

Report No. CCEER 93-2

**EVALUATION OF THE RESPONSE OF  
THE APTOS CREEK BRIDGE  
DURING THE 1989 LOMA PRIETA EARTHQUAKE**

By  
Saber M. Abdel-Ghaffar  
Emmanuel 'Manos' Maragakis  
Mehdi 'Saïd' Saïdi

A Report for  
California Department of Transportation,  
National Science Foundation,  
and Nevada Department of Transportation

---

**Center for Civil Engineering Earthquake Research**  
Department of Civil Engineering/258  
University of Nevada  
Reno, Nevada 89557

January 1993

## ABSTRACT

This report is one of a series that results from the study "Effect of the Aptos Creek bridge suffered some damage during the Loma Prieta earthquake of October 17, 1989. This bridge is located approximately \*\* miles southwest of the epicenter. The focus of the analysis for this bridge study was the nonlinear behavior of the expansion joint elements. Several parameters were studied in details. Parametric studies were carried out to determine the effect of cable restrainers and intermediate hinge shear bolts on the response of the bridge. Finally, based on the analytical results in conjunction with the damage report, a general conclusion regarding the analysis capability is deduced. Detailed mathematical procedures simulating nonlinear behavior of the expansion joints are included in the study.

## CONTENTS

ABSTRACT	II
ACKNOWLEDGEMENT	III
LIST OF FIGURES	IV
LIST OF TABLES	X
<b>1 INTRODUCTION</b>	<b>1</b>
1-1 STATEMENT OF THE PROBLEM	1
1-2 REVIEW OF RELEVANT RESEARCH INVESTIGATION	1
1-3 OBJECTIVE AND SCOPE	
1-4 DESCRIPTION OF THE COMPUTER PROGRAMS	
1-4.1 IMAGES-3D	
1-4.2 NEABS	
1-5 THE LOMA PRIETA EARTHQUAKE	
<b>2 DESCRIPTION OF THE BRIDGE</b>	
2.1 DESCRIPTION OF THE BRIDGE	
2.5 RETROFITTING	
2.6 EARTHQUAKE DAMAGE	
<b>3 ANALYTICAL MODEL</b>	
3.1 LINEAR ANALYTICAL MODEL	
3.2 NONLINEAR ANALYTICAL MODEL	
3.3 SEISMIC EXCITATION	
<b>4 ANALYTICAL RESULTS</b>	
4.1 STRUCTURE PERIODS AND FREQUENCIES	
4.2 PARAMETRIC STUDY AND RESULTS	
4-2.1 NODAL DISPLACEMENT	
4-2.2 JOINT SEPARATION	
4-2.3 ABUTMENT AND PILES	
4-2.4 BEARING BARS	
4-2.5 Hinge BOLTS	

4-2.6 SHEAR PIPES .....  
4-2.7 CABLE RESTRAINERS .....  
4-2.8 IMPACT .....

**5 SUMMARY AND CONCLUSIONS**

## LIST OF FIGURES

<b>Figure 2-1</b>	Schematic Drawing of the Aptos Creek Bridge . . . . .
<b>Figure 2-2</b>	Typical Cross Section of the Bridge . . . . .
<b>Figure 2-3</b>	Fixed Bearing Assembly at both Abutments . . . . .
<b>Figure 2-4</b>	Details of the Middle Expansion Joint . . . . .
<b>Figure 2-5</b>	Details of the Retrofitting at the Abutments . . . . .
<b>Figure 2-6</b>	Details of the Retrofitting at the Middle Expansion Joint . . . . .
<b>Figure 3-1</b>	Idealization of the Lumped Mass, Linear Analytical Model . . . . .
<b>Figure 3-2</b>	Idealization of the Lumped Mass, Nonlinear Analytical Model . . . . .
<b>Figure 3-3</b>	Capitola Fire Station, Transverse Component ( Peak Acceleration = $-462.922 \text{ cm/sec}^2$ at 6.02 sec ) . . . . .
<b>Figure 3-4</b>	Capitola Fire Station, Longitudinal Component ( Peak Acceleration = $-390.792 \text{ cm/sec}^2$ at 8.08 sec ) . . . . .
<b>Figure 4-1</b>	First Ten Mode Shapes for the Aptos Creek Bridge . . . . .
<b>Figure 4-2</b>	Relative Displacement Response at Abutment 1 in the Long. Direction (0" TBG and 1" SG) . . . . .
<b>Figure 4.3</b>	Relative Displacement Response at Abutment 1 in the Trans. Direction (0" TBG and 1" SG) . . . . .
<b>Figure 4.4</b>	Relative Displacement Response at Abutment 1 in the Long. Direction (0" TBG and 1" SG), Motion Normalized to 0.7g . . . . .
<b>Figure 4-5</b>	Relative Displacement Response at Abutment 1 in the Trans. Direction (0" TBG and 1" SG), Motion Normalized to 0.7g . . . . .
<b>Figure 4-6</b>	Relative Displacement Response at the Mid. Exp. Jt. in the Long. Dir. (0" TBG and 1" SG) . . . . .
<b>Figure 4-7</b>	Relative Displacement Response at the Mid. Exp. Jt. in the Trans. Dir. (0" TBG and 1" SG) . . . . .
<b>Figure 4-8</b>	Relative Displacement Response at the Mid. Exp. Jt. in the Long. Dir. (0" TBG, 1" SG, and W/O Shear Bolts) . . . . .

**Figure 4-9** Relative Displacement Response at the Mid. Exp. Jt. in the Trans. Dir. (0" TBG, 1" SG, and W/O Shear Bolts) . . . . .

**Figure 4-10** Relative Displacement Response at Abutment 6 in the Long. Dir. (0" TBG and 1" SG) . . . . .

**Figure 4-11** Relative Displacement Response at Abutment 6 in the Trans. Dir. (0" TBG and 1" SG) . . . . .

**Figure 4-12** Abutment Force Response at Abutment 1 (0" TBG and 1" SG).

**Figure 4-13** Pile Force Response at Abutment 1 (0" TBG and 1" SG) . . . . .

**Figure 4-14** Abutment Force Response at Abutment 6 (0" TBG and 1" SG)

**Figure 4-15** Pile Force Response at Abutment 6 (0" TBG and 1" SG) . . . . .

**Figure 4-16** Abutment Force Response at Abutment 1 (0" TBG, 1" SG, and W/O Shear Bolts) . . . . .

**Figure 4-17** Pile Force Response at Abutment 1 (0" TBG, 1" SG, and W/O Shear Bolts) . . . . .

**Figure 4-18** Abutment Force Response at Abutment 6 (0" TBG, 1" SG, and Shear Bolts) . . . . .

**Figure 4-19** Pile Force Response at Abutment 6 (0" TBG, 1" SG, and W/O Shear Bolts) . . . . .

**Figure 4-20** Abutment Force Response at Abutment 1 (W/O Cables and 1" SG), Motion Normalized to 1.0 g . . . . .

**Figure 4-21** Nonlinear Deformation of Abutment 1 (W/O Cables and 1" SG), Motion Normalized to 1.0 g . . . . .

**Figure 4-22** Pile Force Response at Abutment 1 (W/O Cables and 1" SG), Motion Normalized to 1.0 g . . . . .

**Figure 4-23** Nonlinear Deformation of Piles (W/O Cables and 1" SG), Motion Normalized to 1.0 g . . . . .

**Figure 4-24** Abutment Force Response at Abutment 6 (W/O Cables and 1" SG), Motion Normalized to 1.0 g . . . . .

**Figure 4-25** Nonlinear Deformation of Abutment 6 (W/O Cables and 1" SG), Motion Normalized to 1.0 g . . . . .

**Figure 4-26** Pile Force Response at Abutment 6 (W/O Cables and 1" SG),  
Motion Normalized to 1.0 g . . . . .

**Figure 4-27** Shear Force Response of the Bearing Bars at Abutment 1 in the  
Long. Dir. (0" TBG and 1" SG) . . . . .

**Figure 4-28** Nonlinear Deformation Response of the Bearing Bars in the  
Long. Dir. (0" TBG and 1" SG) . . . . .

**Figure 4-29** Shear Force Response of the Bearing Bars at Abutment 1 in the  
Trans. Dir. (0" TBG and 1" SG) . . . . .

**Figure 4-30** Nonlinear Deformation Response of the Bearing Bars at  
Abutment 1 in the Trans. Dir. (0" TBG and 1" SG) . . . . .

**Figure 4-31** Shear Force Response of the Bearing Bars at Abutment 6 in the  
Long. Dir. (0" TBG and 1" SG) . . . . .

**Figure 4-32** Nonlinear Deformation Response of the Bearing Bars at  
Abutment 6 in the Long. Dir. (0" TBG and 1" SG) . . . . .

**Figure 4-33** Shear Force Response of the Bearing Bars at Abutment 6 in the  
Trans. Dir. (0" TBG and 1" SG) . . . . .

**Figure 4-34** Nonlinear Deformation Response of the Bearing Bars at  
Abutment 6 in the Trans. Dir. (0" TBG and 1" SG) . . . . .

**Figure 4-35** Shear Force Response of the Bearing Bars at Abutment 1 in the  
Long. Dir. (0" TBG, 1" SG, and W/O shear Bolts) . . . . .

**Figure 4-36** Nonlinear Deformation Response of the Bearing Bars at  
Abutment 1 in the Long. Dir. (0" TBG, 1" SG, and W/O shear  
Bolts) . . . . .

**Figure 4-37** Shear Force Response of the Bearing Bars at Abutment 1 in the  
Trans. Dir. (0" TBG, 1" SG, and W/O Shear Bolts) . . . . .

**Figure 4-38** Nonlinear Deformation Response of the Bearing Bars at  
Abutment 1 in the Trans. Dir. (0" TBG, 1" SG, and W/O Shear  
Bolts) . . . . .

**Figure 4-39** Shear Force Response of the Bearing Bars at Abutment 6 in the  
Long. Dir. (0" TBG, 1" SG, and W/O Shear Bolts) . . . . .

**Figure 4-40** Nonlinear Deformation Response of the Bearing Bars at Abutment 6 in the Long. Dir. (0" TBG, 1" SG, and W/O Shear Bolts) . . . . .

**Figure 4-41** Shear Force Response of the Bearing Bars at Abutment 6 in the Trans. Dir. (0" TBG, 1" SG, and W/O Shear Bolts) . . . . .

**Figure 4-42** Nonlinear Deformation Response of the Bearing Bars at Abutment 6 in the Trans. Dir. (0" TBG, 1" SG, and W/O Shear Bolts) . . . . .

**Figure 4-43** Shear Force Response of the Shear Bolts at the Mid. Exp. Jt. in the Long. Dir. (0" TBG and 1" SG) . . . . .

**Figure 4-44** Nonlinear Deformation Response of the Shear Bolts at the Mid. Exp. Jt. in the Long. Dir. (0" TBG and 1" SG) . . . . .

**Figure 4-45** Shear Force Response of the Shear Bolts at the Mid. Exp. Jt. in the Trans. Dir. (0" TBG and 1" SG) . . . . .

**Figure 4-46** Nonlinear Deformation Response of the Shear Bolts at the Mid. Exp. Jt. in the Trans. Dir. (0" TBG and 1" SG) . . . . .

**Figure 4-47** Shear Force Response of the Shear Bolts at the Mid. Exp. Jt. in the Long. Dir. (0" TBG and 1" SG), Motion Normalized to 0.7g . . . . .

**Figure 4-48** Nonlinear Deformation Response of the Shear Bolts at the Mid. Exp. Jt. in the Long. Dir. (0" TBG and 1" SG), Motion Normalized to 0.7g . . . . .

**Figure 4-49** Shear Force Response of the Shear Bolts at the Mid. Exp. Jt. in the Trans. Dir. (0" TBG and 1" SG), Motion Normalized to 0.7g . . . . .

**Figure 4-50** Nonlinear Deformation Response of the Shear Bolts at the Mid. Exp. Jt. in the Trans. Dir. (0" TBG and 1" SG), Motion Normalized to 0.7g . . . . .

**Figure 4-51** Shear Force Response of the Shear Pipes at the Mid. Exp. Jt. in the Trans. Dir. (0" TBG and 1" SG) . . . . .

**Figure 4-52** Nonlinear Deformation Response of the Shear Pipes at the Mid. Exp. Jt. in the Trans. Dir. (0" TBG and 1" SG) . . . . .

- Figure 4-53** Shear Force Response of the Shear Pipes at the Mid. Exp. Jt. in the Trans. Dir. (0" TBG and 1" SG, and W/O Shear Bolts) . . .
- Figure 4-54** Nonlinear Deformation Response of the Shear Pipes at the Mid. Exp. Jt. in the Trans. Dir. (0" TBG and 1" SG, and W/O Shear Bolts) . . . . .
- Figure 4-55** Tie-Bar-Force Response of the Restrainers at Abutment 1 (0" TBG and 1" SG) . . . . .
- Figure 4-56** Tie-Bar-Force Response of the Restrainers at the Mid. Exp. Jt. (0" TBG and 1" SG) . . . . .
- Figure 4-57** Tie-Bar-Force Response of the Restrainers at Abutment 6 (0" TBG and 1" SG) . . . . .
- Figure 4-58** Tie-Bar-Force Response of the Restrainers at Abutment 1 (0" TBG and 1" SG), Motion Normalized to 1.0 g . . . . .
- Figure 4-59** Tie-Bar-Force Response of the Restrainers at the Mid. Exp. Jt. (0" TBG and 1" SG), Motion Normalized to 1.0 g . . . . .
- Figure 4-60** Tie-Bar-Force Response of the Restrainers at Abutment 6 (0" TBG and 1" SG), Motion Normalized to 1.0 g . . . . .
- Figure 4-61** Relative Displacement Response at Abutment 1 in the Long. Direction (0" TBG and 1" SG), Motion Normalized to 1.0 g . .
- Figure 4-62** Relative Displacement Response at Abutment 1 in the Long. Direction (W/O Cables and 1" SG), Motion Normalized to 1.0 g.
- Figure 4-63** Relative Displacement Response at the Mid. Exp. Jt. in the Long. Dir. (W/O Cables and 1" SG), Motion Normalized to 1.0 g . . . . .
- Figure 4-64** Relative Displacement Response at Abutment 6 in the Long. Dir. (W/O Cables and 1" SG), Motion Normalized to 1.0 g . . .

## LIST OF TABLES

<b>Table 3-1</b>	Section Properties . . . . .
<b>Table 3-2</b>	Abutment Foundation Spring Coefficients . . . . .
<b>Table 3-3</b>	Expansion Joint Properties . . . . .
<b>Table 4-1</b>	Structural Periods and Participation Factors . . . . .
<b>Table 4-2</b>	Symbols used in the Tables and Graphs . . . . .
<b>Table 4-3</b>	Analysis Identification Number . . . . .
<b>Table 4-4</b>	Maximum Absolute Displacement of the Expansion Joint Nodes
<b>Table 4-5</b>	Maximum Absolute Displacement of the Expansion Joint Nodes
<b>Table 4-6</b>	Maximum Relative Displacement at the Expansion Joints . . . . .
<b>Table 4-7</b>	Maximum Longitudinal Abutment and Pile Force and Deformations . . . . .
<b>Table 4-8</b>	Maximum Nonlinear Deformation at the Expansion Joints . . . . .
<b>Table 4-9</b>	Permanent Deformation at the Expansion Joints . . . . .
<b>Table 4-10</b>	Maximum Cable Restrainer Forces Used at both Abutments and the Intermediate Expansion Joint . . . . .

# CHAPTER 1

## INTRODUCTION

### 1-1 STATEMENT OF THE PROBLEM

The damage caused to the bridge structure during the San Fernando earthquake of February 9, 1971, demonstrated the critical needs for both theoretically and experimental research related directly to the seismic effects on the bridge structures. In order to get a better understanding of seismic effects on bridge structures, it is imperative to study the seismic damages to a similar existing bridges during the previous earthquakes. The characteristic of the damage encompassed three major forms. These forms include weakness of the superstructure, weakness of the substructure, and weakness of the surrounding soils.

Most of the bridge damages during the great Alaskan earthquake of March 27, 1964 were caused by the substructure failure resulting from large ground displacements, settlements, and loss of bearing capacity. Evaluation of the resistance of the existing bridge components. Evaluation of the structural integrity. Bridge column/ foundation connections have proven to be a weak detail in past earthquakes. In order to quantify structural resistance it is necessary to establish ultimate strength and deformation capacity of a typical connections for a standard columns. Appropriate retrofit measures can then be developed for strengthening this detail. Once the strengths of typical existing connection details have been determined deficiencies including insufficient embedment length and bar anchorage can be addressed.

Analytically and experimental studies are required prior to using retrofit concepts in the field, as the concepts must be shown to be practical and cost effective. Current bridge design practice is to consider seismic excitation in each global direction separately. Certain internal force components are sensitive to simultaneous excitations from different directions. It would therefore appear that earthquake resistant design would be appreciably

approved, by considering simultaneous base motion excitation to the structure.

## **1-2 REVIEW OF RELEVANT RESEARCH INVESTIGATION**

Few analytical and experimental investigations have been carried out in the past to determine the effect of the different components of the expansion joint on the total response of the bridge. In recent years, the influence of the expansion joint on the seismic response of structural system has become increasingly important.

## **1-2 OBJECTIVE AND SCOPE**

Chapter 2 of this report describes the geometry of the bridge, the retrofitting of the bridge, and the damage the bridge experienced during the Loma Prieta earthquake. Chapter 3 presents in details the mathematical model used in studying the nonlinearity of the bridge. Chapter 4 represents the analytical results of the investigation. Chapter 5 summarizes the conclusions and recommendations.

Various parameter studies have been carried out for the bridge to study the effect of the shear bolts and the cable restrainers.

## **1-3 DESCRIPTION OF COMPUTER PROGRAMS**

Two computer programs have been used in this study to get the overall dynamic behavior of the Aptos Creek bridge. A brief description of each computer program is listed below:-

### **1-3.1 IMAGES-3D**

The computer program IMAGES-3D, Interactive Microcomputer Analysis and Graphics of Engineering System-3 Dimensional (version 1.6), was used in the frequency analysis of the bridge [3]. This a finite element analysis program that can be used for modal and linear-elastic static and dynamic analyses of two and three dimensional structures. In this study, it was only necessary to use IMAGES-3D for the purpose of modal analysis for the Aptos Creek bridge. The modal analysis was performed to calculate the frequencies, mode shapes,

and participation factors for the bridge. These dynamic characteristics were necessary as input for the nonlinear program used in this study. More details regarding the computer program can be found in reference 3.

### **1-3.2 NEABS-86**

The computer program NEABS, Nonlinear Earthquake Analysis of Bridge System, was developed by Tseng and Penzien to perform nonlinear dynamic analysis of bridge systems [16]. NEABS can evaluate the dynamic time-history response of a discrete system subjected to dynamic loadings and support motions at supporting bridge columns and abutments. This computer program uses step-by-step direct integration method with either constant acceleration or linear acceleration method in the integration. The program support the following elements:

- 1- Elastic straight beam elements.
- 2- Linear Boundary Spring Elements.
- 3- Nonlinear Expansion Joints (modelled by elasto-plastic).
- 4- Hysteretic elasto-plastic elements to model the nonlinearity of columns.
- 5- Degrading Bi-linear model to model the nonlinearity of columns (not used any more).

### **1-5 THE LOMA PRIETA EARTHQUAKE**

The Loma Prieta earthquake occurred at 5:04 p.m. (local time) on October 17, 1989. The main shock magnitude was estimated as 7.1 on the Richter scale. This earthquake was the largest on the San Andrese fault since the great San Francesico earthquake of 1906 ( $M = 8.3$ ). The earthquake epicenter was about 10 miles northwest of Santa Cruz, 60 miles south-southwest of San Francesico, and its focal depth was about 11 miles beneath the earth surface. The strong shaking lasted only about 10 seconds. The earthquake caused extensive damages to buildings, bridges, and other structures.

## CHAPTER 2

### BRIDGE DESCRIPTION AND DAMAGE

#### 2.1 DESCRIPTION OF THE BRIDGE

The Aptos Creek bridge is located about 6 miles east of Santa Cruz in Santa Cruz County, connecting Santa Cruz with Watsonville. The bridge was designed in 1946 according to the 1943 AASHO (American Association of State Highway Official) specifications for highway bridges. The construction of the bridge was completed and the bridge was opened to traffic in 1949.

Figure 2-1 presents a schematic drawing of the Aptos Creek bridge. The bridge is a five span reinforced concrete slab girder type structure with an expansion joint located in Span 3, about 11 feet away from bent number four. It should be noted that the middle expansion joint divides the structure into two continuous frames. The first frame, referred to as Frame I, extends between abutment 1 and the interior expansion joint. Frame II extends between the interior expansion joint and abutment 6. The total length of the bridge is 260 feet. The first four spans are 56 feet long each, whereas the fifth span is 32 feet long. The overall width of the bridge is 62 feet. None of the bridge supports or joints are skewed.

The superstructure consists of ten reinforced concrete girders supporting a 6.5" thick slab. The beams are cast monolithically with the slab which in turn is cast monolithically into a continuous cap. The cap is cantilevered over the columns to support the exterior girders. The bent cap cross sectional dimensions are 4' wide and 9' deep between the columns, then the depth is tapered to 5'-7" at both ends of the bent cap. All the dimensions of the bent caps are identical. The typical cross section dimension for the girders are 1'-6" wide and 4'-6" deep. Diaphragms are provided at mid spans and at both ends of the deck to increase the torsional capacity of the superstructure. These diaphragms are 10" wide, 2'-4" deep, and 4'-10" long. It should be noted that these diaphragms were cast monolithically with the superstructure. Figure 2-2

shows typical cross sections of the superstructure and the substructure of the bents.

The columns of each bent are pinned at the footings. Each pin consists of a concrete neck cast monolithically with the footing. The typical cross sectional dimensions of the columns and the column neck are 4' X 6' and 3' X 4'-4" respectively. The hinge reinforcement consists of six square dowels, each having a cross section of 1 1/4" X 1 1/4". The dowels are placed in a scissor pattern, thus preventing transmission of moments from the columns to the foundations. The dowels were placed 2' apart symmetric about the column transverse centerline. The column reinforcement consists of square bars, each having a cross section of 1 1/8" X 1 1/8" ..

The columns of each bent are attached to a combined reinforced concrete footing. Bents number two and three have additional plain concrete sub-foundation. The configuration of the column base and footing is shown in Fig. 2-2.

At each abutment, the bridge girders are supported on metal bearing bars. The fixed bearing provides pinned connections between the girders and the abutments. Each bearing bar is 3" X 3" X 1'-3 1/2". The bars at each bearing are welded to a bottom plate. The joint configuration allows for one inch movement in each of the transverse and the longitudinal directions. The bottom plate is anchored to the abutment by means of two bolts. The bearing bars are located under the girders at both abutments. Figure 2-3 shows a typical bearing assembly. The bearing mechanism allows for thermal and shrinkage movements along the longitudinal and transverse axes of the bridge.

The intermediate expansion joint is fitted with two steel angles as shown in Figure 2-4 to minimize friction. Each angle is 6 X 4 X 3/8". The intermediate expansion joint is designed to allow rotations about all axes and translation in both horizontal directions, and to restrain the relative displacement in the vertical direction. The two angles are tied together with  $\phi$  3/8" bolts at 5' intervals as shown in section A-A of Figure 2-4. At the

Intermediate expansion joint the longitudinal and the transverse translations are restrained by shear bolts. The seat gap was specified, in the blue print, at both abutments and at the intermediate expansion joint as 1 inch. The seat gaps were filled with molged expansion joint material at the time of the construction. Figure 2-4 shows details of the middle expansion joint.

At both ends, the bridge is supported on standard seat type abutments, which in turn are supported on steel piles. The abutment wall width has a constant thickness of 1 foot and clear height of 4'-11". The centerline of the metal bearing bar is located at a distance of one foot from the abutment back wall. The wing wall is connected to the abutment wall through &&&. At abutment 1 there is 10 battered piles of length 60 feet and at abutment 6 there is 10 battered piles of length 40 feet. These piles have an individual design capacity of 40 tons. The battered piles have slope 1 to 3. The combined footing used at bents 2 and 3 have dimensions of 8' deep X 60' long X 4' deep and at bents 4 and 5 have dimensions of 7' wide X 60' long X 4' deep.

The specified concrete used for this bridge has minimum compressive strength of 3000 psi, and the steel was specified as grade 50.

## **2.2 RETROFITTING**

The Aptos Creek bridge was retrofitted in 1983 to mitigate potential damage due to future seismic activity. Horizontal earthquake restrainer units were placed at the abutments and at the intermediate hinge. At both abutments, there are 6 restrainer units, with cables in a through loop configuration. Each end of the loop is attached to the abutment, and thus there are two attachment points for each restrainer unit. Figure 2-5 shows the details of the retrofitting at the abutments. At the middle expansion joint there are 4 restrainer units tying the expansion joint with the bent number four. Each one of these restrainer units consists of five 3/4" cables. Two galvanized steel pipes of 3 3/4" in diameter filled with concrete are placed across the intermediate expansion joint to provide dowels action to resist the relative

transverse movement. Figure 2-6 shows the details of the retrofitting at the middle expansion joint. The longitudinal hinge restrainers are provided with a gap to accommodate the expected movements due to change in the temperature. In addition to that, the hinge opening was adjusted during the construction accommodate the expected seasonal temperature change. At both abutments and middle hinge, all the restrainers and the steel pipes are symmetrical about the longitudinal axes of the bridge.

### **2.3 EARTHQUAKE DAMAGE**

Following the Loma Prieta earthquake of October 17, 1989, Caltrans (California Department of Transportation) engineers conducted preliminary inspections of more than 1500 bridge structures in the area affected by the earthquake. One of those bridges was the Aptos Creek which suffered some damage during the earthquake.

According to the Caltrans report, the right and the left curtain walls at abutment 1 were cracked and spalled (3 1/2" X 4 1/2" X 1'). Also there was a large spall in the overhang soffit above the curtain walls (2 1/2' X 1 1/2').

The superstructure moved transversely and came to rest after it moved one inch to the left of abutment number one. All the bottom plate anchor bolts were sheared off and the ends of the groute pads have broken loose due to the movement.

## CHAPTER 3

### ANALYTICAL MODELS

#### 3.1 LINEAR ANALYTICAL MODEL

The primary objective of this report is to study the response of the Aptos Creek bridge under the 1989 Loma Prieta earthquake with particular emphasis on the nonlinear phase of the behavior. In order to determine the frequencies of the bridge, it was necessary to build a linear mathematical model. Figure 3-1 shows the lumped mass model used to idealize the linear mathematical model. The computer program IMAGES-3D was used to conduct the linear analysis for the bridge.

The linear analytical model idealizes the structure as an assemblage of line members coinciding with the center line of the structural elements. Since the center line of the deck does not intersect with the center line of the bent cap in elevation, very stiff vertical elements were used to connect the deck to the bent. It should be noted that the bent cap properties were adjusted, by increasing the moment of inertia in the three direction, to account for the additional stiffness, resulting from the construction of the cap as an integral part of the superstructure. The rigid elements that represent the bent caps were used to model the transverse displacements of the columns with respect to the center line of the bridge. The structure is assumed to be supported by a rigid foundation at the bents. In view of the high strength of the soil and the large plane of the combined footings, the rigid foundation assumptions appears to be satisfactory.

The modulus of elasticity for the concrete was calculated from Ref. 10.

---

$$E_c = 57,000 \sqrt{f'_c}$$

where  $f'_c$  is the design strength of the concrete. The Poisson's ratio for the concrete was taken equal to 0.2. The unit weight of the superstructure was

increased to 175 pcf to account for the paving materials and superstructure.

The two columns monolithic bents were modelled as continuous frames. To simulate the freedom of rotation at the intermediate expansion joint, moment releases in all three coordinate directions were used at one end of the beam. The element properties, cross sectional area, moment of inertia, and torsional constant are shown in Table 3-1. The total moment of inertia and the gross area were used for the columns and the beams without any deductions in the frequency analysis and the nonlinear analysis.

**Table 3-1 Section Properties.**

Location	$A$ (ft <sup>2</sup> )	$I_z$ (ft <sup>4</sup> )	$I_y$ (ft <sup>4</sup> )	$J$ (ft <sup>4</sup> )	$E$ (ksi)
Deck	59.38	188.645	30102.5	53.17	449571.
Column	24.0	72.0	32.0	77.2	449571.
Bent Cap	1000.0	1000.0	100000	1000.0	449571.

All the bent supports were assumed to be pinned to the rigid footings. Foundation flexibility was considered only at the abutments. The foundation flexibility at the abutments was modelled as an equivalent set of linear springs. The abutments soil spring coefficients were calculated based on the Caltrans approach. {which includes linear elastic boundary spring elements at the foundation/abutment interface}. It should be noted that fifty percent reduction in the longitudinal direction was taken to account for the development of the passive pressure at only one abutment at any instant. If the full passive resistance was used at both abutments, the total structure stiffness would be very high. In order to prevent unrealistically high stiffness, one half of the total stiffness is allocated to each abutment. In calculating the stiffness of the abutment, the wing wall was added according to Caltrans way.

**Table 3-2** Abutment Foundation Spring Coefficients.

Spring Coefficients	$K_x$ (kips/ft)	$K_y$ (kips/ft)	$K_z$ (kips/ft)	$K_{\theta x}$ (k-ft/rad)	$K_{\theta y}$ (k-ft/rad)	$K_{\theta z}$ (k-ft/rad)
Abutments 1 & 6						

Since NEABS (Nonlinear Earthquake Analysis of Bridge System) [8] requires the Rayleigh damping, it was necessary to calculate the mass and the stiffness proportional damping coefficients. The relative stiffness damping coefficient ( $\alpha$ ) and the absolute mass damping ( $\beta$ ) were calculated based on the calculated frequencies and assumed damping ratio 5% for all mode shapes. The first and the second normal modes of vibration were used to find the coefficients  $\alpha$  and  $\beta$ .

$$DampingFactor = \alpha [M] + \beta [k]$$

$$\zeta_1 = \frac{1}{2 \omega_1} (\alpha + \beta \omega_1^2)$$

$$\zeta_2 = \frac{1}{2 \omega_2} (\alpha + \beta \omega_2^2)$$

where

$\alpha$  Mass-proportional damping.

$\beta$  Stiffness-proportional damping.

[M] Mass matrix.

[K] Stiffness matrix

$\zeta_1$  and  $\zeta_2$  Damping factors for the first two modes.

$\omega_1$  and  $\omega_2$  Circular frequencies of the first two mode shape.

### **3.2 NONLINEAR ANALYTICAL MODEL**

The mathematical model used for the nonlinear analysis is similar to the linear model which was used for the frequency analysis. The deck of the

bridge and the columns were modelled as linear elastic straight beam elements. Each span was subdivided into four straight beam elements, while each column was subdivided into three beam elements[13]. The nonlinear mathematical model used to idealize the bridge is shown in fig. 3-2. The hinge element was introduced to simulate the followings; the force in the tie bars, the friction between the bridge deck and the impact between the deck and the abutment when the hinge gap close up.

For the presence of the nonlinear analysis it was necessary to calculate the different element stiffnesses and yield forces. At both abutments, the metal bearing bars were modelled by using nonlinear expansion joint elements. In the longitudinal direction, the stiffness of the bearings was calculated by considering the contribution from both bending and shearing of the bearing bar and the elongation of the anchor bolts. By imposing a unit displacement, the bearing spring coefficients were determined. Under the assumption that the bearing bar and the anchor bolt springs are connected in series, the total spring coefficient was determined.

Bending plus shear stiffness can be calculated as:

$$K = \frac{12 EI}{(1 + 4\beta) L^3}$$

where

$$\beta = \frac{3 EI}{G A L^2} \qquad G = \frac{E}{2 (1 + \nu)}$$

E	Modulus of Elasticity	G	Shear Modulus
A	Shear Area	L	Length of the Member
$\nu$	Poisson's Ratio	I	Moment of Inertia

Axial anchor bolt stiffness can be calculated as;

E	Modulus of Elasticity	A	Axial area of the bolt
---	-----------------------	---	------------------------

$$K = \frac{E A}{L}$$

L Length of the bolt

$K_{\text{equivalent}}$  Equivalent Stiffness.

$K_{\text{bearing}}$  Bearing Bar Stiffness (Bending + Shear).

$K_{\text{anchor}}$  Anchor Bolt Stiffness (Axial).

$$\frac{1}{K_{\text{equivalent}}} = \frac{1}{K_{\text{bearing}}} + \frac{1}{K_{\text{anchor}}}$$

Since NEABS can only take six tie bars, the ten bearing bar stiffnesses were transformed to six. It was necessary to provide five transnational springs and one torsional spring in order to accommodate the expansion joint coordinates. The torsional spring coefficient was determined based only on the longitudinal springs of the bearing bars and their distance from the center line of the bridge. The vertical degree of freedom was assumed to be fixed. At the expansion joint the superstructure could rotate freely about the longitudinal axis and about the transverse axis.

The lateral stiffness of the piles was modelled by using another expansion joint active only in tension. At both abutments, the beam element representing the superstructure was connected to the boundary spring through the expansion joints. Nonlinear expansion joint elements, however, were included at both abutments to more accurately model the connections at the end of the girders. The abutments were modeled with boundary spring elements connected in series with the hinge element. A summary of the spring coefficients used for the boundary spring elements is shown in table 3-2.

Due to the fact that no damage occurred in the columns due to the Loma Prieta earthquake, nonlinear behavior was not accounted for in the columns.

The computer program NEABS [8] was used to perform the nonlinear analysis of the structure.

At each abutment it was necessary to provide eight expansion joints. Four of these elements represented the nonlinearity of the bearing bars and the anchor bolts, two in the longitudinal direction, and two in the transverse direction. Two of the remaining expansion joints represented the nonlinearity of the lateral stiffness of both the abutments and the piles. Finally, the remaining two expansion joints represented the nonlinear behavior of the cable restrainers and the impact between the abutment and the deck.

At the middle expansion joint 8 expansion joints were provided. Four of these elements were necessary to model the nonlinearity behavior of the shear bolts, two in the longitudinal directions, and two in the transverse directions. Two of the remaining expansion joint represented the nonlinear behavior of the shear pipes in the transverse direction. Finally, the remaining two expansion joints represented the nonlinear behavior of the cable restrainers and the impact between the two parts of the superstructure.

Equivalent tensile stiffness and yield force of the cable restrainer units were calculated using the following equations [13];

$$K_r = \frac{E A_r N_r}{L}$$

$$F_y = \sigma_y A_r N_r$$

where

E	Modulus of Elasticity after initial yielding = 18,000 ksi
F <sub>y</sub>	Yield stress in the restrainer (176.1 ksi)
A <sub>r</sub>	Area of the restrainer (0.222 in <sup>2</sup> for 3/4" cables)
L	Length of the restrainer
N <sub>r</sub>	Number of cables in the restrainer unit

The input parameters used to model the different types of the expansion

joint hinge properties are shown in Table 3-3.

### 3.3 SEISMIC EXCITATION

17 ~~257~~  
Motion caused by the Loma Prieta earthquake was recorded by the California Strong Motion Instrumentation Program (CSMIP) [16]. Base motion was used to excite the bridge in orthogonal direction. The exciting force used in this study was selected with the objective of representing the actual excitation at the bridge site during the Loma Prieta earthquake. Instrumentation was installed at Capitola fire station and indicated a peak ground acceleration of 0.3984g in the longitudinal direction and of 0.4719g in the transverse direction. The fire station is located about 4.0 miles away from the bridge site. It was assumed that the bridge site experienced the same accelerations as the Capitola fire station during the earthquake. This assumption is valid if the underlying soils were firm and thus did not contribute to site amplification. The longitudinal motion was in a direction parallel to the bridge deck centerline and the transverse motion was perpendicular to the bridge deck.

The north south axis of the fire station was approximately parallel to the longitudinal axis of the bridge. Thus it seemed reasonable to assign the north-south component of the earthquake record to the longitudinal direction of the bridge, and accordingly the east-west component of the transverse direction of the bridge.

Plots of the time history motions are shown in Figures 3-3 and 3-4. The time intervals used for the earthquake and the analysis were respectively 0.02 second and 0.005 seconds. It was felt that more refined intervals for analysis would provide greater accuracy. The recorded length of the motion is 39.98 seconds. It was decided to use only 8.8 seconds to reduce the computational effort.

**Table 3-3** Input Parameters for the Different Expansion Joints.

	Yield Force (Kips)	Stiffness (kips/ft)	Seat-Gap (ft)	Tie-Bar-Gap (ft)	No. of Cables	Cable Locations	Impact
Abutment Hinge	1771.5	74604.0	0.0833	0.0	1	0.0	0.0
Piles Hinge	100.0	1200.0	0.0833	0.0	6	± 3.083	0.0
Abutment Bearing	104.72	56018.9	0.0	0.0	6	± 3.083	0.0
Abutment Bearing	104.72	56018.9	1.0	0.0	6	± 0.02	0.0
Abutment Retrofitted	78.188	532.8	0.0833	0.0833	6	± 3.083	0.0
Hinge Shear Bolts	44.2	72746.4	0.0	0.0	6	± 3.083	0.0
Hinge Shear Bolts	44.2	72746.4	1.0	0.0	6	± 0.02	0.0
Hinge Shear Pipes	64.0	148896.0	1.0	0.01	2	± 0.1	0.0
Hinge Retrofitted	195.47	1393.95	0.0833	0.0625	4	± 18.5	0.0
Impact Hinge	1.0	1.0	.0833	0.0	---	---	180000.

## CHAPTER 4

### ANALYTICAL RESULTS

#### 4.1 STRUCTURE PERIODS AND FREQUENCIES

The computer program IMAGES-3D was used to perform the modal analysis of the Aptos Creek bridge. The first ten mode shapes, periods, and participation factors were calculated for the bridge and are presented in table 4-1. Figure 4-1 shows the first ten mode shape of the bridge. Closer examination of the mode shapes and the participation factors indicated that there were three patterns of response behavior. The first type of response was predominantly transverse as indicated in the plots for modes 1, 3, 4, and 10. In this case the bent cap was rotating as a rigid body in a horizontal plane, elastically restrained by the columns. The bent cap rotation had a tendency to introduce opposite shear forces in the tops of the columns normal to the plane of the bent. Corresponding to these shear forces are moments in a vertical plane perpendicular to the plane of the bent. Mode 2 characterizes the second pattern which includes the longitudinal mode of vibration. The third pattern of vibration, which is predominantly vertical, occurs in modes 5, 6, 7, 8, and 9 as shown in Figure 4-1. The contribution of these modes to the final response of the bridge is minimal.

Closer inspection of the mode shapes, as covered above, indicates the structure behaved predominantly in the transverse direction. It is interesting to note that the bridge is significantly weaker in the transverse direction, when compared to the longitudinal direction.

The intermediate expansion joint was modelled as a hinge in accordance with Caltrans design guidelines. For this reason, different element stiffnesses, customarily used, were not accounted for. The expansion joints that are located at the abutments were disregarded, thus the bridge deck was directly connected to the abutment springs. Evidence of coupling between Frame I and

Frame II is apparent due to these assumptions. The coupling effect is most visible in the first pattern of vibration which characterizes the transverse response of the bridge.

In this study, only the first two mode shapes were used to calculate Rayleigh damping coefficients as shown in Chapter 2. A uniform damping coefficients of 5% was selected for all mode shapes. Therefore the effect of variation of modal damping was not included in this study.

**Table 4-1** Structural Periods and Participation Factors.

Mode Shape	Periods	Participation Factor		
		X	Y	Z
Mode 1	0.7445	0.0112	-0.00024	1.328
Mode 2	0.5048	1.087	0.00078	-0.00454
Mode 3	0.3814	0.0207	0.00079	0.09318
Mode 4	0.2526	-0.0233	-0.4621	0.9122
Mode 5	0.2016	-0.0349	0.1781	-0.01302
Mode 6	0.1662	-0.1091	-0.4193	-0.0006918
Mode 7	0.1469	-0.0609	1.591	0.00833
Mode 8	0.1453	-0.0479	-0.7155	0.0319
Mode 9	0.1337	-0.0084	1.787	0.01667
Mode 10	0.1187	0.00131	0.02077	0.1274

## 4.2 PARAMETRIC STUDY AND RESULTS

The objective of the study was to investigate overall response of the bridge components, with particular emphasis on the cable restrainers and hinge shear bolts. Overall response included a detailed study of expansion joint components such as shear pipes, bearing bars, hinge separation, and impact. Table 4-2 presents the seven cases studied. The parameter that were varied in the study were the tie bars and hinge shear bolts, as evident in the table.

To investigate the effect of the shear bolts on the overall response of the bridge, two cases were considered. In the first case the hinge shear bolts were fully intact (Case 1), while in the second case, the hinge shear bolts were removed.

The effect of the cable restrainers on the overall response was initially determined by changing the tie-bar-gap. Since the cable restrainers experienced insignificant force under the given ground excitation, it was decided to increase the base motion. This was accomplished by normalizing the base motion to 0.7g and 1.0g in both directions as shown in cases 4 and 6. The previous two cases were compared to results obtained by removing the cable restrainers as covered in cases 5 and 7.

The following symbols will enable the reader to interpret data in the tables and graphs:

**Table 4-2** Symbols used in the Tables and Graphs.

Symbols	Interpretation	Symbols	Interpretation
TBG	Tie-Bar-Gap	SG	Seat-Gap
Long.	Longitudinal	Trans.	Transverse
Abut. (1)	Abutment 1	Abut. (6)	Abutment 6
Mid. Exp. Jt.	Middle Expansion Joint		

The subsequent sections discuss in details the response of different components of the bridge to the above mentioned cases:

**Table 4-3** Analysis Identification Number.

Case	Tie-Bar-Gap (inch)	Shear Bolts	Ground Motion	
			Transverse	Longitudinal
1	0.0	Accounted for	0.4179g	0.3984g
2	0.75	Accounted for	0.4179g	0.3984g
3	0.0	Removed	0.4719g	0.3984g
4	0.0	Accounted for	0.7g	0.7g
5	Without Cables	Accounted for	0.7g	0.7g
6	0.0	Accounted for	1.0g	1.0g
7	Without Cables	Accounted for	1.0g	1.0g

#### **4-2.1 NODE DISPLACEMENT**

Neabs represents the expansion joint as a two nodes with infinitesimal distance in between of them. One of these nodes is acting as a support and the other moves free relative to the first one. Tables 4-3 and 4-4 show the maximum absolute displacement at the free and the support nodes of the expansion joints respectively. The fixed node number for abutment 1, the intermediate expansion joint, and abutment 6 are 1, 40, and 76 respectively. For the bridge components listed above, the free node numbers are 2, 39, and 75 respectively. It should be noted that the free nodes underwent significantly larger displacements in comparison to the fixed nodes.

#### **4-2.2 JOINT SEPARATION**

The maximum longitudinal and transverse joint separations that occurred at both abutments and at the intermediate expansion joint, are tabulated in Table 4-5. The joint separation is the movement of the free node of the

expansion joint relative to the support node. Figures 4-2 through 4-5 show longitudinal and transverse relative displacements at abutment 1 for cases 1 and 4. Figures 4-6 through 4-9 show the same phenomena at the middle expansion joint for cases 1 and 3. Finally Figures 4-10 through 4-11 show only case 1 at abutment 6.

It should be noted that the wave shapes of the longitudinal and transverse directions, for each expansion joint, are almost identical for all cases, with some magnification as input base motion increases. It was also noted that the hinge opening at abutment 1 was much larger than that at abutment 6 in both the longitudinal and transverse directions.

It is apparent from considering the tables and graphs, that relative displacement in the transverse direction was much larger than in the longitudinal direction. This characteristic was noted for all cases. This difference can be attributed to the significant difference in stiffness between Frames I and II.

The difference in the longitudinal and transverse relative displacement between the cases, with or without cable restrainers was not significant. This is in keeping with the fact that the predominant motion of the bridge was in the transverse direction.

Removal of the hinge shear bolts at the intermediate expansion joint did not significantly change the response in both longitudinal and transverse directions. This can be noted by observing Figures 4-6 through 4-9.

#### **4-2.3 ABUTMENT AND PILES**

The maximum longitudinal forces in both abutments and their supporting piles, for all cases, are tabulated in table 4-6. In all studied cases abutment 1 experienced larger forces than abutment 6 as would be expected. The cable bars which were used to model the abutments and the piles did not reach the yield point for the first three cases. Abutment 1 started to yield when the base motion was normalized to 0.7g in both directions. This Yielding was apparent for conditions with or without cable restrainers. When the base motion was

normalized to 1.0g in both directions, both abutments 1 and 6 yielded. By removing the cable restrainers (Case 7), the cable bar representing the piles at abutment 1 yielded. However the pile group at abutment 6 did not yield. Figures 4-12 through 4-26 show the force and the nonlinear deformation time histories in both abutments and piles for the selected cases.

#### **4-2.4 BEARING BAR**

The shear force and the nonlinear deformation indicated that the capacity of the bearing bars at both abutments was exceeded in both the longitudinal and the transverse directions for all cases. Plots of the time history describing the shear force and nonlinear deformation that occurred in the tie-bars, used to model the bearing bars, are shown in figures 4-27 through 4-42 for both longitudinal and transverse directions. As with the abutments, the bearing bars at abutment number 1 exhibited more transverse and longitudinal displacements than the one at abutment 6.

Since NEABS-86 deals with the cable restrainers as members acting only in tension, it was necessary to model the physical expansion joint with two expansion joint elements acting in opposite directions. The time histories for shear force represent output from two NEABS expansion joints. This data has been combined to produce the complete shear force time history. In a similar fashion, nonlinear deformation could only be obtained by using two NEABS expansion joints. To obtain total nonlinear deformation, it was necessary to subtract negative deformation from positive deformation. This approach was also used for shear pipes and shear bolts with respect to shear force and nonlinear deformation.

It is interesting to note that the damage report by Caltrans showed the transverse force at abutment 1 to be much larger than that at abutment 6. Caltrans observed that bearings at abutment 1 had sheared off and the superstructure had come to rest one inch left of the abutment. Ground motion for the analysis from a site located approximately 4 miles from the bridge. This implies that there could be some inaccuracy in the base motion record used for

the analysis due to soil factors, which could have lead to the damage at abutment 6.

#### **4-2.5 HINGE BOLTS**

Figures 4-43 through 4-50 show selected shear force and nonlinear deformation time histories of the hinge bolts. In all studied cases the hinge shear bolts had yielded in both directions.

The condition of the hinge shear bolts could not be determined, subsequent to the earthquake, due to the physical difficulty of investigating the joint (see Fig. 2-4).

#### **4-2.6 SHEAR PIPES**

Plots of the shear force and nonlinear deformation of the shear pipes are shown in figures 4-51 through 4-54. The shear pipes experienced the same force and nonlinear deformation as the shear bolts in the transverse direction. The only difference between these two responses were in first few seconds in the motions were due to the gap in the shear pipes joint. The maximum shear force in the pipe restrainers reached yield force in all studied cases. The only difference between these two responses was in the first few seconds of motion. This difference can be attributed to the gap in the shear pipe joint.

#### **4-2.7 CABLE RESTRAINERS**

The maximum axial forces and their percentage of the yield force that occurred at the restrainer cables at both abutments and the intermediate expansion joint are tabulated in table 4-9. Figures 4-55 through 4-60 show the cable restrainer force time histories for cases number 1 and 6 at both abutments and at the middle expansion joint. The longitudinal cable restrainers forces were taken directly from the maximum force recorded for the tie bar used in modelling the restrainers. In the studied cases, it is clear that the cables at abutment 1 have much larger forces than at abutment 6. It should be noted that even by magnifying the motion to 1.0g in both directions, these cable bars did not yield. This is due to the fact that the bridge was acting in the transverse direction. Comparison of the longitudinal relative displacements

between cases number 4 and 5 (Table 4-6) showed that the cable restrainers had minimal effect in resisting the motion in the longitudinal direction.

The cable restrainers can be extremely effective in reducing the seismic response of the bridge model, but this rule did not take any place in this bridge. In the analysis with cable restrainers were not reduced because the motion in the transverse direction was much larger than the motion in the longitudinal direction.

When bridge motions are primarily in the longitudinal direction, cable restrainers can be extremely effect in reducing seismic response of the bridge model. However due to the particular mass, stiffness, and geometry of the Aptos Creek bridge, restrainers in this case were not effective

#### **4-2.8 IMPACT**

In the first five studied cases, impact did not occur. This effect can be verified by examining the maximum relative longitudinal displacement on the compression side. One can see clearly that the impact spring did not engage, since the hinge gap did not close on the compression side of the relative displacement response. Impact commenced at abutment 1 when the motion was normalized to 1.0g in both direction (Case 6). Figures 4-61 shows the longitudinal relative displacement at abutment 1 with impact occurring at about 5.9 seconds. By removing the cable restrainers (Case 7) the impact occurred at abutment 1 and at the intermediate expansion joint as shown in figures 4-62 and 4-63. However the hinge gap did not engage at abutment 6, therefore the impact did not occur. It should be noted that even if the response amplitude in the negative direction is suppressed, the rebound effect from collision can appreciably increase the positive response amplitude which follows immediately. This effect can clearly detected when comparing the positive response of cases number 6 and 7 at abutment 1 and the intermediate expansion joint (see Table 4-5).



Table 4-4 Maximum Absolute Displacement of the Expansion Joint Fixed Nodes.

Case	Node 1		Node 40		Node 76	
	Long.	Trans.	Long.	Trans.	Long.	Trans.
1- With 0" TBG and 1" SG	0.02053	0.01808	0.02076	0.06003	0.00895	0.0168
With 3/4" TBG and 1" SG	0.02465	0.04392	0.02235	0.04428	0.00768	0.01597
Without shear bolts	0.0207	0.01733	0.02715	0.06114	0.06342	0.01185
With 0" TBG and 1" SG (0.7g)	0.03494	0.02128	0.04467	0.07766	0.01219	0.0199
(1 ) Without cable restrainers (0.7g)	0.03375	0.01762	0.04718	0.07807	0.01459	0.01994
With 0" TBG and 1" SG (1.0g)	0.04426	0.01727	0.08727	0.1211	0.01603	0.02267
Without cable restrainers (1.0g)	0.0511	0.01706	0.07487	0.1329	0.01621	0.02258

Locations of the Expansion Joint Fixed Nodes

Node 1 is located at abutment 1.

Node 40 is located at the intermediate expansion joint.

Node 76 is located at abutment 6.

Table 4-5 Maximum Absolute Displacement of the Expansion Joint Free Nodes.

Case	Node 2		Node 39		Node 75	
	Long.	Trans.	Long.	Trans.	Long.	Trans.
With 0" TBG and 1" SG	0.03257	0.339	0.03476	0.3534	0.01986	0.09547
With 3/4" TBG and 1" SG	0.04093	0.3058	0.04384	0.3357	0.0214	0.05972
Without shear bolts	0.03324	0.3288	0.03487	0.2762	0.02656	0.01894
With 0" TBG and 1" SG (0.7g)	0.07804	0.5777	0.07939	0.439	0.04362	0.08294
Without cable restrainers (0.7g)	0.07755	0.5645	0.07931	0.474	0.04643	0.08552
With 0" TBG and 1" SG (1.0g)	0.1308	0.8642	0.1349	0.6154	0.08644	0.1259
Without cable restrainers (1.0g)	0.1424	0.9149	0.1439	0.7004	0.0743	0.1172

Locations of the Expansion Joint Free Nodes

Node 2 is located at abutment 1.

Node 39 is located at the intermediate expansion joint.

Node 75 is located at abutment 6.

Table 4-6 Maximum Relative Displacement at the Expansion Joints.

Case	Abut. (1)		Mid. Exp. Jt.		Abut. (6)	
	Long.	Trans.	Long.	Trans.	Long.	Trans.
	With 0" TBG and 1" SG	0.0231	0.3257	0.0248	0.3356	0.0167
With 3/4" TBG and 1" SG	0.0273	0.2921	0.0314	0.3213	0.01672	0.0491
Without shear bolts	0.0217	0.3155	0.0291	0.2817	0.0212	0.016
With 0" TBG and 1" SG (0.7g)	0.0621	0.5635	0.0627	0.4157	0.0383	0.0777
Without cable restrainers (0.7g)	0.0635	0.5512	0.0755	0.4428	0.0394	0.0762
With 0" TBG and 1" SG (1.0g)	0.0945	0.8509	0.0785	0.5594	0.0779	0.1155
Without cable restrainers (1.0g)	0.1263	0.9016	0.1569	0.6514	0.0692	0.1139

**Table 4-7** Maximum Abutment and Pile Force and Deformation .

Case	Abut. (1)			Abut. (6)		
	Abutment Force	Abutment Deform.	Pile Force	Abutment Force	Abutment Deform.	Pile Force
With 0" TBG and 1" SG	909.10	---	27.73	792.50	---	20.03
With 3/4" TBG and 1" SG	1214.0	---	32.78	554.60	---	20.07
Without shear bolts	870.90	---	26.02	607.50	---	25.40
With 0" TBG and 1" SG (0.7g)	1771.0	0.00866	74.49	1324.0	---	45.97
Without cable restrainers (0.7g)	1771.0	0.02000	76.16	1375.0	---	47.31
With 0" TBG and 1" SG (1.0g)	1771.0	0.07072	88.22	1683.0	---	93.50
Without cable restrainers (1.0g)	1771.0	0.06442	100.0	1771.0	8.84E-4	83.00

pile def. =0.06442

**Table 4-8** Maximum Nonlinear Deformation at the Expansion Joints.

Case	Abut. (1)		Mid. Exp. Jt.		Abut. (6)	
	Long.	Trans.	Long.	Trans.	Long.	Trans.
	With 0" TBG and 1" SG	0.01481	0.11952	0.01116	0.1714	0.00826
With 3/4" TBG and 1" SG	0.016423	0.0816	0.01829	0.1095	0.01165	0.01258
Without shear bolts	0.011233	0.1438		0.061		
With 0" TBG and 1" SG (0.7g)	0.03927	0.1907	0.03514	0.1005	0.02496	0.02433
Without cable restrainers (0.7g)	0.04471	0.173	0.05811	0.1356	0.02643	0.01935
With 0" TBG and 1" SG (1.0g)	0.02755	0.2741	0.03934	0.1367	0.05536	0.03393
Without cable restrainers (1.0g)	0.05354	0.3302	0.11621	0.2167	0.05195	0.0285

**Table 4-9 Permanent Nonlinear Deformation at the Expansion Joints.**

Case	Abut. (1)		Mid. Exp. Jt.		Abut. (6)	
	Long.	Trans.	Long.	Trans.	Long.	Trans.
	With 0" TBG and 1" SG	0.01092	0.0208	0.00857	0.0338	0.00608
With 3/4" TBG and 1" SG	0.01104	0.0015	0.00623	0.0423	0.00929	0.00413
Without shear bolts	0.01001	0.1018		0.0233		
With 0" TBG and 1" SG (0.7g)	0.02968	0.1174	0.03514	0.0584	0.02056	0.00666
Without cable restrainers (0.7g)	0.01972	0.0772	0.04089	0.0391	0.021	0.0254
With 0" TBG and 1" SG (1.0g)	0.02095	0.1716	0.00367	0.081	0.05536	0.01812
Without cable restrainers (1.0g)	0.03821	0.1236	0.07451	0.0937	0.00446	0.01455

Table 4-10 Cable Forces and their Percentage of the Yield Force.

Case	Abut. (1)		Mid. Exp. Jt.		Abut. (6)	
	Force	% of YF	Force	% of YF	Force	% of YF
	With 0" TBG and 1" SG	12.31	15.74	34.56	17.68	5.66
Without shear bolts	11.55	14.77	40.53	20.73	4.338	5.55
With 0" TBG and 1" SG (0.7g)	33.08	42.31	87.37	44.7	9.458	12.1
With 0" TBG and 1" SG (1.0g)	39.17	50.1	109.5	56.02	12.02	15.4

% of YF

is the Percentage of the Yield Force

Yield Force of the Abutment Cables

= 78.188 Kips

Yield Force of the Intermediate Hinge Cables

= 195.47 Kips

## CHAPTER 5

### CONCLUSION

Based on the analytical results presented in this report for the bridge studied, the following conclusions were drawn:

- 1- The nonlinear mathematical model developed in this study predicts realistic results under high and low seismic excitations, when compared with damage reports.
- 2- The absolute seismic displacement response of the nodes in the longitudinal direction were much less than the transverse in all the study cases.
- 3- In all cases tie-bar cables did not experience high forces.
- 4- The collision between girders and the abutment and girders with themselves started taking a place after removing the cable and normalizing the motion to 0.7g in both directions.
- 5- The dynamic behavior of the bridge is significantly controlled by the expansion joint components. For that reason, their characteristics must be presented in a modelled realistic form.
- 6- The effect of the vertical excitation on the horizontal, longitudinal and transverse, directions was not taken into account due to the insensitivity of coupling between vertical and horizontal modes.
- 7- The bridge movements at abutment 1 were much larger than the movement at abutment 6. This difference can be attributed to the greater stiffness of frame I relative to frame II.
- 8- The longitudinal cable restrainers were not effective in resisting the motion ( check if they were effective in reducing the transverse response of the bridge model)
- 9- The multiple impact which occurs has a major influence on both amplitude and frequency characteristics of the response. The

rebound from the collision can result in an increased positive response amplitude immediately following the collision.

- 10- The basic mathematical model and the analytical procedures developed in this report as well as the computer program NEABS can be used to predict realistic dynamic response of bridge structure subjected to low or high seismic intensity base excitation.
- 11- The tie bars which were used to represent the nonlinearity of the bearing bars at both abutments had yielded under all conditions studied. The nonlinear deformation at abutment 1 were much larger than the deformation at abutment 6. This difference can be attributed to the considerable difference in relative stiffness of frames I and II.
- 12- The Collapse of the bearing bars of the bridge during the 1989 Loma Prieta earthquake was due to the inability of the bearing bars to take the forces generated by the earthquake. A major portion of that damage was caused by the significant difference in both the transverse and the longitudinal stiffness between frame I and frame II.
- 13- The strength and the stiffness of the bridge columns on each side of the expansion joint are the primary factors which most significantly affect the seismic response characteristics of the bridge.

The nonlinear time history analysis results indicated that all actual cable restrainers experienced very little increase in force. However, bearing bars, shear pipes, and shear bolts experienced considerable forces leading to yielding of structural elements.

## REFERENCES

1. Imbsen, R. A., Penzien, J., "Evaluation of Energy Absorption Characteristics of Highway Bridges Under Seismic Conditions Volume 1", Report No. UCB/EERC-84/17, Earthquake Engineering Research Center, University of California, Berkeley, September 1986.
2. Kawashima, K., Penzien, J., "Correlative Investigations on Theoretical and Experimental Dynamic Behavior of Model Bridge Structure," Report No. UCB/EERC 76-26, Earthquake Engineering Research Center, University of California, Berkeley, July 1976.
3. IMAGES-3D "Interactive Microcomputer Analysis of Graphics of Engineering System-3 Dimensional," Programmed: W. H. Leung, Version 1.61.
4. Ghusn, G. E., Saiidi, M. , " A Simple Hysteretic Element for Biaxial Bending of R/C Columns and Implementation in NEABS-86," Report No. CCEER 86-1, University of Nevada, Reno, July 1986.
5. Lew, H. S., Editor, "Performance of Structures During the Loma Prieta Earthquake of October 17, 1989," NIST Special Publication 778.
6. Imbsen, R. A., Schamber, R. A., "Increased Seismic Resistance of Highway Bridges using Improved Bearing Design Concepts, Volume 1, Bearing Design Concepts and Test Results," A report to U.S. Department of Transportation, Federal Highway Administration.
7. Imbsen, R. A., Nutt, R. V., Penzien, J., "Seismic Response of Bridges-Case Studies," Report No. UCB/EERC 78/14, Earthquake Engineering Research Center, University of California, Berkeley, June 1978.
8. Penzien, J., Imbsen , R. A., Liu, W. D., "NEABS: Nonlinear Earthquake Analysis of Bridge Systems (Users Manual)," NISSEE/Computer Applications, Earthquake Engineering Research Center, University of

California, Berkeley, May 1981.

9. Selna, L. G., "Experimental Evaluation of Performance of Earthquake Restrainer in Box Girder Bridge," ASCE, 1989, pp. 31-40.
10. ACI Committee 318-83, "Building Code Requirements for reinforced Concrete," American Concrete Institute, Detroit, 1983.
11. "Seismic Design of Highway Bridges Workshop Manual," Federal Highway Administration, FHWA-IP-81-2, January 1981.
12. "Bridge Design Aids Manual," State of California, Department of Transportation, Office of the Structure Division, 1991.
13. "Bridge Memo to Designers Manual," State of California, Department of Transportation, Office of the Structure Division, 1991.
14. "Bridge Design Specifications Manual," State of California, Department of Transportation, Office of the Structure Divisions, 1991.
15. Maragakis, E., Saiidi, M., Abdel-Ghaffar, S. M., "Evaluation of the Response of the Whitewater Bridge During the 1986 Palm Spring Earthquake," 8th US-JAPAN Bridge Engineering Workshop, Chicago, IL, May 1992.
- 16- Tesng, W. S., and Penzien, J., "Analytical Investigations of the Seismic Response of Long Multiple-Span Highway Bridges," College of Engineering, U.C. Berkeley, Earthquake Engineering Research Center, Report No. EERC 73-12, June, 1973.
- 17- Shakal, A., M. Huang, M. Reichle, C. Ventura, T. Cao, R. Sherburne, M. Savage, R. Darrah, And C. Peterson. 1989. "CSMIP strong-motion records from the Santa Cruz Mountains (Loma Prieta), California earthquake of 17 October 1989." Report No. OSMS-89-06. Sacramento: California Department of Conservation, Division of Mines and Geology.

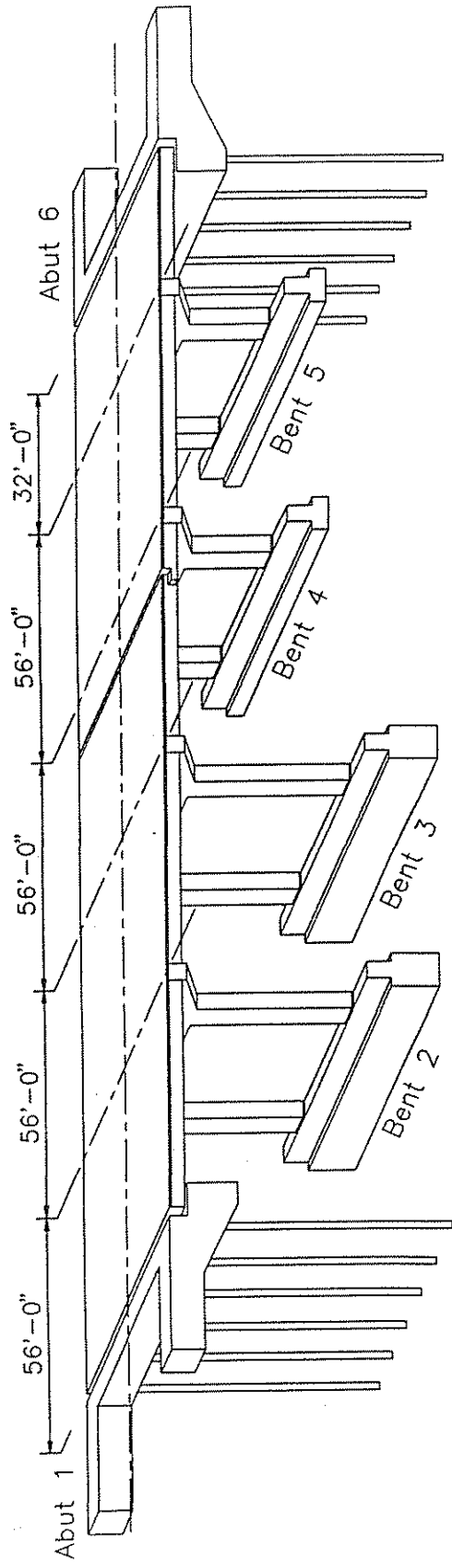


Figure 2-1 Schematic Drawing of the Aptos Creek Bridge.

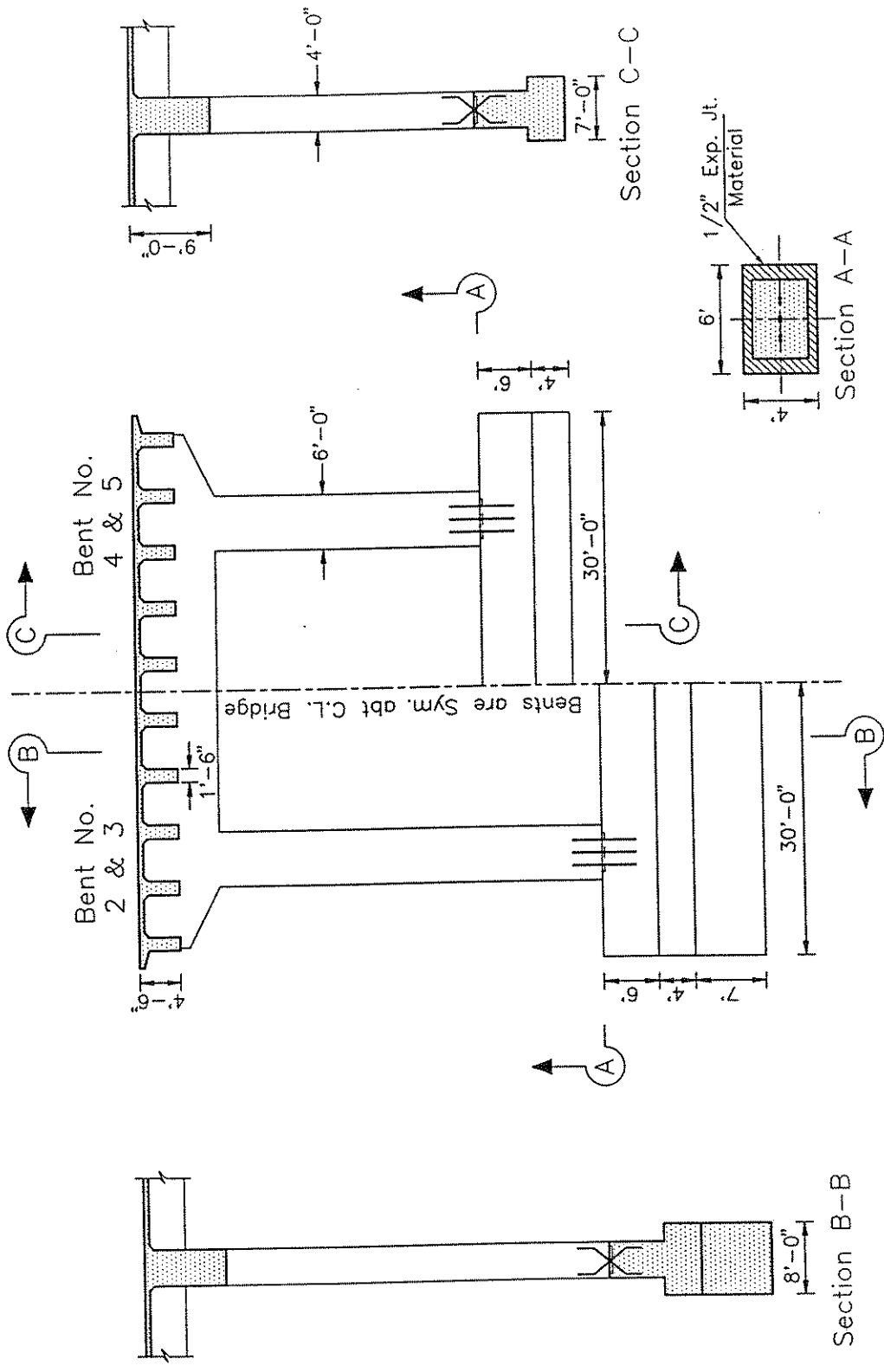


Figure 2-2 Typical Cross Section of the Bridge.

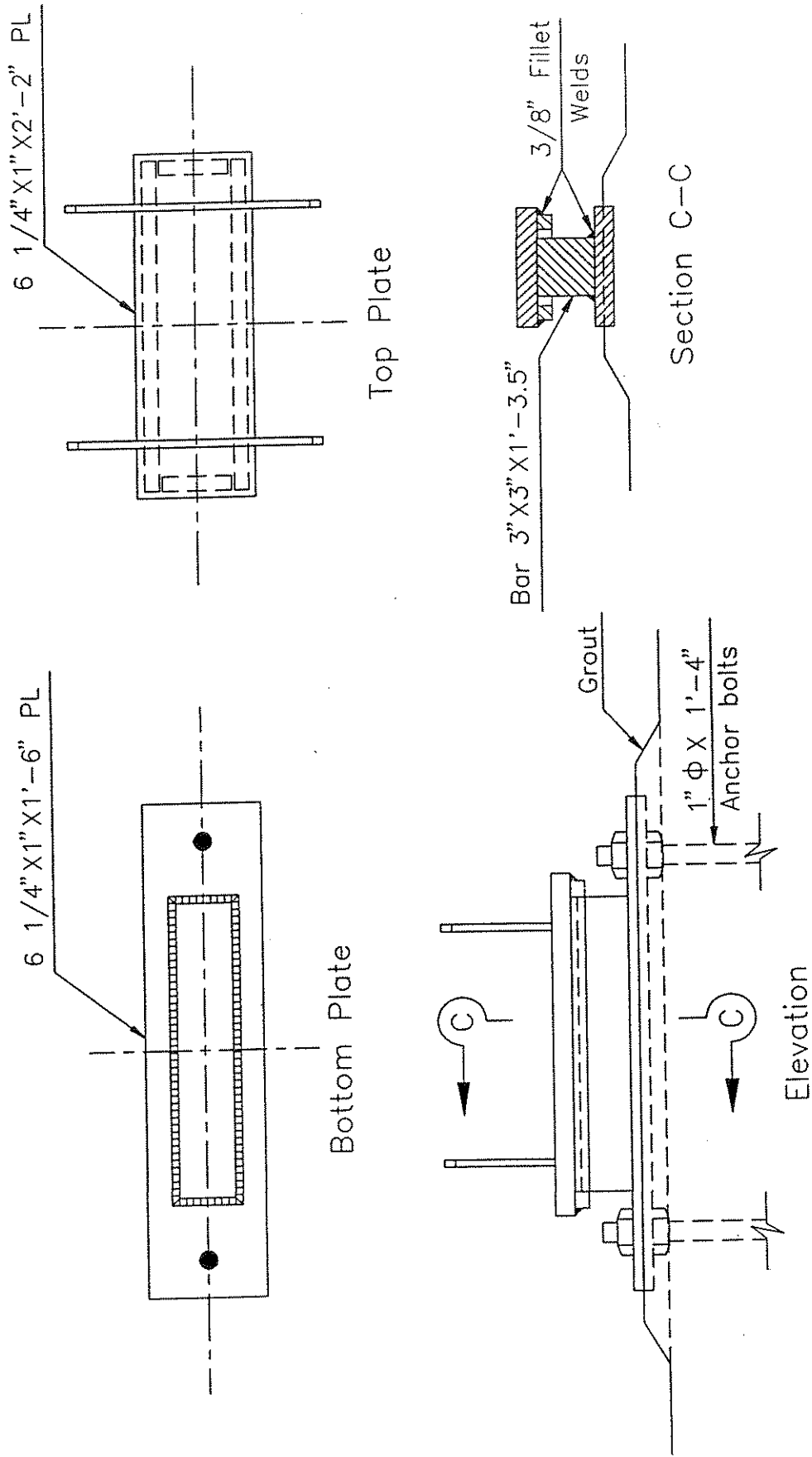
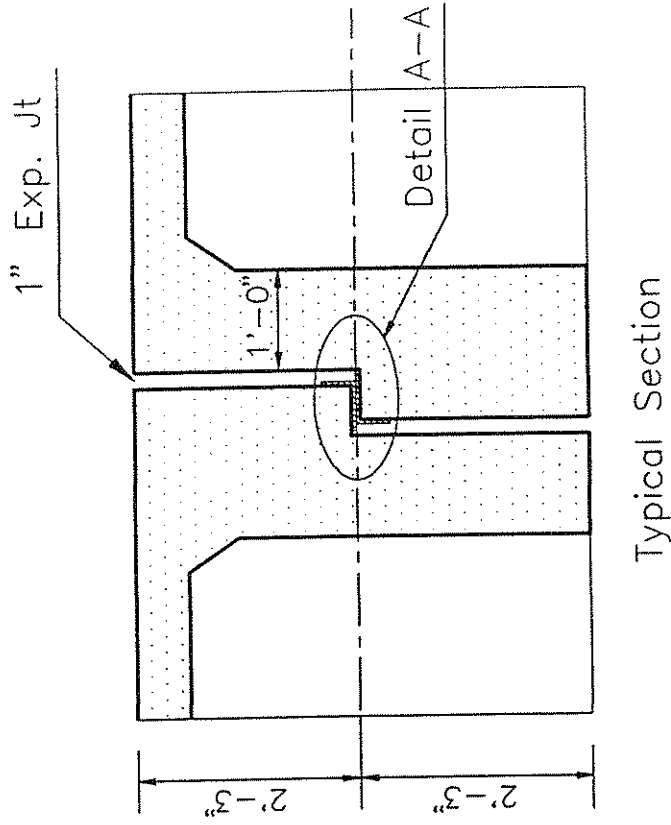
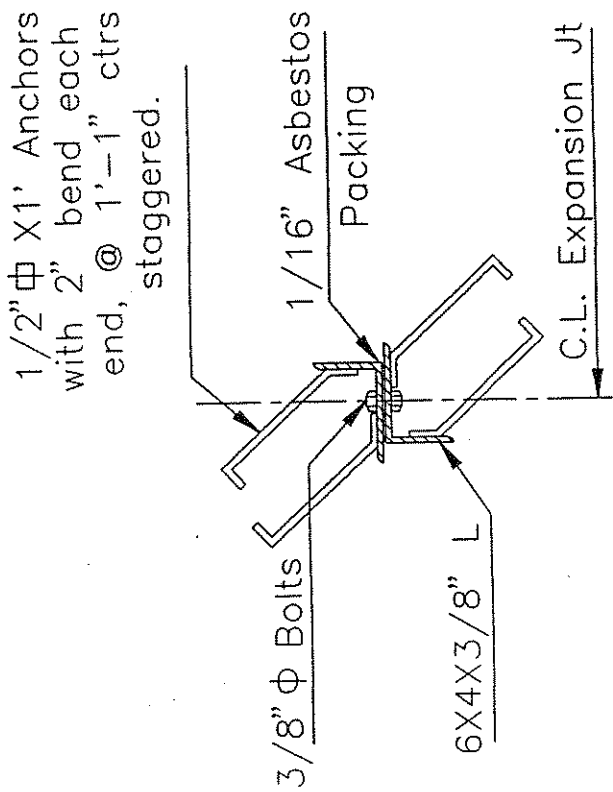


Figure 2-3 Fixed Bearing Assembly at both Abutments.

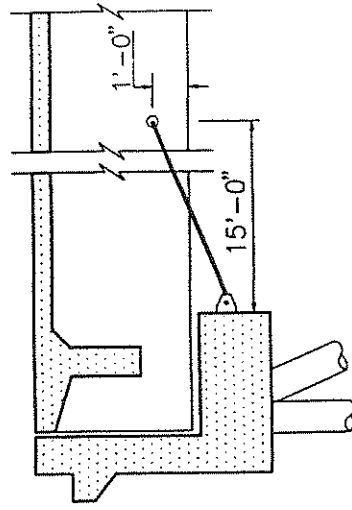
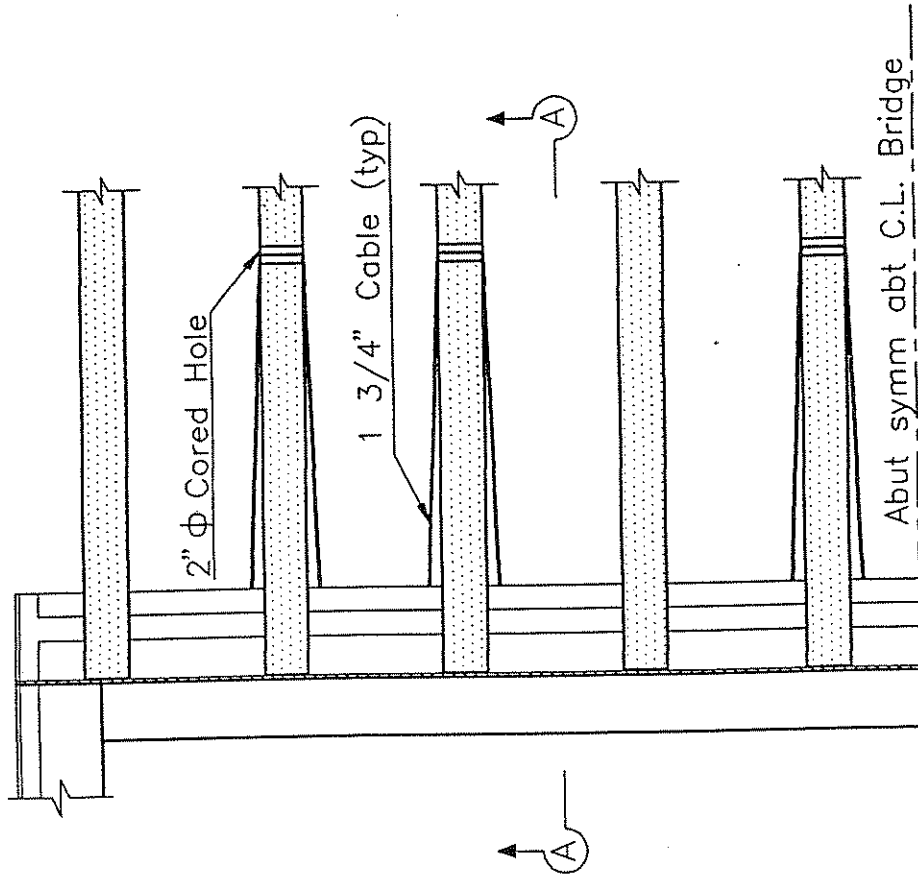


Typical Section



Section A-A

Figure 2-4 Details of the Middle Expansion Joint.



Section A-A

Figure 2-5 Details of the Retrofitting at the Abutments.

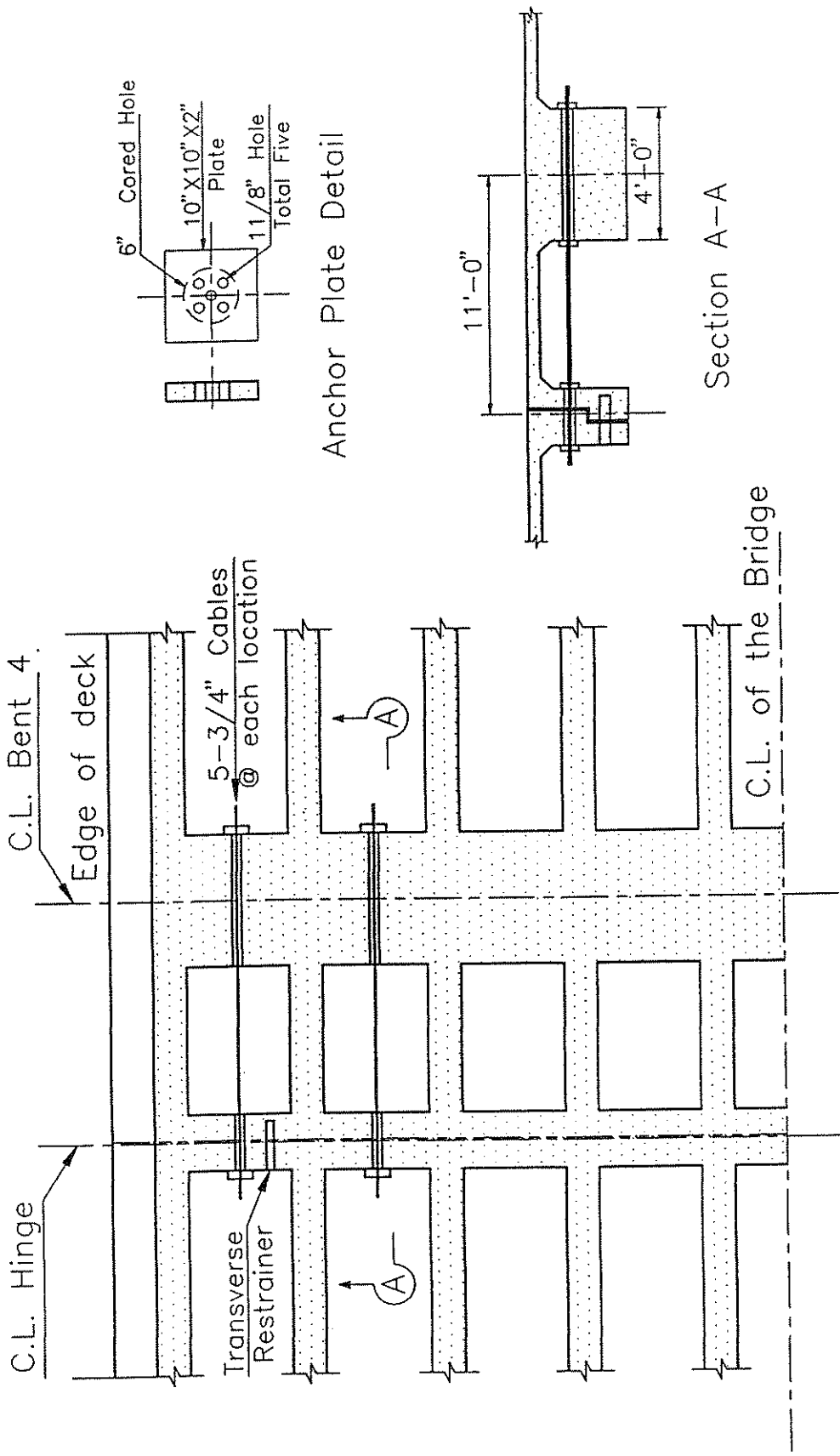


Figure 2-6 Details of the Retrofitting at the Middle Expansion Joint.

Span 3

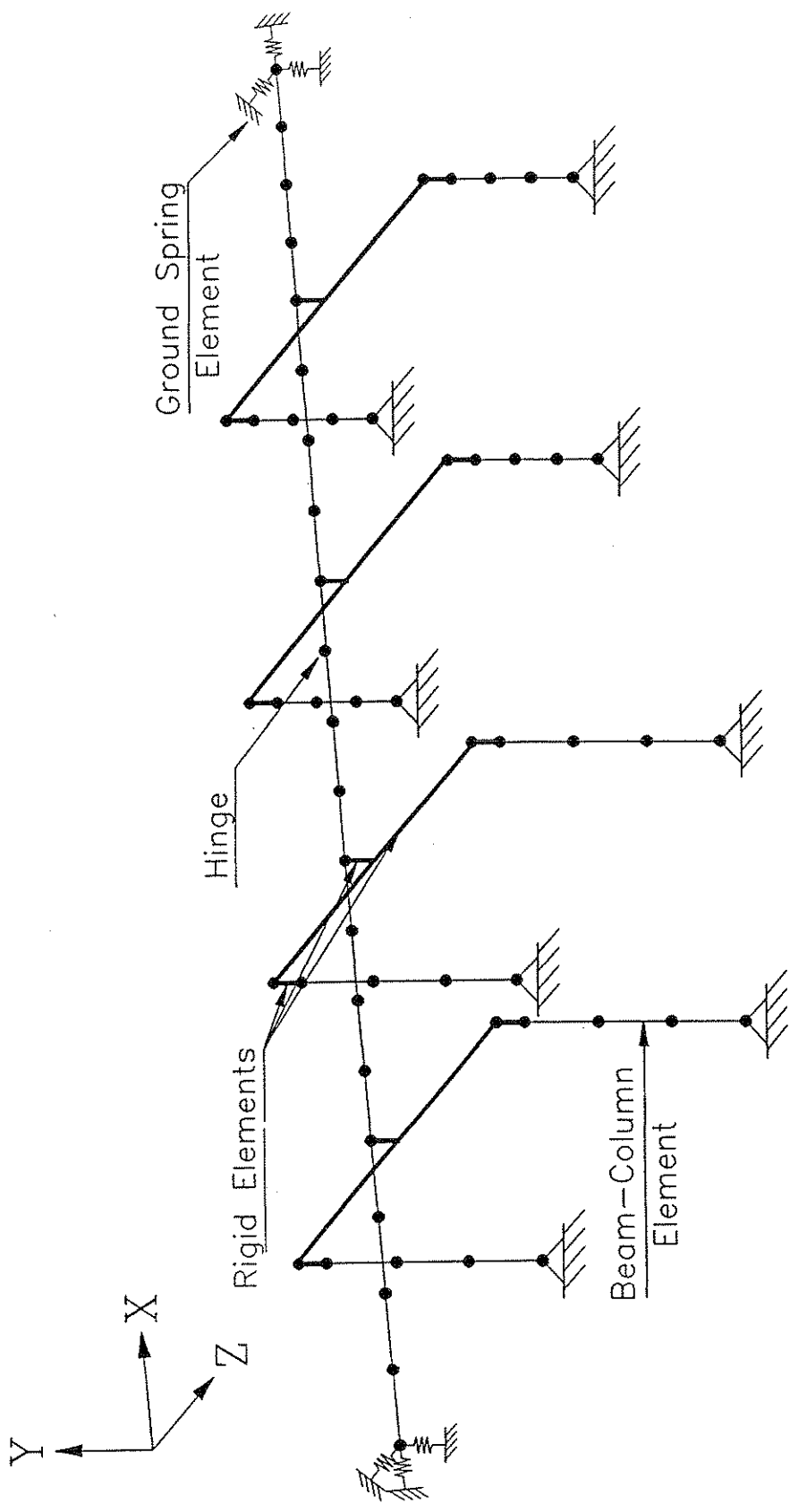


Figure 3-1 Idealization of the Lumped Mass, Linear Analytical Model.

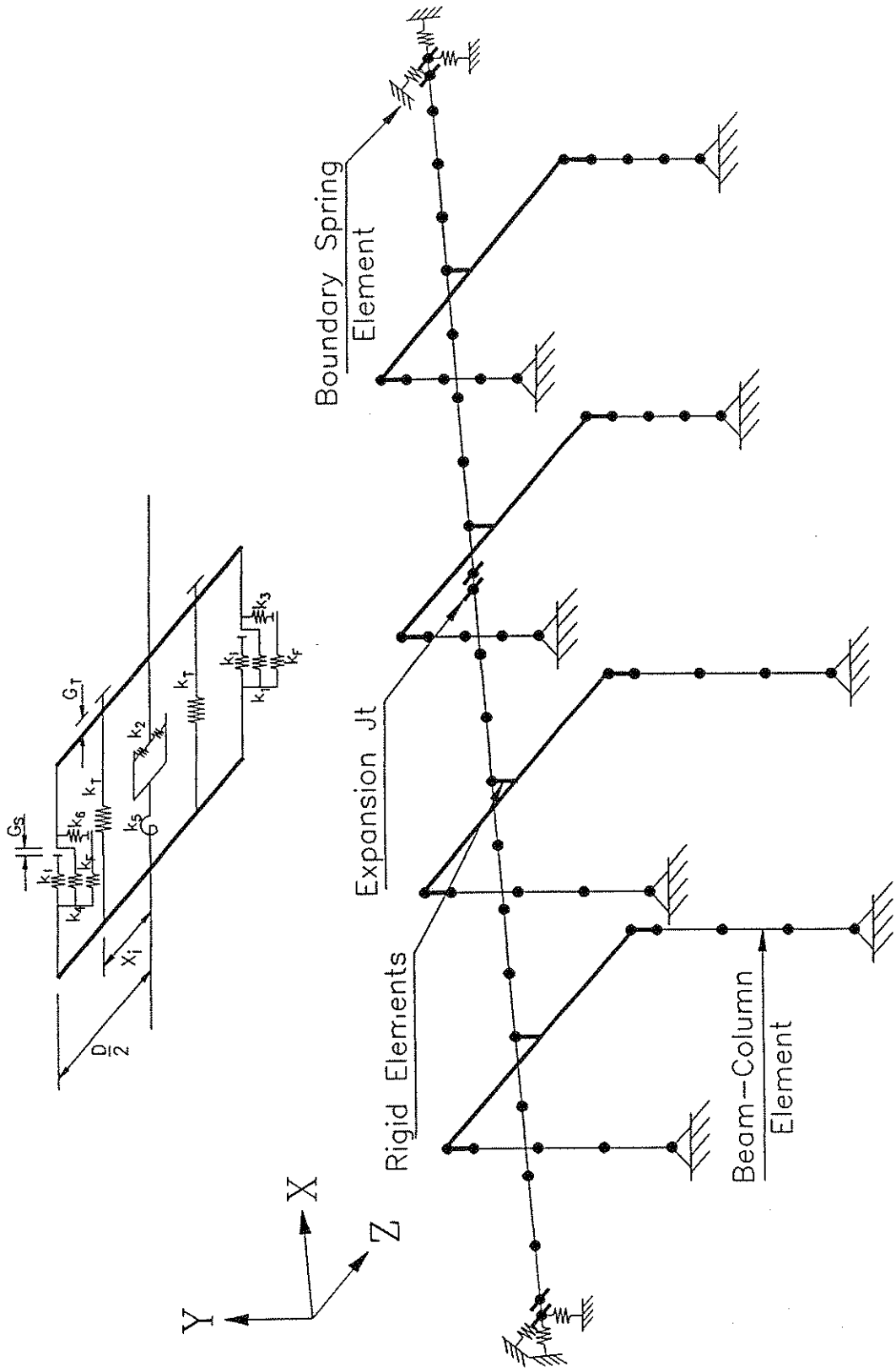
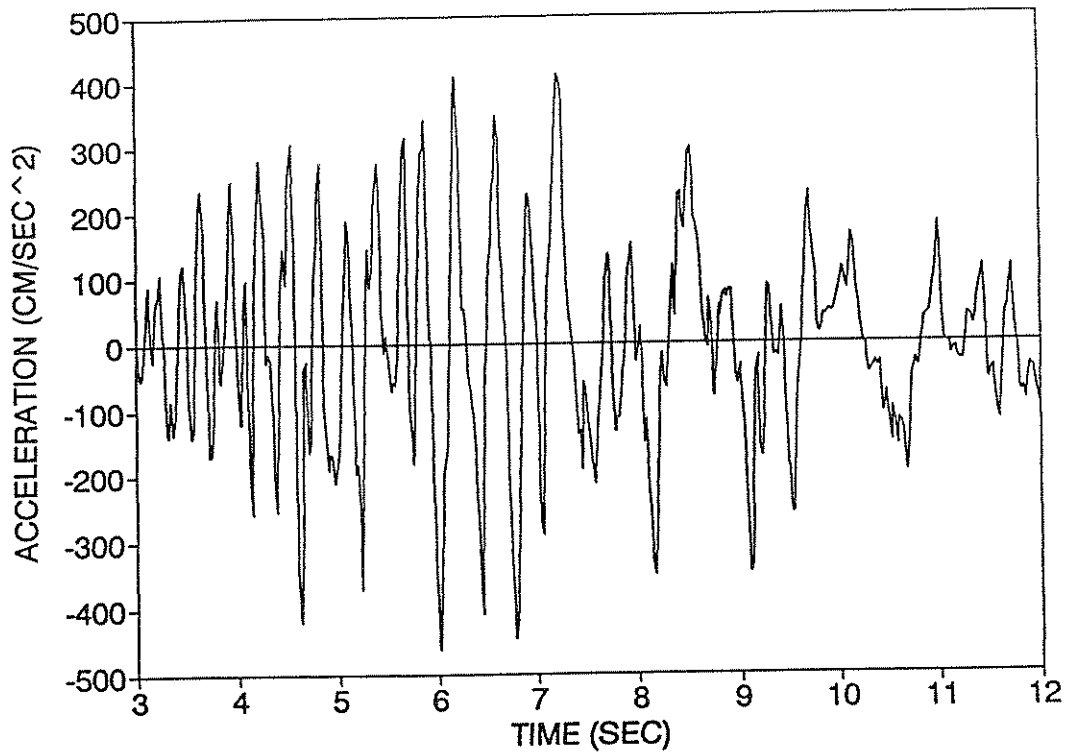
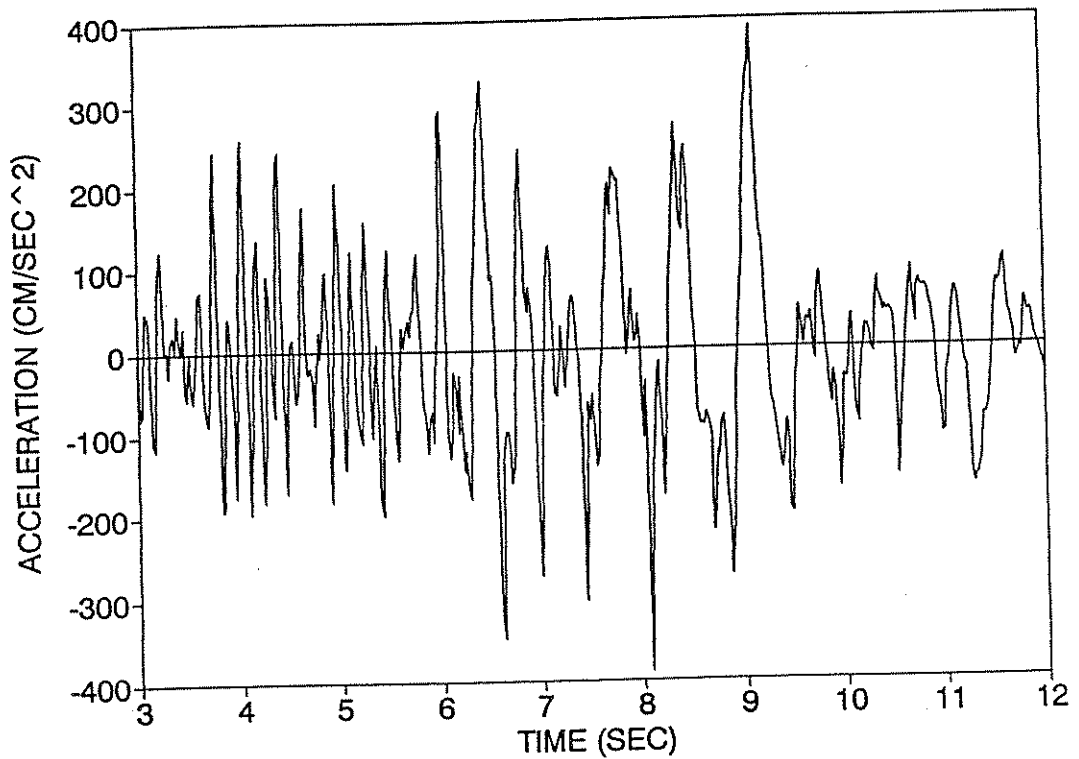


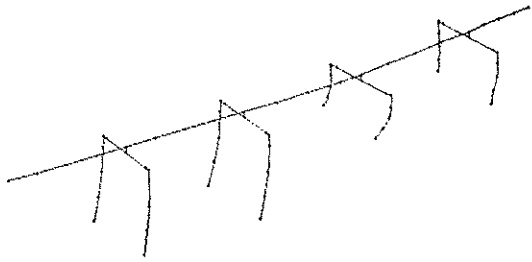
Figure 3-2 Idealization of the Lumped Mass, Nonlinear Analytical Model.



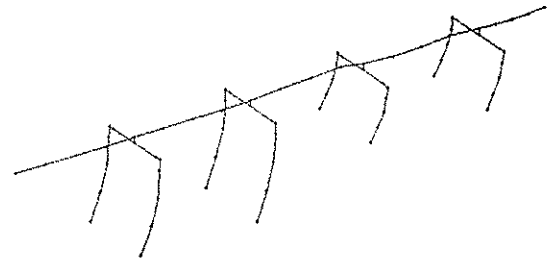
**Figure 3-3** Capitola Fire Station, Transverse Component ( Peak Acceleration =  $-462.922 \text{ cm/sec}^2$  at 6.02 sec ).



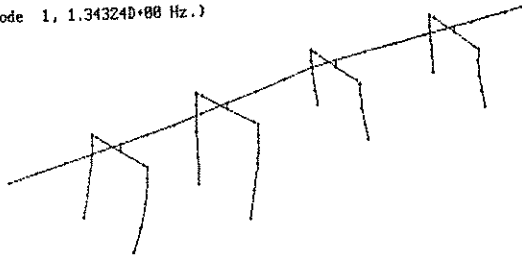
**Figure 3-4** Capitola Fire Station, Longitudinal Component ( Peak Acceleration =  $-390.792 \text{ cm/sec}^2$  at 8.08 sec ).



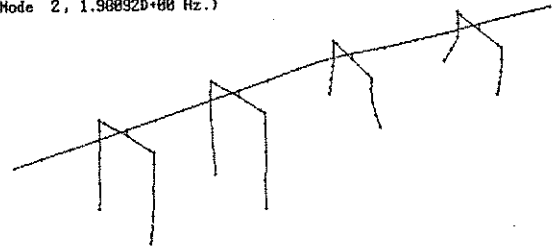
(Mode 1, 1.343240+00 Hz.)



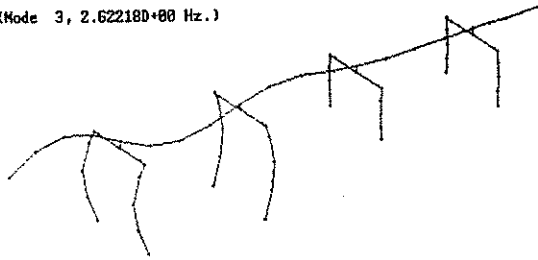
(Mode 2, 1.988920+00 Hz.)



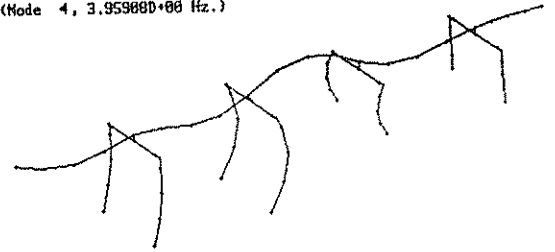
(Mode 3, 2.622180+00 Hz.)



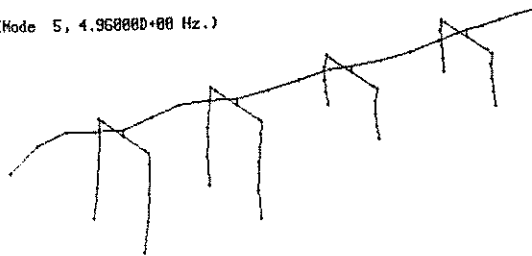
(Mode 4, 3.959880+00 Hz.)



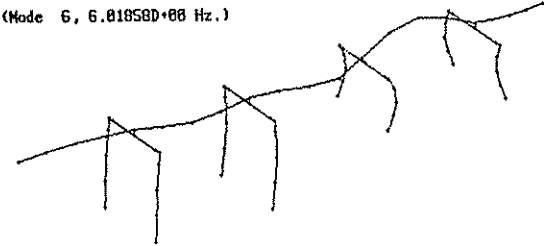
(Mode 5, 4.968880+00 Hz.)



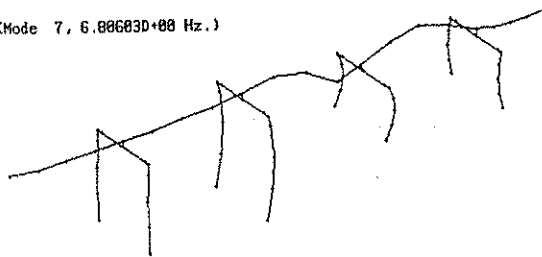
(Mode 6, 6.818580+00 Hz.)



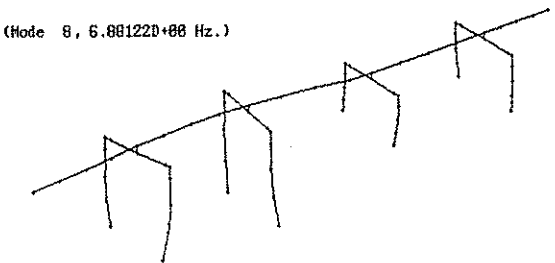
(Mode 7, 6.886830+00 Hz.)



(Mode 8, 8.881220+00 Hz.)



(Mode 9, 7.478210+00 Hz.)



(Mode 10, 8.428350+00 Hz.)

Figure 4-1 First Ten Mode Shapes for the Aptos Creek Bridge.

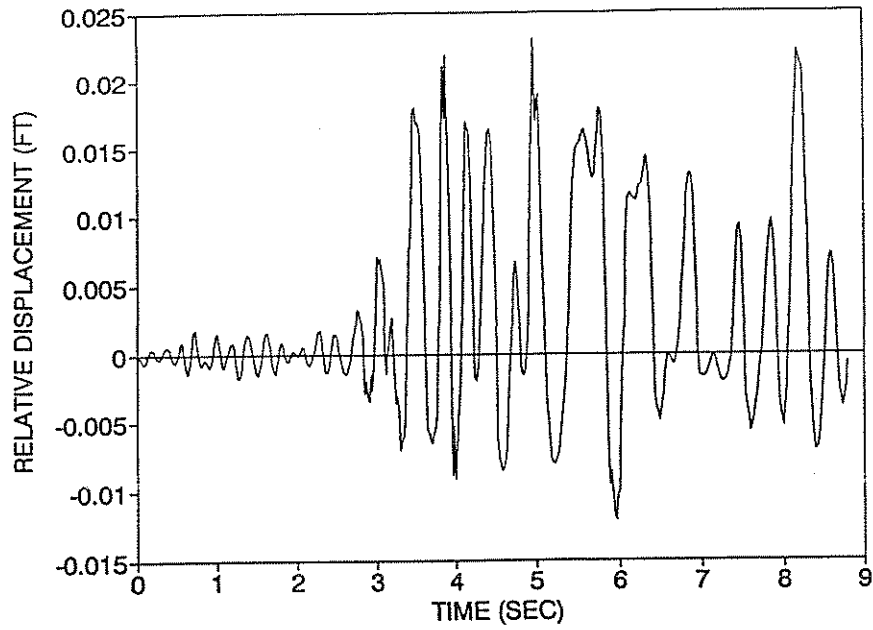


**Figure 4-2** Relative Displacement Response at Abutment 1 in the Long. Direction (0" TBG and 1" SG).

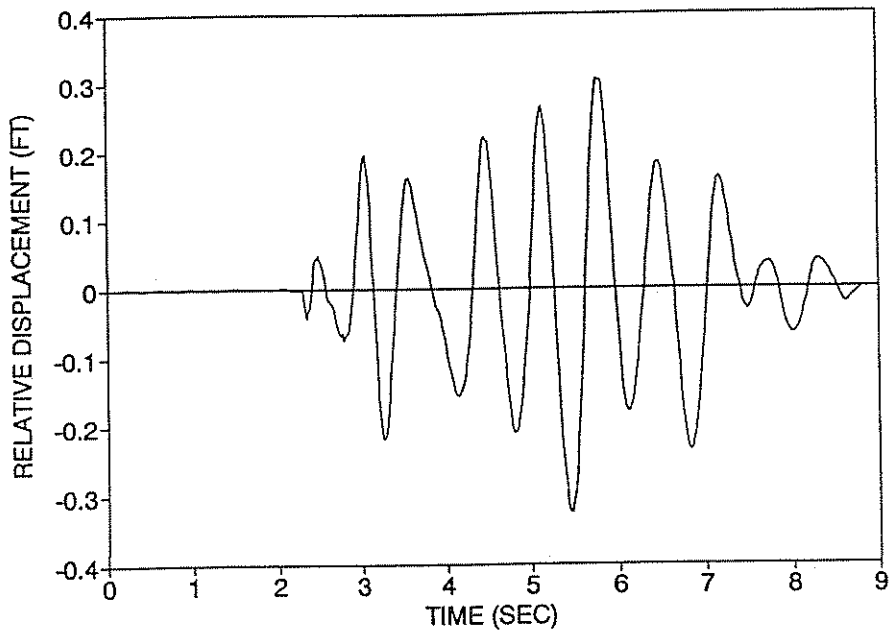


**Figure 4.3** Relative Displacement Response at Abutment 1 in the Trans. Direction (0" TBG and 1" SG).

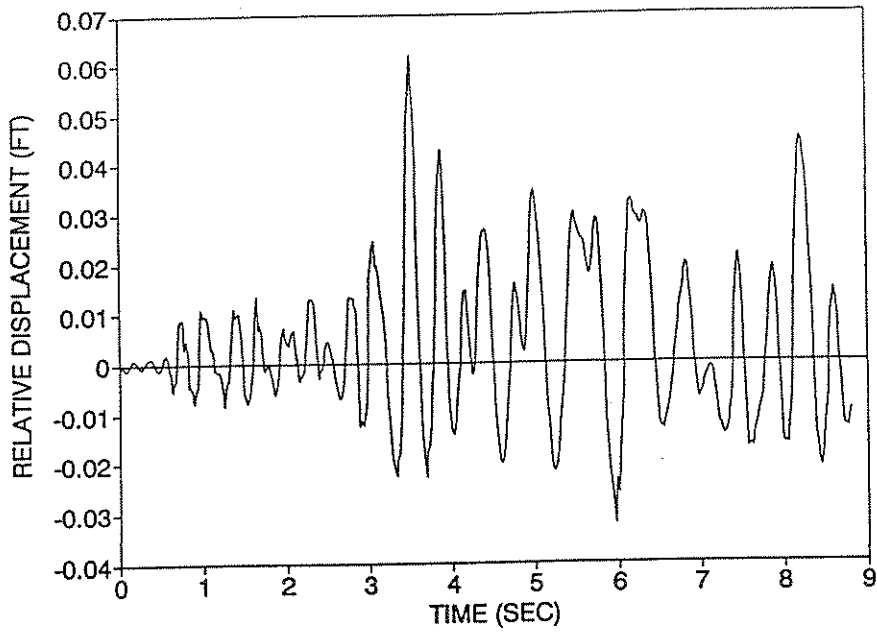


**Figure 4.4** Relative Displacement Response at Abutment 1 in the Long. Direction (0" TBG and 1" SG), Motion Normalized to 0.7g.

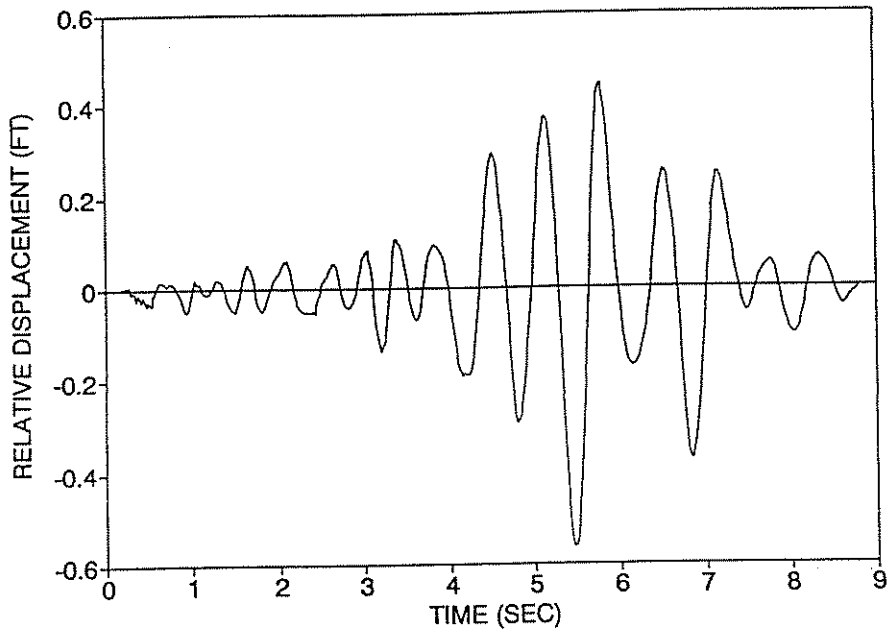


**Figure 4-5** Relative Displacement Response at Abutment 1 in the Trans. Direction (0" TBG and 1" SG), Motion Normalized to 0.7g.

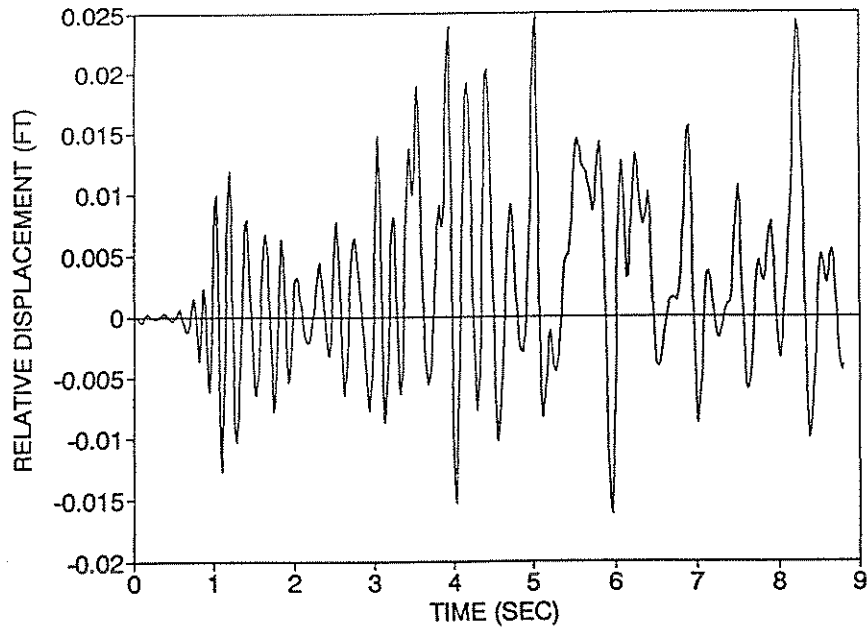


**Figure 4-6** Relative Displacement Response at the Mid. Exp. Jt. in the Long. Dir. (0" TBG and 1" SG).

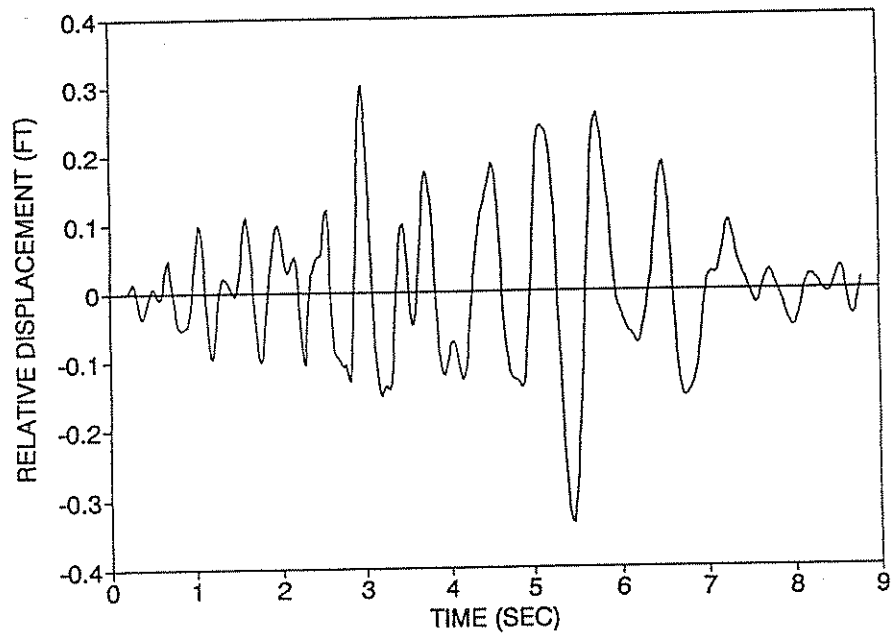


**Figure 4-7** Relative Displacement Response at the Mid. Exp. Jt. in the Trans. Dir. (0" TBG and 1" SG).

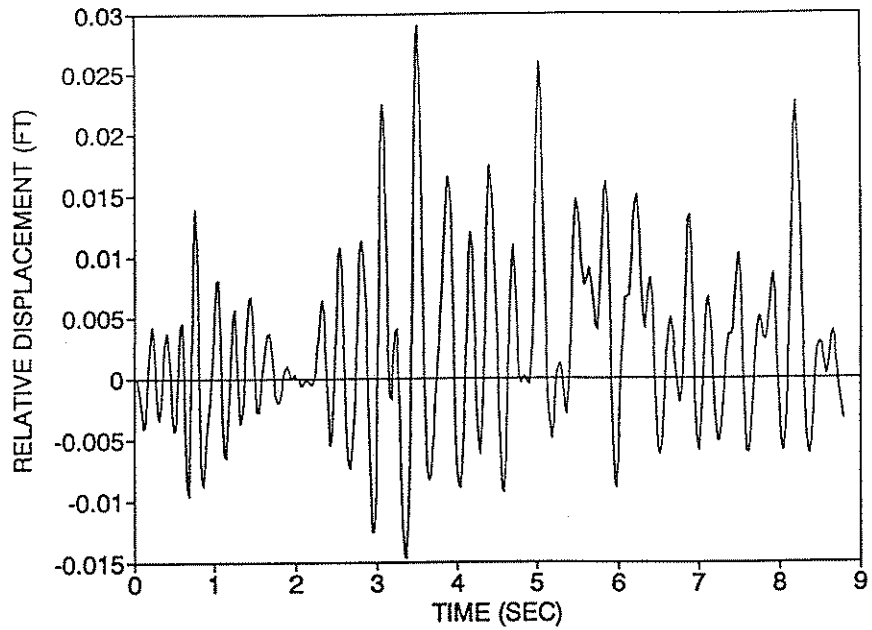


**Figure 4-8** Relative Displacement Response at the Mid. Exp. Jt. in the Long. Dir. (0" TBG, 1" SG, and W/O Shear Bolts).

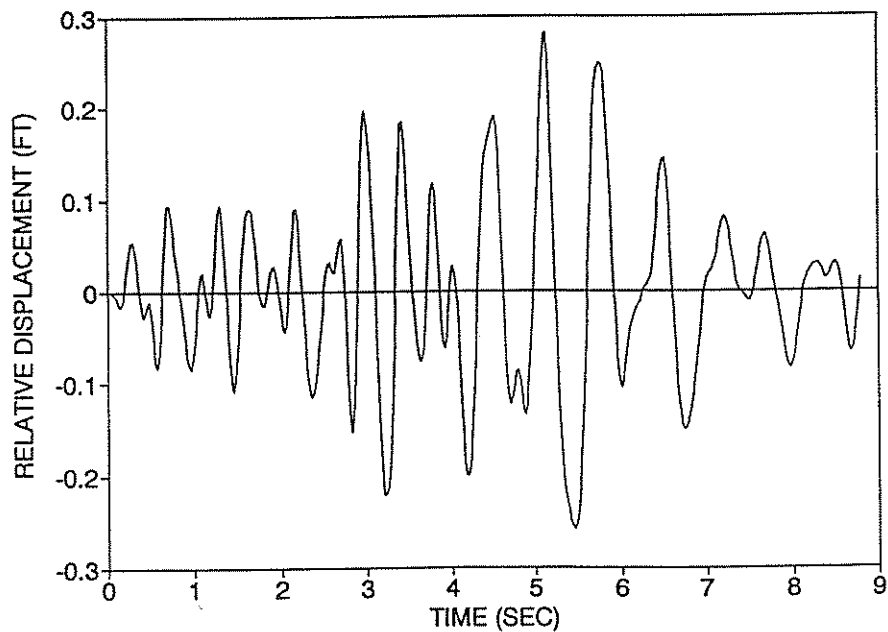


**Figure 4-9** Relative Displacement Response at the Mid. Exp. Jt. in the Trans. Dir. (0" TBG, 1" SG, and W/O Shear Bolts).

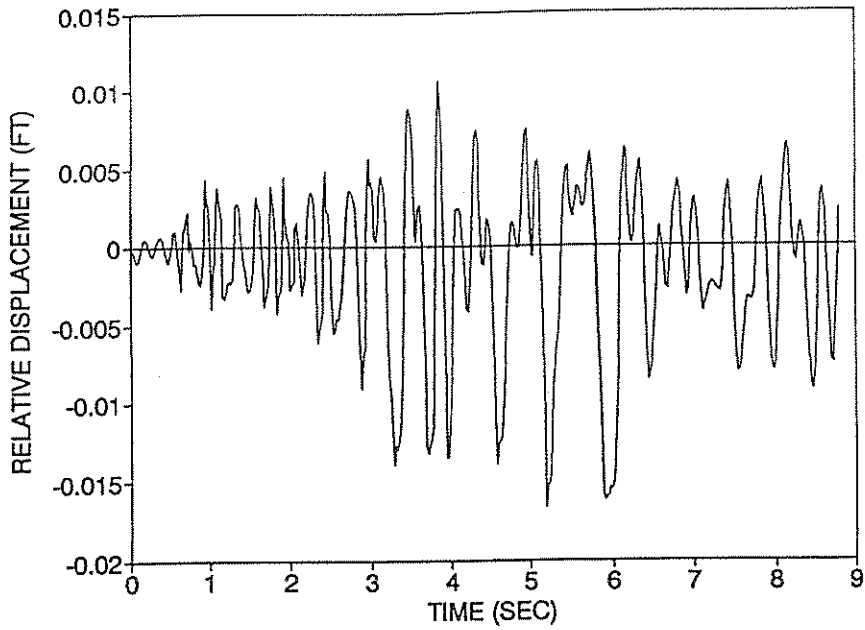


**Figure 4-10** Relative Displacement Response at Abutment 6 in the Long. Dir. (0" TBG and 1" SG).

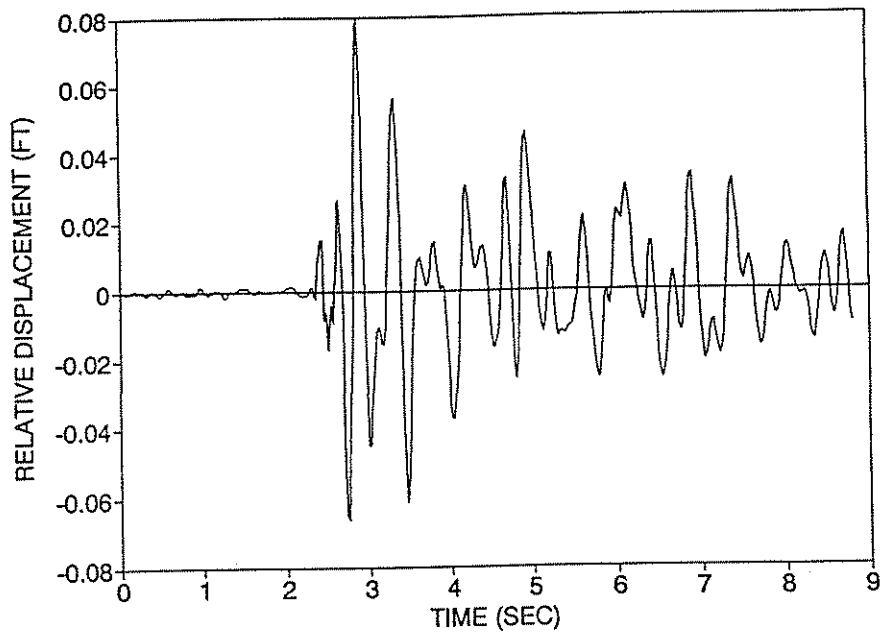


**Figure 4-11** Relative Displacement Response at Abutment 6 in the Trans. Dir. (0" TBG and 1" SG).

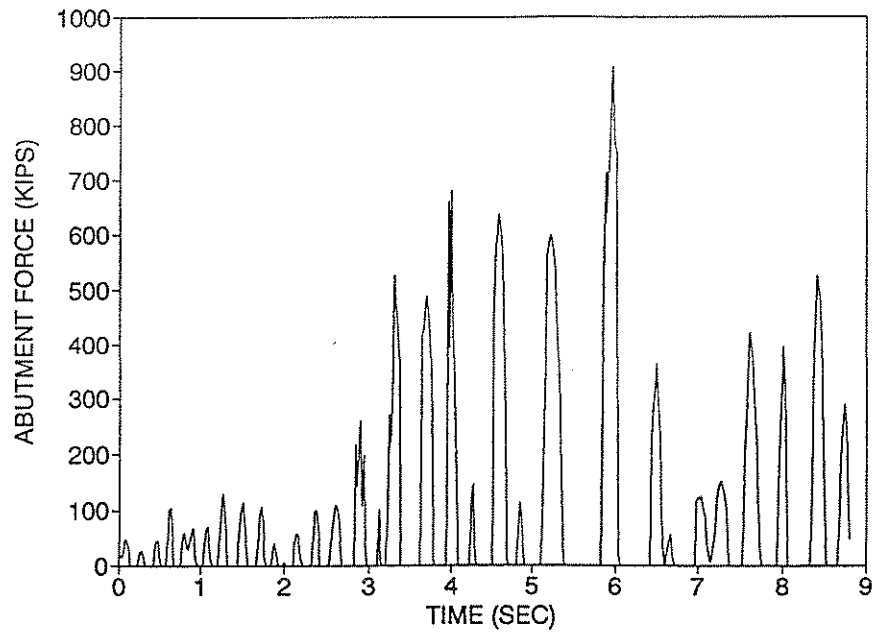


Figure 4-12 Abutment Force Response at Abutment 1 (0" TBG and 1" SG).

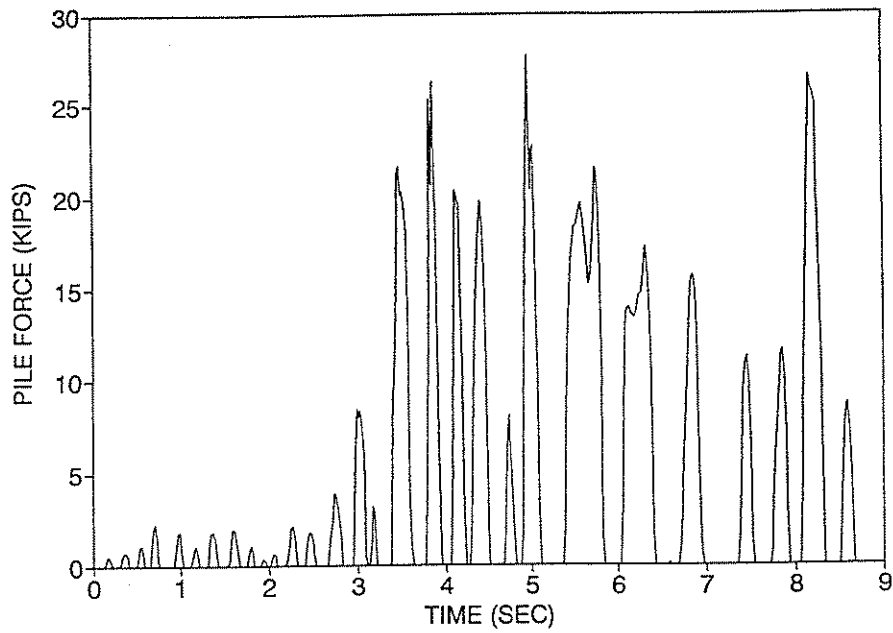
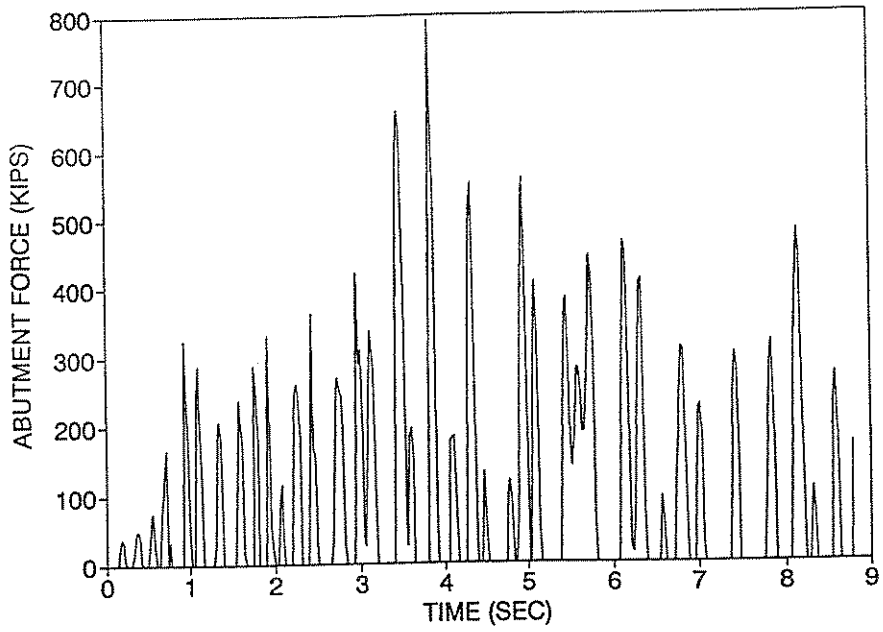
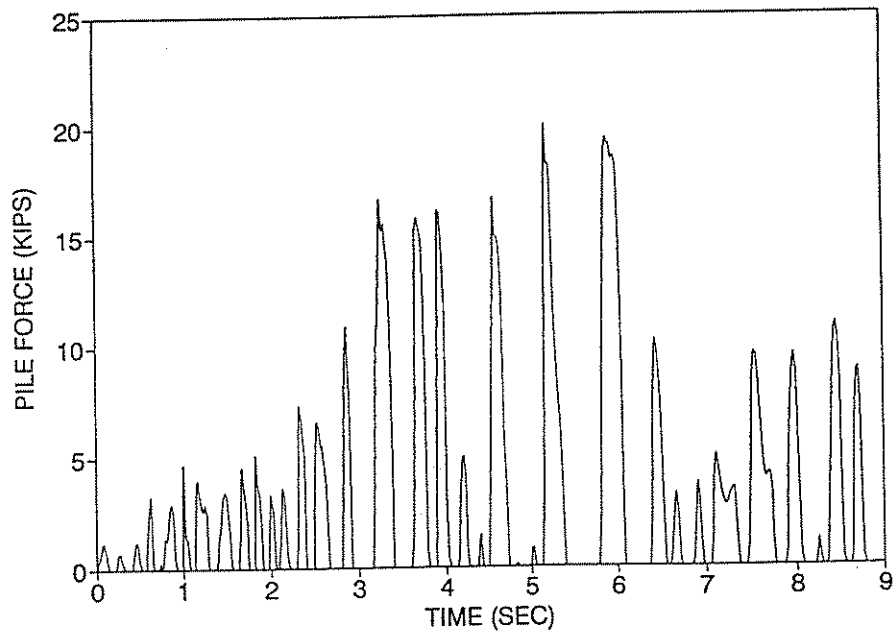


Figure 4-13 Pile Force Response at Abutment 1 (0" TBG and 1" SG).



**Figure 4-14** Abutment Force Response at Abutment 6 (0" TBG and 1" SG).



**Figure 4-15** Pile Force Response at Abutment 6 (0" TBG and 1" SG).

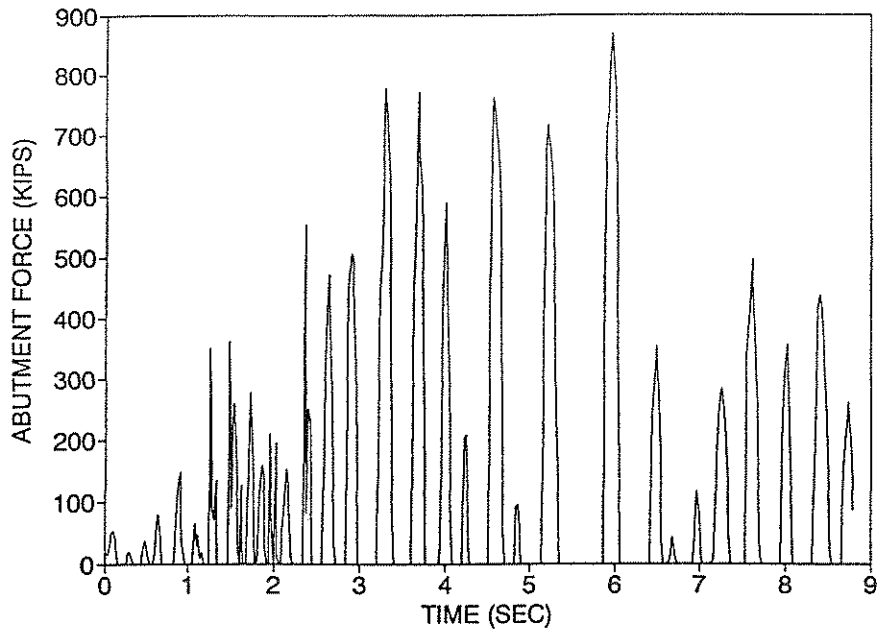


**Figure 4-16** Abutment Force Response at Abutment 1 (0" TBG, 1" SG, and W/O Shear Bolts).

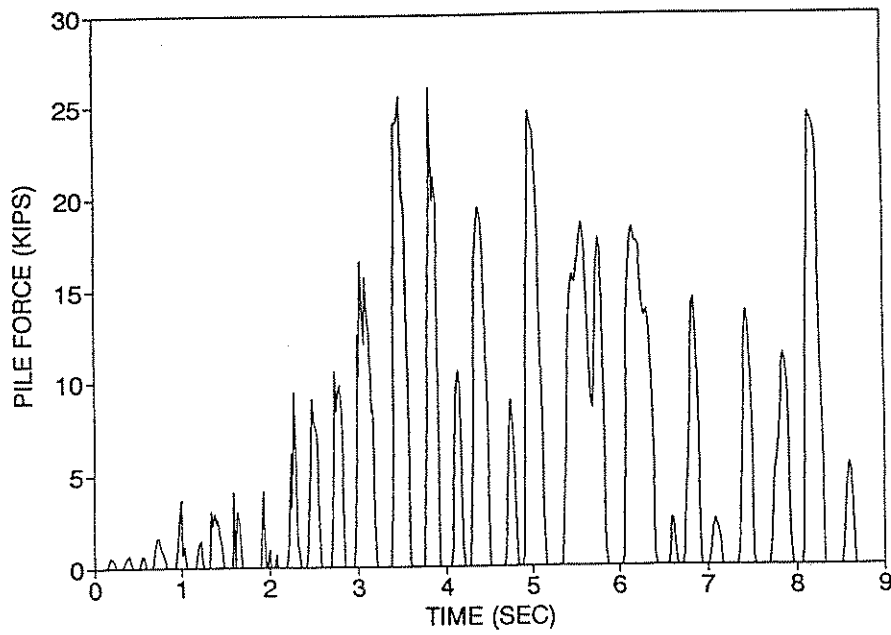


**Figure 4-17** Pile Force Response at Abutment 1 (0" TBG, 1" SG, and W/O Shear Bolts).

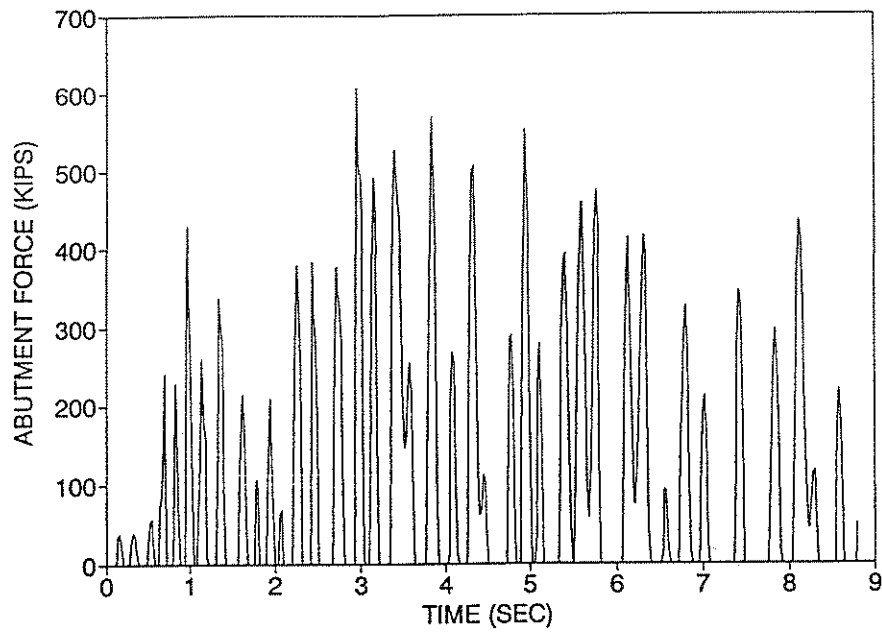


**Figure 4-18** Abutment Force Response at Abutment 6 (0" TBG, 1" SG, and Shear Bolts).

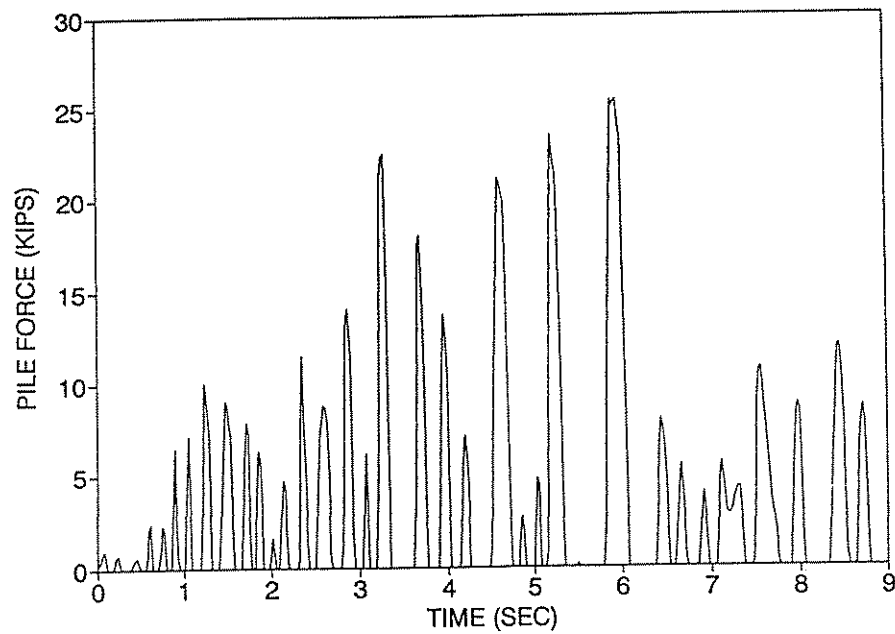


**Figure 4-19** Pile Force Response at Abutment 6 (0" TBG, 1" SG, and W/O Shear Bolts).

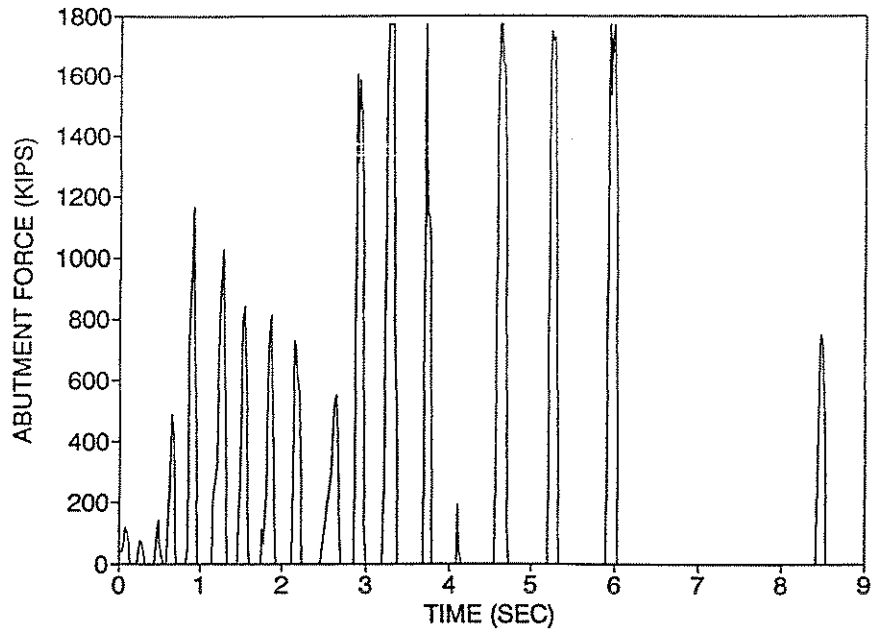


**Figure 4-20** Abutment Force Response at Abutment 1 (W/O Cables and 1" SG), Motion Normalized to 1.0 g.

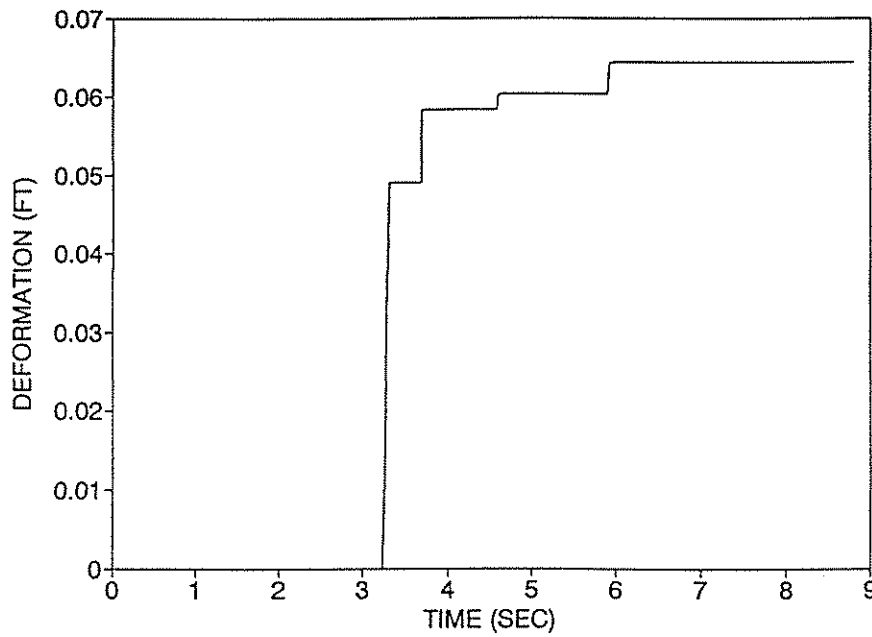


**Figure 4-21** Nonlinear Deformation of Abutment 1 (W/O Cables and 1" SG), Motion Normalized to 1.0 g.

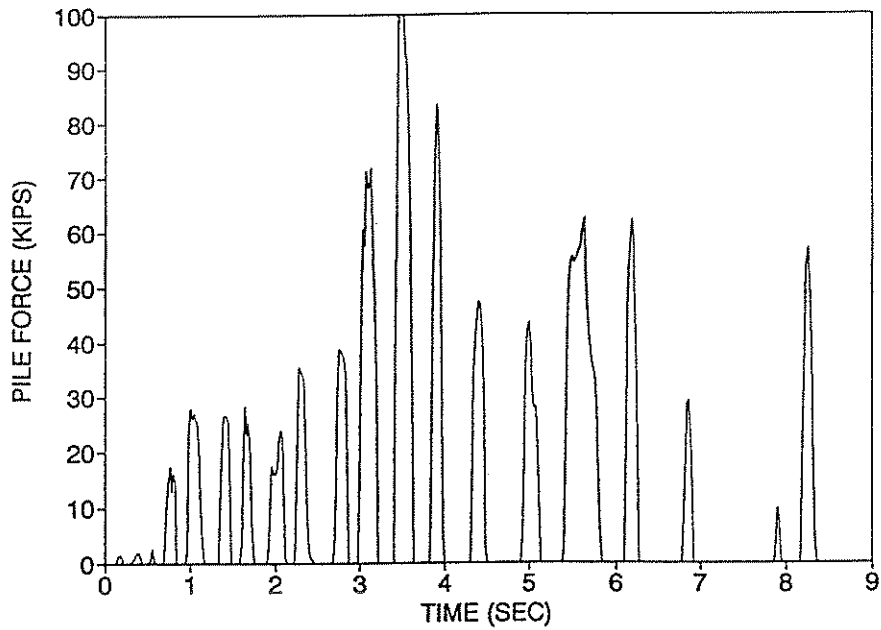


**Figure 4-22** Pile Force Response at Abutment 1 (W/O Cables and 1" SG), Motion Normalized to 1.0 g.

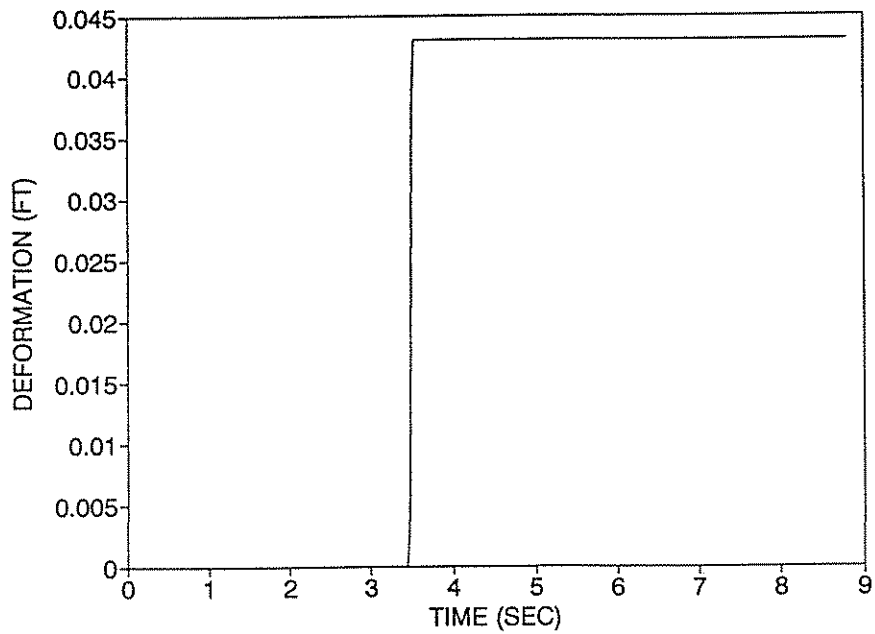


**Figure 4-23** Nonlinear Deformation of Piles (W/O Cables and 1" SG), Motion Normalized to 1.0 g.

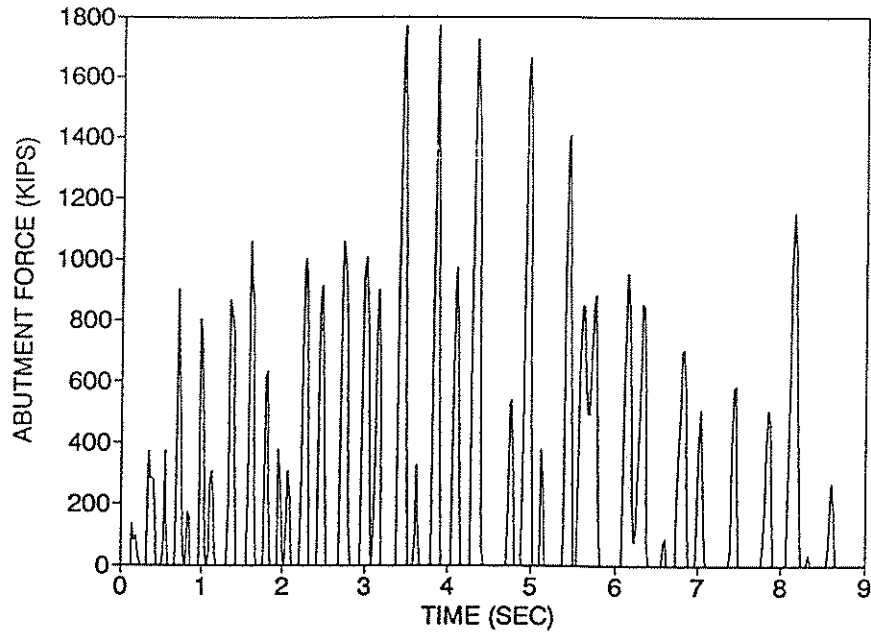


**Figure 4-24** Abutment Force Response at Abutment 6 (W/O Cables and 1" SG), Motion Normalized to 1.0 g.

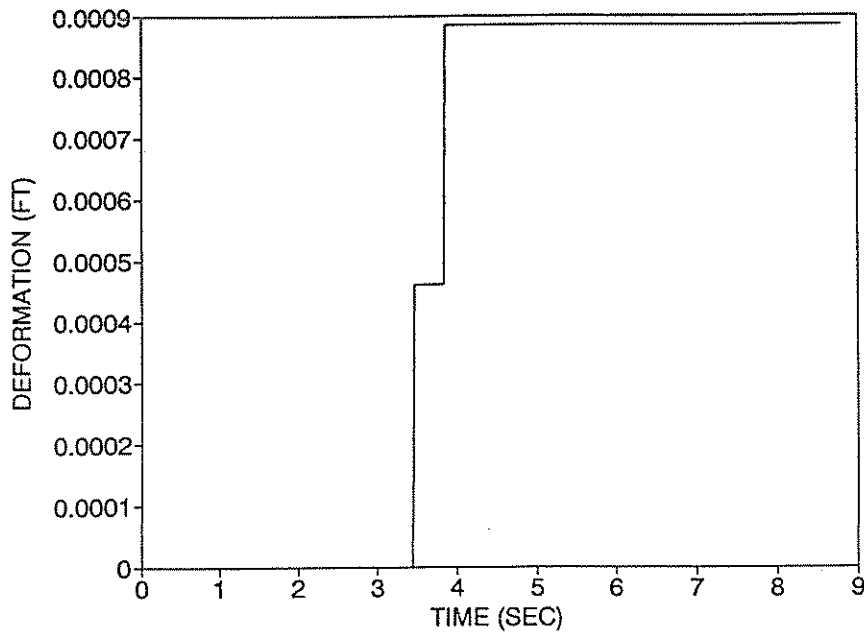


**Figure 4-25** Nonlinear Deformation of Abutment 6 (W/O Cables and 1" SG), Motion Normalized to 1.0 g.

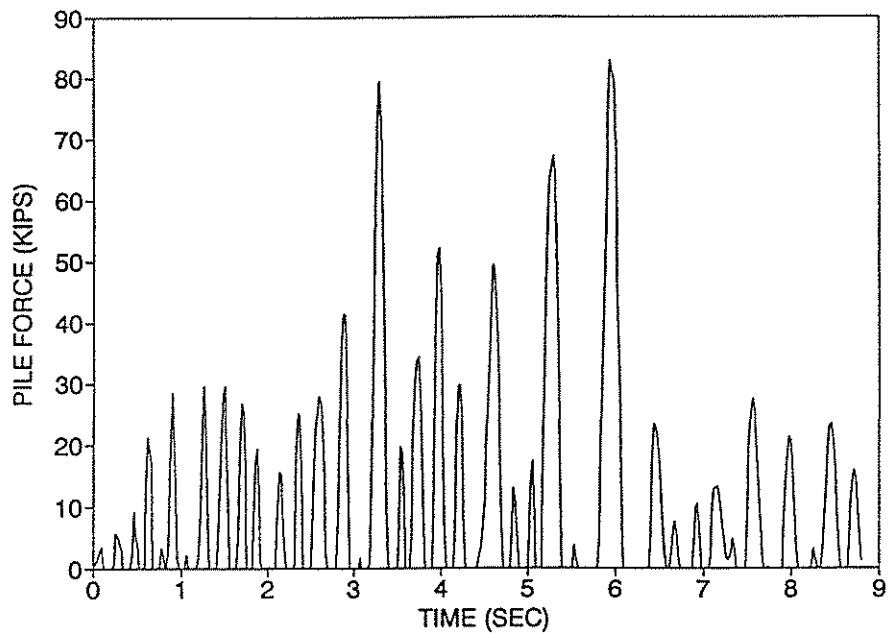


**Figure 4-26** Pile Force Response at Abutment 6 (W/O Cables and 1" SG), Motion Normalized to 1.0 g.

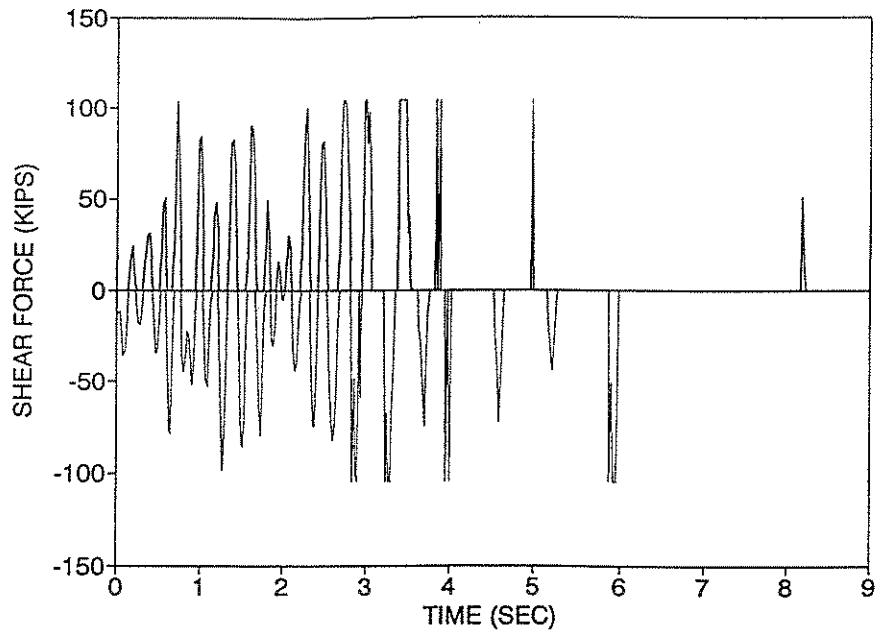


**Figure 4-27** Shear Force Response of the Bearing Bars at Abutment 1 in the Long. Dir. (0" TBG and 1" SG).

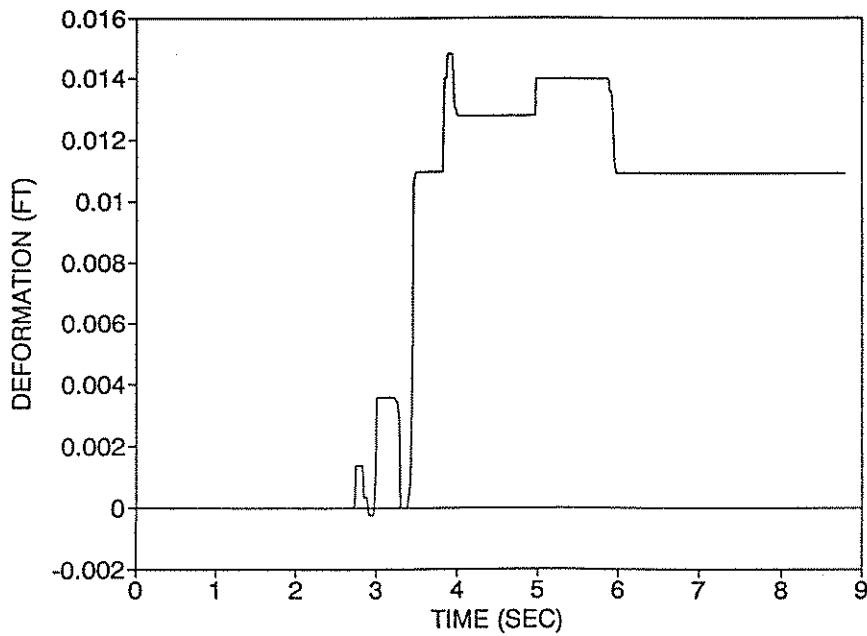


**Figure 4-28** Nonlinear Deformation Response of the Bearing Bars in the Long. Dir. (0" TBG and 1" SG).

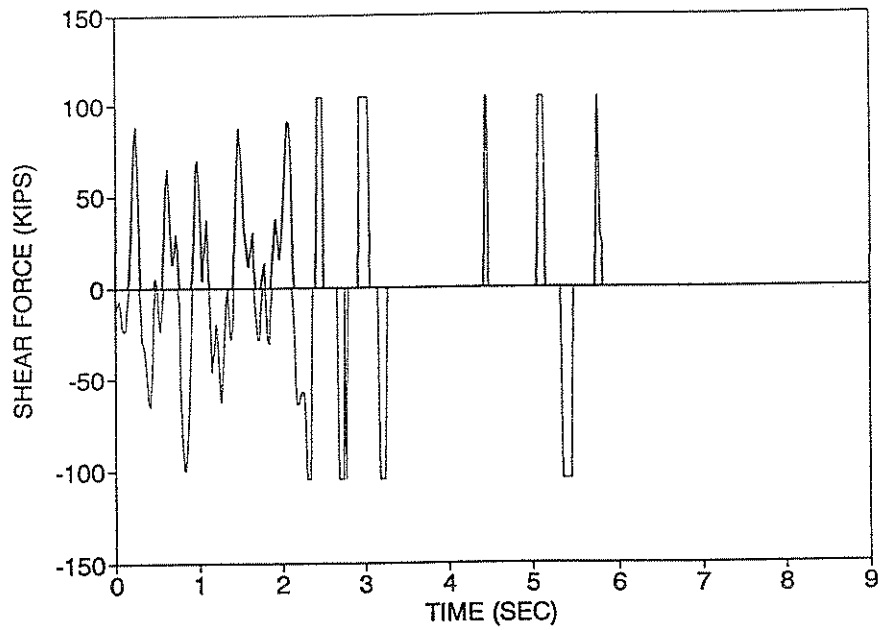


**Figure 4-29** Shear Force Response of the Bearing Bars at Abutment 1 in the Trans. Dir. (0" TBG and 1" SG).

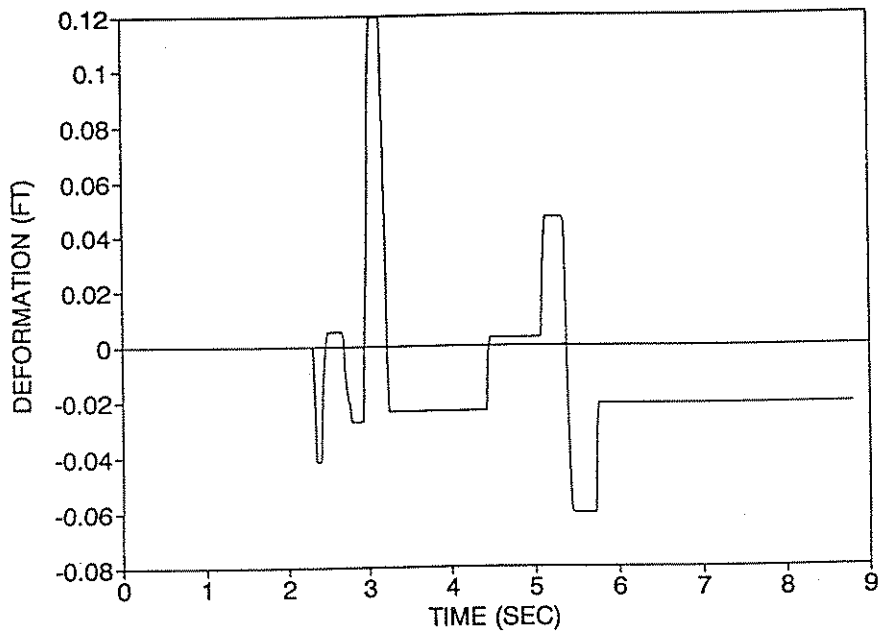


**Figure 4-30** Nonlinear Deformation Response of the Bearing Bars at Abutment 1 in the Trans. Dir. (0" TBG and 1" SG).

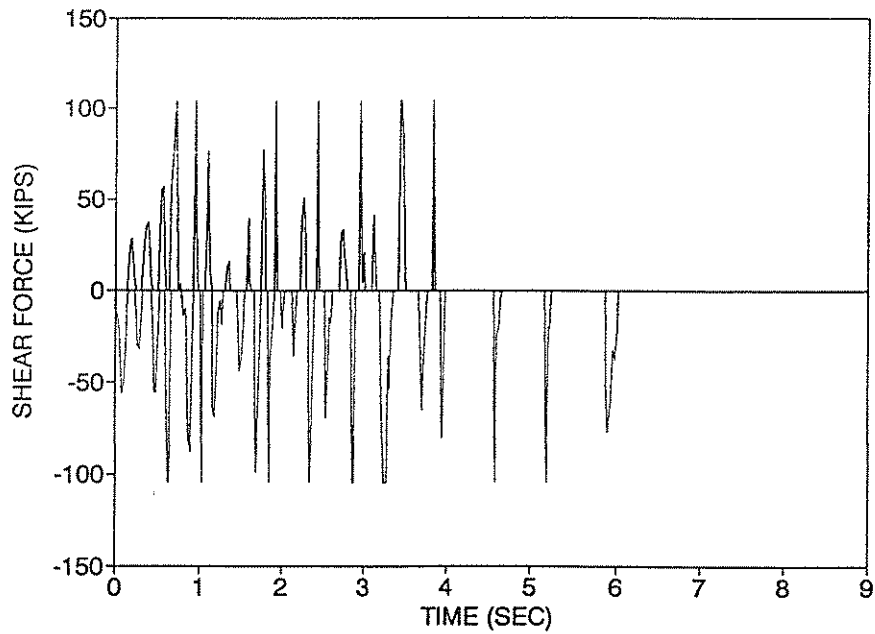


**Figure 4-31 Shear Force Response of the Bearing Bars at Abutment 6 in the Long. Dir. (0" TBG and 1" SG).**

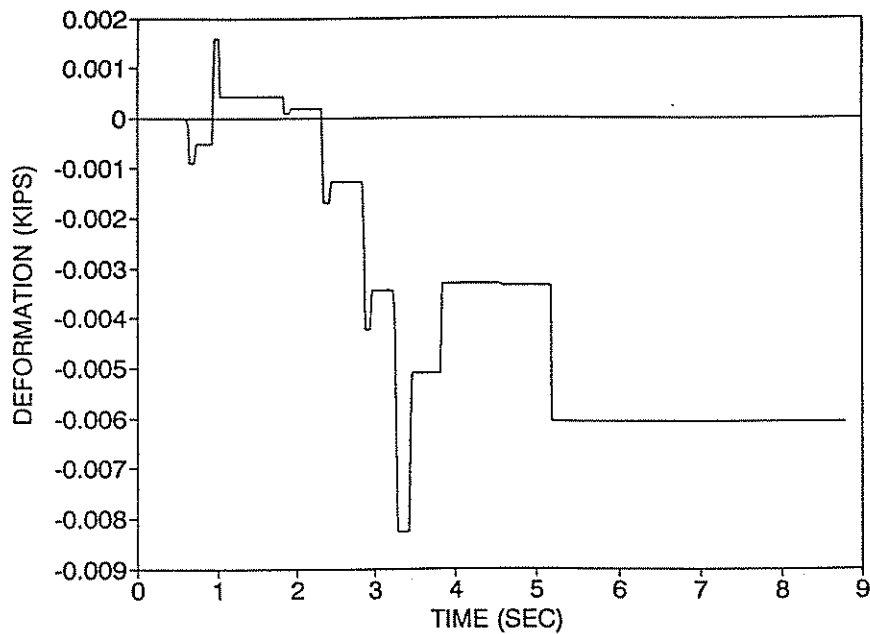


**Figure 4-32 Nonlinear Deformation Response of the Bearing Bars at Abutment 6 in the Long. Dir. (0" TBG and 1" SG).**

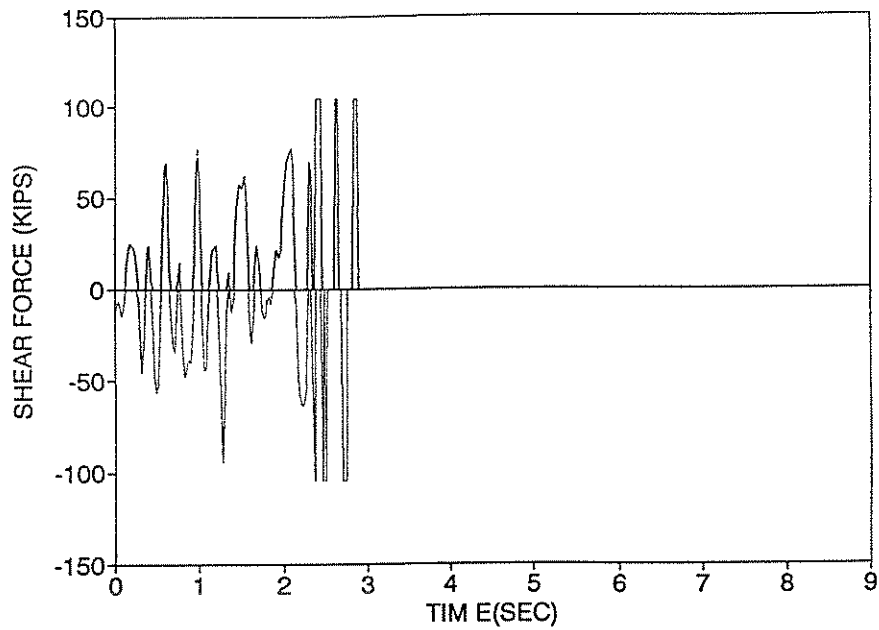


**Figure 4-33** Shear Force Response of the Bearing Bars at Abutment 6 in the Trans. Dir. (0" TBG and 1" SG).

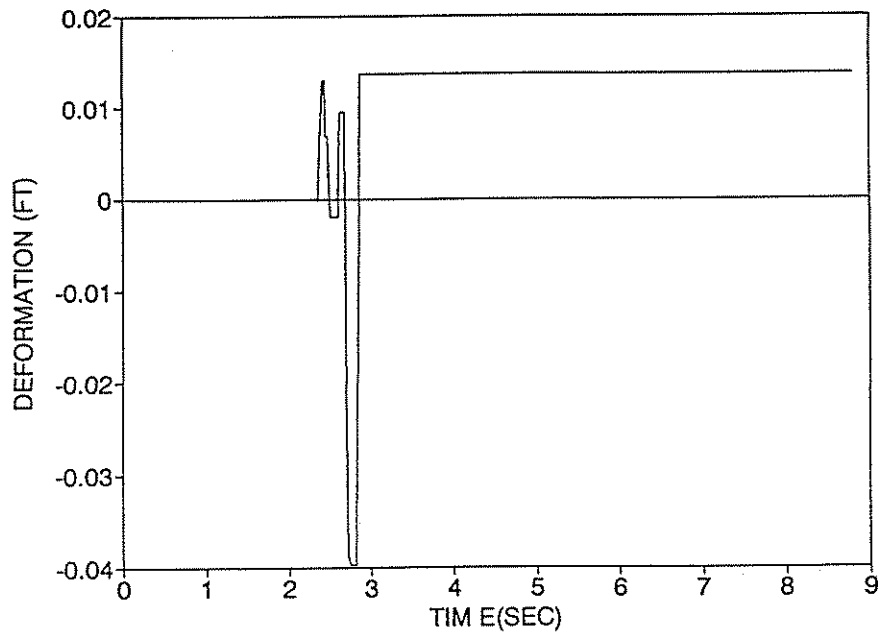


**Figure 4-34** Nonlinear Deformation Response of the Bearing Bars at Abutment 6 in the Trans. Dir. (0" TBG and 1" SG).

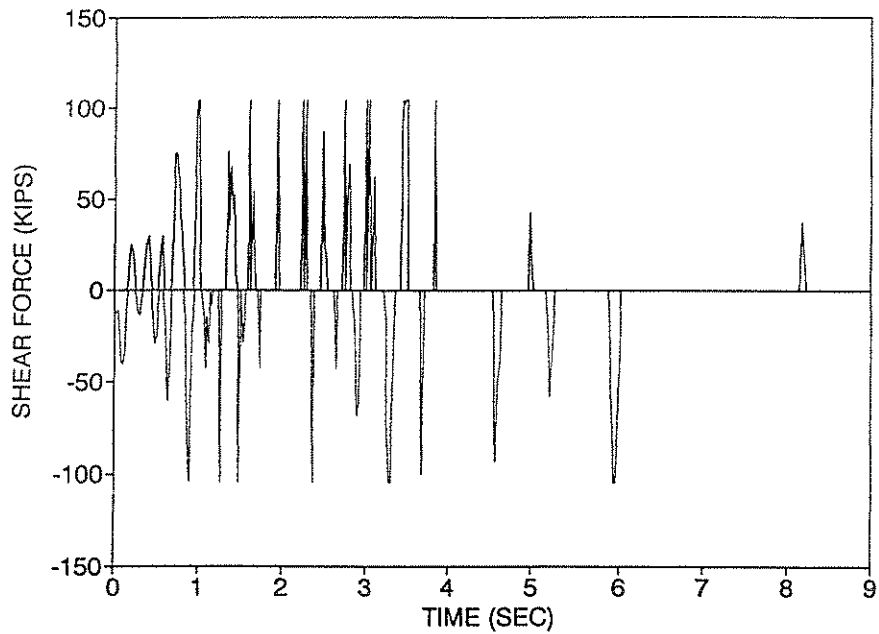


**Figure 4-35** Shear Force Response of the Bearing Bars at Abutment 1 in the Long. Dir. (0" TBG, 1" SG, and W/O shear Bolts).

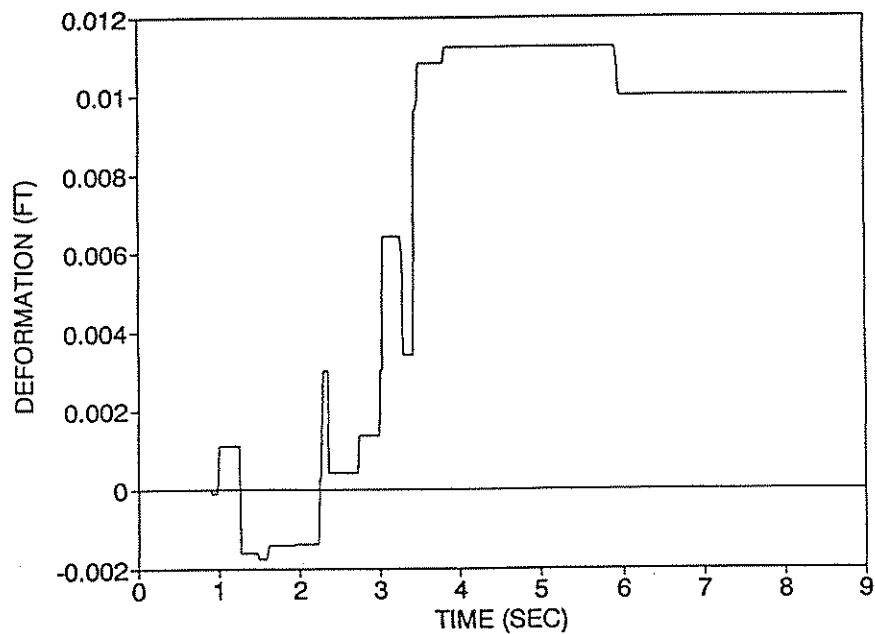


**Figure 4-36** Nonlinear Deformation Response of the Bearing Bars at Abutment 1 in the Long. Dir. (0" TBG, 1" SG, and W/O shear Bolts).

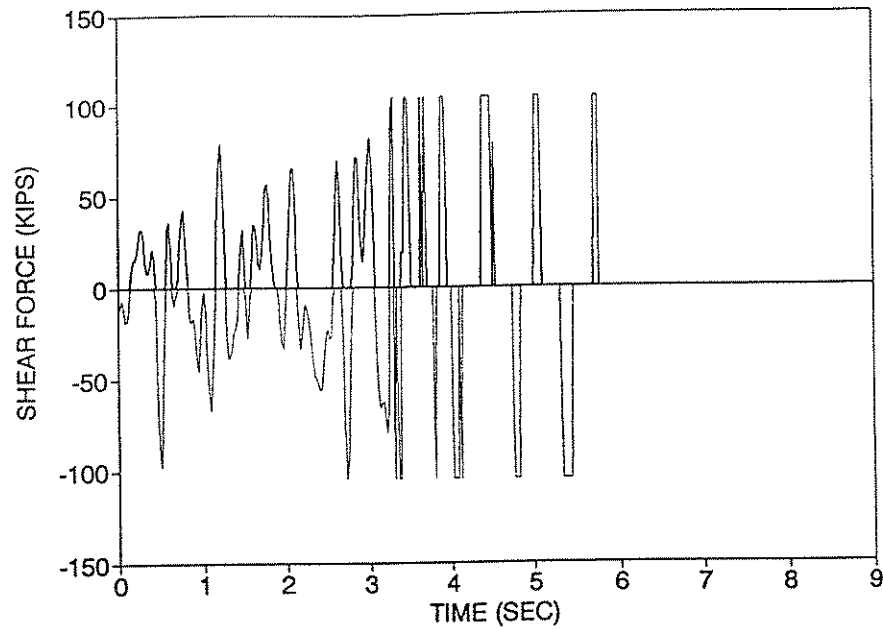


**Figure 4-37** Shear Force Response of the Bearing Bars at Abutment 1 in the Trans. Dir. (0" TBG, 1" SG, and W/O Shear Bolts).

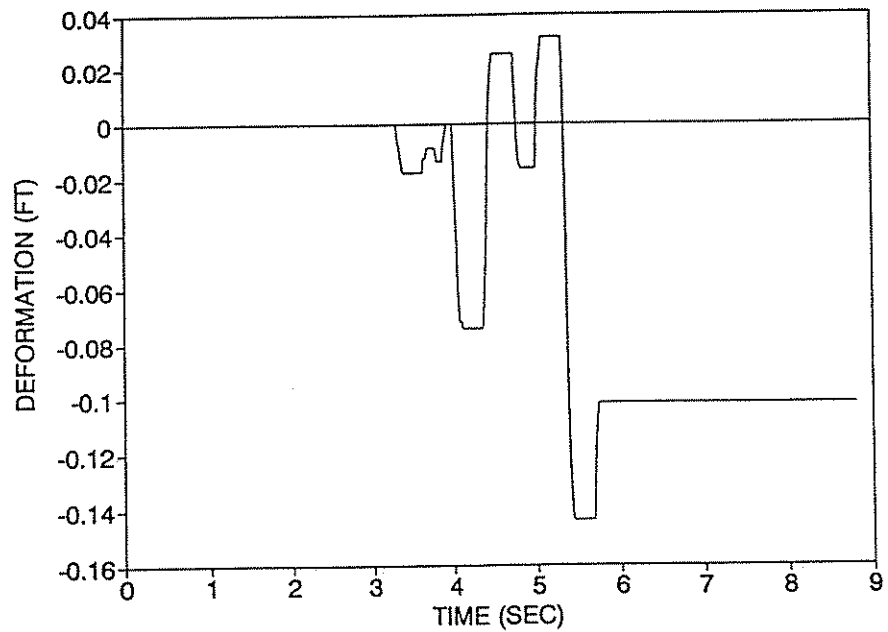


**Figure 4-38** Nonlinear Deformation Response of the Bearing Bars at Abutment 1 in the Trans. Dir. (0" TBG, 1" SG, and W/O Shear Bolts).

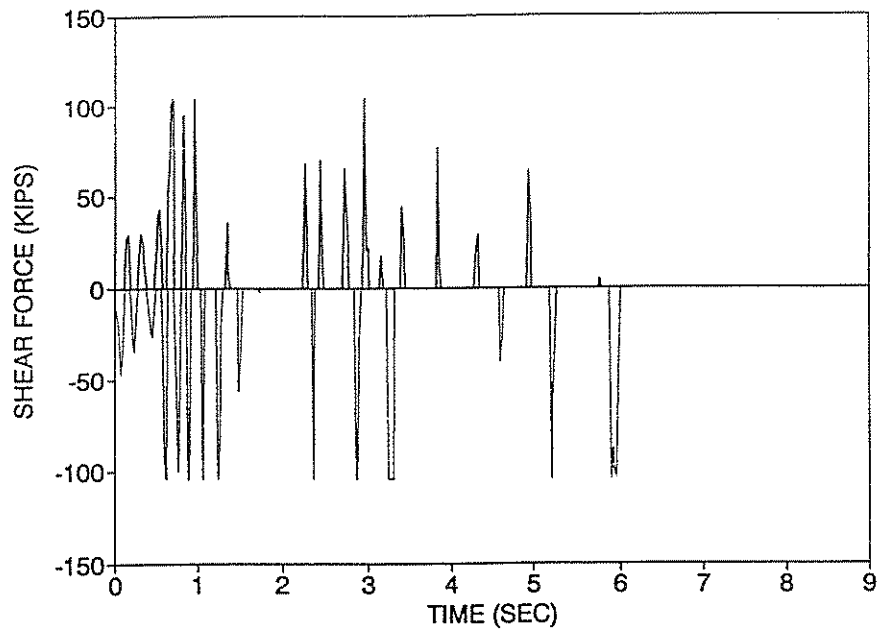


**Figure 4-39** Shear Force Response of the Bearing Bars at Abutment 6 in the Long. Dir. (0" TBG, 1" SG, and W/O Shear Bolts).

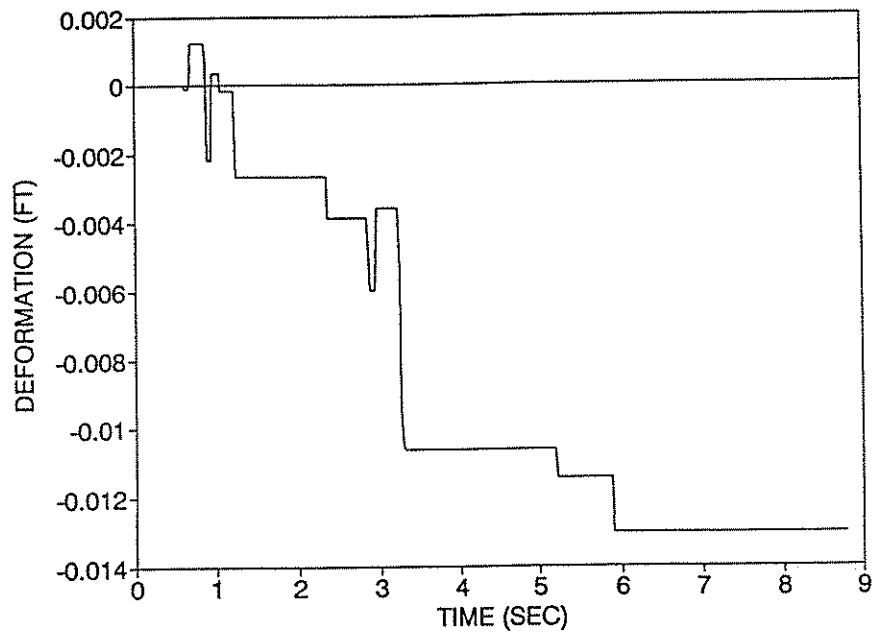


**Figure 4-40** Nonlinear Deformation Response of the Bearing Bars at Abutment 6 in the Long. Dir. (0" TBG, 1" SG, and W/O Shear Bolts).

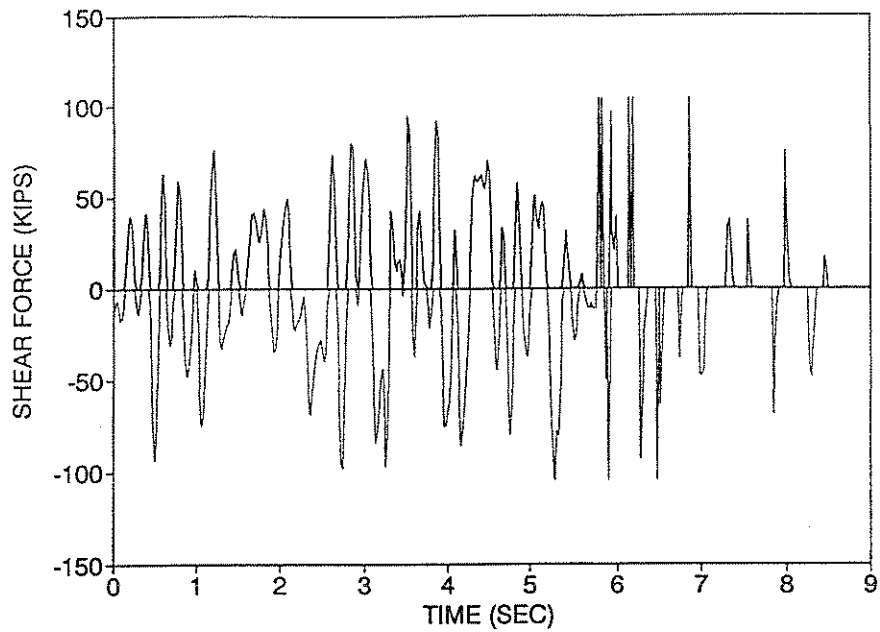


**Figure 4-41** Shear Force Response of the Bearing Bars at Abutment 6 in the Trans. Dir. (0" TBG, 1" SG, and W/O Shear Bolts).

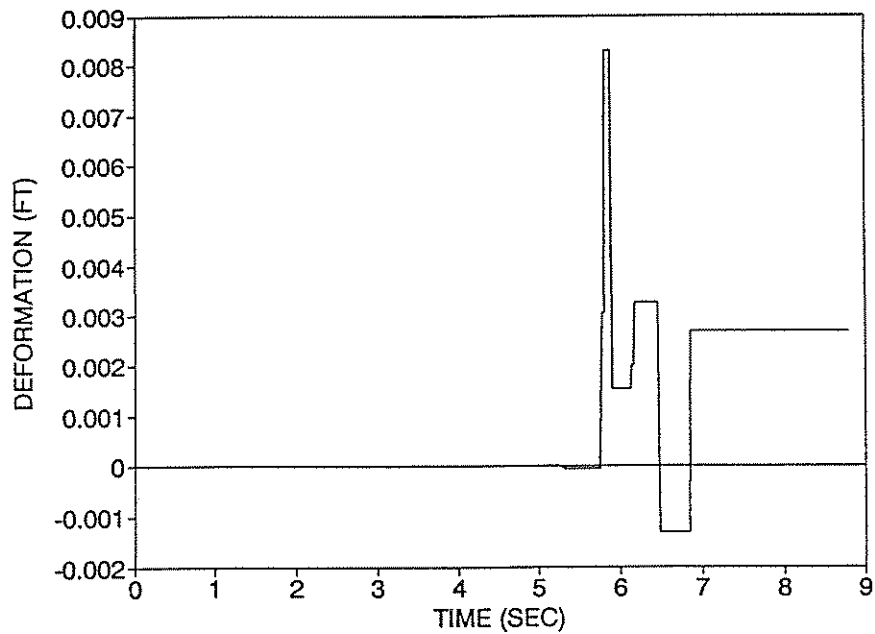


**Figure 4-42** Nonlinear Deformation Response of the Bearing Bars at Abutment 6 in the Trans. Dir. (0" TBG, 1" SG, and W/O Shear Bolts).

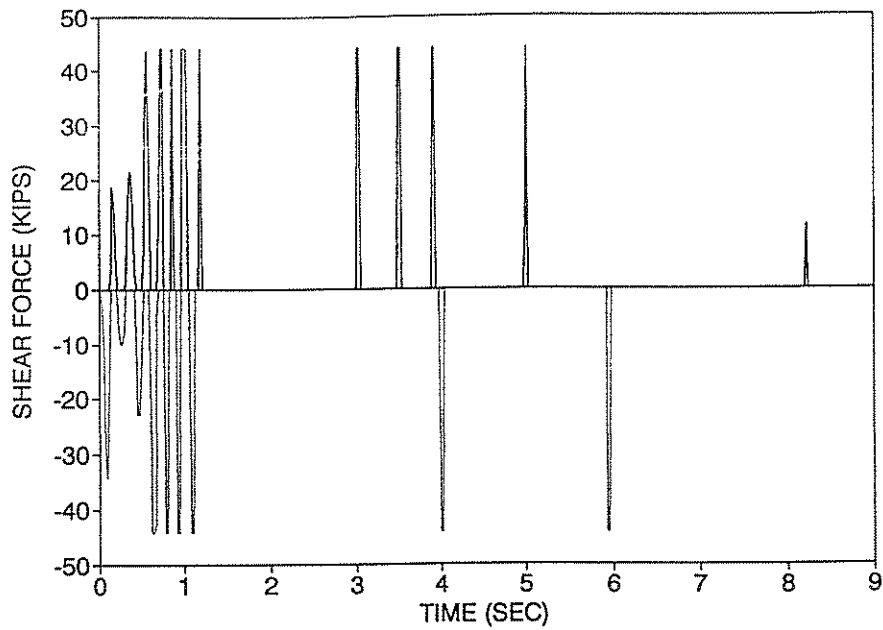


**Figure 4-43** Shear Force Response of the Shear Bolts at the Mid. Exp. Jt. in the Long. Dir. (0" TBG and 1" SG).

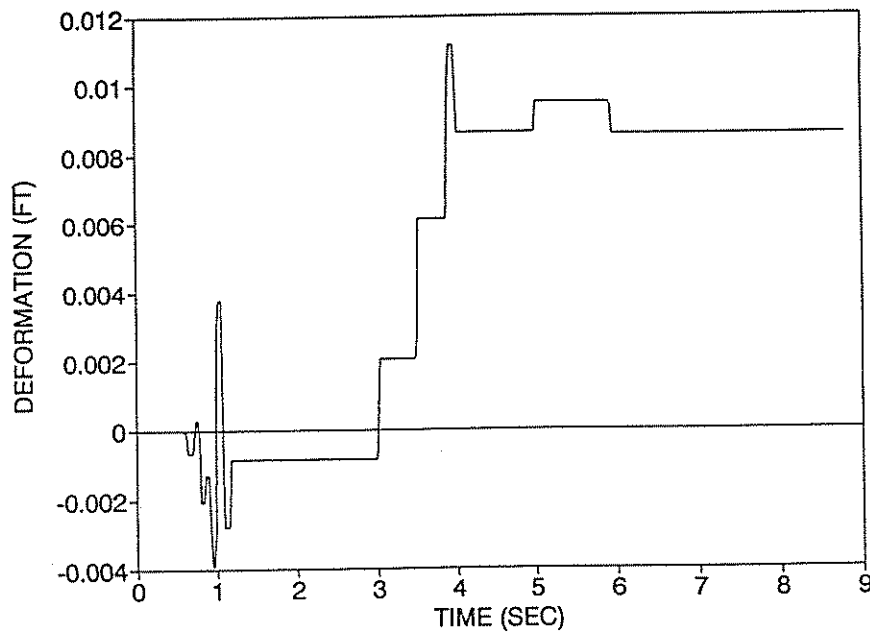


**Figure 4-44** Nonlinear Deformation Response of the Shear Bolts at the Mid. Exp. Jt. in the Long. Dir. (0" TBG and 1" SG).

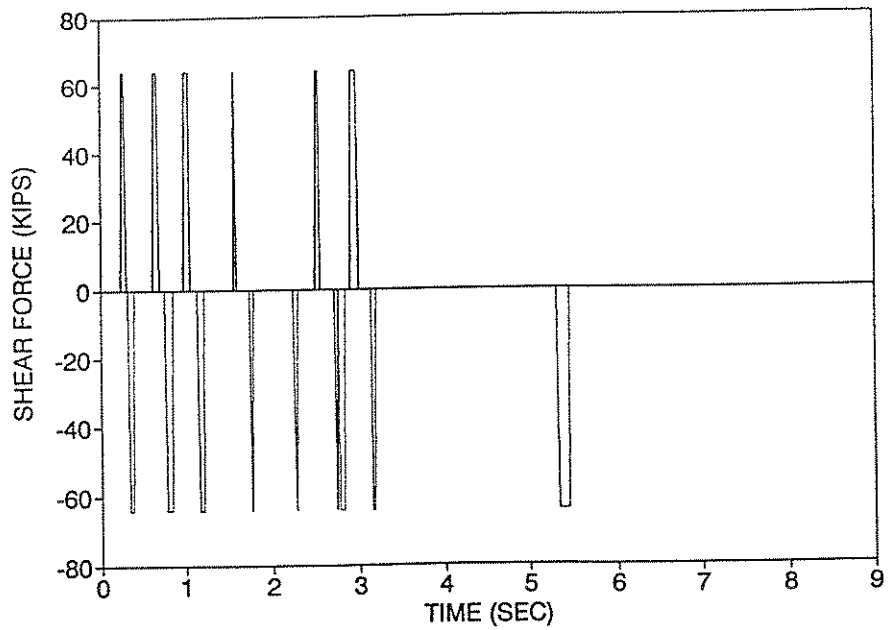


**Figure 4-45** Shear Force Response of the Shear Bolts at the Mid. Exp. Jt. in the Trans. Dir. (0" TBG and 1" SG).

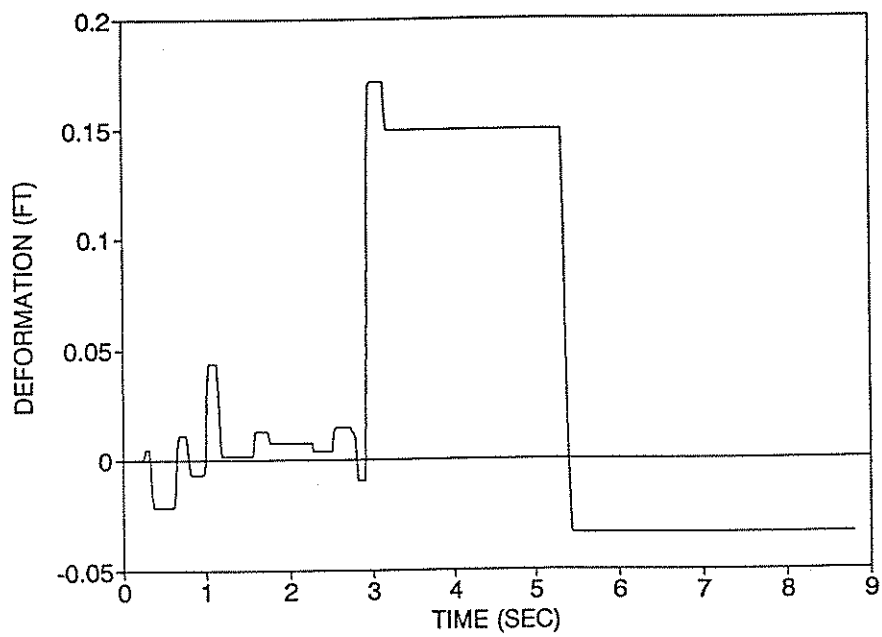


**Figure 4-46** Nonlinear Deformation Response of the Shear Bolts at the Mid. Exp. Jt. in the Trans. Dir. (0" TBG and 1" SG).

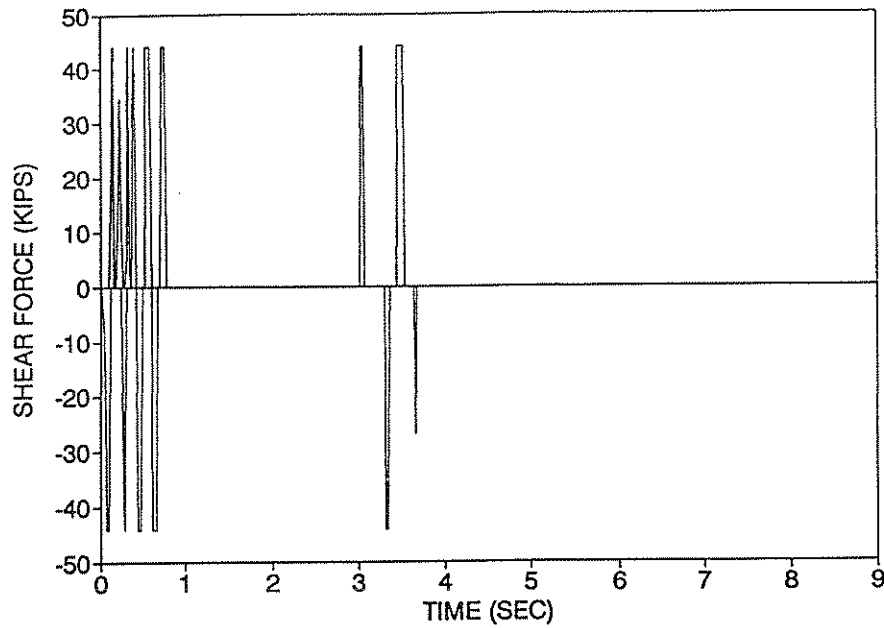


**Figure 4-47** Shear Force Response of the Shear Bolts at the Mid. Exp. Jt. in the Long. Dir. (0" TBG and 1" SG), Motion Normalized to 0.7g.

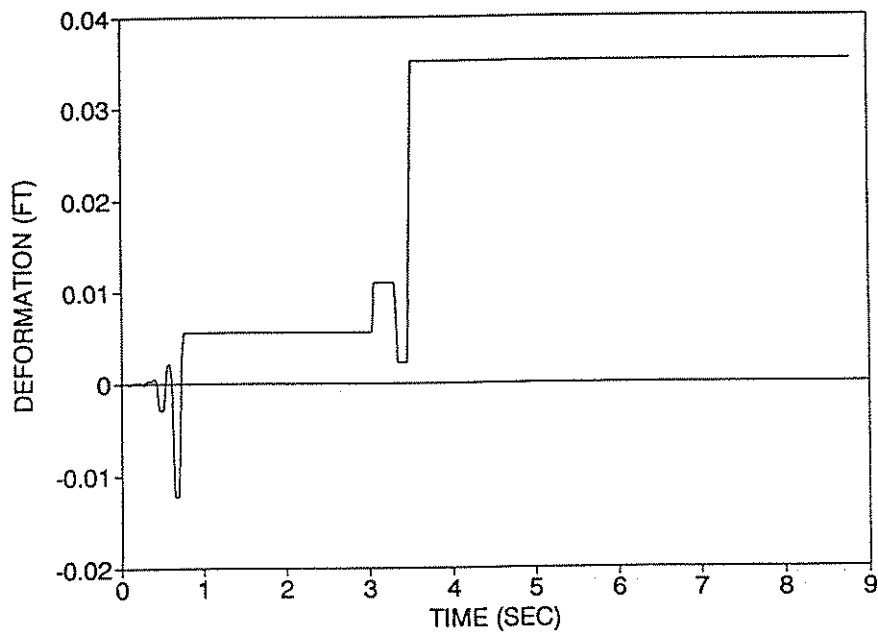


**Figure 4-48** Nonlinear Deformation Response of the Shear Bolts at the Mid. Exp. Jt. in the Long. Dir. (0" TBG and 1" SG), Motion Normalized to 0.7g.

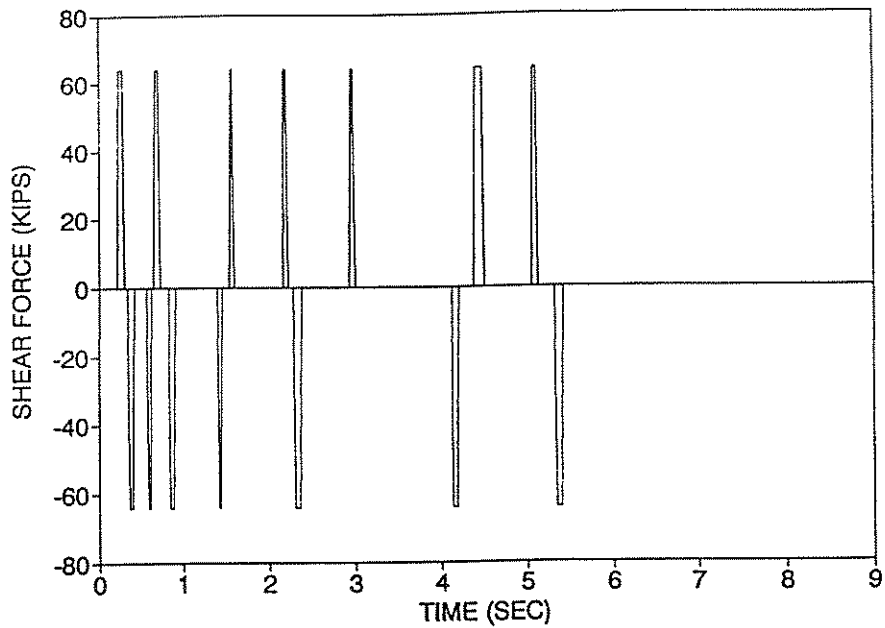


**Figure 4-49** Shear Force Response of the Shear Bolts at the Mid. Exp. Jt. in the Trans. Dir. (0" TBG and 1" SG), Motion Normalized to 0.7g.

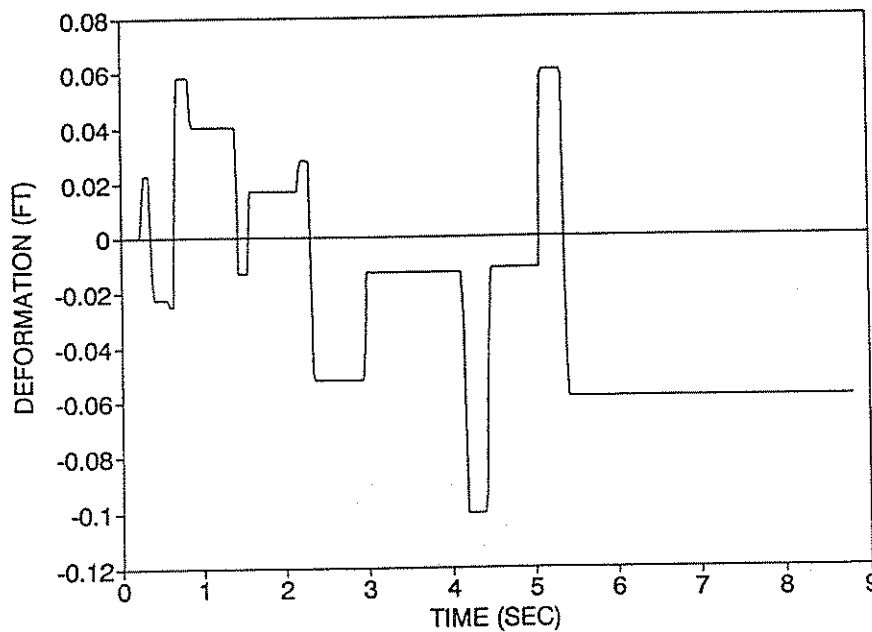


**Figure 4-50** Nonlinear Deformation Response of the Shear Bolts at the Mid. Exp. Jt. in the Trans. Dir. (0" TBG and 1" SG), Motion Normalized to 0.7g.

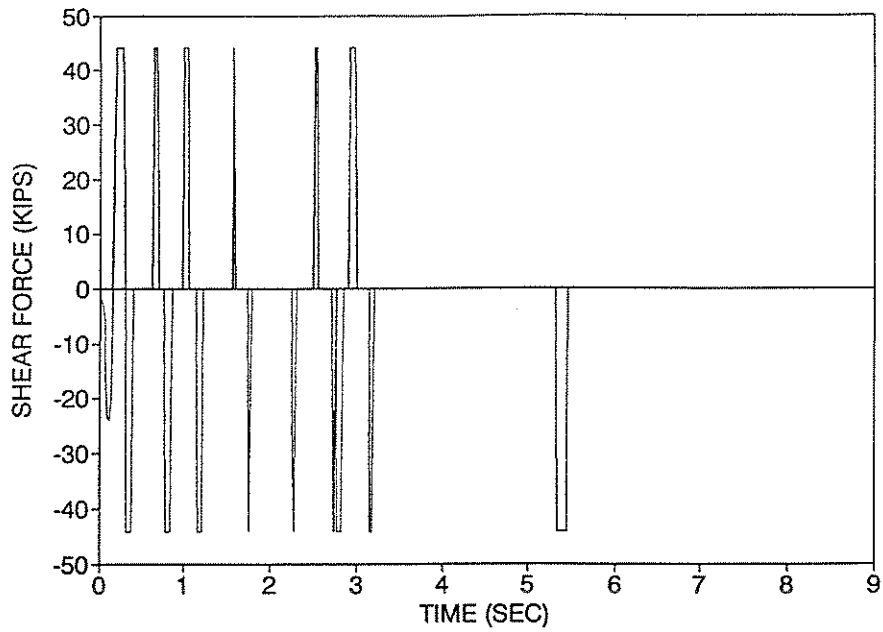


**Figure 4-51** Shear Force Response of the Shear Pipes at the Mid. Exp. Jt. in the Trans. Dir. (0" TBG and 1" SG).

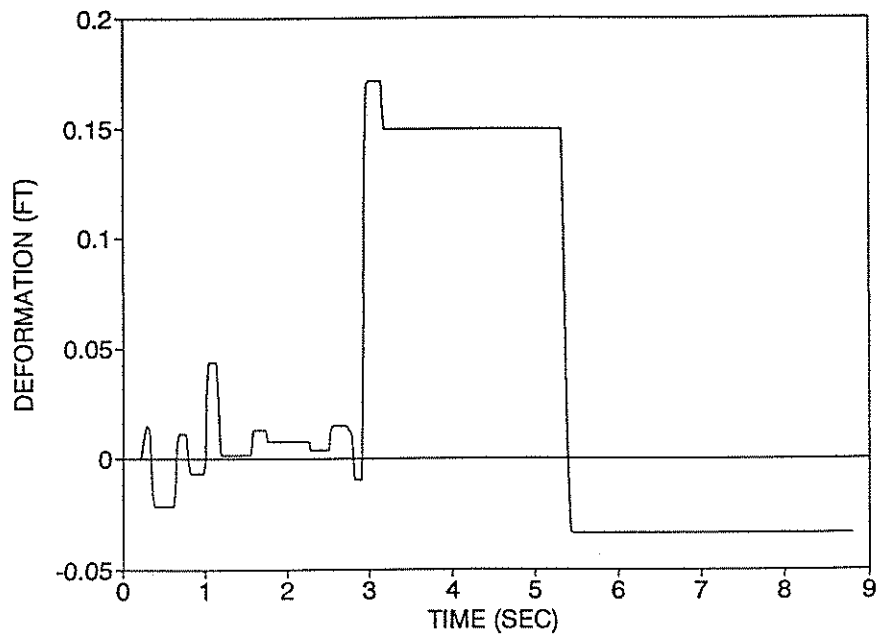


**Figure 4-52** Nonlinear Deformation Response of the Shear Pipes at the Mid. Exp. Jt. in the Trans. Dir. (0" TBG and 1" SG).

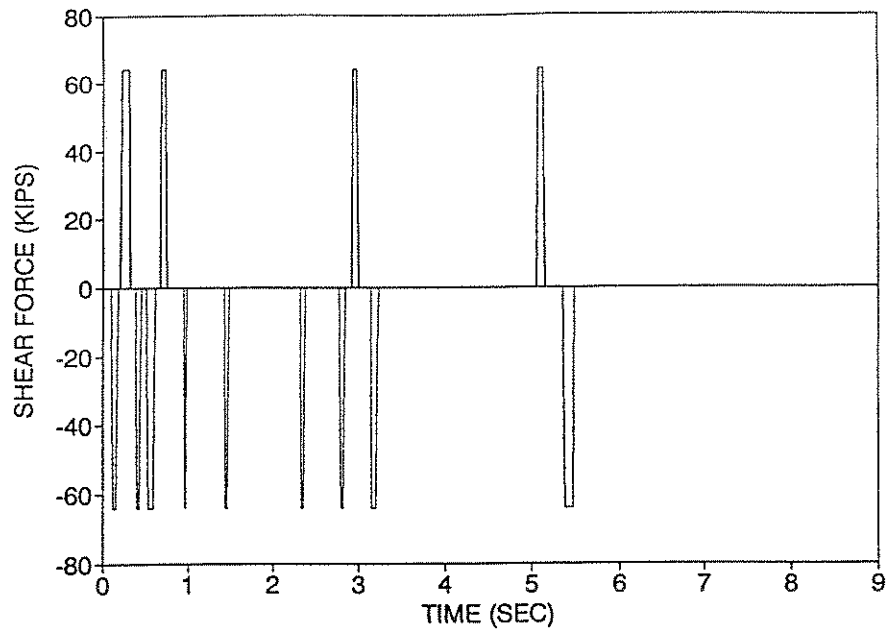


**Figure 4-53** Shear Force Response of the Shear Pipes at the Mid. Exp. Jt. in the Trans. Dir. (0" TBG and 1" SG, and W/O Shear Bolts).

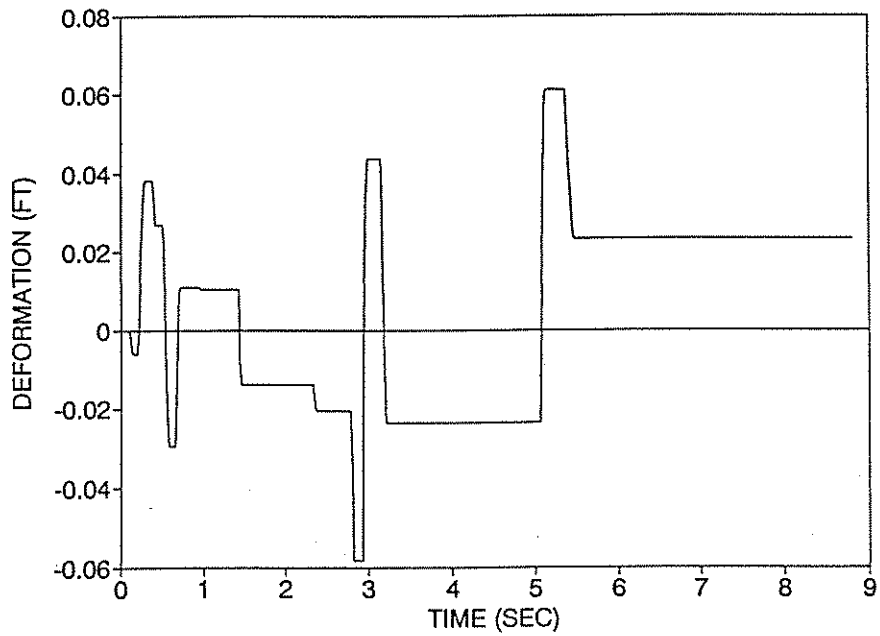


**Figure 4-54** Nonlinear Deformation Response of the Shear Pipes at the Mid. Exp. Jt. in the Trans. Dir. (0" TBG and 1" SG, and W/O Shear Bolts).

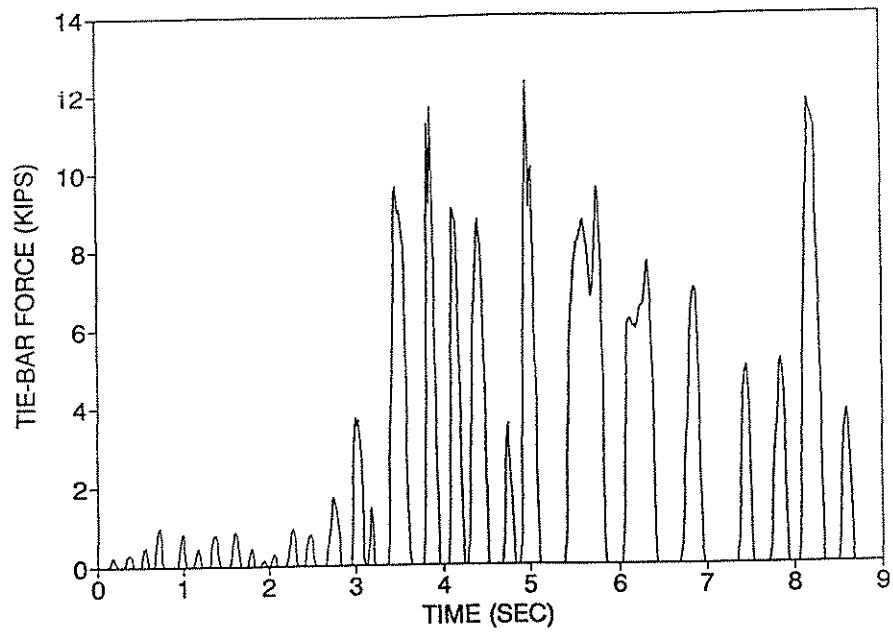


**Figure 4-55** Tie-Bar-Force Response of the Restrainers at Abutment 1 (0" TBG and 1" SG).

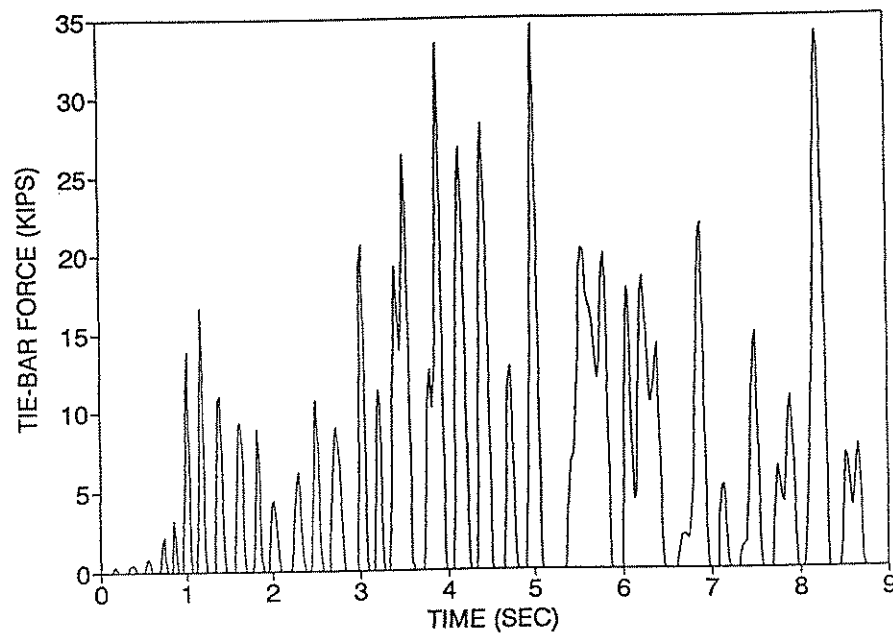


**Figure 4-56** Tie-Bar-Force Response of the Restrainers at the Mid. Exp. Jt. (0" TBG and 1" SG).

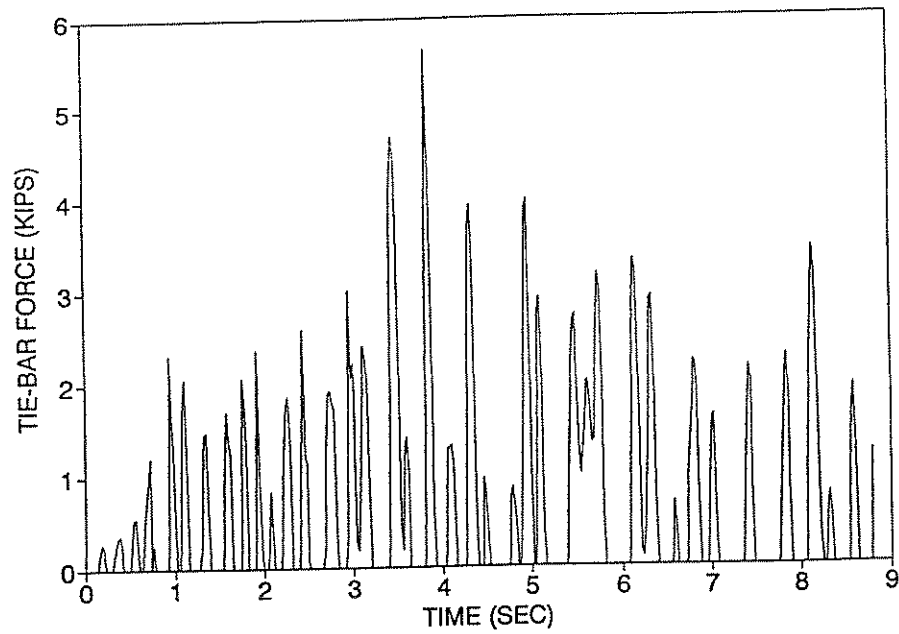


**Figure 4-57** Tie-Bar-Force Response of the Restrainers at Abutment 6 (0" TBG and 1" SG).

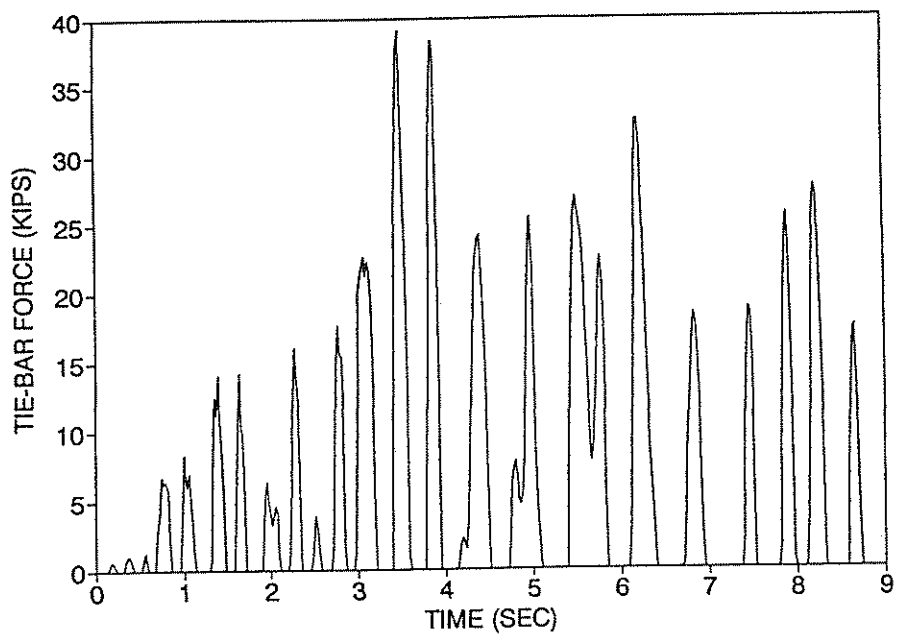


**Figure 4-58** Tie-Bar-Force Response of the Restrainers at Abutment 1 (0" TBG and 1" SG), Motion Normalized to 1.0 g.

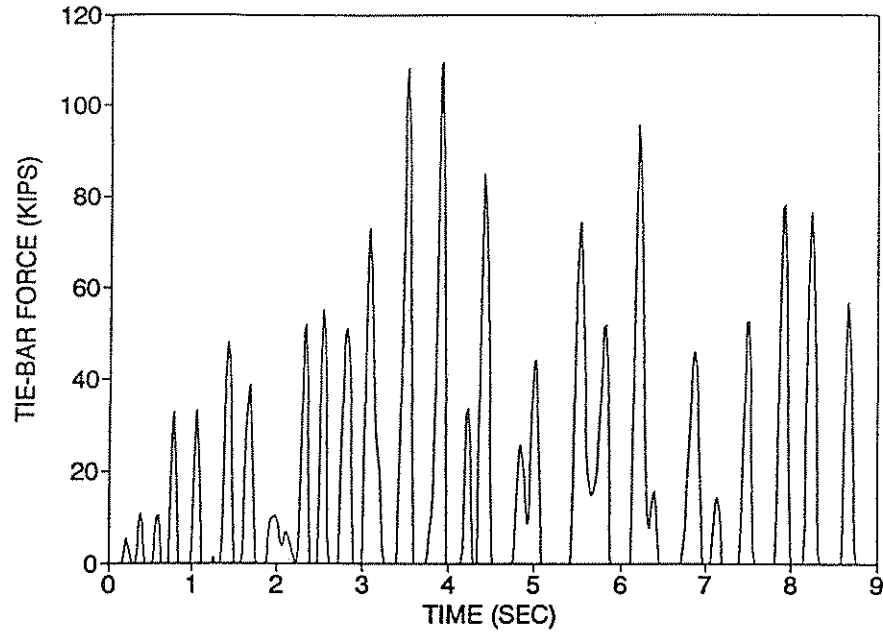


**Figure 4-59** Tie-Bar-Force Response of the Restrainers at the Mid. Exp. Jt. (0" TBG and 1" SG), Motion Normalized to 1.0 g.

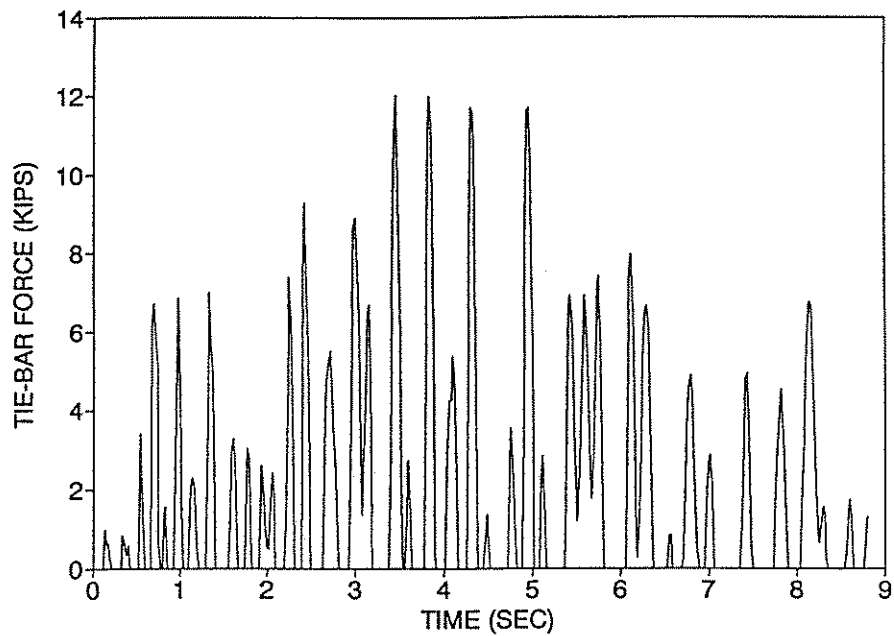


**Figure 4-60** Tie-Bar-Force Response of the Restrainers at Abutment 6 (0" TBG and 1" SG), Motion Normalized to 1.0 g.

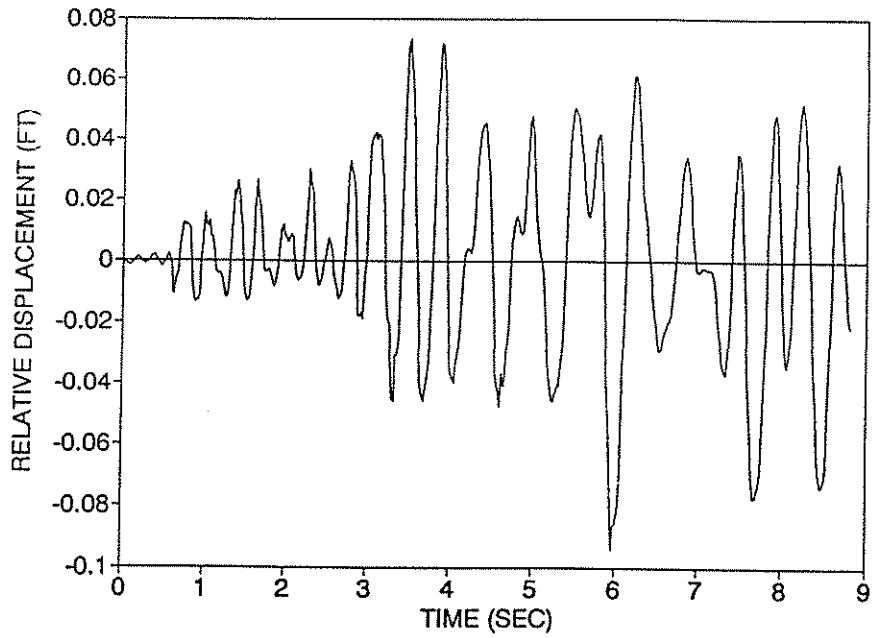


**Figure 4-61** Relative Displacement Response at Abutment 1 in the Long. Direction (0" TBG and 1" SG), Motion Normalized to 1.0 g.

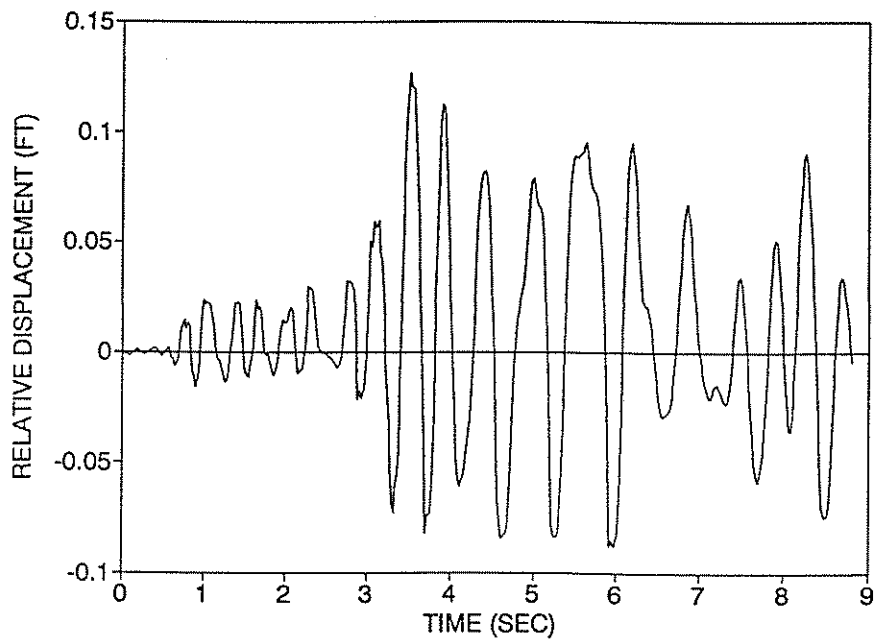


**Figure 4-62** Relative Displacement Response at Abutment 1 in the Long. Direction (W/O Cables and 1" SG), Motion Normalized to 1.0 g.

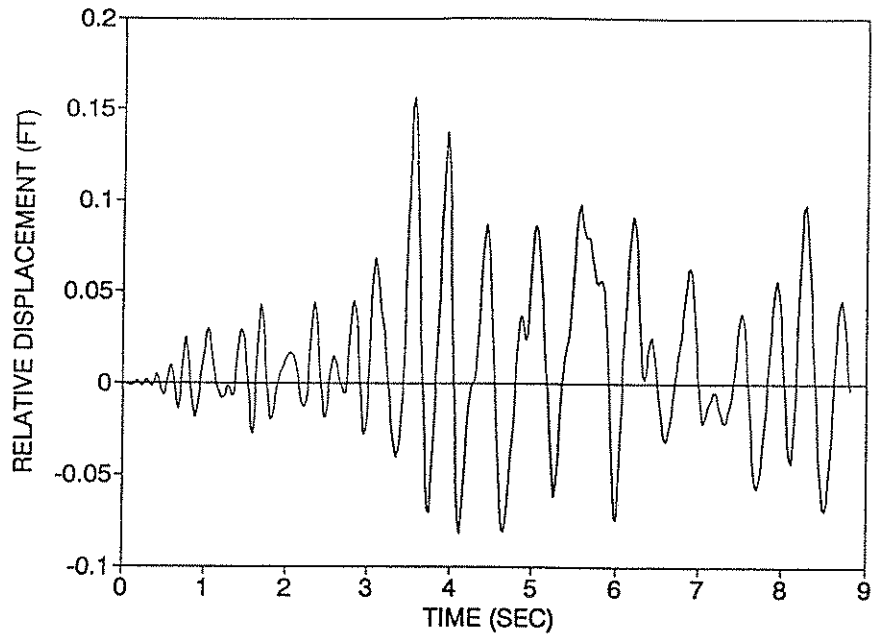


**Figure 4-63** Relative Displacement Response at the Mid. Exp. Jt. in the Long. Dir. (W/O Cables and 1" SG), Motion Normalized to 1.0 g.

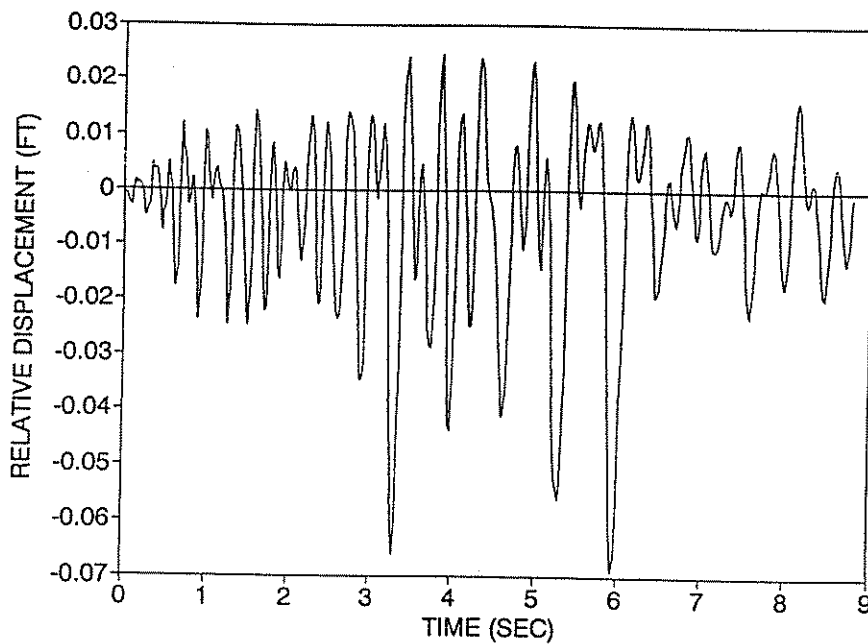


**Figure 4-64** Relative Displacement Response at Abutment 6 in the Long. Dir. (W/O Cables and 1" SG), Motion Normalized to 1.0 g.

## List of CCEER Publications

<u>Report No.</u>	<u>Publication</u>
CCEER-84-1	Saiidi, M., and R. A. Lawver. "User's manual for LZAK-C64, a computer program to implement the Q-model on Commodore 64." <i>Report number CCEER-84-1</i> . Reno: University of Nevada, Department of Civil Engineering. January 1984.
CCEER-84-2	Douglas, B. M., and T. Iwasaki. "Proceedings of the first USA-Japan bridge engineering workshop," held at the Public Works Research Institute, Tsukuba, Japan. <i>Report number CCEER-84-2</i> . Reno: University of Nevada, Department of Civil Engineering. April 1984.
CCEER-84-3	Saiidi, M., J. D. Hart, and B. M. Douglas. "Inelastic static and dynamic analysis of short R/C bridges subjected to lateral loads." <i>Report number CCEER-84-3</i> . Reno: University of Nevada, Department of Civil Engineering. July 1984.
CCEER-84-4	Douglas, B. "A proposed plan for a national bridge engineering laboratory." <i>Report number CCEER-84-4</i> . Reno: University of Nevada, Department of Civil Engineering. December 1984.
CCEER-85-1	Norris, G. M., and P. Abdollaholiae. "Laterally loaded pile response: Studies with the strain wedge model." <i>Report number CCEER-85-1</i> . Reno: University of Nevada, Department of Civil Engineering. April 1985.
CCEER-86-1	Ghusn, G. E., and M. Saiidi. "A simple hysteretic element for biaxial bending of R/C columns and implementation in NEABS-86." <i>Report number CCEER-86-1</i> . Reno: University of Nevada, Department of Civil Engineering. July 1986.
CCEER-86-2	Saiidi, M., R. A. Lawver, and J. D. Hart. "User's manual of ISADAB and SIBA, computer programs for nonlinear transverse analysis of highway bridges subjected to static and dynamic lateral loads." <i>Report number CCEER-86-2</i> . Reno: University of Nevada, Department of Civil Engineering. September 1986.
CCEER-87-1	Siddharthan, R. "Dynamic effective stress response of surface and embedded footings in sand." <i>Report number CCEER-87-1</i> . Reno: University of Nevada, Department of Civil Engineering. June 1987.
CCEER-87-2	Norris, G., and R. Sack. "Lateral and rotational stiffness of pile groups for seismic analysis of highway bridges." <i>Report number CCEER-87-2</i> . Reno: University of Nevada, Department of Civil Engineering. June 1987.

- CCEER-88-1      Orié, J., and M. Saiidi. "A preliminary study of one-way reinforced concrete pier hinges subjected to shear and flexure." *Report number CCEER-88-1*. Reno: University of Nevada, Department of Civil Engineering. January 1988.
- CCEER-88-2      Orié, D., M. Saiidi, and B. Douglas. "A micro-CAD system for seismic design of regular highway bridges." *Report number CCEER-88-2*. Reno: University of Nevada, Department of Civil Engineering. June 1988.
- CCEER-88-3      Orié, D., and M. Saiidi. "User's manual for Micro-SARB, a microcomputer program for seismic analysis of regular highway bridges." *Report number CCEER-88-3*. Reno: University of Nevada, Department of Civil Engineering. October 1988.
- CCEER-89-1      Douglas, B., M. Saiidi, R. Hayes, and G. Holcomb. "A comprehensive study of the loads and pressures exerted on wall forms by the placement of concrete." *Report number CCEER-89-1*. Reno: University of Nevada, Department of Civil Engineering. February 1989.
- CCEER-89-2a      Richardson, J., and B. Douglas. "Dynamic response analysis of the Dominion Road Bridge test data." *Report number CCEER-89-2*. Reno: University of Nevada, Department of Civil Engineering. March 1989.
- CCEER-89-2b      Vrontinos, S., M. Saiidi, and B. Douglas. "A simple model to predict the ultimate response of R/C beams with concrete overlays." *Report number CCEER-89-2*. Reno: University of Nevada, Department of Civil Engineering. June 1989.
- CCEER-89-3      Ebrahimpour, A., and P. Jagadish. "Statistical modeling of bridge traffic loads: A case study." *Report number CCEER-89-3*. Reno: University of Nevada, Department of Civil Engineering. December 1989.
- CCEER-89-4      Shields, J., and M. Saiidi. "Direct field measurement of prestress losses in box girder bridges." *Report number CCEER-89-4*. Reno: University of Nevada, Department of Civil Engineering. December 1989.
- CCEER-90-1      Saiidi, M., E. Maragakis, G. Ghosn, Jr., Y. Jiang, and D. Schwartz. "Survey and evaluation of Nevada's transportation infrastructure, task 7.2—highway bridges, final report." *Report number CCEER-90-1*. Reno: University of Nevada, Department of Civil Engineering. October 1990.
- CCEER-90-2      Abdel-Ghaffar, S., E. Maragakis, and M. Saiidi. "Analysis of the response of reinforced concrete structures during the Whittier earthquake of 1987." *Report*

- number CCEER-90-2.* Reno: University of Nevada, Department of Civil Engineering. October 1990.
- CCEER-91-1 Saiidi, M., E. Hwang, E. Maragakis, and B. Douglas. "Dynamic testing and analysis of the Flamingo Road Interchange." *Report number CCEER-91-1.* Reno: University of Nevada, Department of Civil Engineering. February 1991.
- CCEER-91-2 Norris, G., R. Siddharthan, Z. Zafir, S. Abdel-Ghaffar, and P. Gowda. "Soil-foundation-structure behavior at the Oakland Outer Harbor Wharf." *Report number CCEER-91-2.* Reno: University of Nevada, Department of Civil Engineering. July 1991.
- CCEER-91-3 Norris, G. M. "Seismic lateral and rotational pile foundation stiffness at Cypress." *Report number CCEER-91-3.* Reno: University of Nevada, Department of Civil Engineering. August 1991.
- CCEER-91-4 O'Connor, D. N., and M. Saiidi. "A study of protective overlays for highway bridge decks in Nevada, with emphasis on polyester-styrene polymer concrete." *Report number CCEER-91-4.* Reno: University of Nevada, Department of Civil Engineering. October 1991.
- CCEER-91-5 O'Connor, D. N., and M. Saiidi. "Laboratory studies of polyester-styrene polymer concrete engineering properties." *Report number CCEER-91-5.* Reno: University of Nevada, Department of Civil Engineering. November 1991.
- CCEER-92-1 Straw, D. L., and M. "Saiid" Saiidi. "Scale model testing of one-way reinforced concrete pier hinges subjected to combined axial force, shear and flexure." *Report number CCEER-92-1,* ed. by D. N. O'Connor. Reno: University of Nevada, Department of Civil Engineering. March 1992.
- CCEER-92-2 Wehbe, N., M. Saiidi, and F. Gordaninejad. "Basic behavior of composite sections made of concrete slabs and graphite epoxy beams." *Report number CCEER-92-2.* Reno: University of Nevada, Department of Civil Engineering. August 1992.
- CCEER-92-3 Saiidi, M., and E. Hutchens. "A study of prestress changes in a post-tensioned bridge during the first 30 months." *Report number CCEER-92-3.* Reno: University of Nevada, Department of Civil Engineering. April 1992.
- CCEER-92-4 Saiidi, M., B. Douglas, S. Feng, E. Hwang, and E. Maragakis. "Effects of axial force on frequency of prestressed concrete bridges." *Report number CCEER-92-4.* Reno: University of Nevada, Department of Civil Engineering. August 1992.

- CCEER-92-5 Siddharthan, R., and Zafir, Z. "Response of layered deposits to traveling surface pressure waves." *Report number CCEER-92-5*. Reno: University of Nevada, Department of Civil Engineering. September 1992.
- CCEER-92-6 Norris, G., and Zafir, Z. "Liquefaction and residual strength of loose sands from drained triaxial tests." *Report number CCEER-92-6*. Reno: University of Nevada, Department of Civil Engineering. September 1992.
- CCEER-92-7 Douglas, B. "Some thoughts regarding the improvement of the University of Nevada, Reno's national academic standing." *Report number CCEER-92-7*. Reno: University of Nevada, Department of Civil Engineering. September 1992.
- CCEER-92-8 Saiidi, M., E. Maragakis, and S. Feng. "An evaluation of the current Caltrans seismic restrainer design method." *Report number CCEER-92-8*. Reno: University of Nevada, Department of Civil Engineering. October 1992.
- CCEER-92-9 O'Connor, D. N., M. Saiidi, and E. A. Maragakis. "Effect of hinge restrainers on the response of the Madrone Drive Undercrossing during the Loma Prieta earthquake." *Report number CCEER-92-9*. Reno: University of Nevada, Department of Civil Engineering. December 1992.
- CCEER-92-10 O'Connor, D. N., and M. Saiidi. "Laboratory studies of polyester concrete: Compressive strength at elevated temperatures and following temperature cycling, bond strength to portland cement concrete, and modulus of elasticity." *Report number CCEER-92-10*. Reno: University of Nevada, Department of Civil Engineering. December 1992.

## ABSTRACT

This report is one of a series that results from the study "Evaluation of the Effects of the Seismic Retrofitting on the Earthquake Response of Highway Bridges". Aptos Creek bridge suffered some damage during the Loma Prieta earthquake of October 17, 1989. This bridge is located approximately six miles southwest of the epicenter. The focus of the analysis for this bridge study was the nonlinear behavior of the bridge elements. Several parameters were studied in details. Parametric studies were carried out to determine the effect of cable restrainers and intermediate hinge shear bolts on the response of the bridge. Finally, based on the analytical results in conjunction with the damage report, a general conclusion regarding the analysis capability is deduced. Detailed mathematical procedures simulating nonlinear behavior of the expansion joints are included in the study.

## ACKNOWLEDGEMENTS

The authors wish to express their sincere appreciation to California Department of Transportation (Caltrans), National science foundation, and Nevada Department of Transportation for funding the project. Special thanks are due to Mr. Jim Gates, the Caltrans senior supervisor bridge engineer, Mr. Mark Yashinsky, the Caltrans project monitor, and Mr. Richard Obisanya, a staff engineer at Caltrans for their cooperation, assistance, and guidance during the course of the study. Their assistance greatly facilitated the progress of the investigation reported herein.

# CONTENTS

ABSTRACT .....	II
ACKNOWLEDGEMENT .....	III
LIST OF FIGURES .....	VI
LIST OF TABLES .....	XI
<b>1 INTRODUCTION .....</b>	<b>1</b>
1.1 STATEMENT OF THE PROBLEM .....	1
1.2 OBJECTIVE .....	1
<b>2 BRIDGE DESCRIPTION AND DAMAGE .....</b>	<b>3</b>
2.1 DESCRIPTION OF THE BRIDGE .....	3
2.2 RETROFITTING .....	5
2.3 EARTHQUAKE DAMAGE .....	6
<b>3 ANALYTICAL MODEL .....</b>	<b>7</b>
3.1 DESCRIPTION OF THE ANALYTICAL MODELS .....	7
3.2 BRIEF DESCRIPTION OF COMPUTER PROGRAMS .....	7
3.2.1 IMAGES-3D .....	7
3.2.2 NEABS-86 .....	8
3.3 LINEAR ANALYTICAL MODEL (IMAGES-3D) .....	8
3.4 RAYLEIGH' S DAMPING COEFFICIENTS .....	10
3.5 NONLINEAR ANALYTICAL MODEL (NEABS-86) .....	11
3.5.1 Bridge Deck and Columns .....	11
3.5.2 Abutment Expansion Joints .....	12
3.5.2.1 Abutment and piles .....	12
3.5.2.2 Abutment Bearing Bars .....	12
3.5.3 Middle Hinge Expansion Joints .....	14
3.5.3.1 Middle Hinge Shear Pipes .....	14
3.5.3.2 Middle Hinge Shear Bolts .....	14

3.5.4	Cable Restrainers .....	14
3.5.5	Impact .....	15
3.6	SEISMIC EXCITATION .....	15
<b>4</b>	<b>ANALYTICAL RESULTS .....</b>	<b>18</b>
4.1	STRUCTURE PERIODS AND FREQUENCIES .....	18
4.2	PARAMETRIC STUDY AND RESULTS .....	19
4-2.1	OVERALL DISPLACEMENT RESPONSE .....	21
4-2.2	RELATIVE DISPLACEMENT RESPONSE .....	22
4-2.3	ABUTMENT AND PILE RESPONSE .....	23
4-2.4	BEARING BARS .....	24
4-2.5	SHEAR BOLTS .....	25
4-2.6	SHEAR PIPES .....	26
4-2.7	CABLE RESTRAINERS .....	27
4-2.8	IMPACT .....	27
<b>5</b>	<b>CONCLUSIONS .....</b>	<b>35</b>
	REFERENCES .....	37
	FIGURES .....	39
	LIST OF CEER PUBLICATIONS .....	83

## LIST OF FIGURES

Figure 2-1	-Schematic Drawing of the Aptos Creek Bridge	39
Figure 2-2	-Typical Cross Section of the Bridge	40
Figure 2-3	-Fixed Bearing Assembly at both Abutments	41
Figure 2-4	-Details of the Middle Expansion Joint	42
Figure 2-5	-Details of the Retrofitting at the Abutments	43
Figure 2-6	-Details of the Retrofitting at the Middle Expansion Joint	44
Figure 3-1	-Idealization of the Lumped Mass, Linear Model	45
Figure 3-2	-Idealization of the Lumped Mass, Nonlinear Model	46
Figure 3-3	-Capitola Fire Station, Transverse Component ( Peak Acceleration = -0.472g at 6.02 sec )	47
Figure 3-4	-Capitola Fire Station, Longitudinal Component ( Peak Acceleration = -0.398g at 8.08 sec )	47
Figure 4-1	-First Ten Mode Shapes for the Aptos Creek Bridge	48
Figure 4-2	-Longitudinal Displacement History at Node 2 near Abutment 1 (3/4" TBG and 1" SG)	49
Figure 4-3	-Transverse Displacement History at Node 2 near Abutment 1 (3/4" TBG and 1" SG)	49
Figure 4-4	-Longitudinal Displacement History at Node 39 near the Middle Hinge (3/4" TBG and 1" SG)	50
Figure 4-5	-Transverse Displacement History at Node 39 near the Middle Hinge (3/4" TBG and 1" SG)	50
Figure 4-6	-Longitudinal Displacement History at Node 75 near Abutment 6 (3/4" TBG and 1" SG)	51
Figure 4-7	-Transverse Displacement History at Node 75 near Abutment 6 (3/4" TBG and 1" SG)	51
Figure 4-8	-Longitudinal Relative Displacement History at Abutment 1 (3/4" TBG and 1" SG)	52
Figure 4-9	-Transverse Relative Displacement History at Abutment 1 (3/4" TBG and 1" SG)	52
Figure 4.10	-Longitudinal Relative Displacement History at the Middle Hinge (3/4" TBG and 1" SG)	53

Figure 4-11	-Transverse Relative Displacement History at the Middle Hinge (3/4" TBG and 1" SG) . . . . .	53
Figure 4-12	-Longitudinal Relative Displacement History at Abutment 6 (3/4" TBG and 1" SG) . . . . .	54
Figure 4-13	-Transverse Relative Displacement History at Abutment 6 (3/4" TBG and 1" SG) . . . . .	54
Figure 4-14	-Longitudinal Relative Displacement History at Abutment 1 (Motion Normalized to 0.7g) . . . . .	55
Figure 4-15	-Transverse Relative Displacement History at Abutment 1 (Motion Normalized to 0.7g) . . . . .	55
Figure 4-16	-Longitudinal Relative Displacement History at the Middle Hinge (Motion Normalized to 0.7g) . . . . .	56
Figure 4-17	-Transverse Relative Displacement History at the Middle Hinge (Motion Normalized to 0.7g) . . . . .	56
Figure 4-18	-Longitudinal Relative Displacement History at Abutment 6 (Motion Normalized to 0.7g) . . . . .	57
Figure 4-19	-Transverse Relative Displacement History at Abutment 6 (Motion Normalized to 0.7g) . . . . .	57
Figure 4-20	-Abutment 1 Force History (3/4" TBG and 1" SG) . . . . .	58
Figure 4-21	-Piles of Abutment 1 Force History (3/4" TBG and 1" SG) . . . . .	58
Figure 4-22	-Abutment 6 Force History (3/4" TBG and 1" SG) . . . . .	59
Figure 4-23	-Piles of Abutment 6 Force History (3/4" TBG and 1" SG) . . . . .	59
Figure 4-24	-Abutment 1 Force History (Motion Normalized to 0.7g) . . . . .	60
Figure 4-25	-Abutment 1 Nonlinear Deformation History (Motion Normalized to 0.7g) . . . . .	60
Figure 4-26	-Abutment 1 Force History (Motion Normalized to 1.0g) . . . . .	61
Figure 4-27	-Abutment 1 Nonlinear Deformation History (Motion Normalized to 1.0 g) . . . . .	61
Figure 4-28	-Abutment 6 Force History (Motion Normalized to 1.0 g) . . . . .	62
Figure 4-29	-Abutment 6 Nonlinear Deformation History (Motion Normalized to 1.0 g) . . . . .	62
Figure 4-30	-Piles of Abutment 1 Force History (Motion Normalized to 1.0 g) . . . . .	63
Figure 4-31	-Piles of Abutment 1 Nonlinear Deformation History (Motion Normalized to 1.0 g) . . . . .	63

Figure 4-32	-Shear Force History of Abutment 1 Bearing Bars in the Long. Dir. (3/4" TBG and 1" SG) . . . . .	64
Figure 4-33	-Nonlinear Deformation History of Abutment 1 Bearing Bars in the Long. Dir. (3/4" TBG and 1" SG) . . . . .	64
Figure 4-34	-Shear Force History of Abutment 1 Bearing Bars 1 in the Trans. Dir. (3/4" TBG and 1" SG) . . . . .	65
Figure 4-35	-Nonlinear Deformation History of Abutment 1 Bearing Bars in the Trans. Dir. (3/4" TBG and 1" SG) . . . . .	65
Figure 4-36	-Shear Force History of Abutment 6 Bearing Bars in the Long. Dir. (3/4" TBG and 1" SG) . . . . .	66
Figure 4-37	-Nonlinear Deformation History of Abutment 6 Bearing Bars in the Long. Dir. (3/4" TBG and 1" SG) . . . . .	66
Figure 4-38	-Shear Force History of Abutment 6 Bearing Bars in the Trans. Dir. (3/4" TBG and 1" SG) . . . . .	67
Figure 4-39	-Nonlinear Deformation History of Abutment 6 Bearing Bars in the Trans. Dir. (3/4" TBG and 1" SG) . . . . .	67
Figure 4-40	-Shear Force History of Abutment 1 Bearing Bars in the Long. Dir. (Motion Normalized to 0.7g) . . . . .	68
Figure 4-41	-Nonlinear Deformation History of Abutment 1 Bearing Bars in the Long. Dir. (Motion Normalized to 0.7g) . . . . .	68
Figure 4-42	-Shear Force History of Abutment 1 Bearing Bars in the Trans. Dir. (Motion Normalized to 0.7g) . . . . .	69
Figure 4-43	-Nonlinear Deformation History of Abutment 1 Bearing Bars in the Trans. Dir. (Motion Normalized to 0.7g) . . . . .	69
Figure 4-44	-Shear Force History of Abutment 6 Bearing Bars in the Long. Dir. (Motion Normalized to 0.7g) . . . . .	70
Figure 4-45	-Nonlinear Deformation History of Abutment 6 Bearing Bars in the Long. Dir. (Motion Normalized to 0.7g) . . . . .	70
Figure 4-46	-Shear Force History of Abutment 6 Bearing Bars in the Trans. Dir. (Motion Normalized to 0.7g) . . . . .	71
Figure 4-47	-Nonlinear Deformation History of Abutment 6 Bearing Bars in the Trans. Dir. (Motion Normalized to 0.7g) . . . . .	71
Figure 4-48	-Shear Force History of the Middle Hinge Shear Bolts in the Long. Dir. (3/4" TBG and 1" SG) . . . . .	72
Figure 4-49	-Nonlinear Deformation History of the Middle Hinge Shear Bolts in the Long. Dir. (3/4" TBG and 1" SG) . . . . .	72

Figure 4-50	-Shear Force History of the Middle Hinge Shear Bolts in the Trans. Dir. (3/4" TBG and 1" SG) . . . . .	73
Figure 4-51	-Nonlinear Deformation History of the Middle Hinge Shear Bolts in the Trans. Dir. (3/4" TBG and 1" SG) . . . . .	73
Figure 4-52	-Shear Force History of the Middle Hinge Shear Bolts in the Long. Dir. (Motion Normalized to 0.7g) . . . . .	74
Figure 4-53	-Nonlinear Deformation History of the Middle Hinge Shear Bolts in the Long. Dir. (Motion Normalized to 0.7g) . . . . .	74
Figure 4-54	-Shear Force History of the Middle Hinge Shear Bolts in the Trans. Dir. (Motion Normalized to 0.7g) . . . . .	75
Figure 4-55	-Nonlinear Deformation History of the Middle Hinge Shear Bolts in the Trans. Dir. (Motion Normalized to 0.7g) . . . . .	75
Figure 4-56	-Shear Force History of the Middle Hinge Shear Pipes in the Trans. Dir. (3/4" TBG and 1" SG) . . . . .	76
Figure 4-57	-Nonlinear Deformation History of the Middle Hinge Shear Pipes in the Trans. Dir. (3/4" TBG and 1" SG) . . . . .	76
Figure 4-58	-Shear Force History of the Middle Hinge Shear Pipes in the Trans. Dir. (0" TBG, 1" SG, and W/O Shear Bolts) . . . . .	77
Figure 4-59	-Nonlinear Deformation History of the Middle Hinge Shear Pipes in the Trans. Dir. (0" TBG, 1" SG, and W/O Shear Bolts) . . . . .	77
Figure 4-60	Tie Bar Force History of Abutment 1 Restrainers (0" TBG and 1" SG) . . . . .	78
Figure 4-61	-Tie Bar Force History of the Middle Hinge Restrainers (0" TBG and 1" SG) . . . . .	78
Figure 4-62	-Tie Bar Force History of Abutment 6 Restrainers (0" TBG and 1" SG) . . . . .	79
Figure 4-63	-Tie Bar Force History of Abutment 1 Restrainers (Motion Normalized to 1.0 g) . . . . .	79
Figure 4-64	-Tie Bar Force History of the Middle Hinge Restrainers (Motion Normalized to 1.0 g) . . . . .	80
Figure 4-65	-Tie Bar Force History of Abutment 6 Restrainers (Motion Normalized to 1.0 g) . . . . .	80
Figure 4-66	-Longitudinal Relative Displacement History at Abutment 1 (Motion Normalized to 1.0 g) . . . . .	81
Figure 4-67	-Longitudinal Relative Displacement History at the Middle Hinge (Motion Normalized to 1.0 g) . . . . .	81

Figure 4-68 -Longitudinal Relative Displacement History at Abutment 6 (Motion Normalized to 1.0 g) ..... 82

## LIST OF TABLES

Table 3-1	-Section Properties . . . . .	10
Table 3-2	-Abutment Foundation Spring Coefficients . . . . .	10
Table 3-3	-Input Parameters for the Different Expansion Joints . . . . .	17
Table 4-1	-Structural Periods and Participation Factors . . . . .	19
Table 4-2	-Symbols used in the Tables and Graphs . . . . .	20
Table 4-3	-Symbols used in the Tables and Graphs . . . . .	21
Table 4-4	-Maximum Displacement of the Expansion Joint Fixed Nodes . . . . .	28
Table 4-5	-Maximum Displacement of the Expansion Joint Free Nodes . . . . .	29
Table 4-6	-Maximum Relative Displacement at the Expansion Joints . . . . .	30
Table 4-7	-Maximum Longitudinal Abutment and Pile Forces and Deformations	31
Table 4-8	-Maximum Nonlinear Deformation at the Expansion Joints . . . . .	32
Table 4-9	-Permanent Nonlinear Deformation at the Expansion Joints . . . . .	33
Table 4-10	-Maximum Cable Restrainer Forces and their Percentage of the Yield Forces . . . . .	34

# CHAPTER 1

## INTRODUCTION

### 1.1 STATEMENT OF THE PROBLEM

The damage caused to bridge structures during the San Fernando earthquake of February 9, 1971, demonstrated the critical need for both theoretical and experimental research related to the seismic response of highway bridges. In order to gain a better understanding of the seismic effects on bridge structures, it is imperative to study the seismic damages to similar existing bridges during previous earthquakes. The characteristics of damage to bridge structures, include three major forms. These forms include weakness of the superstructure, substructure, and surrounding soils.

One of the most complicated elements in bridge structures is the expansion joint as it exhibits significant nonlinearities during an earthquake. The nonlinearity of the expansion joint is influenced by its many components. Few analytical and experimental investigations have been carried out in the past to determine the effect of the different components of the expansion joint on the total response of the bridge. In recent years, the influence of the expansion joint on the seismic response of structural system has become increasingly important.

### 1.2 OBJECTIVE

This report is one of a series that results from a study entitled "*Evaluation of Effects of the Seismic Retrofitting on the Earthquake Response of Highway Bridges*". The main goals of the overall project are as follows;

- 1- To review the actual performance of highway bridge hinge restrainers during the 1989 Loma Prieta earthquake.
- 2- To select some bridges for analysis according to structure type, geometry, location, and sustained damage.

- 3- To develop detailed mathematical models to represent the selected bridges with particular emphasis on the expansion joint components.
- 4- To simulate the Loma Prieta earthquake on the mathematical models of the selected bridges and study their responses.
- 5- To carry out a parametric study of these bridges to determine the effect of stronger earthquakes, influence of cable restrainers and other retrofitting devices.
- 6- To review the restrainer design procedures and identify refinement if needed.

The study presented in this report is a part of the third, fourth and fifth objectives as outlined above. The report represents the results of the detailed study of the restrainer cable effectiveness on the Aptos Creek bridge.

## CHAPTER 2

### BRIDGE DESCRIPTION AND DAMAGE

#### 2.1 DESCRIPTION OF THE BRIDGE

The Aptos Creek bridge is located about six miles east of Santa Cruz in Santa Cruz County, connecting Santa Cruz with Watsonville. The bridge was designed in 1947 according to the 1943 AASHO (American Association of State Highway Officials) specifications for highway bridges. The construction of the bridge was completed and the bridge was opened to traffic in 1949.

Figure 2-1 presents a schematic drawing of the Aptos Creek bridge. The bridge is a five span reinforced concrete slab girder type structure with an expansion joint located in span three, about eleven feet away from bent number four. It should be noted that the middle expansion joint divides the structure into two continuous frames. The first frame, referred to as *frame I*, extends between abutment 1 and the interior expansion joint. *Frame II* extends between the interior expansion joint and abutment 6. The total length of the bridge is 260 feet. The first four spans are 56 feet long each, whereas the fifth span is 32 feet long. The overall width of the bridge is 62 feet. None of the bridge supports or joints are skewed.

The superstructure consists of ten reinforced concrete girders supporting a 6.5" thick slab. The beams are cast monolithically with the slab which in turn is cast monolithically into a continuous cap. The cap is cantilevered over the columns to support the exterior girders. The bent cap cross sectional dimensions are 4' wide and 9' deep between the columns, then the depth is tapered to 5'-7" at both ends of the bent cap. All the dimensions of the bent caps are identical. The typical cross section dimensions for the girders are 1'-6" wide and 4'-6" deep. Diaphragms are provided at mid spans and at both ends of the deck to increase the torsional capacity of the superstructure. These diaphragms are 10" wide, 2'-4" deep, and 4'-10" long, and they are cast

monolithically with the superstructure. Figure 2-2 shows typical cross sections of the superstructure and the bents.

The columns of each bent are pinned at the footings. Each pin consists of a concrete neck cast monolithically with the footing. The typical cross sectional dimensions of the columns and the column neck are 4' X 6' and 3' X 4'-4" respectively. The hinge reinforcement consists of six square dowels, each having a cross section of 1 1/4" X 1 1/4". The dowels are placed in a scissor pattern, thus preventing transmission of moments from the columns to the foundations. The dowels were placed 2' apart symmetrically about the column transverse centerline. The column reinforcement consists of square bars, each having a cross section of 1 1/8" X 1 1/8".

The columns of each bent are attached to a combined reinforced concrete footing. Bents number two and three have additional plain concrete sub-foundation. The configuration of the column base and footing is shown in Figure 2-2.

At each abutment, the bridge girders are supported on metal bearing bars. The fixed bearing provides pinned connections between the girders and the abutments. Each bearing bar is 3" X 3" X 1'-3 1/2". The bars at each bearing are welded to a bottom plate. The joint configuration allows for one inch movement in each of the transverse and the longitudinal directions. The bottom plate is anchored to the abutment by two bolts. The bearing bars are located under the girders at both abutments. Figure 2-3 shows a typical bearing assembly. The bearing mechanism allows for thermal and shrinkage movements along the longitudinal and transverse axes of the bridge. The intermediate expansion joint is fitted with two steel angles as shown in Figure 2-4 to minimize friction. Each angle is 6 X 4 X 3/8". The intermediate expansion joint is designed to allow rotations about all axes and translation in both horizontal directions, and to restrain the relative displacement in the vertical direction. The two angles are tied together with  $\phi$  3/8" bolts at 5' intervals as shown in section A-A of Figure 2-4. At the Intermediate expansion

joint the longitudinal and the transverse translations are restrained by shear bolts. The seat gap was specified, in the blue prints, at both abutments and at the intermediate expansion joint as 1 inch. The seat gaps were filled with molged expansion joint material at the time of construction. Figure 2-4 shows details of the middle expansion joint.

At both ends, the bridge is supported on standard seat-type abutments, which in turn are supported on steel piles. The abutment wall width has a constant thickness of 1 foot and clear height of 4'-11". The centerline of the metal bearing bar is located at a distance of one foot from the abutment back wall. The wing wall is connected to the abutment wall through shear dowels. At abutment 1 there are 10 battered piles, each 60 feet long and at abutment 6 there are 10 battered piles, each 40 feet long. These piles have an individual design capacity of 40 tons. The battered piles have slope 1 to 3. The combined footings used at bents 2 and 3 have dimensions of 8' wide X 60' long X 4' deep and at bents 4 and 5 they have dimensions of 7' wide X 60' long X 4' deep.

The specified concrete used for this bridge has minimum compressive strength of 3000 psi, and the steel was specified as grade 50.

## **2.2 RETROFITTING**

The Aptos Creek bridge was retrofitted in 1983 to mitigate potential damage due to future seismic activity. Horizontal earthquake restrainer units were placed at the abutments and at the intermediate hinge. At both abutments, there are 6 restrainer units, with cables in a through loop configuration. Each end of the loop is attached to the abutment, and thus there are two attachment points for each restrainer unit. Figure 2-5 shows the details of the retrofitting at the abutments. At the middle expansion joint there are four restrainer units tying the expansion joint with bent number four. Each one of these restrainer units consists of five 3/4" cables. Two galvanized steel pipes of 3 3/4" in diameter filled with concrete are placed across the

intermediate expansion joint to provide dowels action to resist the relative transverse movement. Figure 2-6 shows the details of the retrofitting at the middle expansion joint. The longitudinal hinge restrainers are provided with a gap to accommodate the expected movements due to change in the temperature. In addition to that, the hinge opening was adjusted during the construction to accommodate the expected seasonal temperature change. At both abutments and the middle hinge, all the restrainers and the steel pipes are symmetrical about the longitudinal axis of the bridge.

### **2.3 EARTHQUAKE DAMAGE**

Following the Loma Prieta earthquake of October 17, 1989, *Caltrans* (California Department of *Transportation*) engineers conducted preliminary inspections of more than 1500 bridge structures in the area affected by the earthquake. One of those bridges was the Aptos Creek, which suffered some damage during the earthquake.

According to the Caltrans damage report, the right and the left curtain walls at abutment 1 were cracked and spalled (3 1/2" X 4 1/2" X 1'). Also there was a large spall in the overhang soffit above the curtain walls (2 1/2' X 1 1/2').

The superstructure moved transversely and came to rest after it moved one inch to the left of abutment number one. All the bottom plate anchor bolts were sheared off and the ends of the groute pads had broken loose due to the movement.

## CHAPTER 3

### ANALYTICAL MODELS

#### 3.1 DESCRIPTION OF THE ANALYTICAL MODELS

In order to evaluate the dynamic response of the bridge during the 1989 Loma Prieta Earthquake, two types of analysis were considered in this study. The first type, a modal analysis of the structure, was used to determine the mode shapes and corresponding frequencies. This analysis was needed to determine the Rayleigh's damping coefficients which are required as input for the second stage of analysis. Also, interpretation of the analysis allows one to predict the overall response of the bridge. The study was performed using the computer program *IMAGES-3D* [3]. Subsequent to obtaining the Rayleigh's damping coefficients, a nonlinear time-history analysis was completed to predict the nonlinear behavior of the different bridge elements. This analysis was performed by comparing the results from the computer program with the observed performance of the bridge during the 1989 earthquake. The computer program *NEABS-86* [4,8] was used to perform this kind of analysis.

#### 3.2 BRIEF DESCRIPTION OF COMPUTER PROGRAMS

Two computer programs have been used in this study to get the overall dynamic behavior of the Aptos Creek bridge. A brief description of each computer program is listed below:-

##### 3.2.1 IMAGES-3D

The computer program *IMAGES-3D*, *Interactive Microcomputer Analysis and Graphics of Engineering System-3D*imensional (version 1.6), was used in the frequency analysis of the bridge [3]. This is a finite element analysis program that can be used for modal, linear-elastic static, and dynamic analyses of two and three dimensional structures. In this study, it was only necessary to use *IMAGES-3D* for the purpose of modal analysis for the Aptos Creek

bridge. The modal analysis was performed to calculate the frequencies, mode shapes, and participation factors for the bridge. These dynamic characteristics were necessary as input for the nonlinear program used later in this study. More details regarding the computer program can be found in reference [3].

### **3.2.2 NEABS-86**

The computer program *NEABS*, *Nonlinear Earthquake Analysis of Bridge System*, was developed by Tseng and Penzien to perform nonlinear dynamic analysis of bridge systems [16]. *NEABS* can evaluate the dynamic time-history response of a discrete system subjected to dynamic loadings and support motions at bridge columns and abutments. This computer program uses a step-by-step direct integration method with either constant or linear acceleration method in the integration. The program supports the following elements:

- 1- Elastic straight beam elements.
- 2- Linear Boundary Spring Elements.
- 3- Nonlinear Expansion Joints (modeled by elasto-plastic elements).
- 4- Hysteretic elasto-plastic elements to model the nonlinearity of columns.
- 5- Degrading Bi-linear model to model the nonlinearity of columns (currently not in use).

### **3.3 LINEAR ANALYTICAL MODEL (IMAGES-3D)**

The primary objective of this study is the analysis of response of the Aptos Creek bridge under the 1989 Loma Prieta earthquake with particular emphasis on the nonlinear behavior of the structure. In order to determine the frequencies of the bridge, it was necessary to build a linear mathematical model. Figure 3-1 shows the lumped mass model used to idealize the linear behavior of the bridge. The computer program *IMAGES-3D* [3] was used for the linear analysis.

The linear analytical model idealizes the structure as an assemblage of line members coinciding with the center line of the structural elements. Since

the center line of the deck does not intersect with the center line of the bent cap in elevation, very stiff vertical elements were used to connect the deck to the bent elements. It should be noted that the bent cap properties were adjusted, by increasing the moment of inertia in the three directions, to account for the additional stiffness, resulting from the construction of the cap as an integral part of the superstructure. The rigid elements that represent the bent caps were used to model the transverse displacements of the columns with respect to the center line of the bridge. The structure is assumed to be supported by a rigid foundation at the bents. In view of the high strength of the soil and the large plane of the combined footings, the rigid foundation assumption appears to be satisfactory.

The modulus of elasticity for the concrete was calculated by using the following formula [10]:

$$E_c = 57,000 \sqrt{f_c} \quad 3-1$$

where  $f_c$  is the design strength of the concrete. The Poisson's ratio ( $\nu$ ) for the concrete was taken equal to 0.2. The unit weight ( $\gamma$ ) of the superstructure was increased to 175 pcf to account for the paving materials.

The two column monolithic bents were modeled as continuous frames. To simulate the freedom of rotation at the intermediate expansion joint, moment releases in all three coordinate directions were used at one end of the beam. The element properties, cross sectional area, moment of inertia, and torsional constant are shown in Table 3-1. The total moments of inertia and the gross areas were used for the columns and the beams, without any deductions in the frequency analysis and the nonlinear analysis.

**Table 3-1 Section Properties.**

Location	$A$ (ft <sup>2</sup> )	$I_z$ (ft <sup>4</sup> )	$I_y$ (ft <sup>4</sup> )	$J$ (ft <sup>4</sup> )	$E$ (ksi)
Deck	59.38	188.645	30102.5	53.17	449571.
Column	24.0	72.0	32.0	77.2	449571.
Bent Cap	1000.0	1000.0	100000	1000.0	449571.

All the bent supports were assumed to be pinned to the rigid footings. Foundation flexibility was considered only at the abutments. The foundation flexibility at the abutments was modeled by equivalent sets of linear springs. The abutments soil spring coefficients were calculated based on the *Bridge Design Aids* manual [12], which is a methodology for the calculation of linear elastic boundary spring elements at the foundation/abutment interface. Since the soil springs are activated only when they are subjected to compression, only one abutment spring is active at a time. To account for this, the longitudinal abutment stiffnesses were reduced by fifty percent. In calculating the transverse stiffness of the abutment, two thirds of the wing wall stiffness was added according to the Caltrans method. The abutment spring coefficients are shown in Table 3-2. These values are the stiffness of the total system including the abutment wall, piles, and wing walls.

**Table 3-2 Abutment Foundation Spring Coefficients.**

Spring Coefficients	$K_x$ (kips/ft)	$K_y$ (kips/ft)	$K_z$ (kips/ft)	$K_{\theta x}$ (k-ft/rad)	$K_{\theta y}$ (k-ft/rad)	$K_{\theta z}$ (k-ft/rad)
Abutments 1 & 6	74604	10 <sup>6</sup>	46231	0.0	0.0	0.0

### **3.4 RAYLEIGH' S DAMPING COEFFICIENTS**

Since the computer program *NEABS-86* (*Nonlinear Earthquake Analysis of Bridge System-86*) [8] uses the Rayleigh damping approach, it was necessary to calculate the mass and the stiffness proportional damping coefficients. The

relative stiffness damping coefficient ( $\alpha$ ) and the absolute mass damping ( $\beta$ ) were calculated based on the natural frequencies and an assumed damping ratio of 5% for all mode shapes. The first two natural frequencies were used to find the coefficients  $\alpha$  and  $\beta$ . The procedure for calculating the damping matrix according to the Rayleigh damping methodology is briefly described below [18]:

$$[C] = \alpha [M] + \beta [K] \quad 3-2$$

$$\zeta_1 = \frac{1}{2 \omega_1} (\alpha + \beta \omega_1^2) \quad 3-3$$

$$\zeta_2 = \frac{1}{2 \omega_2} (\alpha + \beta \omega_2^2) \quad 3-4$$

where  $\alpha$  is the mass-proportional damping,  $\beta$  is the stiffness-proportional damping,  $[C]$  is the damping matrix,  $[M]$  is the mass matrix,  $[K]$  is the stiffness matrix, ( $\zeta_1$  and  $\zeta_2$ ) are the damping factors for the first two modes, and ( $\omega_1$  and  $\omega_2$ ) are the circular frequencies of the first two mode shape.

### **3.5 NONLINEAR ANALYTICAL MODEL (NEABS-86)**

For the nonlinear analysis of the bridge, the computer program *NEABS-86* was used [4]. The mathematical model consists of 76 element nodes, 21 reference nodes, 72 linear elastic straight beam-column elements, 2 boundary spring elements, and 24 expansion joint elements. The nonlinear mathematical model used to idealize the bridge is shown in Figure 3-2. For the nonlinear analysis it was necessary to calculate the different element stiffnesses and yield forces. The structure of the mathematical model used for the nonlinear analysis is similar to the one of the linear model which was used for the frequency analysis except the following:

#### **3.5.1 Bridge Deck and Columns**

The bridge deck and the columns were modeled as linear elastic straight

beam elements. Each span was subdivided into four straight beam elements, while each column was subdivided into three beam elements [13]. The element properties of the bridge deck, the columns, and the bent caps are shown in Table 3-1.

Due to the fact that no damage occurred to the bridge columns during the Loma Prieta earthquake, no hysteretic elements were used to represent the top and the bottom connections of the columns.

### 3.5.2 Abutment Expansion Joints

At each abutment it was necessary to provide eight expansion joint elements. Four of these elements were used to represent the nonlinearity of the bearing bars and the anchor bolts, two in the longitudinal direction, and two in the transverse direction. Two of the remaining expansion joints modeled the nonlinearity of the lateral stiffness of both the abutments and the piles. Finally, the remaining two expansion joints represented the nonlinear behavior of the cable restrainers and the impact between the abutment and the deck.

#### 3.5.2.1 Abutment and Piles

In the longitudinal direction of the bridge, each abutment was modeled as a nonlinear expansion joint. These springs become active only when the bridge moves toward the soil. The abutment springs were calculated based on the Caltrans approach [12] that is assumed based on 200 kips/inch per line foot of the abutment. The yield force of the abutment was calculated based on an approximate abutment effective soil stress of 7.7 ksf. The pile springs were calculated based on the same approach that is 40 kips/inch for OSD standard 45 ton and 75 ton piles. The yield force for each pile was taken equal to 40 kips [12]. In the lateral directions, the rest of the springs were modeled as linear boundary spring elements. A summary of the spring coefficients used for the boundary spring elements is shown in Table 3-2.

#### 3.5.2.2 Abutment Bearing Bars

At both abutments, the metal bearing bars were modeled by using nonlinear expansion joint elements. In the longitudinal and transverse

directions, the stiffness of the bearings was calculated by considering the contribution from both bending and shearing of the bearing bar and the elongation of the anchor bolts. This elongation is caused by the rotation of the bearing plate, which is considered to be rigid (Figure 2.3). By imposing a unit displacement, the bearing spring coefficients were determined.

The bending stiffness including shear deformation can be calculated as:

$$K = \frac{12 EI}{(1 + 4\beta) L^3} \quad 3-5$$

where

$$\beta = \frac{3 EI}{G A L^2} \quad G = \frac{E}{2 (1 + \nu)} \quad 3-6$$

$E$  is the modulus of elasticity,  $G$  is the shear modulus,  $A$  is the shear area of the bearing bar,  $L$  is the bar length,  $\nu$  is the Poisson's ratio, and  $I$  is the moment of Inertia of the bearing bar.

The axial anchor bolt stiffness can be calculated as;

$$K = \frac{E A_b}{L_b} \quad 3-7$$

where  $E$  is the modulus of elasticity,  $A_b$  is the axial area of the bolt, and  $L_b$  is the length of the bolt.

Then assuming that the bearing bar and the anchor bolt springs are connected in series, the equivalent stiffness of the system can be calculated as:

$$\frac{1}{K_{equivalent}} = \frac{1}{K_{bearing}} + \frac{1}{K_{anchor}} \quad 3-8$$

where  $K_{equivalent}$  is the equivalent stiffness of the system,  $K_{bearing}$  is the bearing bar stiffness (*including bending and shear*), and  $K_{anchor}$  is the anchor bolt stiffness (*axial*).

### 3.5.3 Middle Hinge Expansion Joints

At the middle expansion joint eight expansion joint elements were used. Four of these elements were necessary to model the nonlinearity behavior of the shear bolts, two in the longitudinal direction, and two in the transverse direction. Two of the remaining expansion joint elements represented the nonlinear behavior of the shear pipes in the transverse direction. Finally, the remaining two expansion joint elements represented the nonlinear behavior of the cable restrainers and the impact between the adjacent parts of the superstructure.

#### 3.5.3.1 Middle Hinge Shear Pipes

At the middle expansion joint, the galvanized steel pipes were modeled by using two nonlinear expansion joints in the transverse direction. The stiffness was calculated by treating the middle part of the galvanized steel pipe as a column fixed from both sides. The contribution from both bending and shearing was considered. The equations used to calculate the stiffness of the shear pipes are the same as equations 3-5 and 3-6. In these equations,  $L$  represents the diameter of the pipe plus the seat gap. The yield force was calculated based on the Caltrans approach [13] assuming that the effective area of the bearing is thirty percent of the shear pipe circumference.

#### 3.5.3.2 Middle Hinge Shear Bolts

At the middle expansion joint, the shear bolts used to connect the two frames were modeled by two expansion joints in the transverse direction and another two in the longitudinal direction. The stiffness of the shear bolts were calculated by treating the shear bolts as fixed-fixed column. The contribution from bending and shear was considered. Equations 3-5 and 3-6 were used to calculate the stiffnesses. The yield force of the shear bolts were determined from the AISC manual [19].

### 3.5.4 Cable Restrainers

The cable restrainers were modeled with another expansion joint element. The equivalent tensile stiffness and yield force of the cable restrainer units were

calculated using the following equations [13]:

$$K_r = \frac{E A_r N_r}{L_r} \quad 3-9$$

$$F_y = \sigma_y A_r N_r \quad 3-10$$

where  $E$  is the modulus of elasticity after initial yielding and it is equal to 18,000 ksi,  $F_y$  is the yield stress in the restrainer (176.1 ksi),  $A_r$  is the area of the restrainer (0.222 in<sup>2</sup> for 3/4" cables),  $L_r$  is the length of the restrainer, and  $N_r$  is the number of cables in the restrainer unit.

### **3.5.5 Impact**

To take account of the joint collisions, impact springs were incorporated into the analytical model. The impact stiffness was taken equal to 180000 kips/ft. This stiffness is nearly the same as the magnitude of the longitudinal stiffness of the beam elements representing the superstructure [2].

The input parameters used to model the different types of the expansion joint hinge properties are shown in Table 3-3.

## **3.6 SEISMIC EXCITATION**

Motions caused by the Loma Prieta earthquake were recorded by the California Strong Motion Instrumentation Program (CSMIP) [17] in several locations. The ground acceleration used in this study was selected with the objective of representing the actual excitation at the bridge site during the Loma Prieta earthquake. Seismographic instruments were installed at Capitola fire station and indicated a peak ground acceleration of 0.3984g in the north-south direction and of 0.4719g in the east-west direction. The fire station is located about four miles away from the bridge site. It was assumed that the bridge site experienced the same accelerations as the Capitola fire station during the earthquake. This assumption is valid if the underlying soils were relatively stiff and thus did not contribute to significant site amplification.

The north-south axis of the fire station was approximately parallel to the longitudinal axis of the bridge. Thus, it seemed reasonable to assign the north-south component of the earthquake record to the longitudinal direction of the bridge, and accordingly the east-west component of the transverse direction of the bridge.

Plots of the acceleration records are shown in Figures 3-3 and 3-4. The time intervals used for the earthquake record was 0.02 seconds. However, for the analysis an interval of 0.005 seconds was used. This refinement was necessary for more accurate results. The total recorded length of the motion is 39.98 seconds. It was decided to use only 8.8 seconds to reduce the computational effort.

To investigate the effects of the magnitude of the ground motion on the bridge response two more amplification of longitudinal and transverse excitation were used. In the first one, both the longitudinal and the transverse record were normalized to a 0.7g peak ground acceleration. In the second one, the normalized peak general acceleration was equal to 1.0g.

Table 3-3 Input Parameters for the Different Expansion Joints.

	Yield Force (Kips)	Stiffness (kips/ft)	Seat-Gap (ft)	Tie-Bar-Gap (ft)	No. of Cables	Cable Locations	Impact
Abutment Hinge	1771.5	74604.0	0.0833	0.0	1	0.0	0.0
Piles Hinge	100.0	1200.0	0.0833	0.0	6	± 3.083	0.0
Abutment Bearing	104.72	56018.9	0.0	0.0	6	± 3.083	0.0
Abutment Bearing	104.72	56018.9	1.0	0.0	6	± 0.02	0.0
Abutment	78.188	532.8	0.0833	0.0833	6	± 3.083	0.0
Hinge Shear Bolts	44.2	72746.4	0.0	0.0	6	± 3.083	0.0
Hinge Shear Bolts	44.2	72746.4	1.0	0.0	6	± 0.02	0.0
Hinge Shear Pipes	64.0	148896.	1.0	0.01	2	± 0.1	0.0
Hinge Retrofitted	195.47	1393.95	0.0833	0.0625	4	± 18.5	0.0
Impact Hinge	1.0	1.0	0.0833	0.0	---	---	180000.

## CHAPTER 4

### ANALYTICAL RESULTS

#### 4.1 STRUCTURE PERIODS AND FREQUENCIES

The computer program *IMAGES-3D* [3] was used to perform the modal analysis of the Aptos Creek bridge. The first ten mode shapes, periods, and participation factors were calculated for the bridge and are presented in Table 4-1. Figure 4-1 shows the first ten mode shapes of the bridge. Closer examination of the mode shapes and the participation factors indicated that there were three patterns of response behavior. The first type of response was predominantly transverse as indicated in the plots for modes 1, 3, 4, and 10. In this case the bent cap was rotating as a rigid body in a horizontal plane, elastically restrained by the columns. The bent cap rotation had a tendency to introduce opposite shear forces in the tops of the columns normal to the plane of the bent. Corresponding to these shear forces are moments in a vertical plane perpendicular to the plane of the bent. Mode 2 characterizes the second pattern which includes the longitudinal mode of vibration. The third pattern of vibration, which is predominantly vertical, occurs in modes 5, 6, 7, 8, and 9 as shown in Figure 4-1. The contribution of these modes to the final response of the bridge is minimal.

Closer inspection of the mode shapes, as covered above, indicates the structure behaved predominantly in the transverse direction. It is interesting to note that the bridge is significantly weaker in the transverse direction, when compared to the longitudinal direction.

In the linear analysis, the intermediate expansion joint was modeled as a hinge in accordance with Caltrans design guidelines [12]. For this reason, different element stiffnesses, customarily used, were not accounted for. The expansion joints that are located at the abutments were disregarded, thus the bridge deck was directly connected to the abutment springs. Evidence of

coupling between *frame I* and *frame II* is apparent due to these assumptions. The coupling effect is most visible in the first pattern of vibration which characterizes the transverse response of the bridge.

In this study, only the first two mode shapes were used to calculate Rayleigh's damping coefficients as discussed in Chapter 2. A uniform damping coefficients of 5% was selected for all mode shapes. Therefore the effect of variation of modal damping was not included in this study.

**Table 4-1** Structural Periods and Participation Factors.

Mode Shape	Periods (Sec)	Participation Factors		
		X	Y	Z
Mode 1	0.7445	0.0112	-0.00024	1.328
Mode 2	0.5048	1.087	0.00078	-0.00454
Mode 3	0.3814	0.0207	0.00079	0.09318
Mode 4	0.2526	-0.0233	-0.4621	0.9122
Mode 5	0.2016	-0.0349	0.1781	-0.01302
Mode 6	0.1662	-0.1091	-0.4193	-0.0006918
Mode 7	0.1469	-0.0609	1.591	0.00833
Mode 8	0.1453	-0.0479	-0.7155	0.0319
Mode 9	0.1337	-0.0084	1.787	0.01667

#### **4.2 PARAMETRIC STUDY AND RESULTS**

The main objective of the study was to investigate the overall response of the bridge components to the Loma Prieta earthquake, with particular emphasis on the cable restrainers and hinge shear bolts. The overall response included a detailed study of expansion joint components such as cable restrainers, shear pipes, bearing bars as well as hinge separation and impact. To perform a complete investigation of the role of the hinge elements on the performance of the bridge, eight different cases were studied. A summary of these cases is

presented in Table 4-2.

**Table 4-2** Analysis Identification Number.

Case	Tie-Bar-Gap <i>(inch)</i>	Shear Bolts	Ground Motion	
			Transverse	Longitudinal
1	0.0	Accounted for	0.4179g	0.3984g
2	Without Cables	Accounted for	0.4179g	0.3984g
3	3/4	Accounted for	0.4179g	0.3984g
4	0.0	Removed	0.4719g	0.3984g
5	0.0	Accounted for	0.7g	0.7g
6	Without Cables	Accounted for	0.7g	0.7g
7	0.0	Accounted for	1.0g	1.0g
8	Without Cables	Accounted for	1.0g	1.0g

In the first case the bridge was subjected to the Capitola fire station seismic record. In the second case the cable restrainers were removed in order to compare with the first case and identify their role on the seismic response of the bridge. In the third case the tie-bar-gap was reduced to 3/4", while in the fourth case the middle expansion shear bolts were removed. In cases number 5 and 6, the response of the bridge with and without the cable restrainers respectively was analyzed for higher level of ground motions. This was accomplished by normalizing the Capitola fire station record to 0.7g peak ground acceleration in both plane directions. Similarly in cases number 7 and 8, the response of the bridge was evaluated with and without cable restrainers, but the structure was subjected to seismic excitation with peak ground acceleration of 1.0g in both plane directions.

The following symbols will enable the reader to interpret data in the tables and graphs:

**Table 4-3** Symbols used in the Tables and Graphs.

Symbols	Interpretation	Symbols	Interpretation
<b>TBG</b>	<b>Tie-Bar-Gap</b>	<b>SG</b>	<b>Seat-Gap</b>
<b>Long.</b>	<b>Longitudinal</b>	<b>Trans.</b>	<b>Transverse</b>
<b>Abut. (1)</b>	<b>Abutment 1</b>	<b>Abut. (6)</b>	<b>Abutment 6</b>
<b>Mid. Exp. Jt.</b>	<b>Middle Expansion Joint</b>		

The subsequent sections discuss in detail the response of different components of the bridge to the above mentioned cases.

#### **4-2.1 OVERALL DISPLACEMENT RESPONSE**

In *NEABS* the expansion joint is represented by two nodes with infinitesimal distance between them. One of these nodes is acting as a support and the other moves free relative to the first one. Tables 4-4 and 4-5 show the maximum superstructure displacements for all cases at the free and the support nodes of the expansion joints respectively. The fixed node numbers for abutment 1, the intermediate expansion joint, and abutment 6 are 1, 40, and 76 respectively. For the bridge components listed above, the free node numbers are 2, 39, and 75 respectively. It can be noted from these tables that the free nodes underwent significantly larger displacements in comparison to the fixed nodes. Some selected overall displacement response histories are discussed in more details below.

Figures 4-2 through 4-7 show the overall superstructure displacement time histories for case number 3. This is the case that represented more closely the way the bridge was actually retrofitted since in the retrofitting drawings the cable restrainers are shown to have an initial sag, which is represented by the

3/4" Tie-Bar-Gap. It can be seen from these figures that the longitudinal displacements were relatively small compared to the transverse displacements. Also, the displacements at abutment 1 were much larger than the displacement at abutment 6. This is probably due to the fact that frame number two is stiffer than frame number one. The transverse movement at abutment 1 was as high as 4", which is consistent with the observed damage described in the damage report. The displacement response histories were then calculated for case number 2, in which the cable restrainers were removed. It was found that the response in this case were almost identical with the response in case number 3. This indicates that the cable restrainers were not activated at this level of excitations and therefore they did not play a major role in the response of the bridge.

#### **4-2.2 RELATIVE DISPLACEMENT RESPONSE**

The maximum longitudinal and transverse hinge separations that occurred at both abutments and at the intermediate expansion joint, are tabulated in Table 4-6. The hinge separation is the movement of the free node of the expansion joint relatively to the support node. The complete time histories for case number 3 with 3/4" TBG and 1" SG are shown in Figures 4-8 through 4-13. As it was discussed above, at this level of excitation the cable restrainers were not activated and therefore the relative displacement responses with and without the cables were the same. Figures 4-14 through 4-19 show the complete time histories for cases number 5 and 6 with the motion normalized to 0.7g in both direction. In these graphs the solid lines represent case No. 5 with the cable restrainers, while the dashed lines represent case No. 6 with the cable restrainers removed.

Based on the results shown in the tables and the graphs, the following remarks can be made;

- 1- The wave shapes of the longitudinal and transverse directions, for each expansion joint, are almost identical for all cases, with some magnification as the input base motion increases.

- 2- The hinge opening at abutment 1 was much larger than that at abutment 6 in both the longitudinal and transverse directions for all cases. This difference can be attributed to the significant difference in stiffness between *frames I* and *II*.
- 3- The relative displacement in the transverse direction was larger than in the longitudinal direction for all cases. This is consistent with the earlier remark that the predominant motion of the bridge was in the transverse direction.
- 4- Removal of the hinge shear bolts at the intermediate expansion joint did not significantly change the response in both the longitudinal and the transverse directions.
- 5- The difference in the longitudinal and transverse relative displacements between the cases with or without cable restrainers was not significant.
- 6- In general, the maximum longitudinal relative displacements in the cases without cable restrainers were higher than the cases with cable restrainers.
- 7- By amplifying the peak ground acceleration to 0.7g and 1.0g, the restrainers were activated and helped in reducing the maximum movements.

#### **4-2.3 ABUTMENT AND PILES RESPONSE**

The maximum longitudinal forces and deformations of both abutments and their supporting piles, for all cases, are tabulated in Table 4-7. In all the cases studied abutment 1 experienced larger forces than abutment 6. This was expected since *frame I* of the bridge is more flexible than *frame II*. The cable bar elements which were used to model the abutments and the piles did not reach the yield point in the first four cases. Abutment 1 started to yield when the base motion was normalized to 0.7g in both directions. Figures 4-24 and 4-25 show the abutment 1 force history and its corresponding nonlinear deformation. The solid lines in these graphs represent the case with cable restrainers and the dashed lines represent the case with the cable restrainers

removed. It can be seen from these figures, that the yielding was apparent for conditions with or without cable restrainers. However, in the case without cable restrainers the abutment yielded earlier. When the base motion was normalized to 1.0g in both directions, only abutment 1 yielded. Figures 4-26 through 4-29 show the force and the nonlinear deformation time histories at abutments 1 and 6 in cases number 7 and 8.

Based on these figures one can see that abutment 1 yielded in both cases, while abutment 6 yielded only when the restrainers were removed (case number 8). Figures 4-30 and 4-31 show the pile force and nonlinear deformation time histories for cases number 7 and 8 of the piles at abutment 1. It is obvious that the piles yielded only when the cable restrainers were removed.

#### **4-2.4 BEARING BAR**

Since in *NEABS-86* the cable restrainer elements are acting only in tension, it was necessary to model the abutments bearing bars with two expansion joint elements acting in opposite directions. Each shear force or nonlinear deformation time history represents the output from two *NEABS-86* expansion joints. This data has been combined to produce the complete shear force time history. In a similar fashion, nonlinear deformation could only be obtained by using two *NEABS-86* expansion joints. To obtain total nonlinear deformation, it was necessary to subtract the negative deformation from the positive deformation. This approach was also used for the shear pipes and the shear bolts to produce the shear force and the nonlinear deformation time histories.

Plots of the time history describing the shear forces and the nonlinear deformations that occurred in the tie-bars used to model the bearing bars, are shown in Figures 4-32 through 4-47 for both longitudinal and transverse directions. Figures 4-32 through 4-39 show the response histories of the abutment bearing bars for case number 3. These figures are primarily used to illustrate the method which was used to calculate the response of the bearing

bars. The solid lines in the shear force responses in Figures 4-32 through 4-39 represent the response from one expansion joint, while the dashed lines represent the response from the other expansion joint acting in opposite direction. As mentioned above, both expansion joints elements were necessary to model the bearing bars. In Figures 4-40 through 4-47, the solid lines represent the response with the cable restrainers existing and the dashed lines represent the response with the cable restrainers removed. It can be seen that the presence of the cable restrainers did not have any significant difference on the response of the abutment bearing bars. The only exception was the direction of the nonlinear deformation time history at abutment 6, shown in Figure 4-47.

The shear force and the nonlinear deformation indicated that the capacity of the bearing bars at both abutments was exceeded in both the longitudinal and the transverse directions for all cases shown in Figures 4-32 through 4-47. As with the abutments, the bearing bars at abutment number 1 exhibited higher transverse and longitudinal displacements than the ones at abutment 6.

It should be noted that the force and the nonlinear deformation time histories of Figures 4-37 and 4-39 indicate damage at abutment 6 bearing bars in case number 3, which represents more closely the response of the bridge to the Loma Prieta Earthquake. However, no such damage was mentioned in the Caltrans damage report. This could be due to some discrepancies between the earthquake record used in this study and the actual excitation the bridge was subjected to.

#### **4-2.5 SHEAR BOLTS**

Figures 4-48 through 4-51 show the shear force and nonlinear deformation time histories of the hinge shear bolts for case No. 3. Figures 4-52 through 4-55 show the superimposed shear force and nonlinear deformation of the shear bolts for cases number 5 and 6. In all studied cases the hinge shear bolts had yielded in both directions. The presence of the cable restrainers did not appear to make any significant difference even at higher levels of

excitations.

The condition of the hinge shear bolts could not be determined, following the earthquake, due to the physical difficulty of investigating the joint (Figure 2-4).

#### **4-2.6 SHEAR PIPES**

Plots of the superimposed shear force and nonlinear deformation of the shear pipes are shown in Figures 4-56 through 4-59 for cases number 5, 6, and 7. The shear pipes experienced the same force and nonlinear deformation as the shear bolts in the transverse direction. The only difference between these two responses were in the first few seconds of the motions. This difference can be attributed to the gap in the shear pipe joint. The shear pipes yielded in all the cases studied.

#### **4-2.7 CABLE RESTRAINERS**

The longitudinal cable restrainer forces were calculated directly from the maximum force recorded for the tie bar used in modeling the restrainers. The maximum axial forces and their percentage of the yield force that occurred at the restrainer cables at both abutments and the intermediate expansion joint are tabulated in Table 4-10. Figures 4-60 through 4-65 show the cable restrainer force time histories for cases number 1 and 7 at both abutments and at the middle expansion joint.

Based on the table and the figures, the following remarks can be made:

- 1- In all the studied cases, it is clear that the cable restrainers at abutment 1 have much larger forces than at abutment 6.
- 2- It should be noted that even after magnifying the motion to 1.0g in both directions, the cable bars did not yield. This is probably due to the fact that the predominant response of the bridge was in the transverse direction.

In general, as studies of other structures have indicated that the cable restrainers can be very effective in reducing the longitudinal vibration of a bridge. However, this was not the case with the Aptos Creek bridge. The

restrainers had a minor effect on the longitudinal response of the bridge.

#### **4-2.8 IMPACT**

In the first six studied cases, impact did not occur. This fact can be verified by examining the maximum relative longitudinal displacements of the expansion joints. None of these displacements was enough to close the corresponding gaps. Impact occurred only at abutment 1 when the motion was normalized to 1.0g in both directions and with the cable restrainers present (case number 7). Figure 4-66 shows the longitudinal relative displacement at abutment 1 with impact occurring at about 6.0 seconds. By removing the cable restrainers (case number 8) the impact occurred at abutment 1 and at the intermediate expansion joint as shown in figures 4-66 and 4-67. However, the hinge gap did not close at abutment 6 as shown in Figure 4-68, therefore the impact did not occur.

**Table 4-4** Maximum Displacement of the Expansion Joint Fixed Nodes.

Case	Node 1		Node 40		Node 76	
	Long. (inch)	Trans. (inch)	Long. (inch)	Trans. (inch)	Long. (inch)	Trans. (inch)
1- With 0" TBG and 1" SG	0.24636	0.21696	0.24912	0.72036	0.1074	0.2016
2- Without Cables and 1" SG	0.2958	0.52704	0.2682	0.53136	0.09220	0.19164
3- With 3/4" TBG and 1" SG	0.2958	0.52704	0.2682	0.53136	0.09220	0.19164
4- Without shear bolts	0.2484	0.20796	0.3258	0.73728	0.76104	0.1422
5- With 0" TBG and 1" SG (0.7g)	0.41928	0.25536	0.53604	0.93192	0.14628	0.2388
6- Without cable restrainers (0.7g)	0.405	0.21144	0.56616	0.93684	0.17508	0.23928
7- With 0" TBG and 1" SG (1.0g)	0.53112	0.20724	1.04724	1.4532	0.19236	0.27204
8- Without cable restrainers (1.0g)	0.6132	0.20472	0.89844	1.5948	0.19452	0.27096

Locations of the Expansion Joint Fixed Nodes

- Node 1 is located at abutment 1.
- Node 40 is located at the intermediate expansion joint.
- Node 76 is located at abutment 6.

Table 4-5 Maximum Displacement of the Expansion Joint Free Nodes.

Case	Node 2		Node 39		Node 75	
	Long. (inch)	Trans. (inch)	Long. (inch)	Trans. (inch)	Long. (inch)	Trans. (inch)
1- With 0" TBG and 1" SG	0.39084	4.068	0.41712	4.2408	0.23832	1.14564
2- Without Cables and 1" SG	0.49116	3.6696	0.52608	4.0284	0.2568	0.71664
3- With 3/4" TBG and 1" SG	0.49116	3.6696	0.52608	4.0284	0.2568	0.71664
4- Without shear bolts	0.39888	3.9456	0.41844	3.3144	0.31872	0.22728
5- With 0" TBG and 1" SG (0.7g)	0.93648	6.9324	0.95268	5.268	0.52344	0.99528
6- Without cable restrainers (0.7g)	0.9306	6.774	0.95172	5.688	0.55716	1.02624
7- With 0" TBG and 1" SG (1.0g)	1.5696	10.3704	1.6188	7.3848	1.03728	1.5108
8- Without cable restrainers (1.0g)	1.7088	10.9788	1.7268	8.4048	0.8916	1.4064

Locations of the Expansion Joint Free Nodes

- Node 2 is located at abutment 1.
- Node 39 is located at the intermediate expansion joint.
- Node 75 is located at abutment 6.

**Table 4-6** Maximum Relative Displacement at the Expansion Joints.

Case	Abut. (1)		Mid. Exp. Jt.		Abut. (6)	
	Long. (inch)	Trans. (inch)	Long. (inch)	Trans. (inch)	Long. (inch)	Trans. (inch)
1- With 0" TBG and 1" SG	0.2772	3.9084	0.2976	4.0272	0.2004	0.96
2- Without Cables and 1" SG	0.3276	3.5052	0.3768	3.8556	0.20064	0.5892
3- With 3/4" TBG and 1" SG	0.3276	3.5052	0.3768	3.8556	0.20064	0.5892
4- Without shear bolts	0.2604	3.786	0.3492	3.3804	0.2544	0.192
5- With 0" TBG and 1" SG (0.7g)	0.7452	6.762	0.7524	4.9884	0.4596	0.9324
6- Without cable restrainers (0.7g)	0.762	6.6144	0.906	5.3136	0.4728	0.9144
7- With 0" TBG and 1" SG (1.0g)	1.134	10.2048	0.942	6.7128	0.9348	1.386
8- Without cable restrainers (1.0g)	1.5156	10.8192	1.8828	7.8168	0.8304	1.3668

Table 4-7 Maximum Abutment and Pile Forces and Deformations.

Case	Abutment (1)			Abutment (6)		
	Abutment Force (kips)	Abutment Deform. (inch)	Pile Force (kips)	Abutment Force (kips)	Abutment Deform. (kips)	Pile Force (kips)
1- With 0" TBG and 1" SG	909.10	---	27.73	792.50	---	20.03
2- Without Cables and 1" SG	1214.0	---	32.78	554.60	---	20.07
3- With 3/4" TBG and 1" SG	1214.0	---	32.78	554.60	---	20.07
4- Without shear bolts	870.90	---	26.02	607.50	---	25.40
5- With 0" TBG and 1" SG (0.7g)	1771.0	0.10392	74.49	1324.0	---	45.97
6- Without cable restrainers (0.7g)	1771.0	0.24	76.16	1375.0	---	47.31
7- With 0" TBG and 1" SG (1.0g)	1771.0	0.84864	88.22	1683.0	---	93.50
8- Without cable restrainers (1.0g)	1771.0	0.77304	100.0	1771.0	0.01061	83.00

pile def. = 0.77304 Inch

Table 4-8 Maximum Nonlinear Deformation at the Expansion Joints.

Case	Abutment (1)		Mid. Exp. Jt.		Abutment (6)	
	Long. (inch)	Trans. (inch)	Long. (inch)	Trans. (inch)	Long. (inch)	Trans. (inch)
1- With 0" TBG and 1" SG	0.17772	1.43424	0.13392	2.0568	0.09912	0.04764
2- Without Cables and 1" SG	0.17772	1.43424	0.13392	2.0568	0.09912	0.04764
3- With 3/4" TBG and 1" SG	0.19708	0.9792	0.21948	1.314	0.1398	0.15096
4- Without shear bolts	1.34796	1.7256		0.732		
5- With 0" TBG and 1" SG (0.7g)	0.47124	2.2884	0.42168	1.206	0.2995	0.29196
6- Without cable restrainers (0.7g)	0.53652	2.076	0.69732	1.6272	0.31716	0.2322
7- With 0" TBG and 1" SG (1.0g)	0.3306	3.2892	0.47208	1.6404	0.66432	0.40716
8- Without cable restrainers (1.0g)	0.64248	3.9624	1.39452	2.6004	0.6234	0.342

Table 4-9 Permanent Nonlinear Deformation at the Expansion Joints.

Case	Abut. (1)		Mid. Exp. Jt.		Abut. (6)	
	Long. (inch)	Trans. (inch)	Long. (inch)	Trans. (inch)	Long. (inch)	Trans. (inch)
1- With 0" TBG and 1" SG	0.13104	0.2496	0.10284	0.4056	0.07296	0.16428
2- Without Cables and 1" SG	0.13248	0.018	0.07476	0.5076	0.11148	0.04956
3- With 3/4" TBG and 1" SG	0.13248	0.018	0.07476	0.5076	0.11148	0.04956
4- Without shear bolts	0.12	1.2216		0.2796		
5- With 0" TBG and 1" SG (0.7g)	0.35616	1.4088	0.42168	0.7008	0.24672	0.07992
6- Without cable restrainers (0.7g)	0.23664	0.9264	0.49068	0.4692	0.252	0.3048
7- With 0" TBG and 1" SG (1.0g)	0.2514	2.0592	0.0404	0.972	0.66432	0.21744
8- Without cable restrainers (1.0g)	0.45852	1.4832	0.89412	1.1244	0.05352	0.1746

**Table 4-10** Cable Forces and their Percentage of the Yield Force.

Case	Abut. (1)		Mid. Exp. Jt.		Abut. (6)	
	Force (kips)	% of YF	Force (kips)	% of YF	Force (kips)	% of YF
1- With 0" TBG and 1" SG	12.31	15.74	34.56	17.68	5.66	7.24
4- Without shear bolts	11.55	14.77	40.53	20.73	4.338	5.55
5- With 0" TBG and 1" SG (0.7g)	33.08	42.31	87.37	44.7	9.458	12.1
7- With 0" TBG and 1" SG (1.0g)	39.17	50.1	109.5	56.02	12.02	15.4

% of YF is the Percentage of the Yield Force

Yield Force of the Abutment Cables = 78.188 Kips

Yield Force of the Intermediate Hinge Cables = 195.47 Kips

## CHAPTER 5

### CONCLUSIONS

Based on the analytical results presented in this report, the following conclusions and general remarks can be made:

- 1- The nonlinear mathematical model developed in this study predicts realistic seismic response results, when compared with damage reports.
- 2- The absolute seismic displacement response of the nodes in the longitudinal direction were smaller than the transverse in all the cases studied.
- 3- In all cases tie-bar cables did not experience high forces.
- 4- The collision between the girders and the abutments as well as between the adjacent part of the superstructure at the middle expansion joint occurred after removing the cable restrainers and normalizing the motion to 0.7g in both directions.
- 5- The bridge movements at abutment 1 were much larger than the movement at abutment 6. This difference can be attributed to the greater stiffness of frame I relative to frame II.
- 6- The longitudinal cable restrainers were not critical in resisting the motion in the longitudinal direction.
- 7- The multiple impacts at the abutment and the middle expansion joint have major influence on both the amplitude and the frequency characteristics of the response. The rebound from the collision can result in an increased positive response amplitude immediately following the collision.
- 8- The basic mathematical model and the analytical procedures developed in this report as well as the computer program NEABS can be used to predict realistic dynamic response of bridge

structure subjected to low or high seismic intensity base excitation.

- 9- The tie bars which were used to represent the nonlinearity of the bearing bars at both abutments had yielded in all cases studied. The nonlinear deformations at abutment 1 were larger than the deformation at abutment 6. This difference can be attributed to the considerable difference in relative stiffness of frames I and II.
- 10- The Collapse of the bearing bars at abutment 1 of the bridge during the 1989 Loma Prieta earthquake was due to the inability of the bearing bars to absorb the excessive forces generated by the earthquake. A major portion of that damage was caused by the significant difference in both the transverse and the longitudinal stiffness between frames I and II.
- 11- The strength and the stiffness of the bridge columns, on each side of the expansion joint, are the primary factors which most significantly affect the seismic response characteristics of the bridge.
- 12 The nonlinear time history analysis results indicated that all the cable restrainers experienced low level force. However, bearing bars, shear pipes, and shear bolts experienced considerable forces, which lead to the yielding of these elements.

## REFERENCES

1. Imbsen, R. A., Penzien, J., "Evaluation of Energy Absorption Characteristics of Highway Bridges Under Seismic Conditions Volume 1", Report No. UCB/EERC-84/17, Earthquake Engineering Research Center, University of California, Berkeley, September 1986.
2. Kawashima, K., Penzien, J., "Correlative Investigations on Theoretical and Experimental Dynamic Behavior of Model Bridge Structure," Report No. UCB/EERC 76-26, Earthquake Engineering Research Center, University of California, Berkeley, July 1976.
3. IMAGES-3D "Interactive Microcomputer Analysis of Graphics of Engineering System-3 Dimensional," Programmed: W. H. Leung, Version 1.61.
4. Ghosn, G. E., Saïidi, M. , " A Simple Hysteretic Element for Biaxial Bending of R/C Columns and Implementation in NEABS-86," Report No. CCEER 86-1, University of Nevada, Reno, July 1986.
5. Lew, H. S., Editor, "Performance of Structures During the Loma Prieta Earthquake of October 17, 1989," NIST Special Publication 778.
6. Imbsen, R. A., Schamber, R. A., "Increased Seismic Resistance of Highway Bridges using Improved Bearing Design Concepts, Volume 1, Bearing Design Concepts and Test Results," A report to U.S. Department of Transportation, Federal Highway Administration.
7. Imbsen, R. A., Nutt, R. V., Penzien, J., "Seismic Response of Bridges-Case Studies," Report No. UCB/EERC 78/14, Earthquake Engineering Research Center, University of California, Berkeley, June 1978.
8. Penzien, J., Imbsen, R. A., Liu, W. D., "NEABS: Nonlinear Earthquake Analysis of Bridge Systems (Users Manual)," NISSEE/Computer Applications, Earthquake Engineering Research Center, University of California, Berkeley, May 1981.
9. Selna, L. G., Experimental Evaluation of Performance of Earthquake Restrainer in Box Girder Bridge," ASCE, 1989, pp. 31-40.
10. ACI Committee 318-83, "Building Code Requirements for reinforced Concrete," American Concrete Institute, Detroit, 1983.
11. Seismic Design of Highway Bridges Workshop Manual," Federal Highway Administration, FHWA-IP-81-2, January 1981.

12. "Bridge Design Aids Manual," State of California, Department of Transportation, Office of the Structure Division, 1991.
13. "Bridge Memo to Designers Manual," State of California, Department of Transportation, Office of the Structure Division, 1991.
14. "Bridge Design Specifications Manual," State of California, Department of Transportation, Office of the Structure Divisions, 1991.
15. Maragakis, E., Saiidi, M., Abdel-Ghaffar, S. M., "Evaluation of the Response of the Whitewater Bridge During the 1986 Palm Spring Earthquake," 8th US-JAPAN Bridge Engineering Workshop, Chicago, II, May 1992.
- 16- Tesng, W. S., and Penzien, J., "Analytical Investigations of the Seismic Response of Long Multiple-Span Highway Bridges," College of Engineering, U.C. Berkeley, Earthquake Engineering Research Center, Report No. EERC 73-12, June, 1973.
- 17- Shakal, A., M. Huang, M. Reichle, C. Ventura, T. Cao, R. Sherburne, M. Savage, R. Darrah, And C. Peterson. 1989. "CSMIP strong-motion records from the Santa Cruz Mountains (Loma Prieta), California earthquake of 17 October 1989." Report No. OSMS-89-06. Sacramento: California Department of Conservation, Division of Mines and Geology.
- 18- Saiidi, M., Sozen, A. M. , "Simple and Complex Models for Nonlinear Seismic Response of Reinforced Concrete Structures," Report No. UILU-ENG-79-2013, University of Illinois at Urbana-Champaign, August 1979.

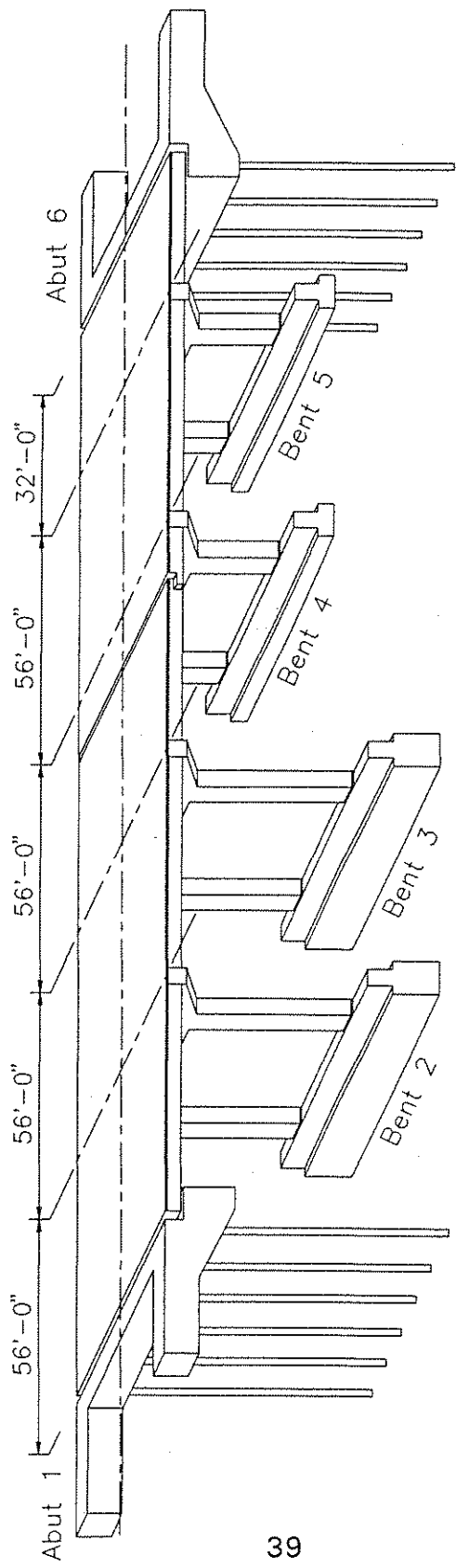


**Figure 2-1** -Schematic Drawing of the Aptos Creek Bridge

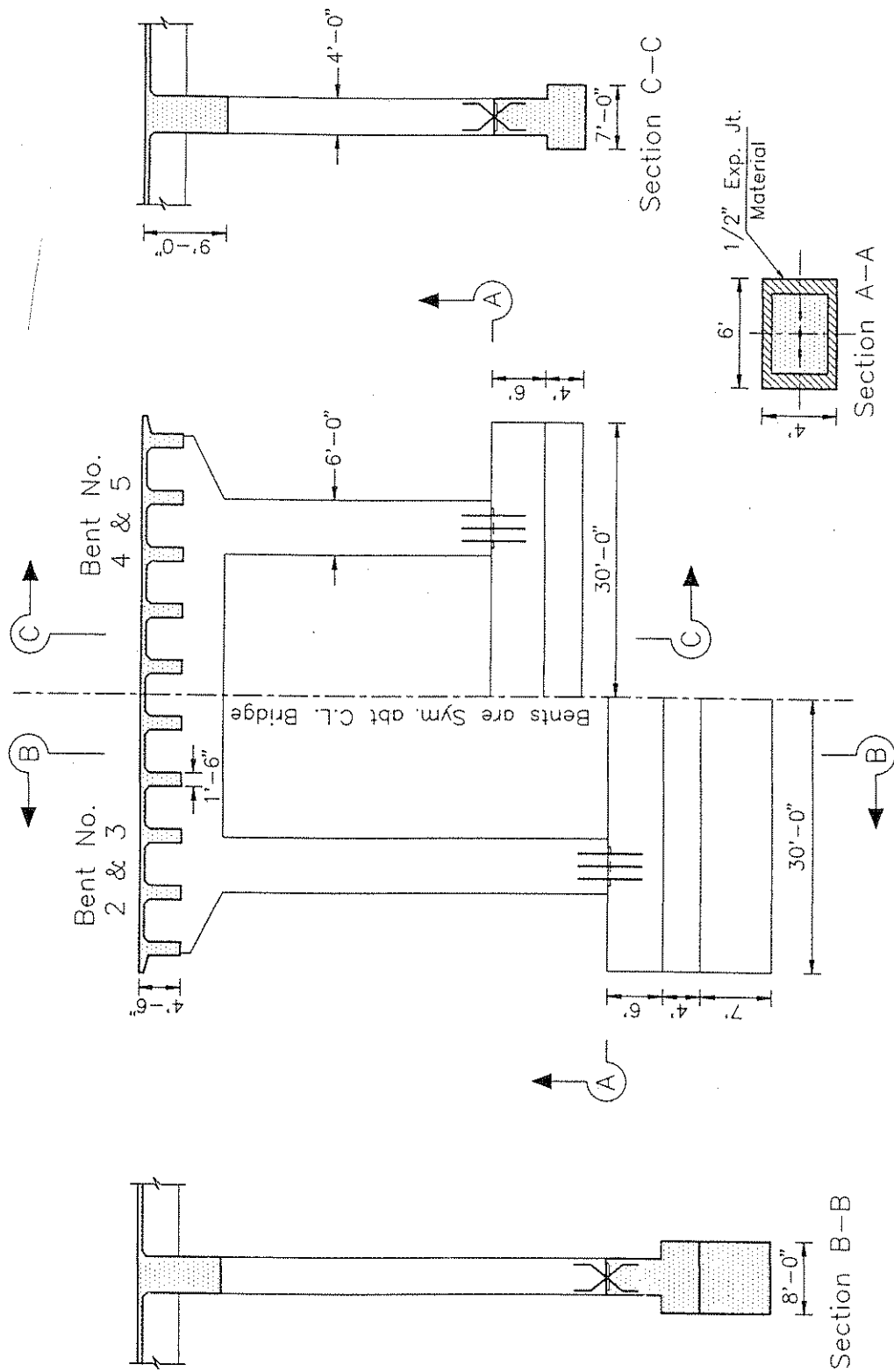


Figure 2-2 - Typical Cross Section of the Bridge

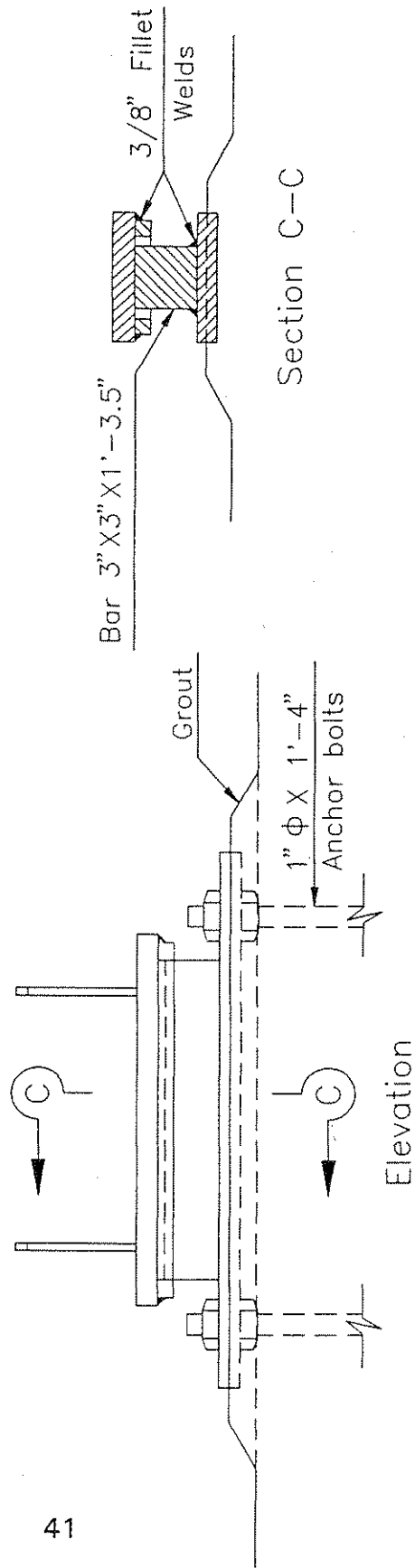
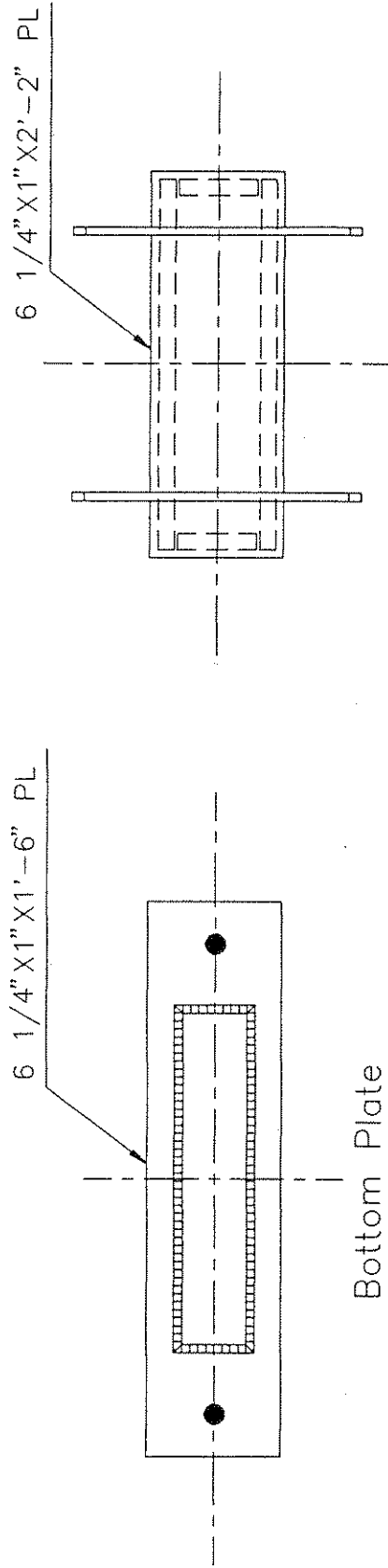


Figure 2-3 -Fixed Bearing Assembly at both Abutments

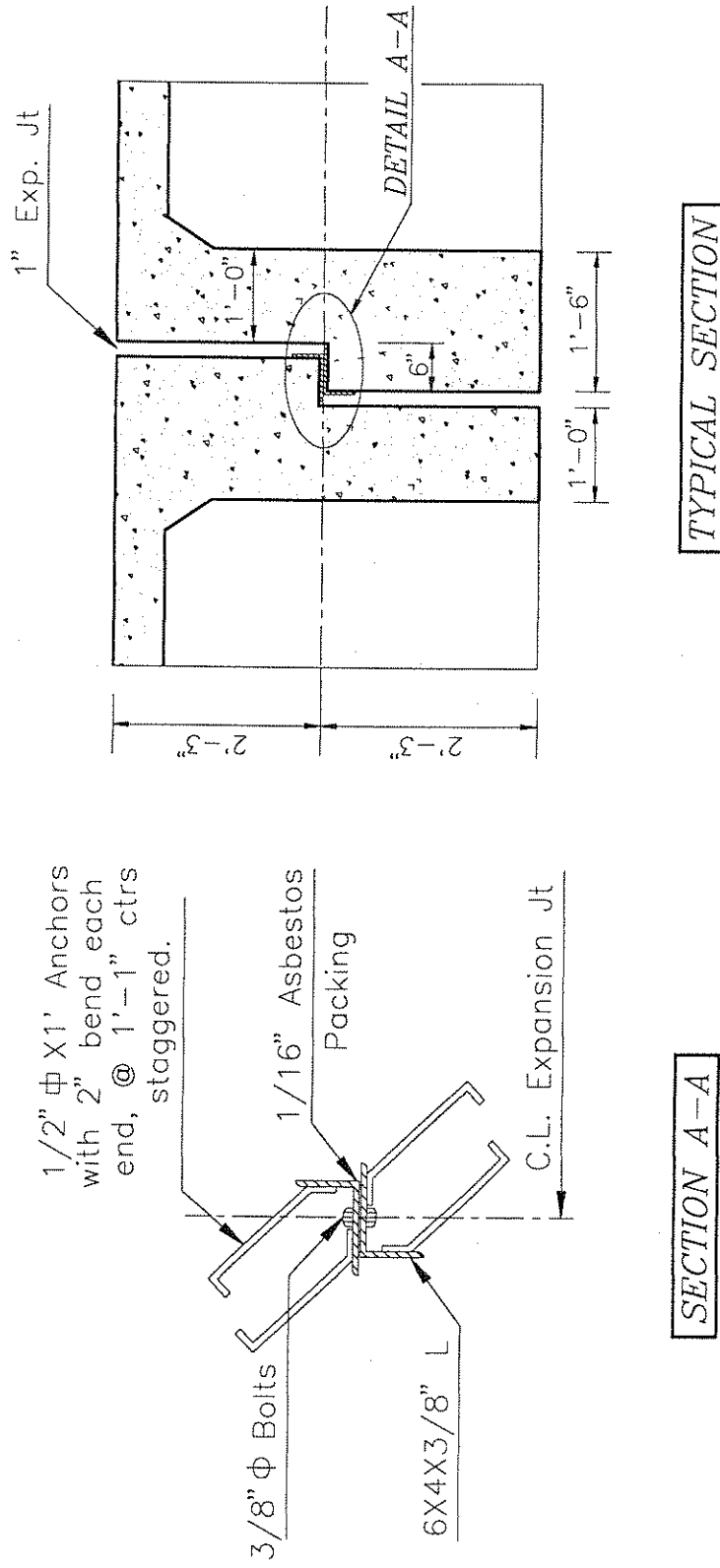


Figure 2-4 -Details of the Middle Expansion Joint

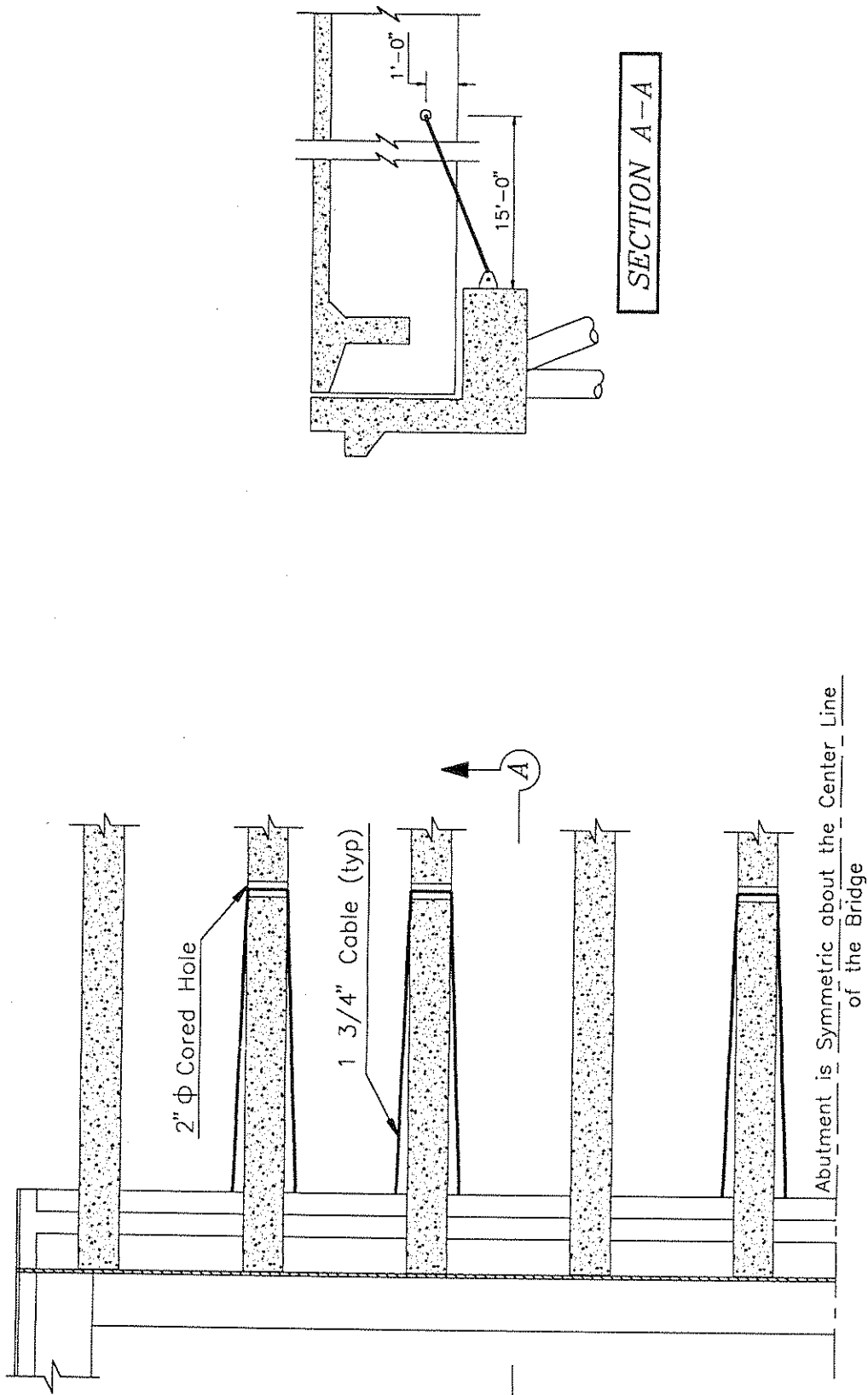


Figure 2-5 -Details of the Retrofitting at the Abutments

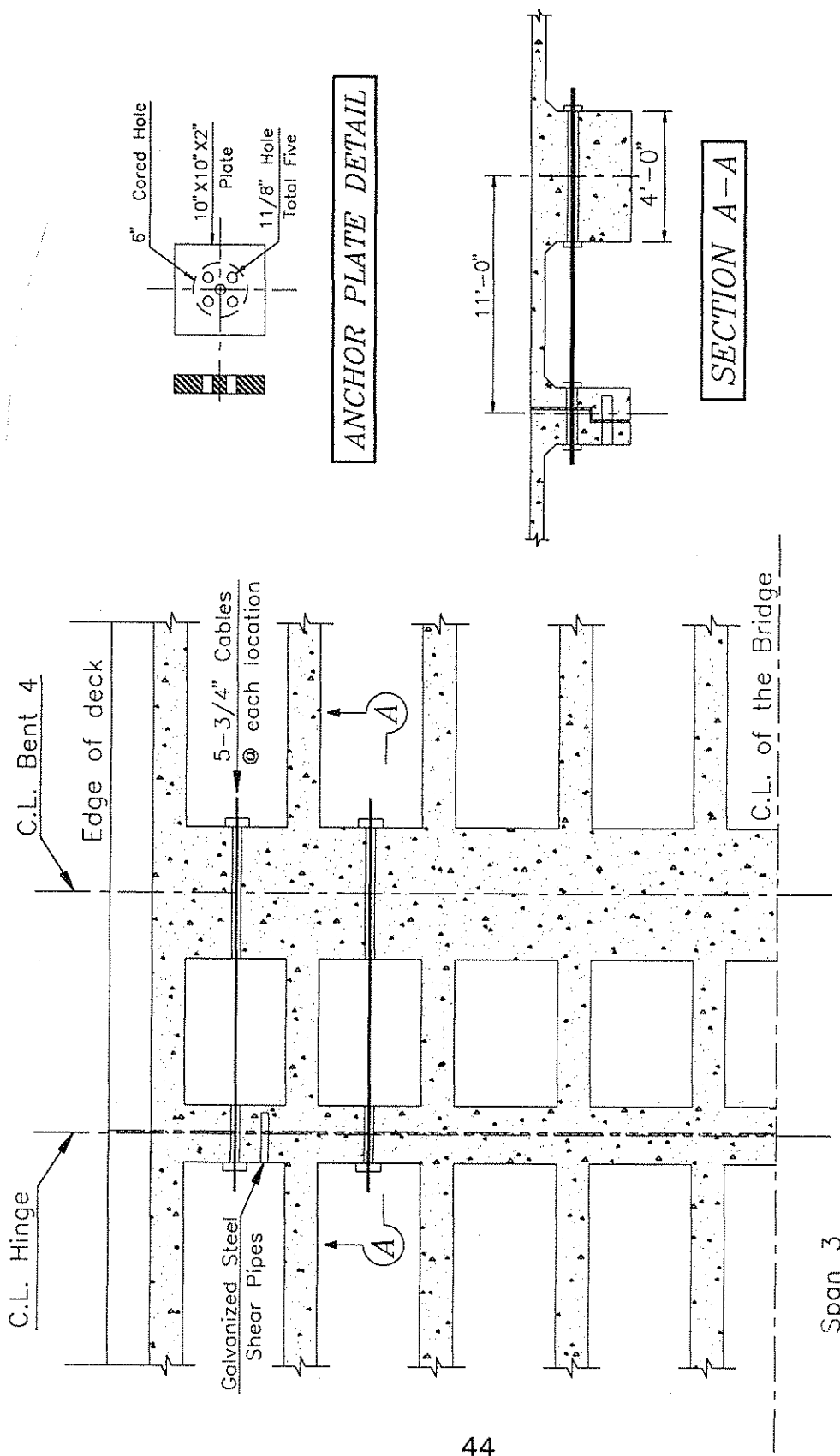


Figure 2-6 -Details of the Retrofitting at the Middle Expansion Joint

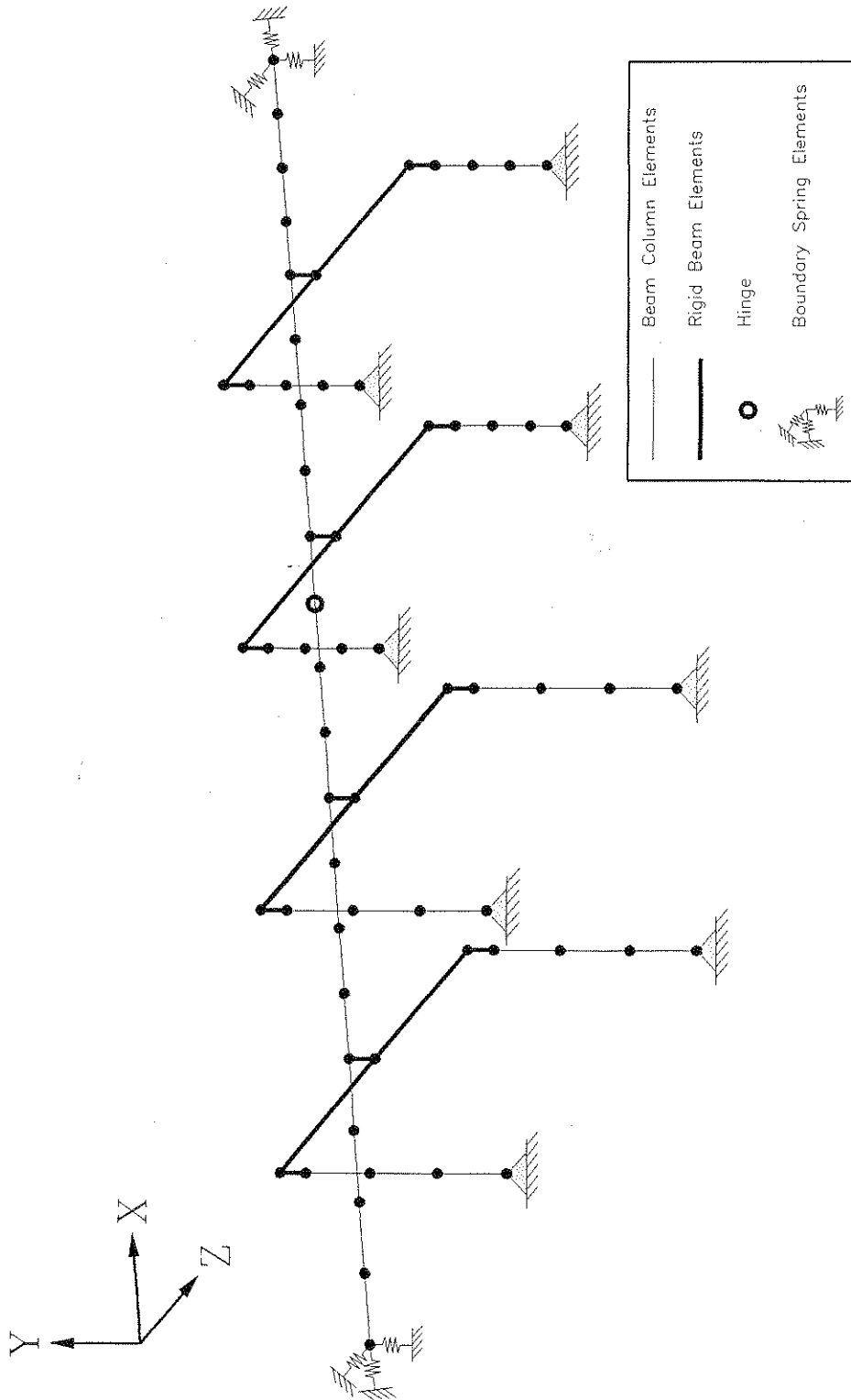


Figure 3-1 -Idealization of the Lumped Mass, Linear Model



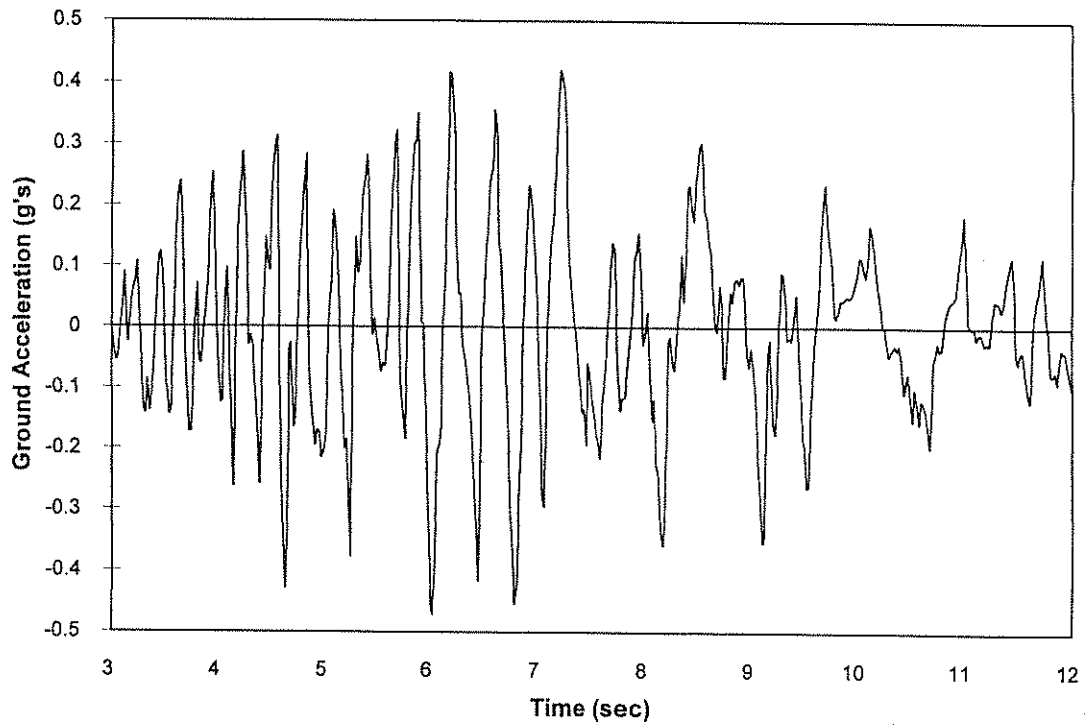


Figure 3-3 -Capitola Fire Station, Transverse Component ( Peak Acceleration = -0.472g at 6.02 sec )

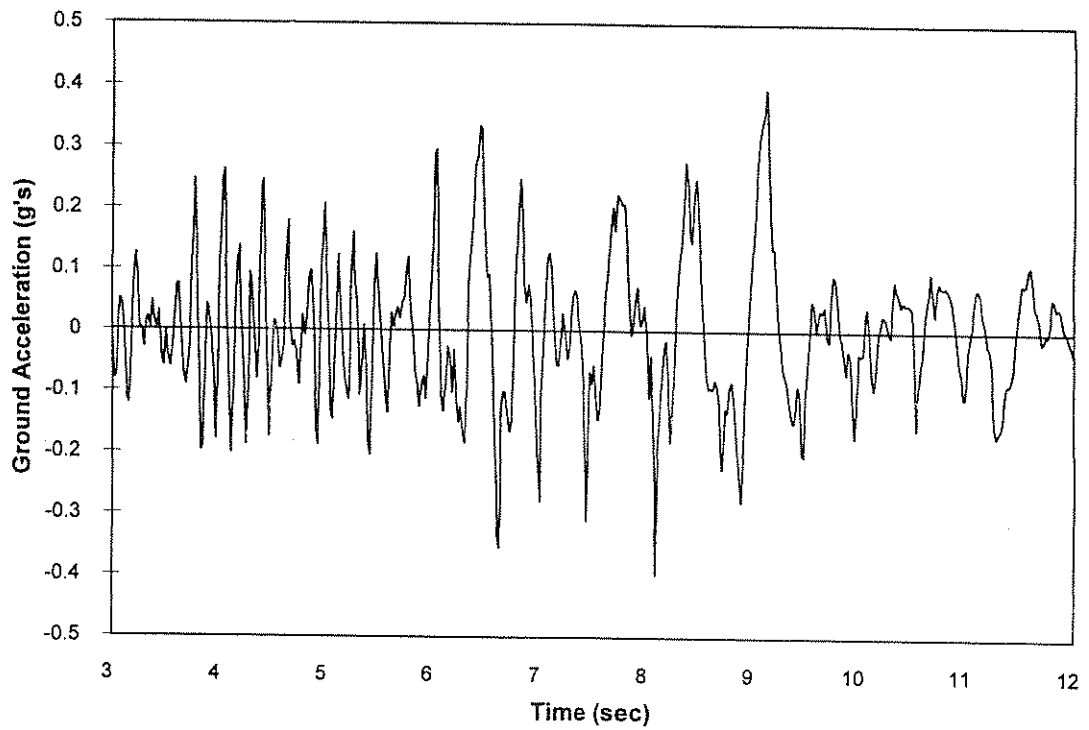


Figure 3-4 -Capitola Fire Station, Longitudinal Component ( Peak Acceleration = -0.398g at 8.08 sec )

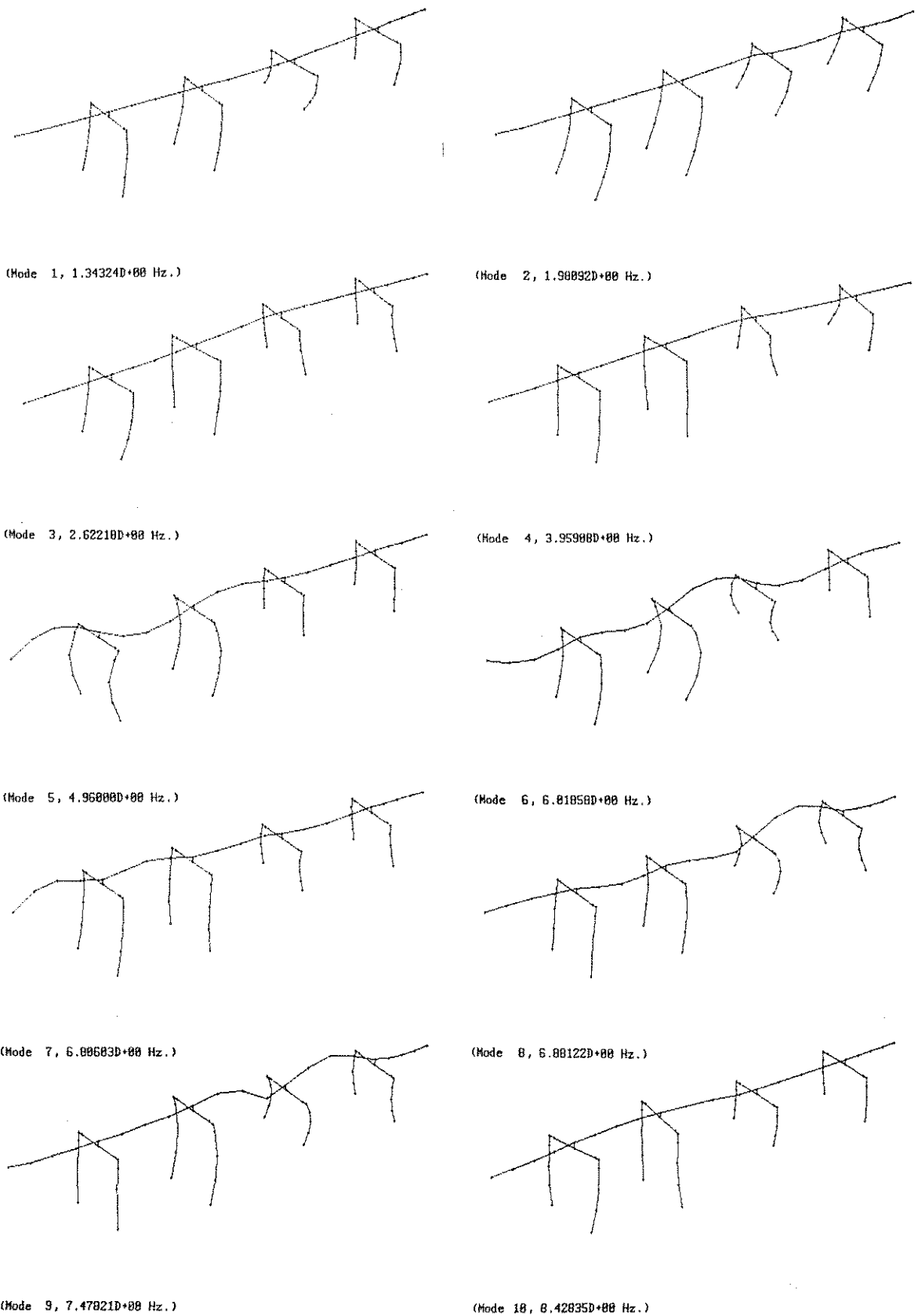


Figure 4-1 First Ten Mode Shapes for the Aptos Creek Bridge.

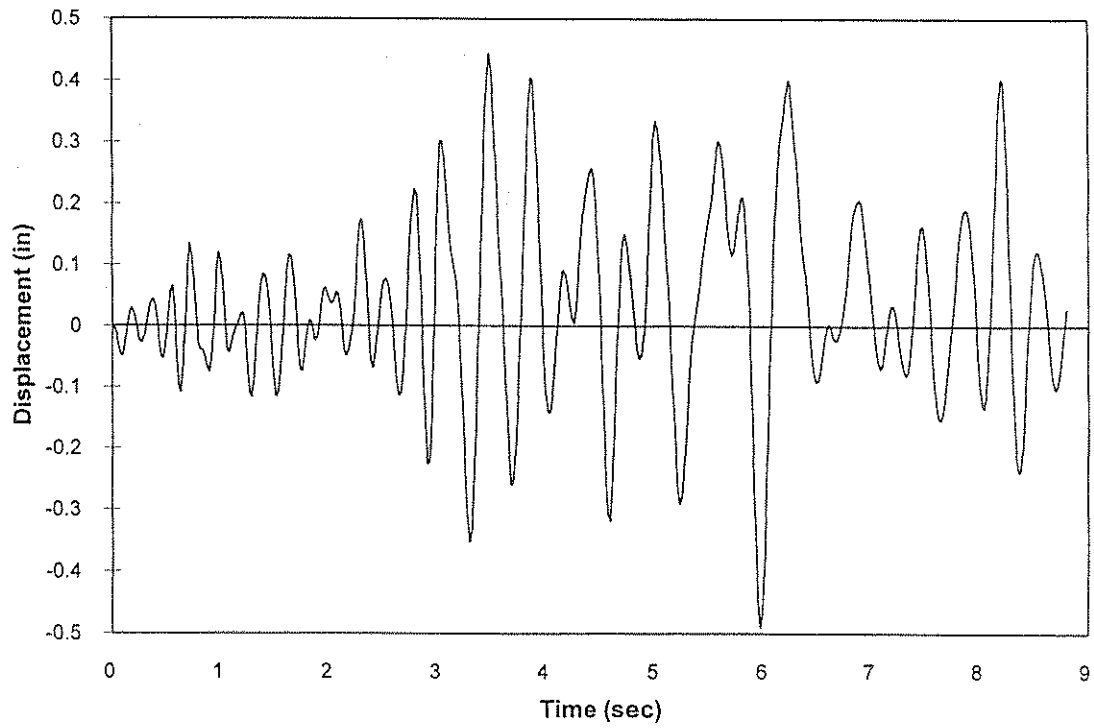


Figure 4-2 -Longitudinal Displacement History at Node 2 near Abutment 1 (3/4" TBG and 1" SG)

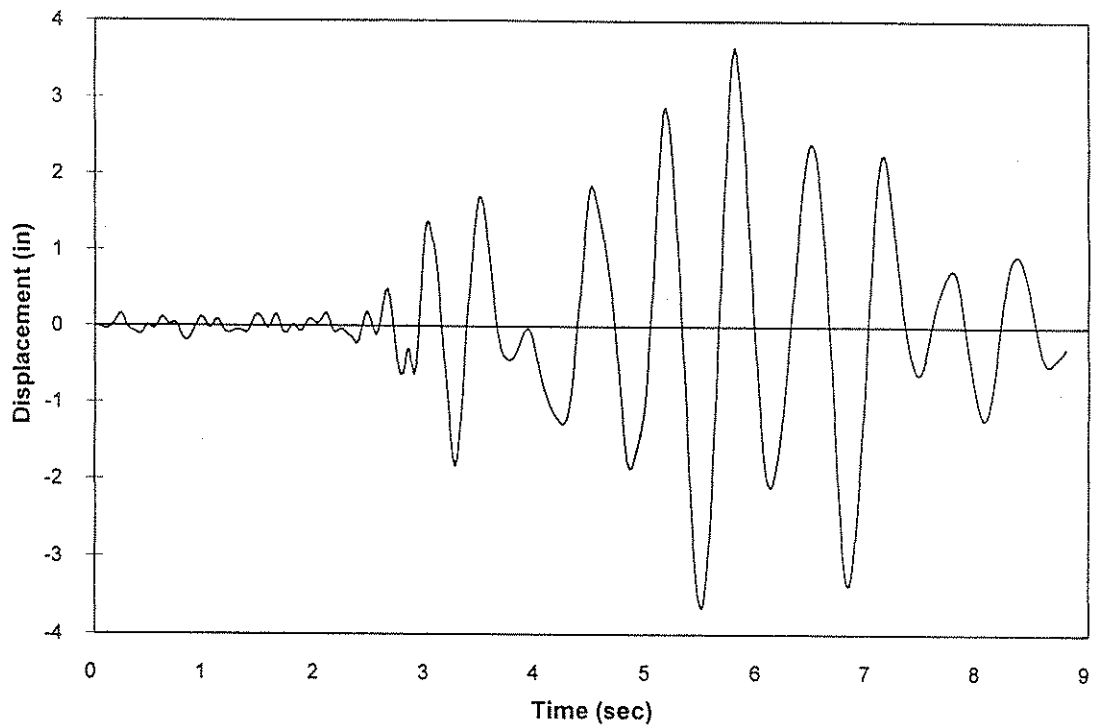
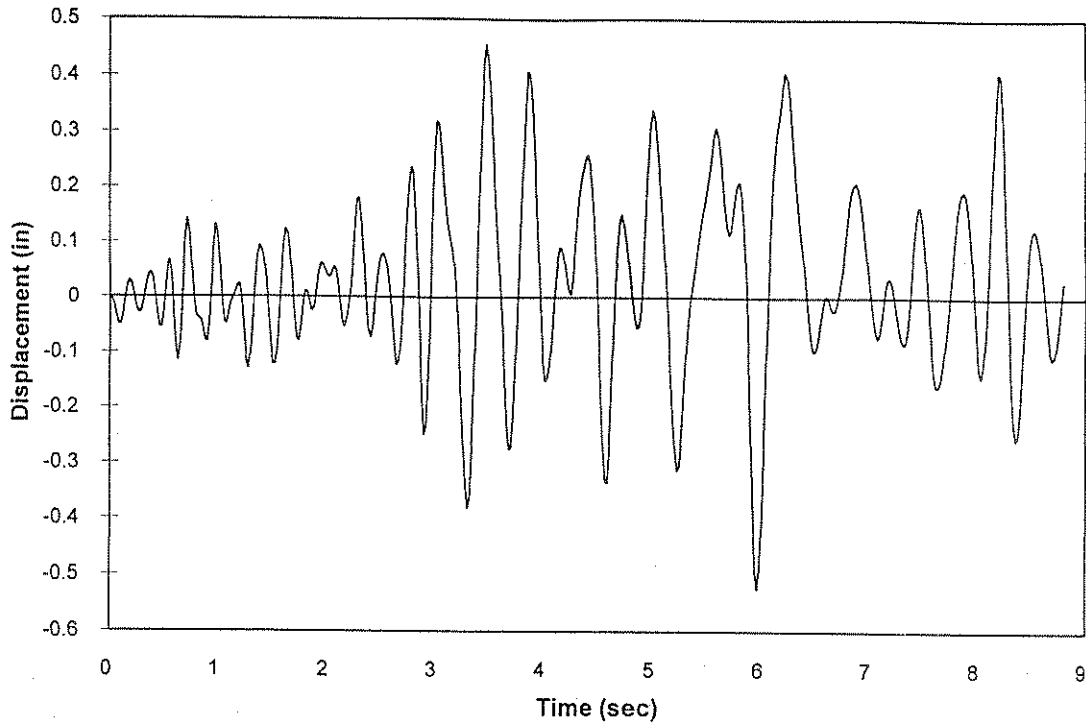
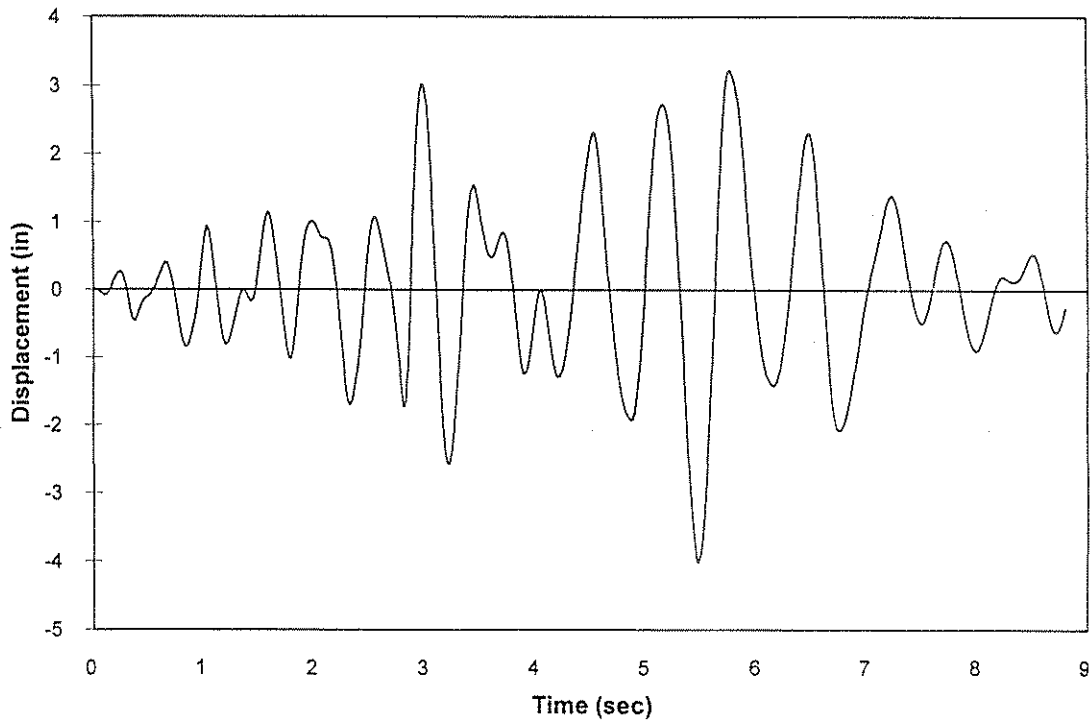


Figure 4-3 -Transverse Displacement History at Node 2 near Abutment 1 (3/4" TBG and 1" SG)



**Figure 4-4** -Longitudinal Displacement History at Node 39 near the Middle Hinge (3/4" TBG and 1" SG)



**Figure 4-5** -Transverse Displacement History at Node 39 near the Middle Hinge (3/4" TBG and 1" SG)

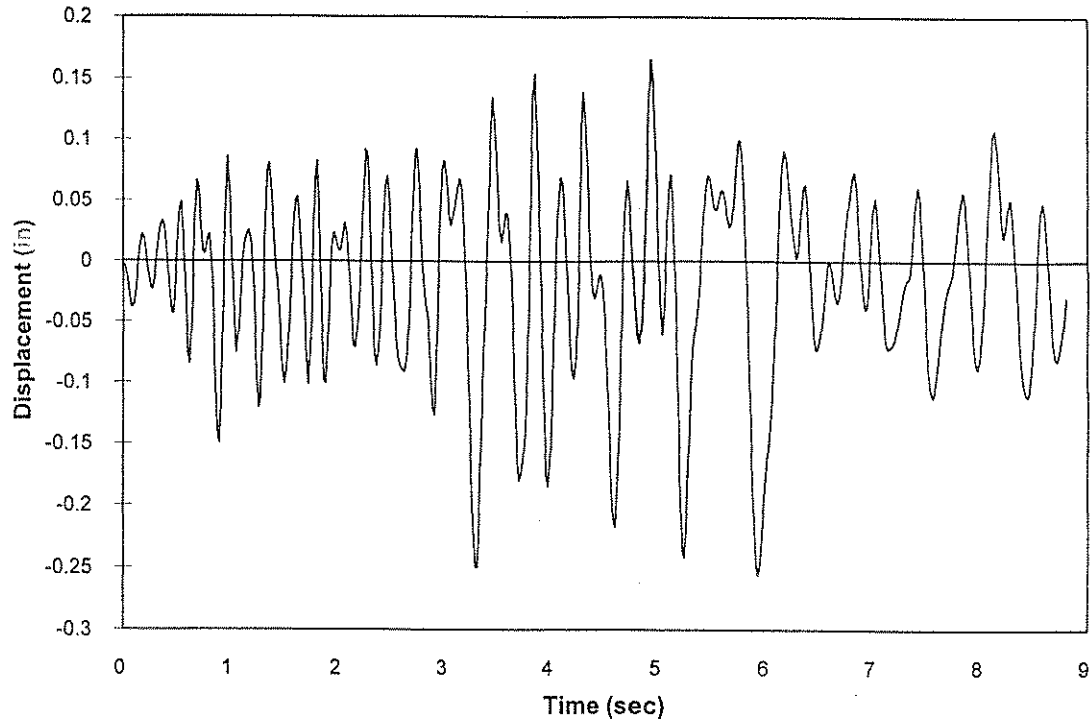


**Figure 4-6** -Longitudinal Displacement History at Node 75 near Abutment 6 (3/4" TBG and 1" SG)

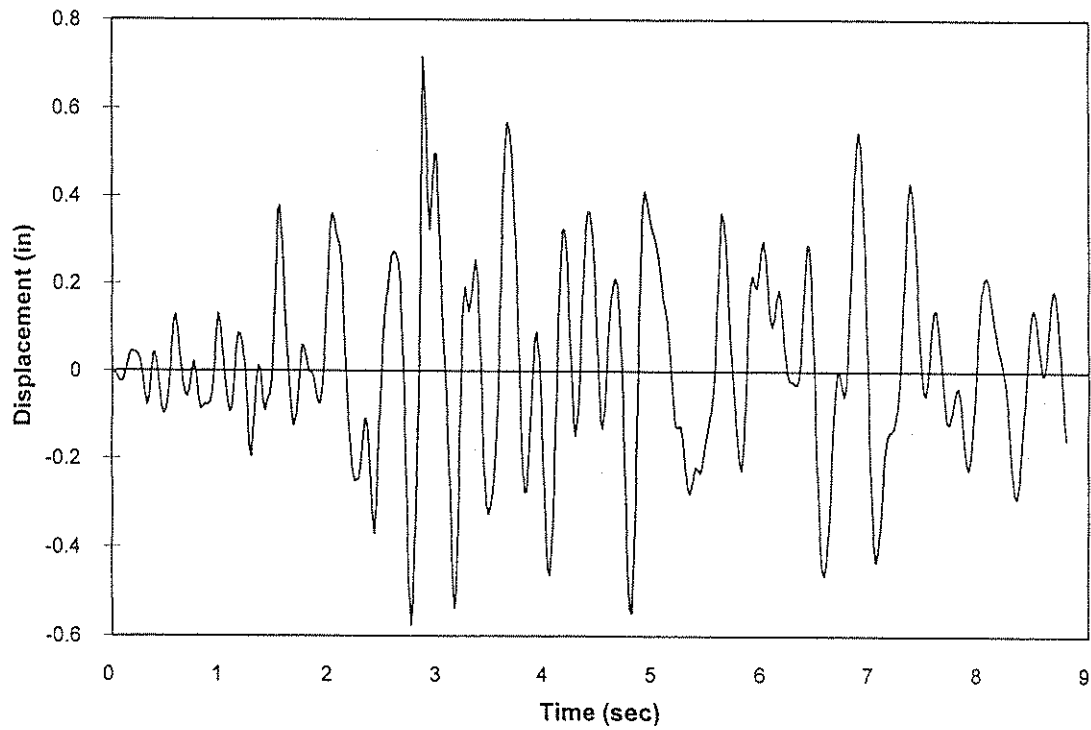


**Figure 4-7** -Transverse Displacement History at Node 75 near Abutment 6 (3/4" TBG and 1" SG)

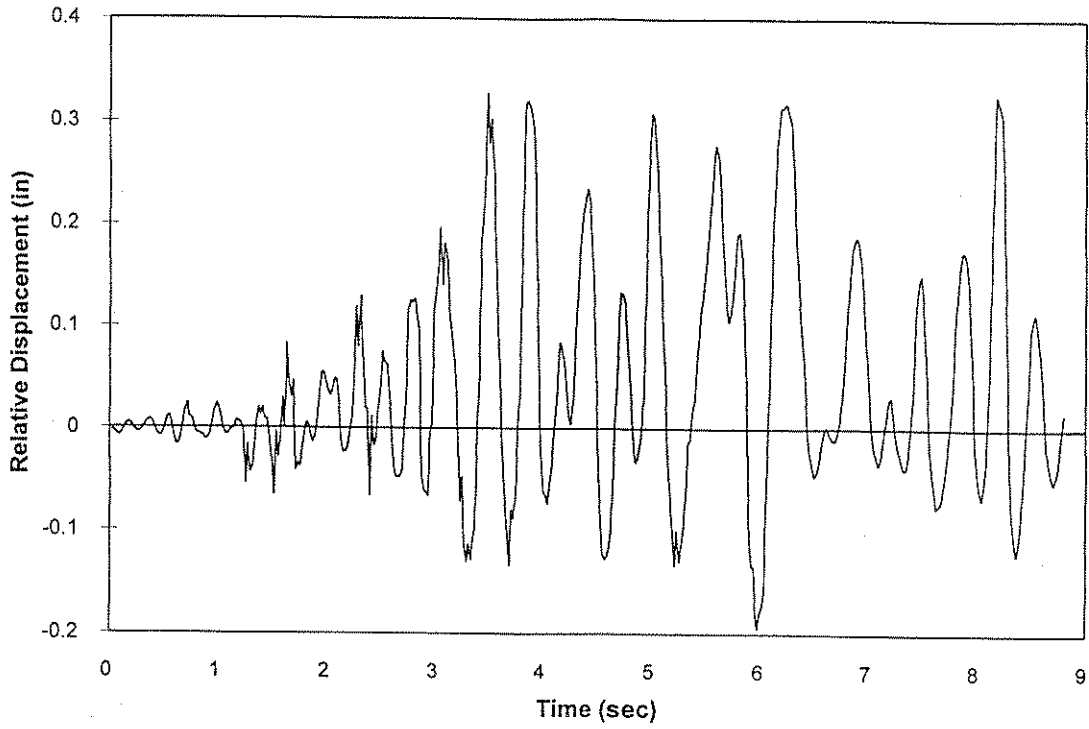


Figure 4-8 -Longitudinal Relative Displacement History at Abutment 1 (3/4" TBG and 1" SG)

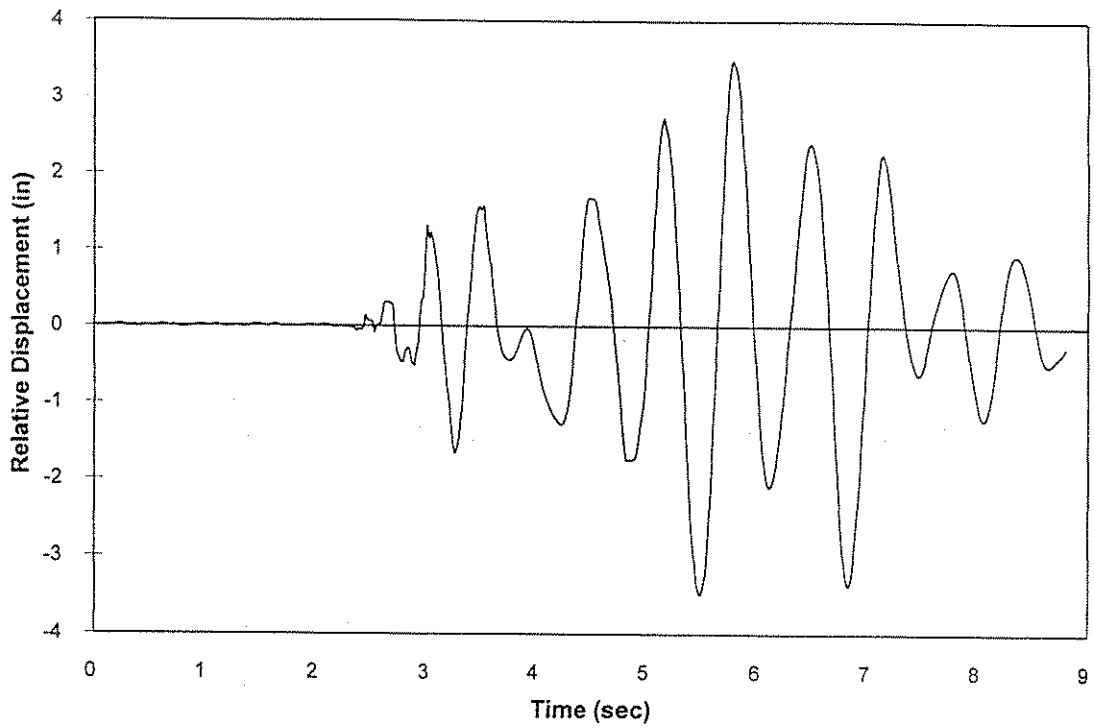
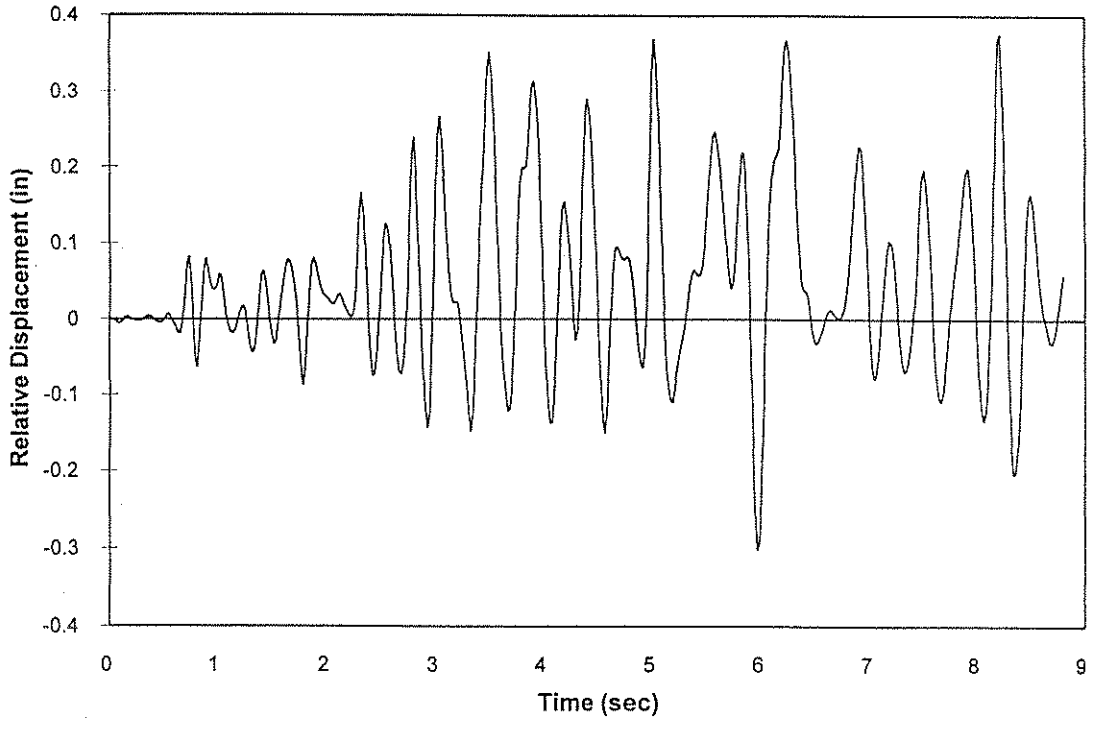
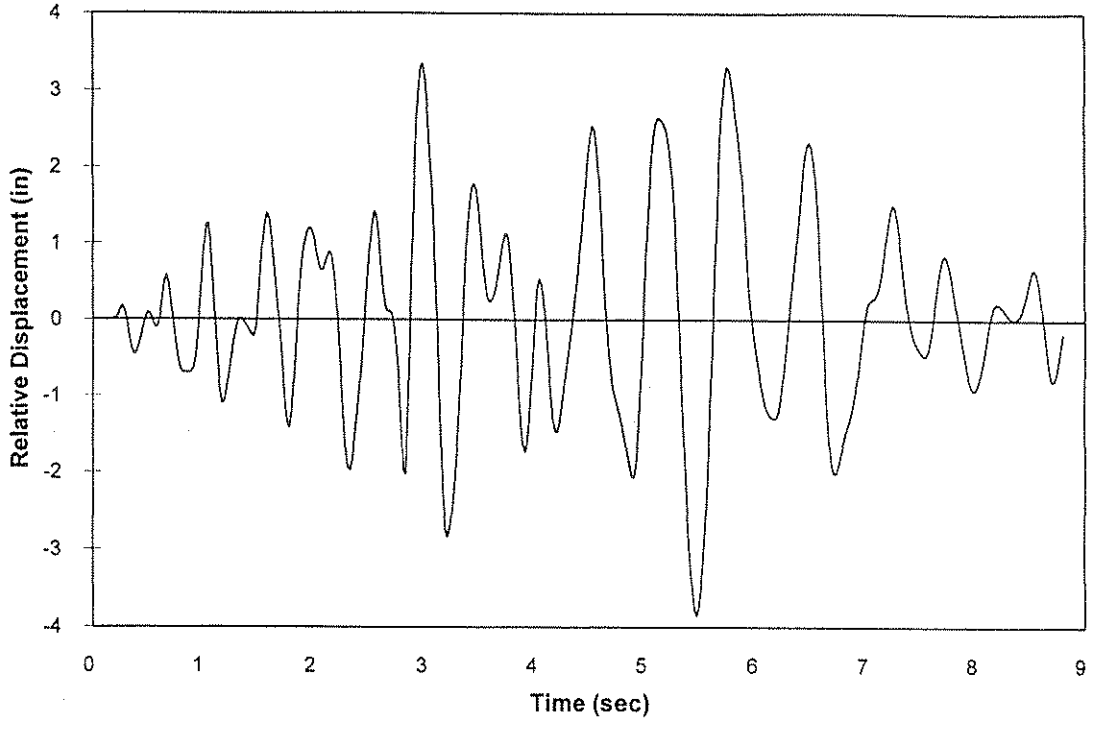


Figure 4-9 -Transverse Relative Displacement History at Abutment 1 (3/4" TBG and 1" SG)



**Figure 4.10** -Longitudinal Relative Displacement History at the Middle Hinge (3/4" TBG and 1" SG)



**Figure 4-11** -Transverse Relative Displacement History at the Middle Hinge (3/4" TBG and 1" SG)

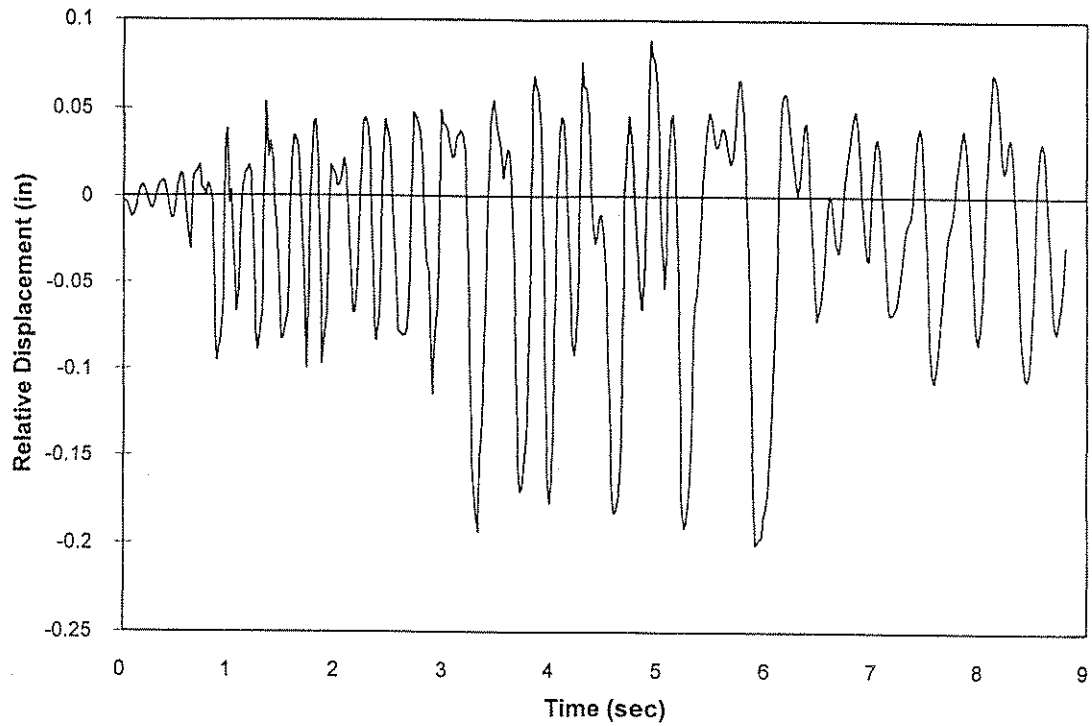


Figure 4-12 -Longitudinal Relative Displacement History at Abutment 6 (3/4" TBG and 1" SG)

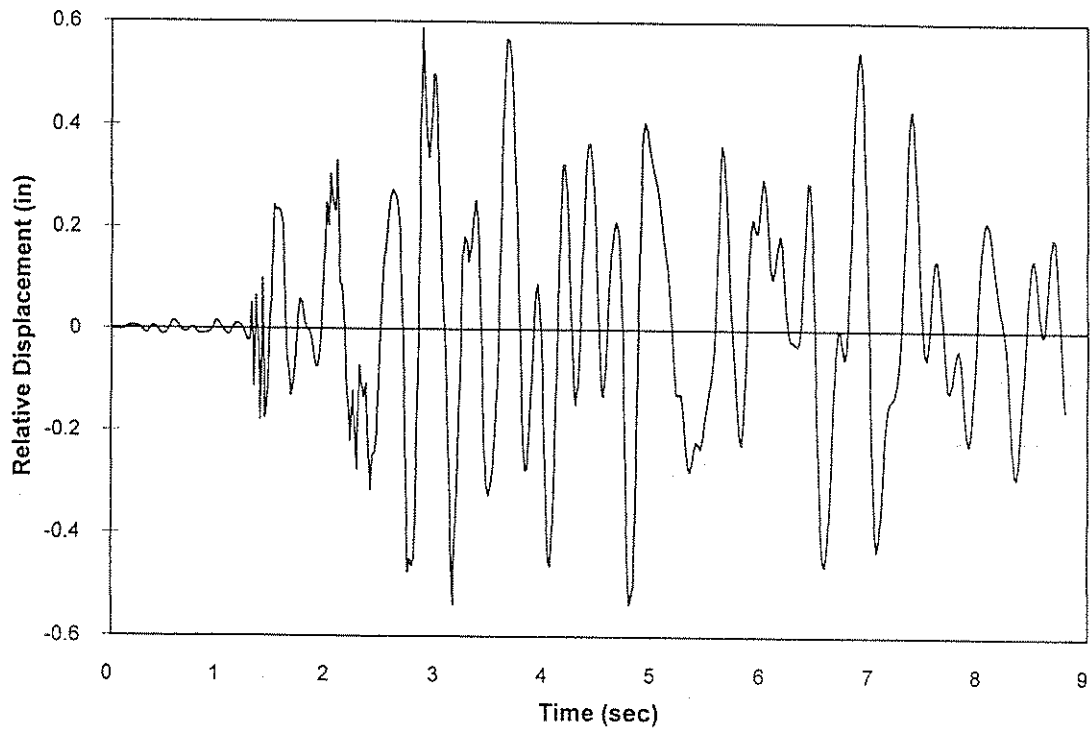


Figure 4-13 -Transverse Relative Displacement History at Abutment 6 (3/4" TBG and 1" SG)

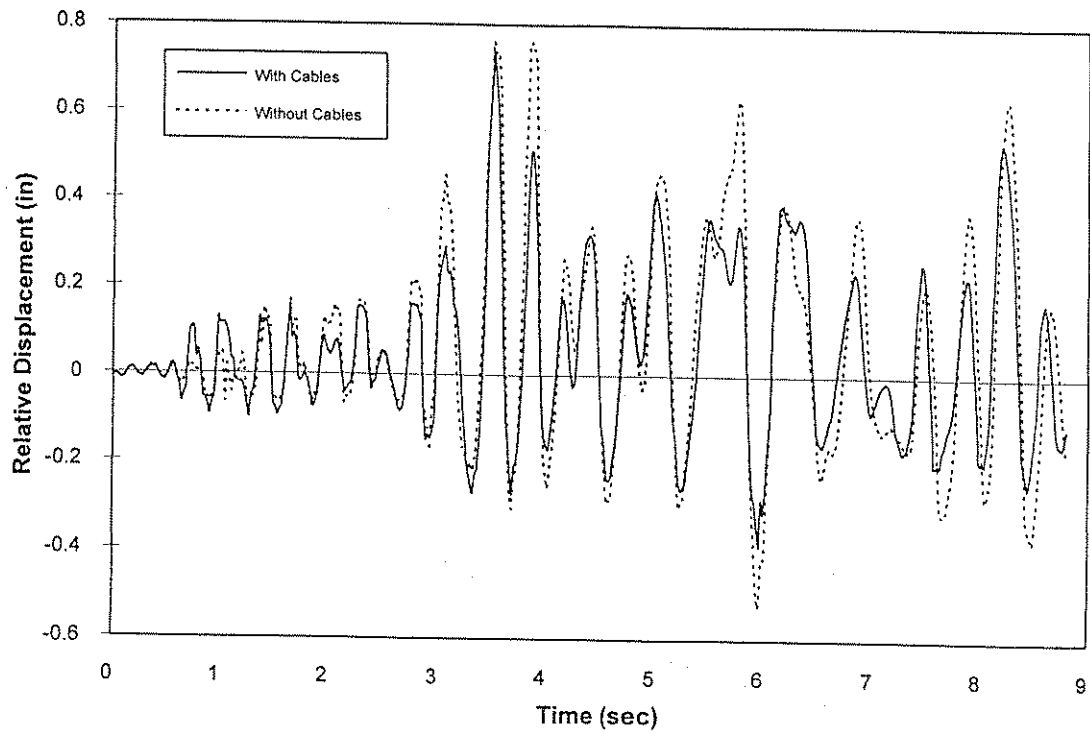


Figure 4-14 -Longitudinal Relative Displacement History at Abutment 1  
(Motion Normalized to 0.7g)

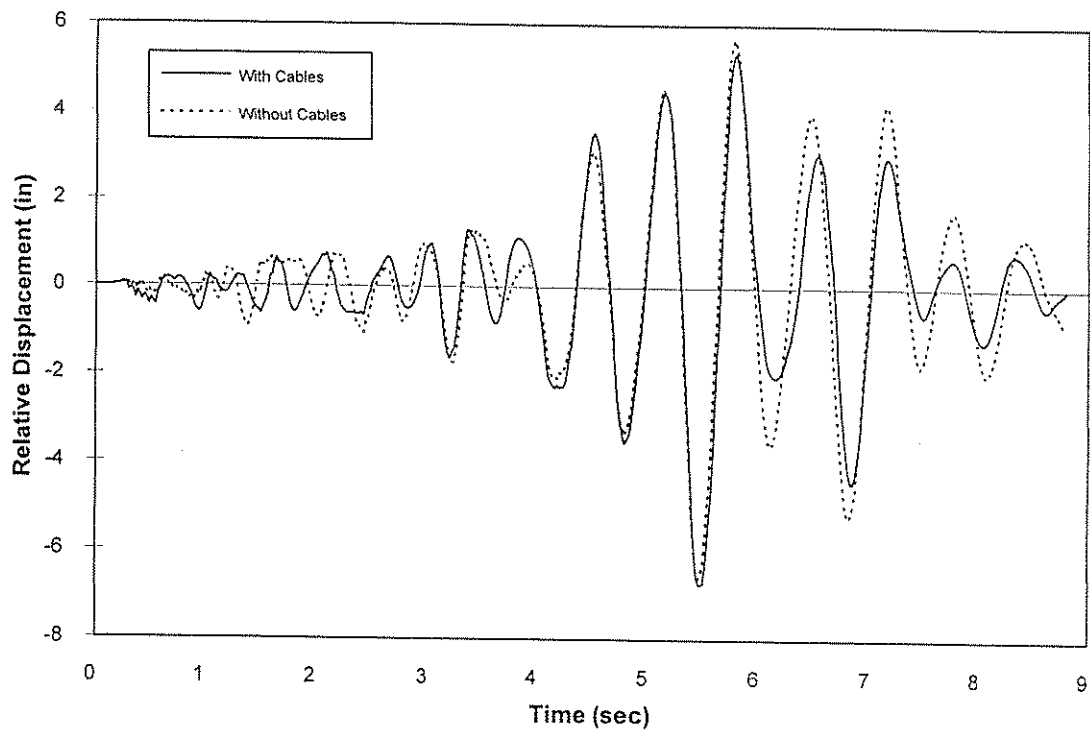


Figure 4-15 -Transverse Relative Displacement History at Abutment 1  
(Motion Normalized to 0.7g)

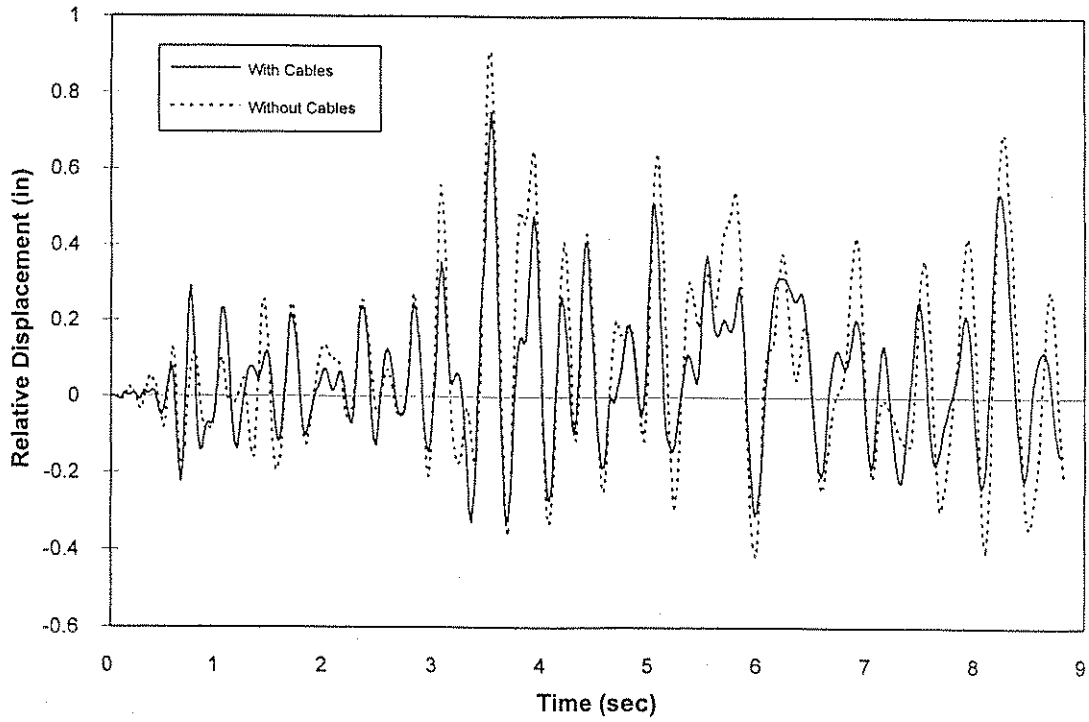


Figure 4-16 -Longitudinal Relative Displacement History at the Middle Hinge (Motion Normalized to 0.7g)

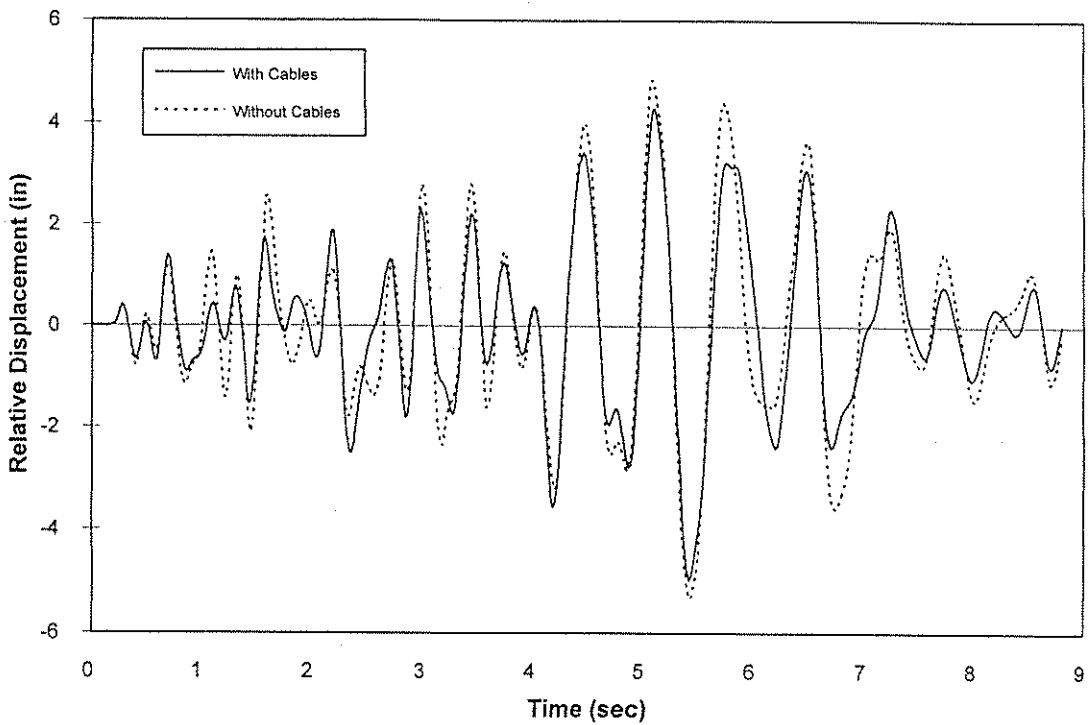


Figure 4-17 -Transverse Relative Displacement History at the Middle Hinge (Motion Normalized to 0.7g)

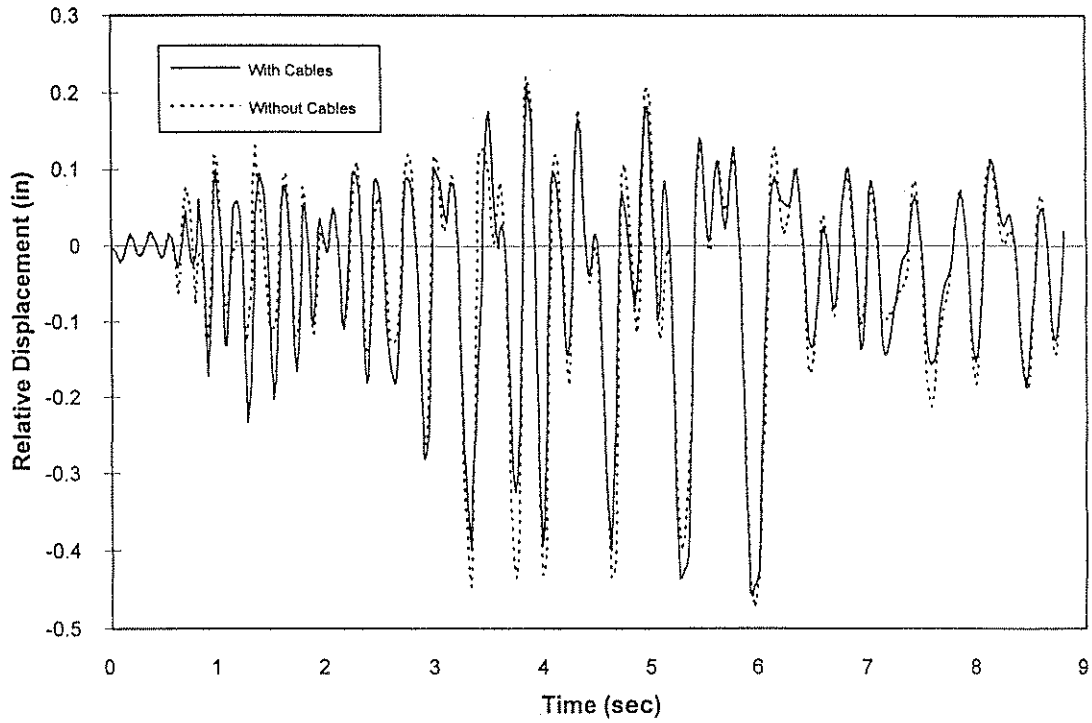


Figure 4-18 -Longitudinal Relative Displacement History at Abutment 6 (Motion Normalized to 0.7g)

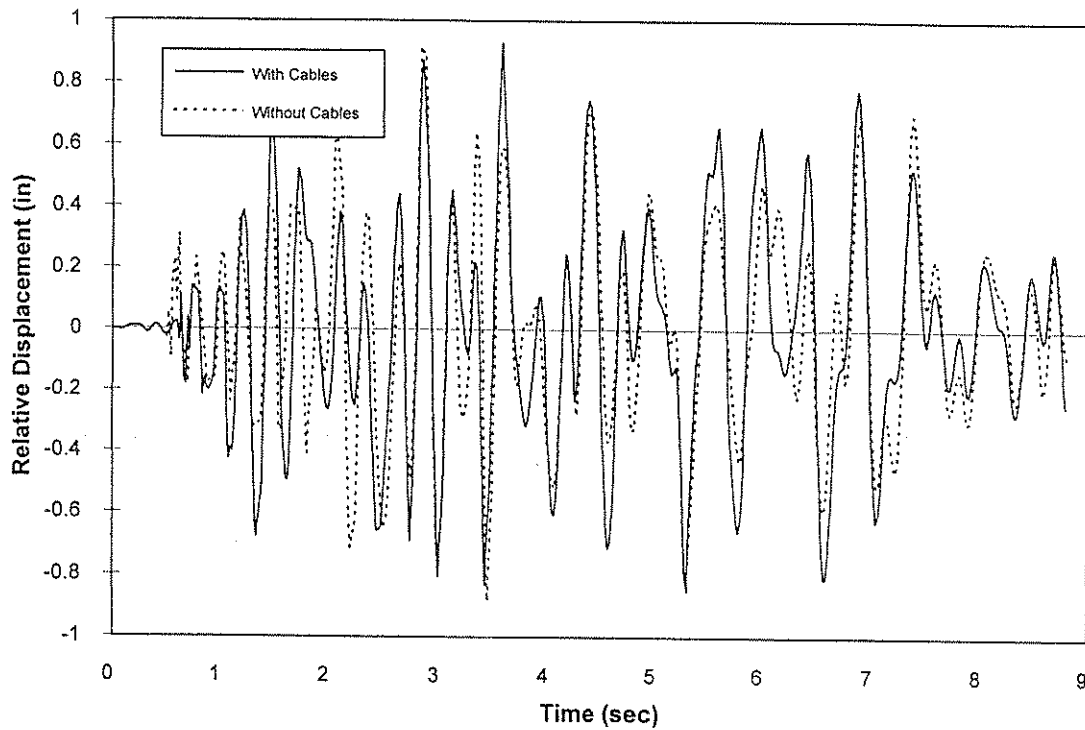


Figure 4-19 -Transverse Relative Displacement History at Abutment 6 (Motion Normalized to 0.7g)

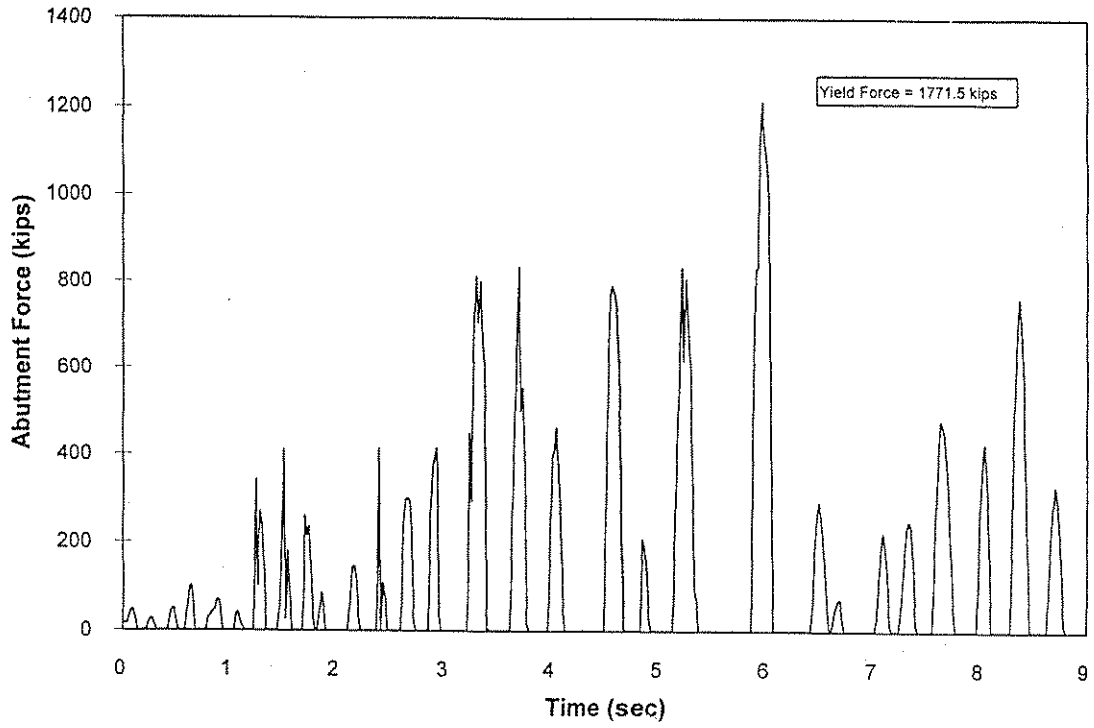


Figure 4-20 -Abutment 1 Force History (3/4" TBG and 1" SG)

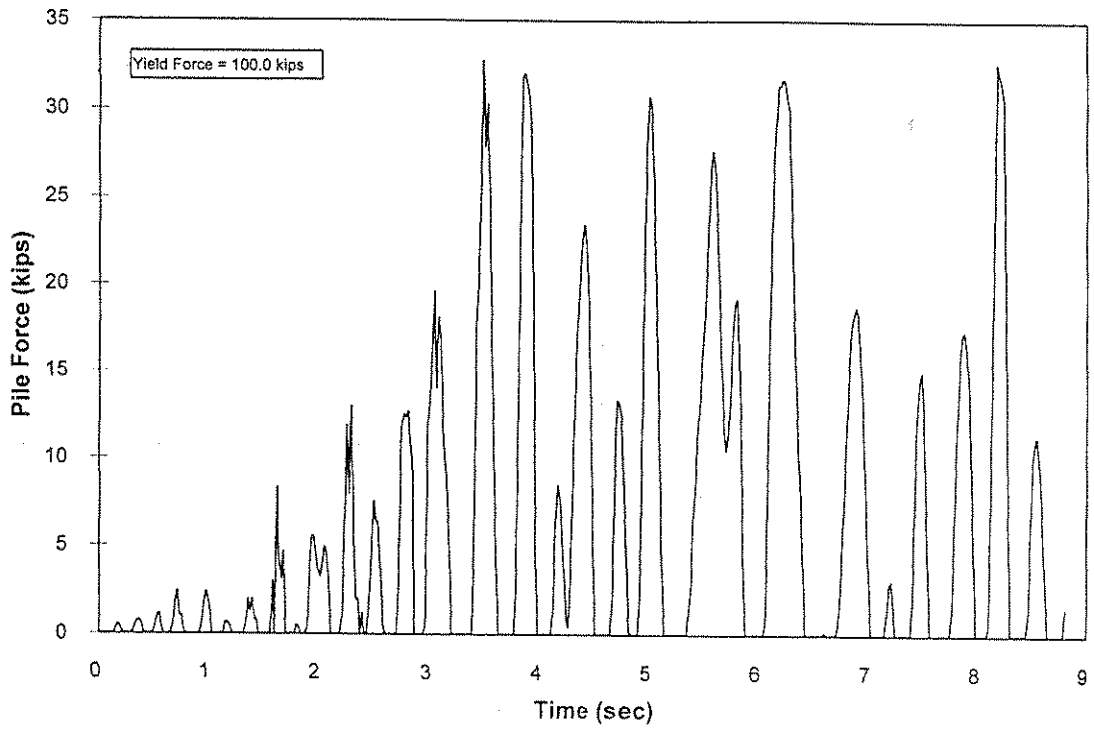


Figure 4-21 -Piles of Abutment 1 Force History (3/4" TBG and 1" SG)

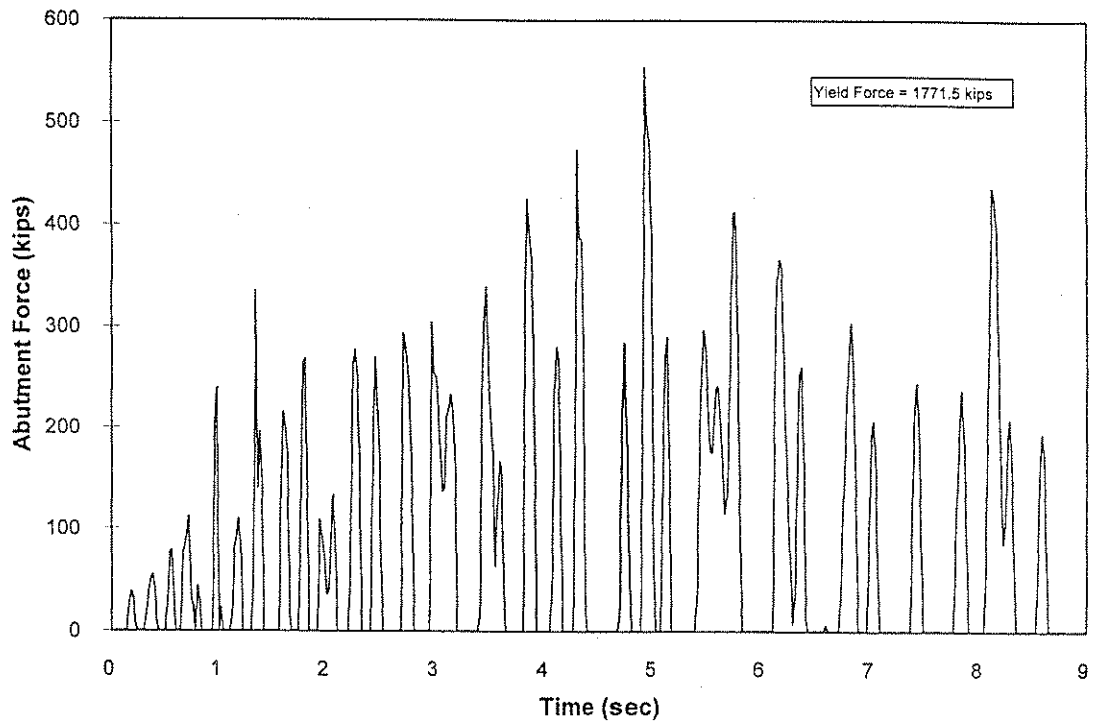


Figure 4-22 -Abutment 6 Force History (3/4" TBG and 1" SG)

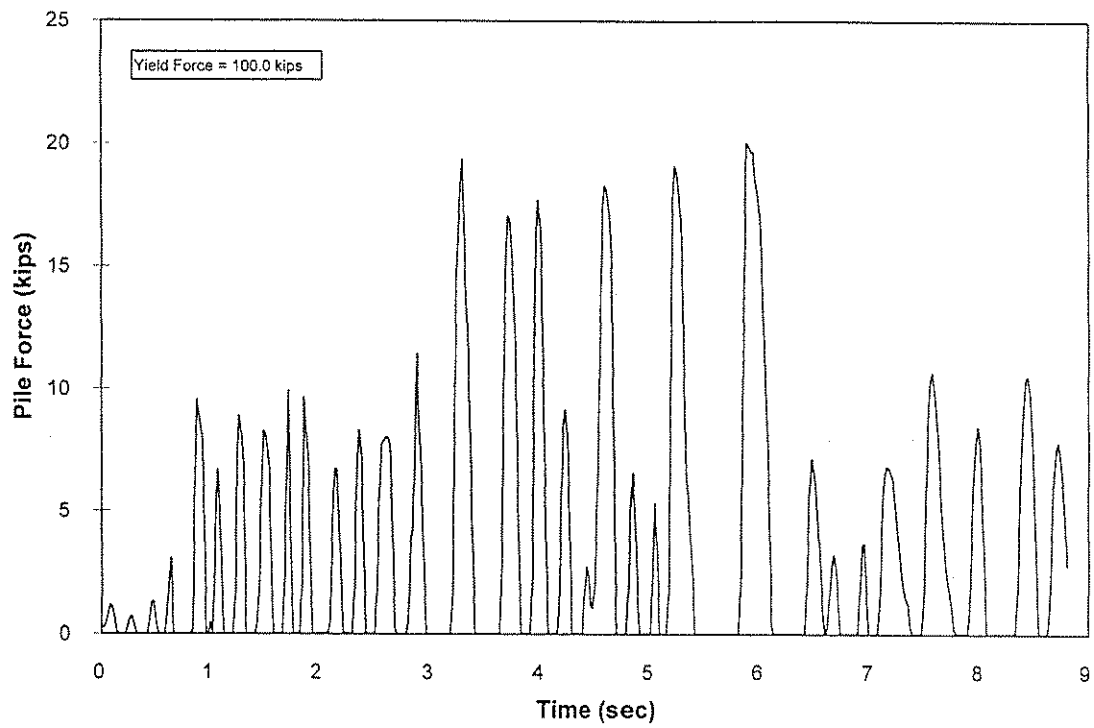


Figure 4-23 -Piles of Abutment 6 Force History (3/4" TBG and 1" SG)

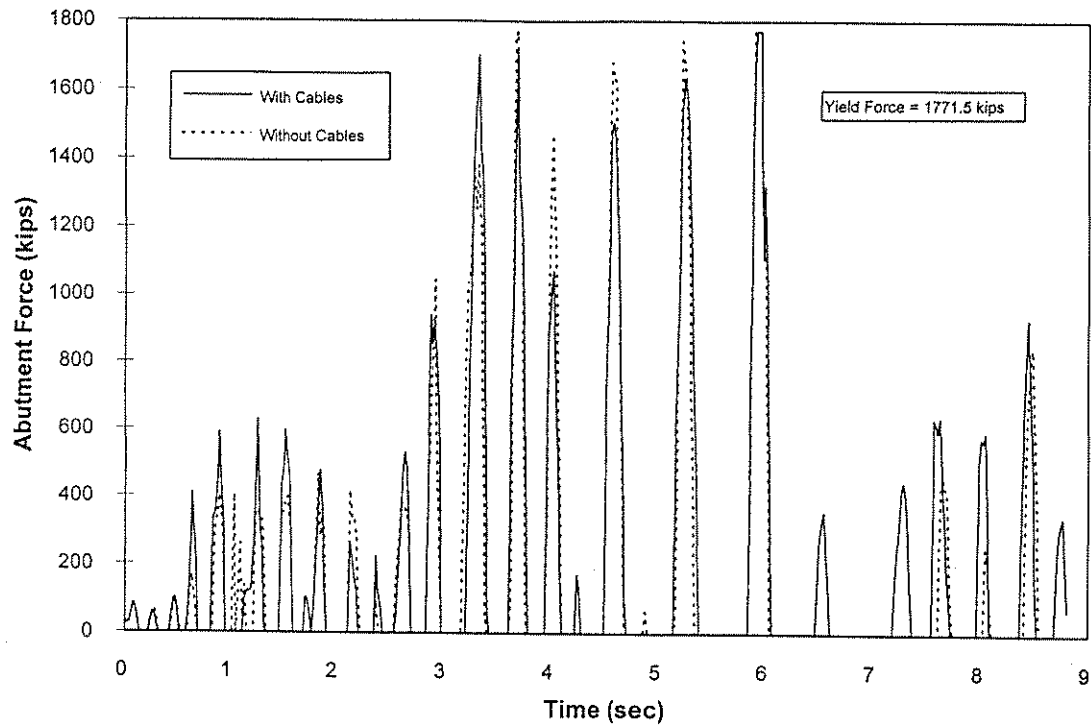


Figure 4-24 -Abutment 1 Force History (Motion Normalized to 0.7g)

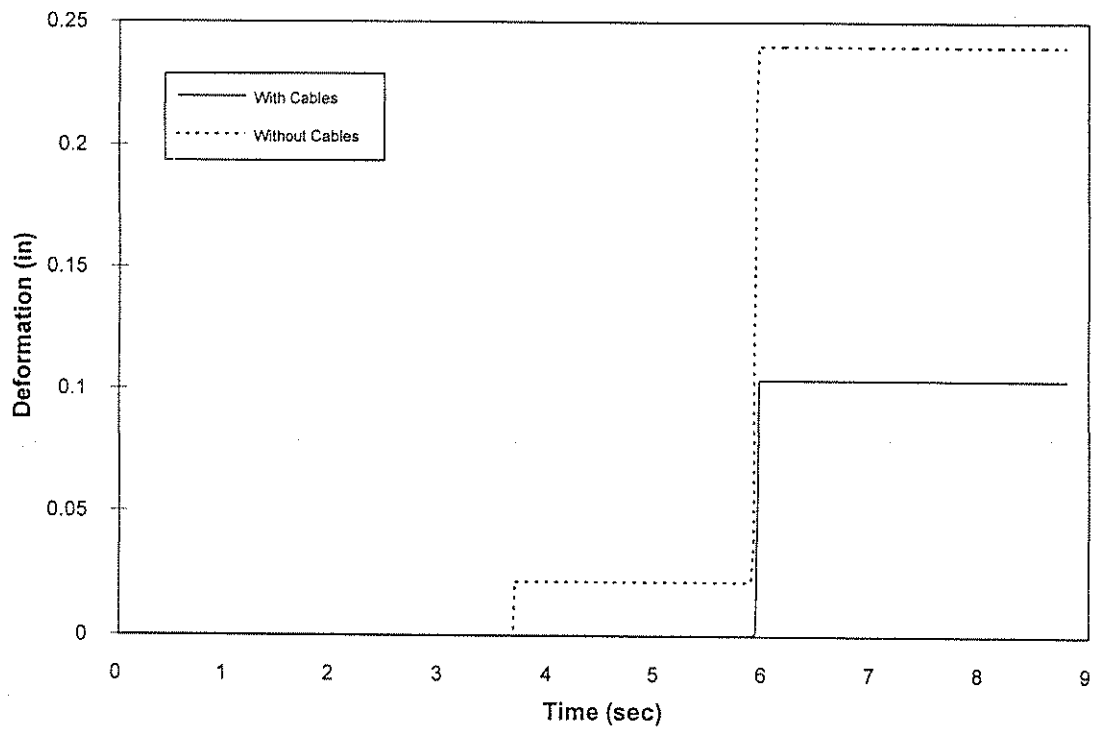


Figure 4-25 -Abutment 1 Nonlinear Deformation History (Motion Normalized to 0.7g)

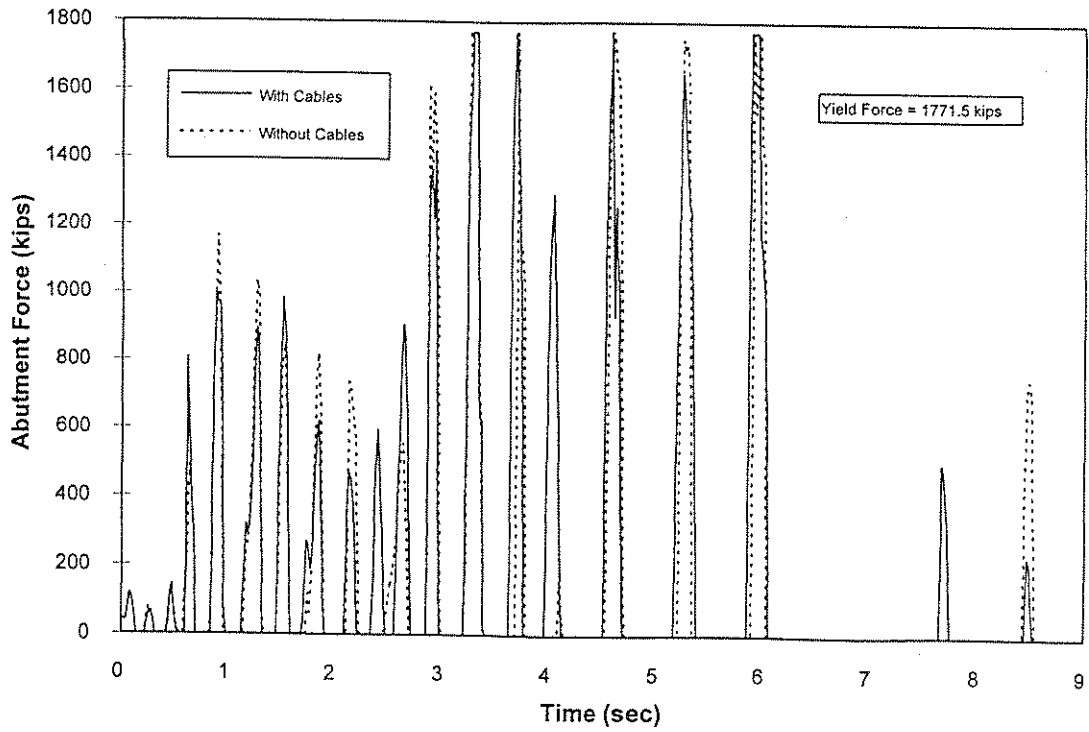


Figure 4-26 -Abutment 1 Force History (Motion Normalized to 1.0g)

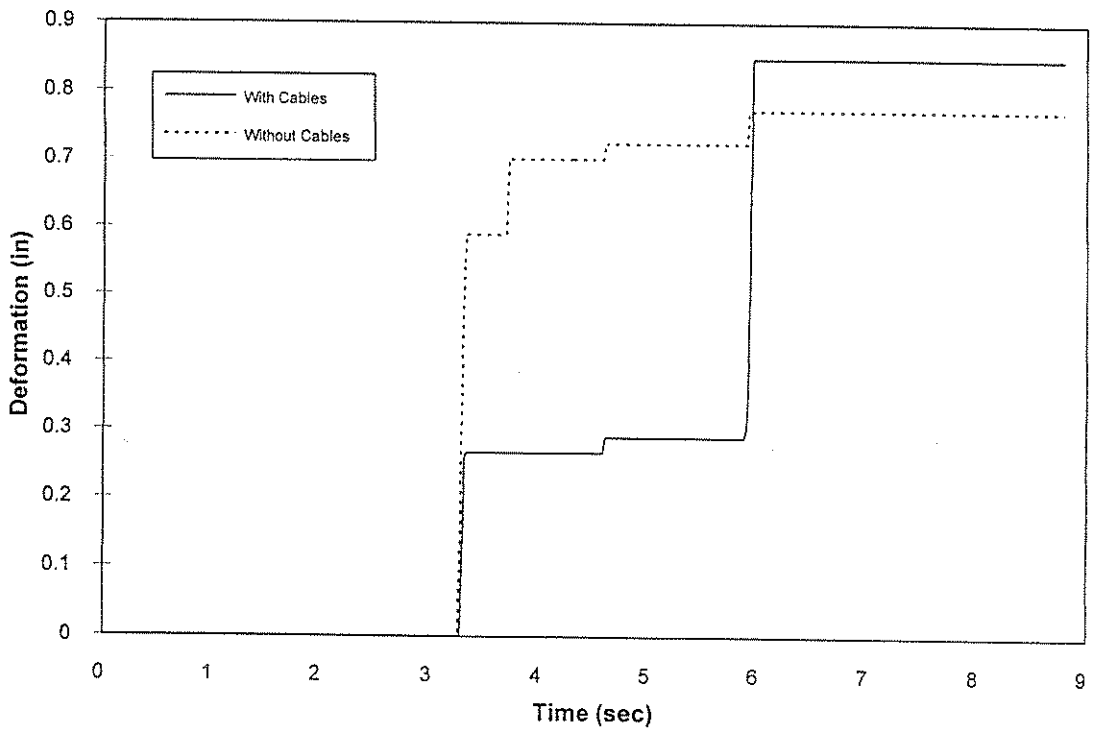


Figure 4-27 -Abutment 1 Nonlinear Deformation History (Motion Normalized to 1.0 g)

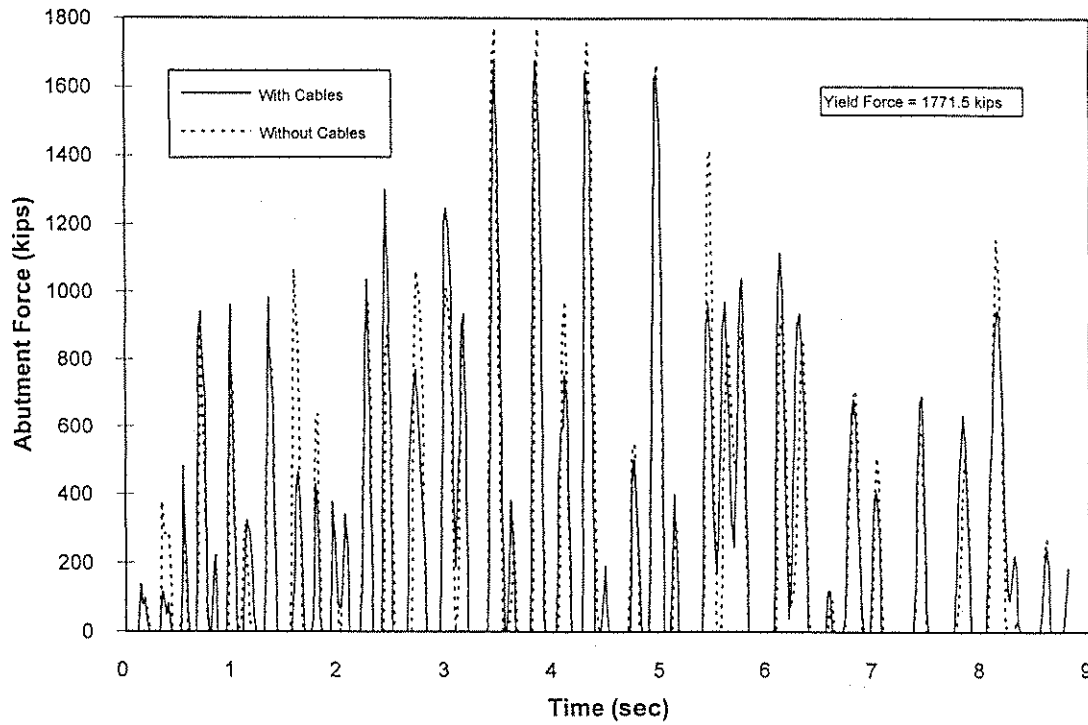


Figure 4-28 -Abutment 6 Force History (Motion Normalized to 1.0 g)

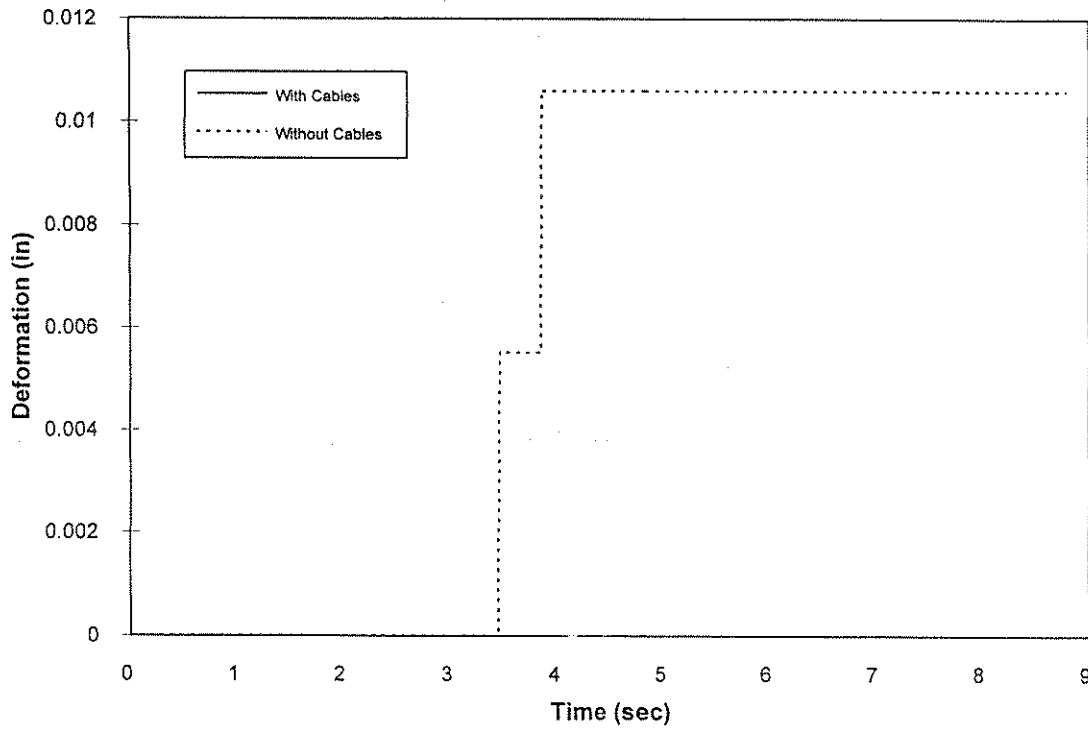


Figure 4-29 -Abutment 6 Nonlinear Deformation History (Motion Normalized to 1.0 g)

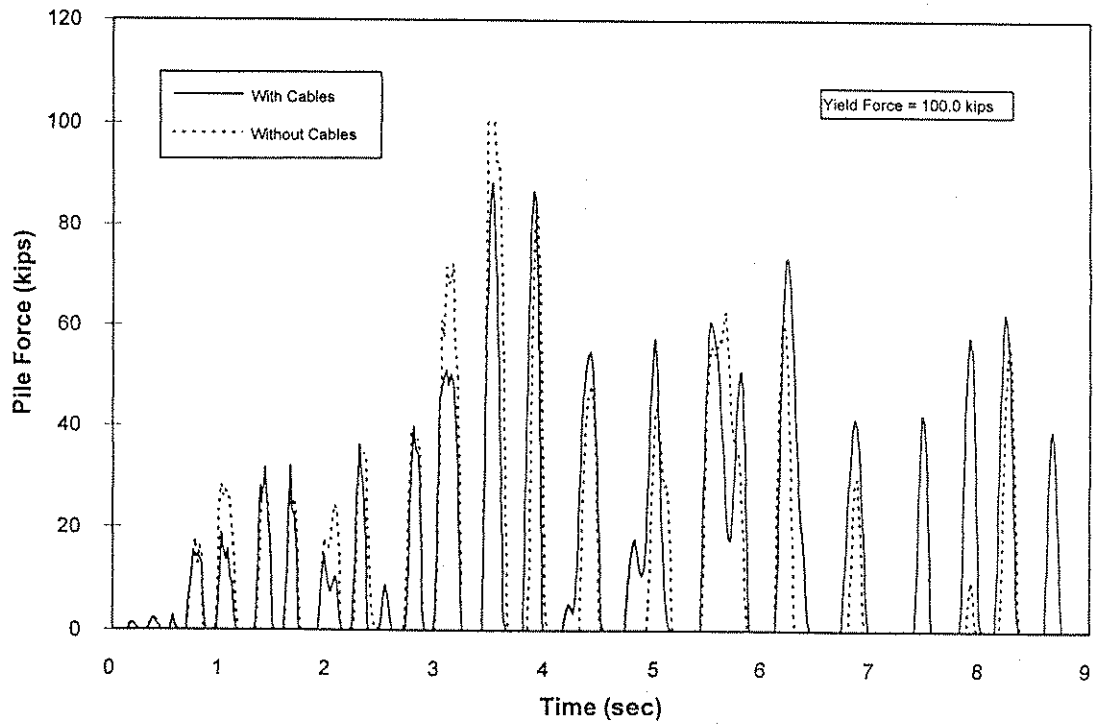


Figure 4-30 -Piles of Abutment 1 Force History (Motion Normalized to 1.0 g)

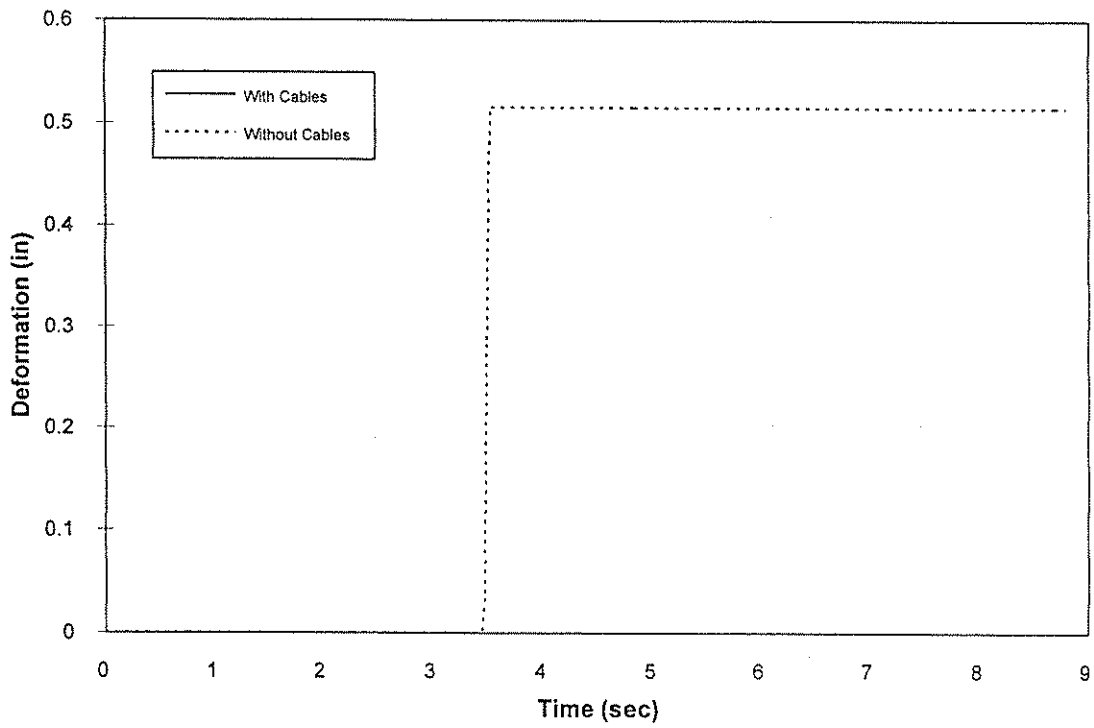


Figure 4-31 -Piles of Abutment 1 Nonlinear Deformation History (Motion Normalized to 1.0 g)

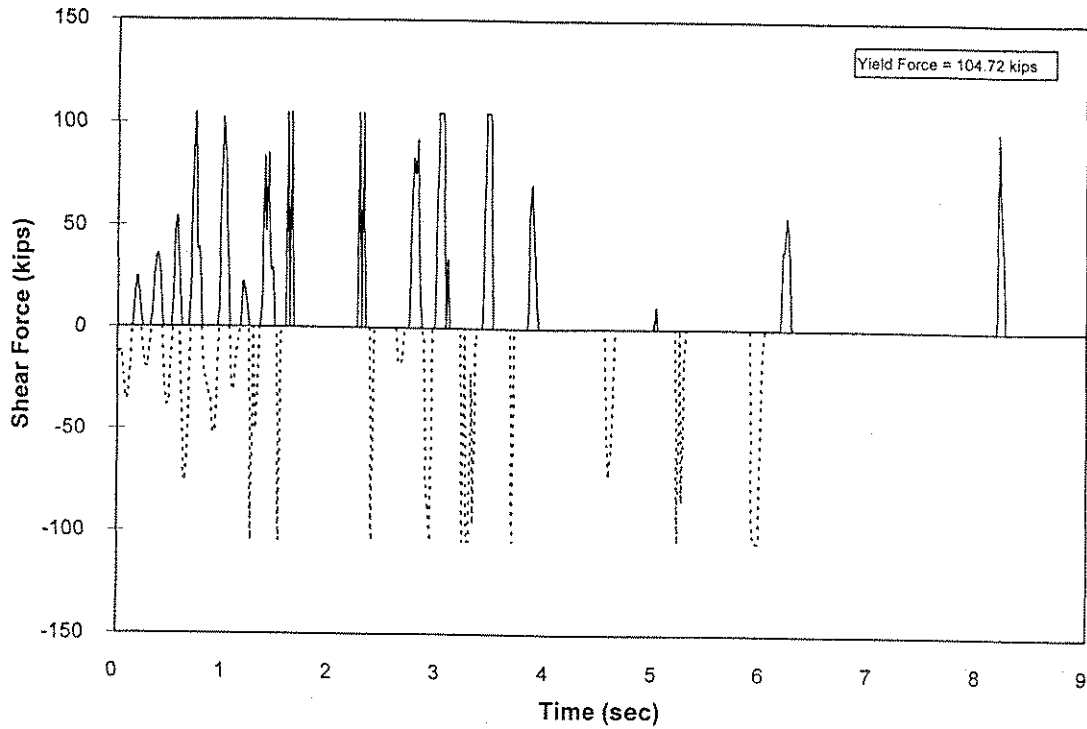


Figure 4-32 -Shear Force History of Abutment 1 Bearing Bars in the Long. Dir. (3/4" TBG and 1" SG)

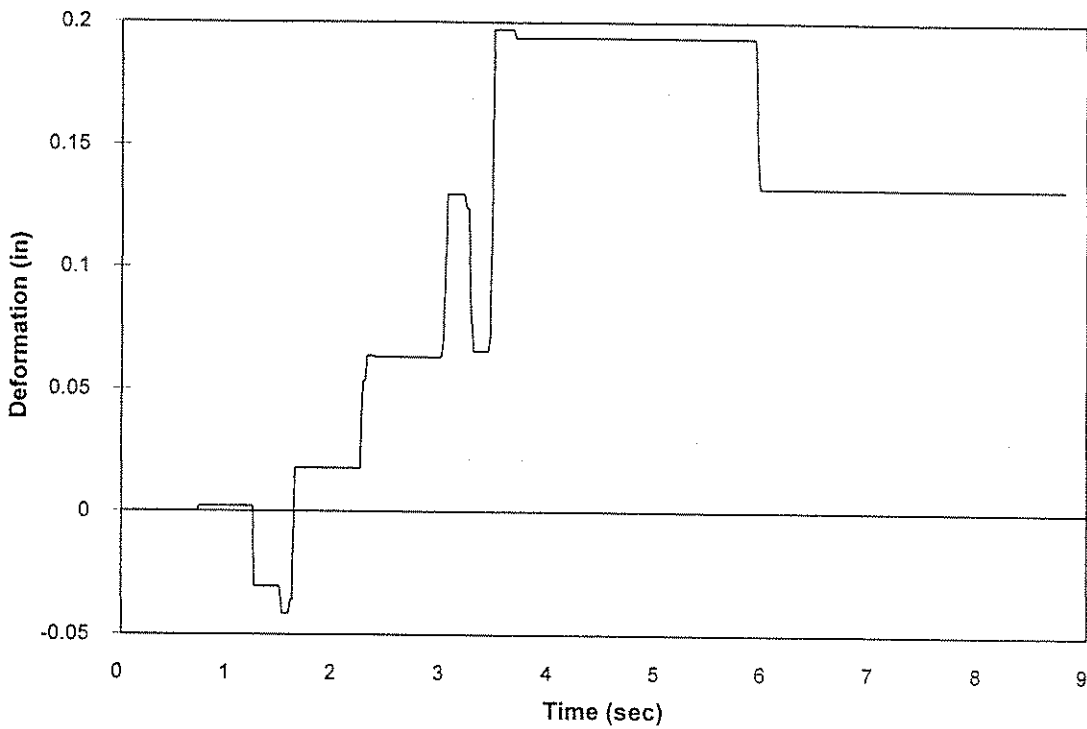


Figure 4-33 -Nonlinear Deformation History of Abutment 1 Bearing Bars in the Long. Dir. (3/4" TBG and 1" SG)

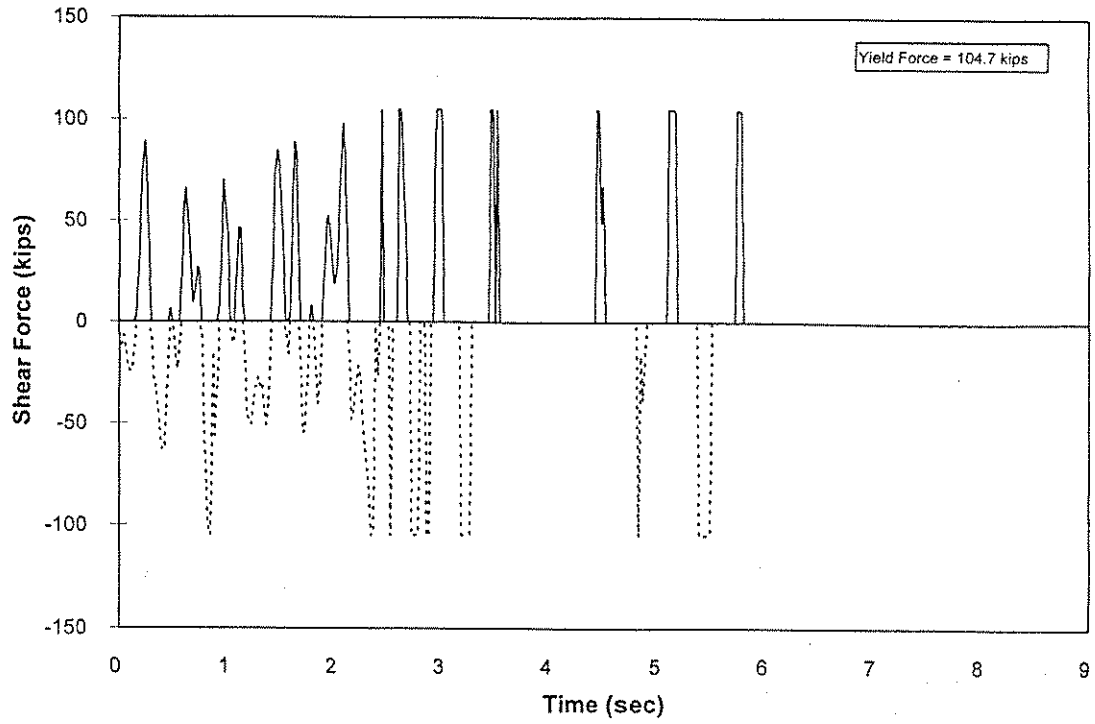


Figure 4-34 -Shear Force History of Abutment 1 Bearing Bars 1 in the Trans. Dir. (3/4" TBG and 1" SG)

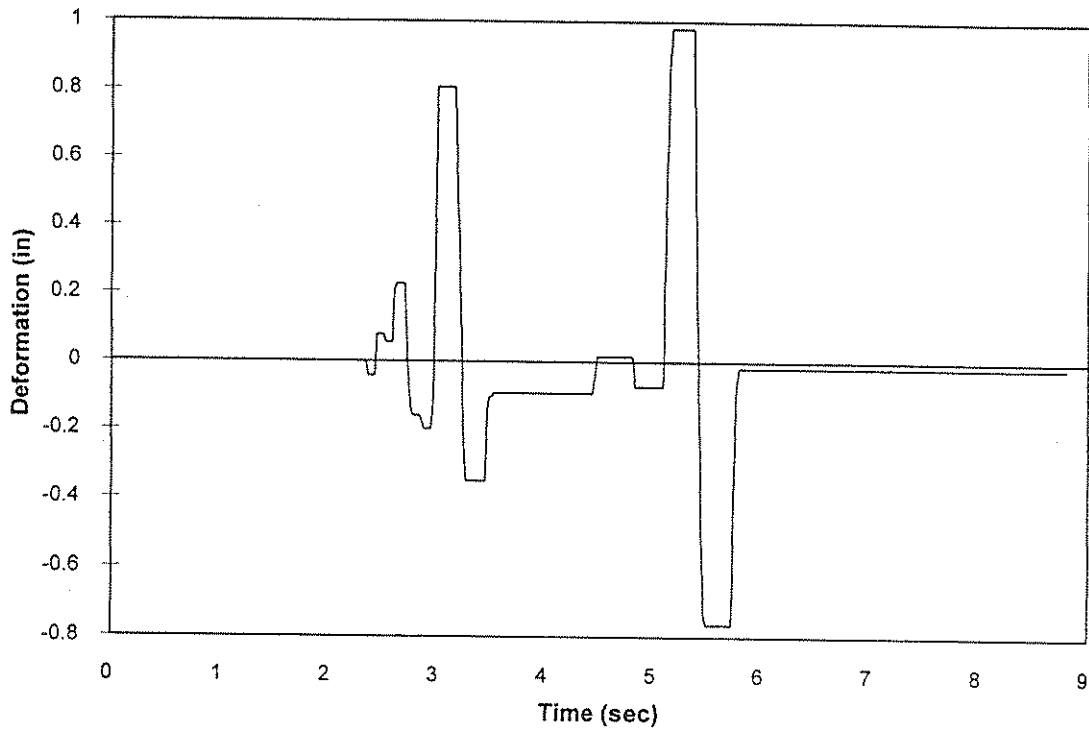


Figure 4-35 -Nonlinear Deformation History of Abutment 1 Bearing Bars in the Trans. Dir. (3/4" TBG and 1" SG)

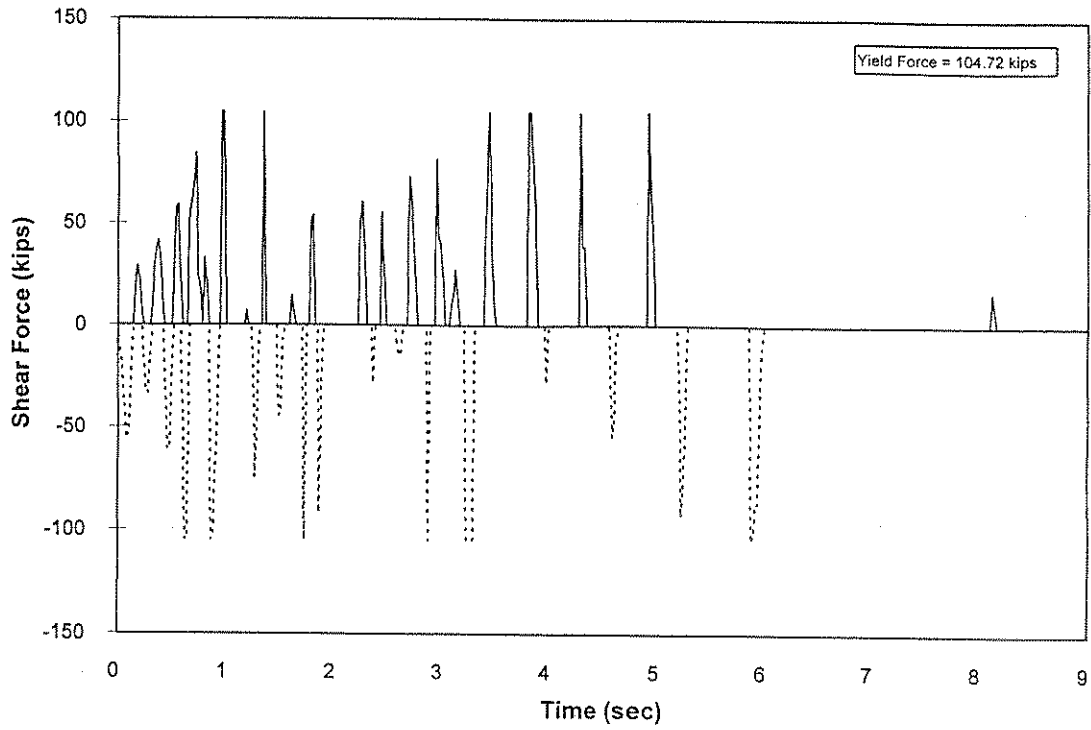


Figure 4-36 -Shear Force History of Abutment 6 Bearing Bars in the Long. Dir. (3/4" TBG and 1" SG)

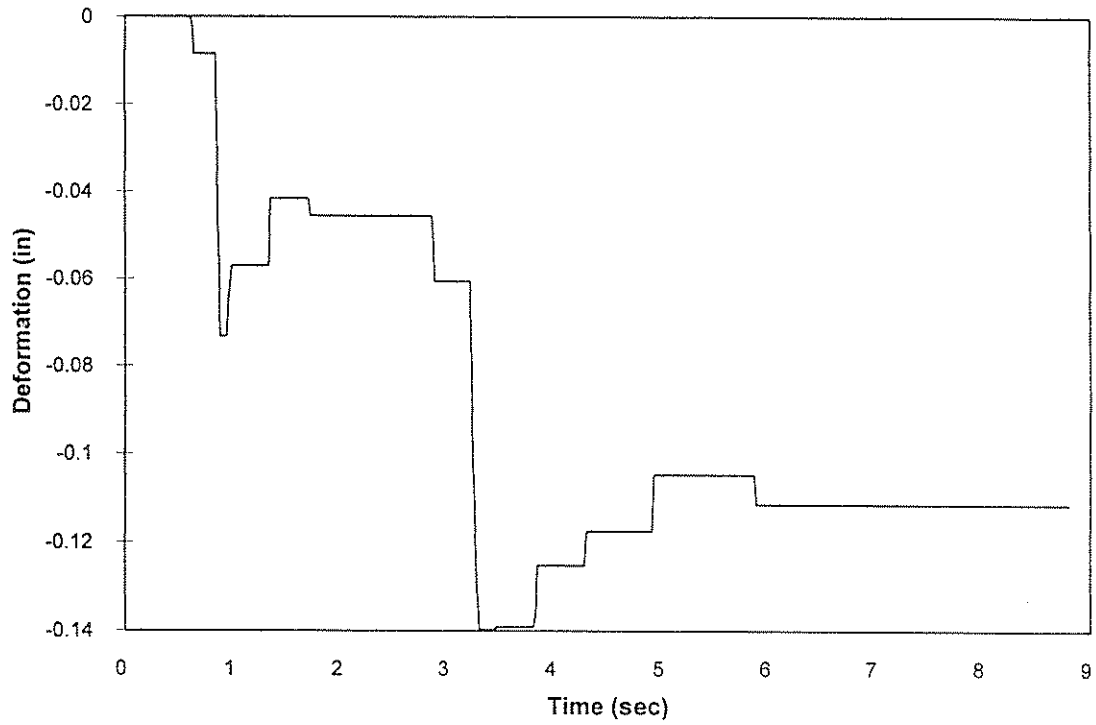


Figure 4-37 -Nonlinear Deformation History of Abutment 6 Bearing Bars in the Long. Dir. (3/4" TBG and 1" SG)

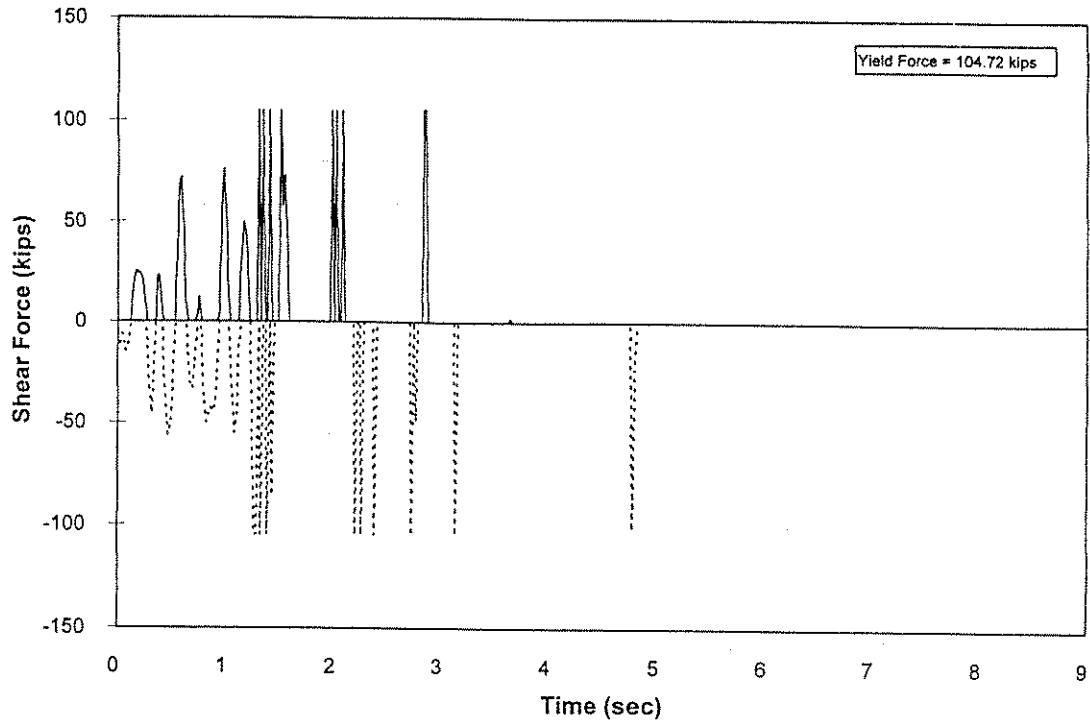


Figure 4-38 -Shear Force History of Abutment 6 Bearing Bars in the Trans. Dir. (3/4" TBG and 1" SG)

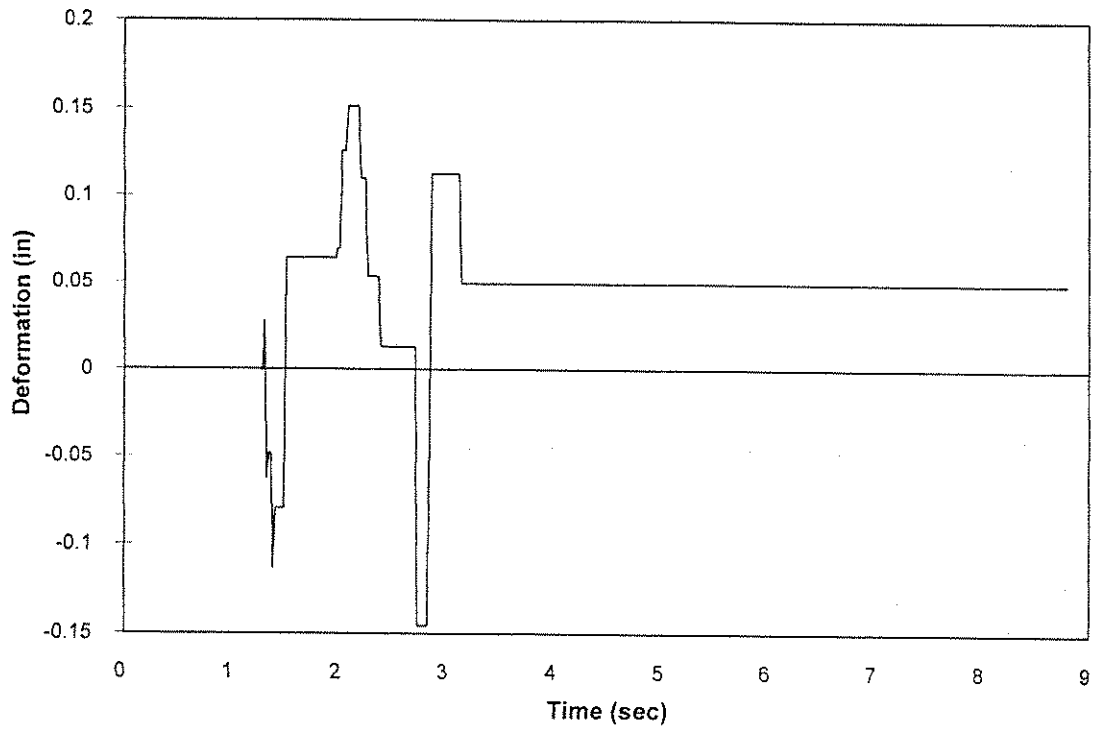


Figure 4-39 -Nonlinear Deformation History of Abutment 6 Bearing Bars in the Trans. Dir. (3/4" TBG and 1" SG)

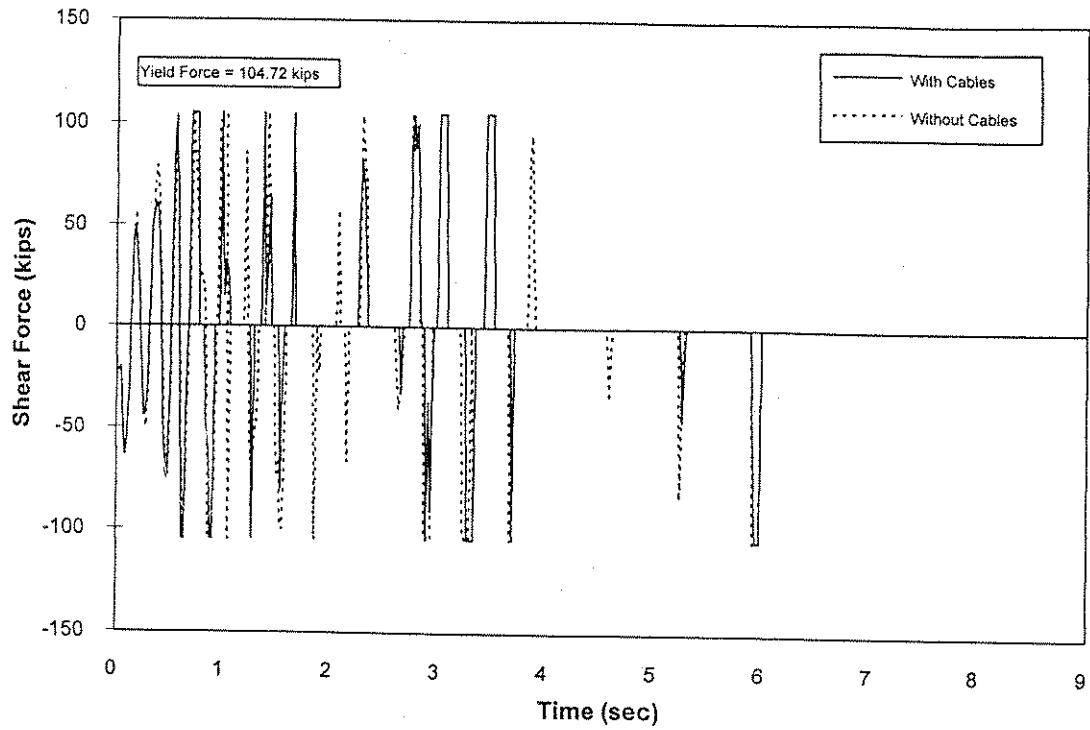


Figure 4-40 -Shear Force History of Abutment 1 Bearing Bars in the Long. Dir. (Motion Normalized to 0.7g)

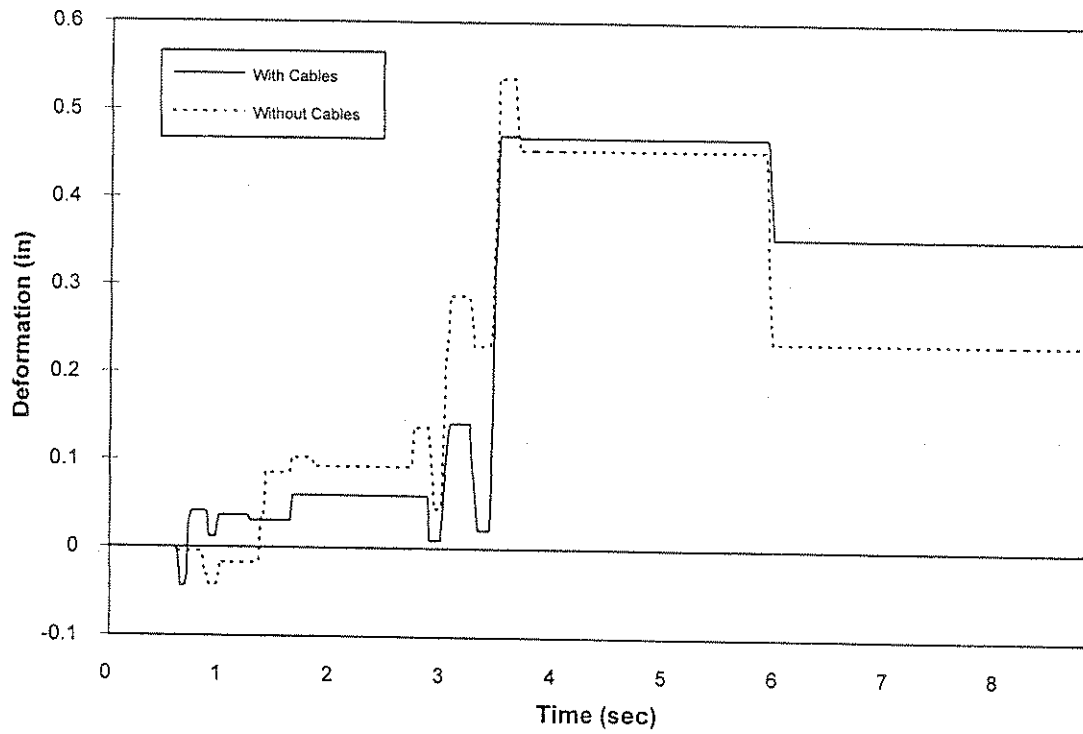


Figure 4-41 -Nonlinear Deformation History of Abutment 1 Bearing Bars in the Long. Dir. (Motion Normalized to 0.7g)

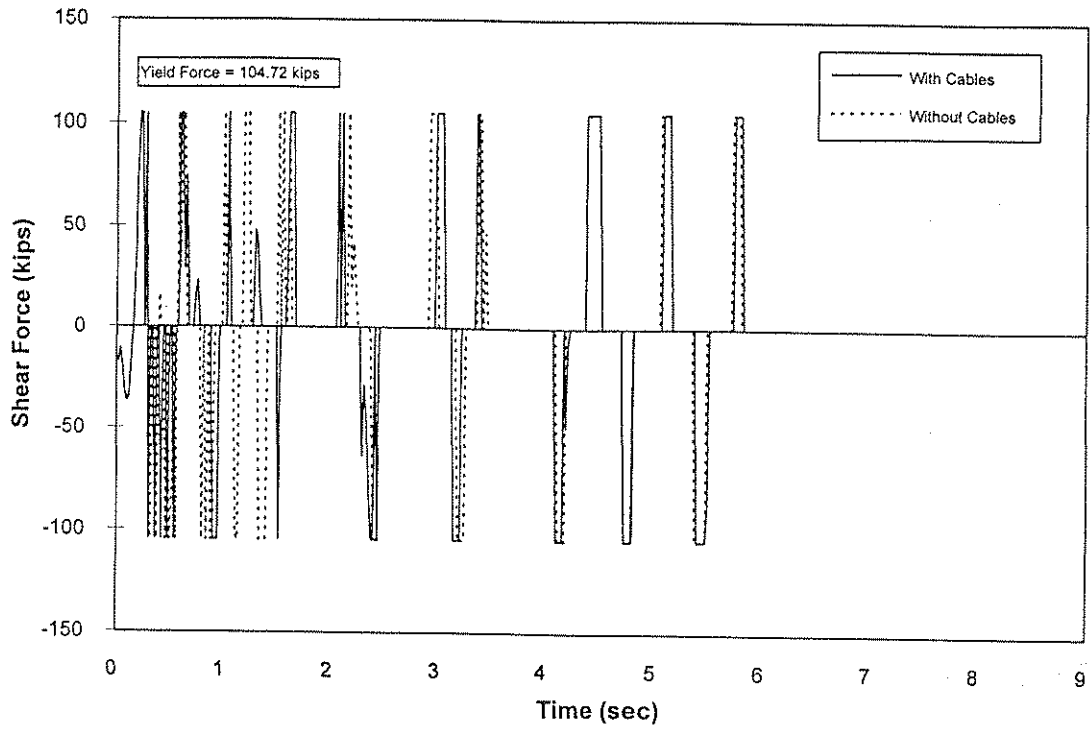


Figure 4-42 -Shear Force History of Abutment 1 Bearing Bars in the Trans. Dir. (Motion Normalized to 0.7g)

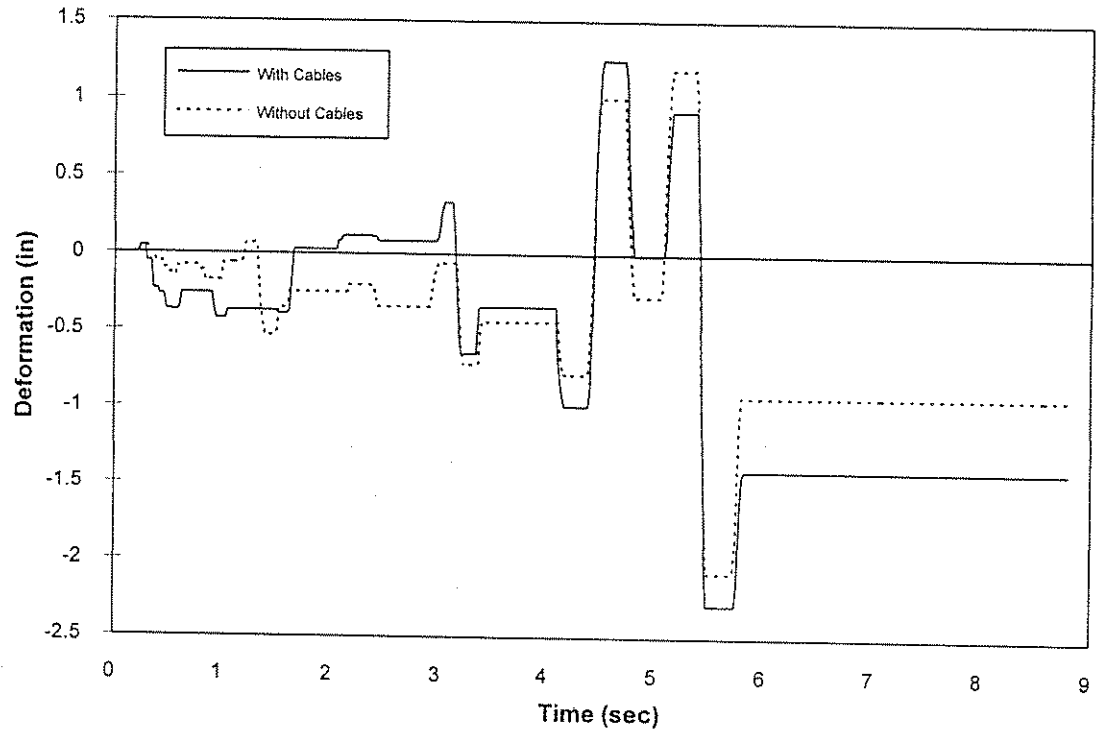


Figure 4-43 -Nonlinear Deformation History of Abutment 1 Bearing Bars in the Trans. Dir. (Motion Normalized to 0.7g)

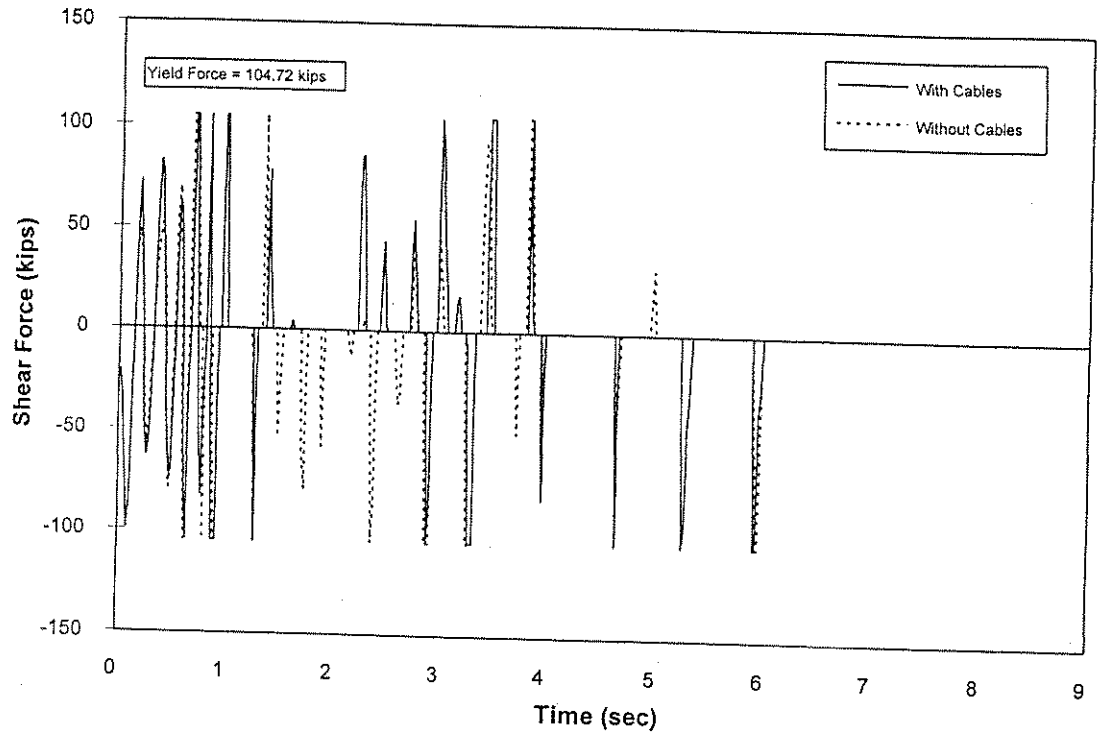


Figure 4-44 -Shear Force History of Abutment 6 Bearing Bars in the Long. Dir. (Motion Normalized to 0.7g)

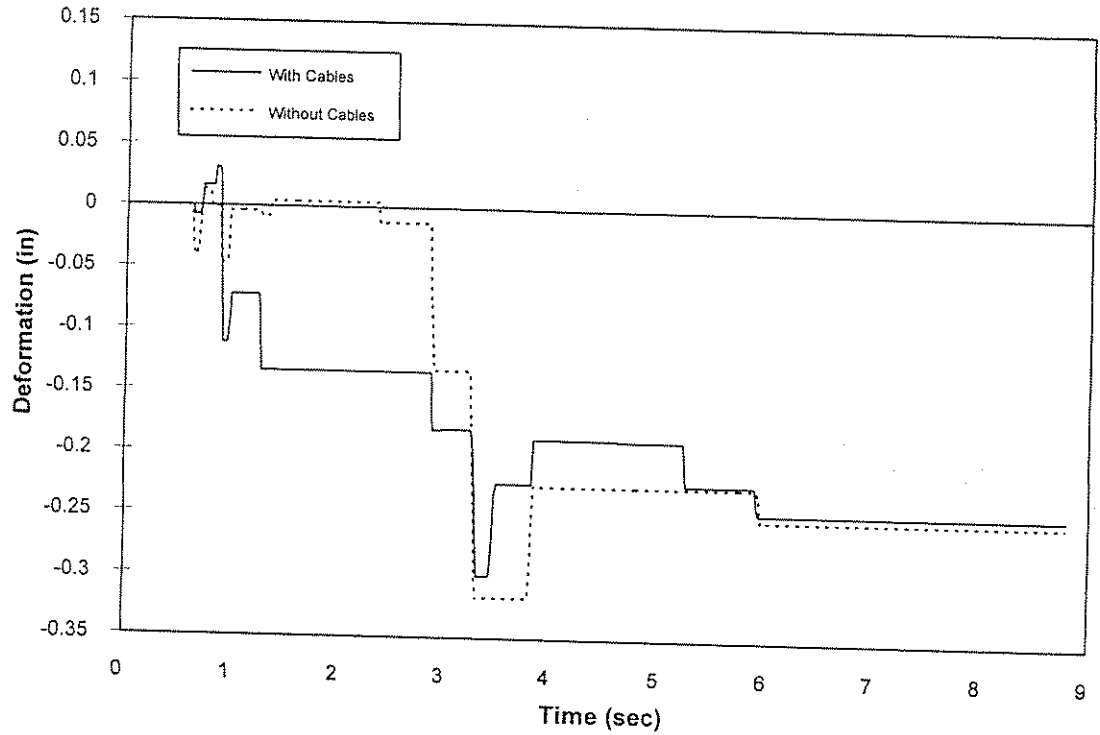


Figure 4-45 -Nonlinear Deformation History of Abutment 6 Bearing Bars in the Long. Dir. (Motion Normalized to 0.7g)

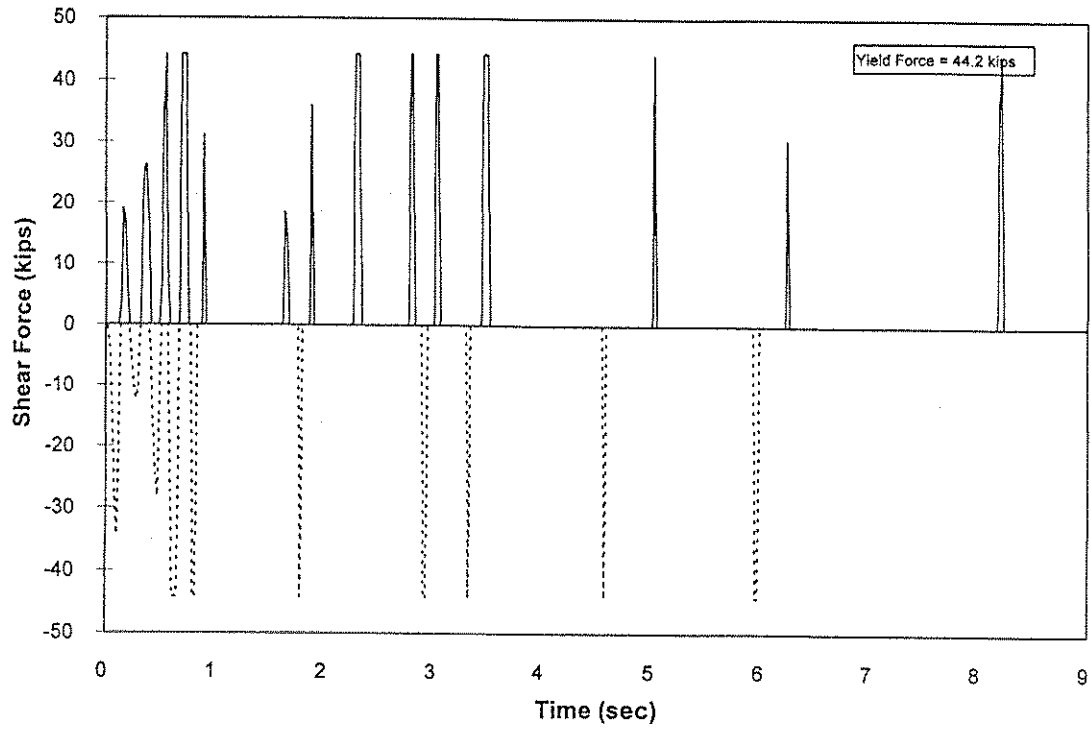


Figure 4-48 -Shear Force History of the Middle Hinge Shear Bolts in the Long. Dir. (3/4" TBG and 1" SG)

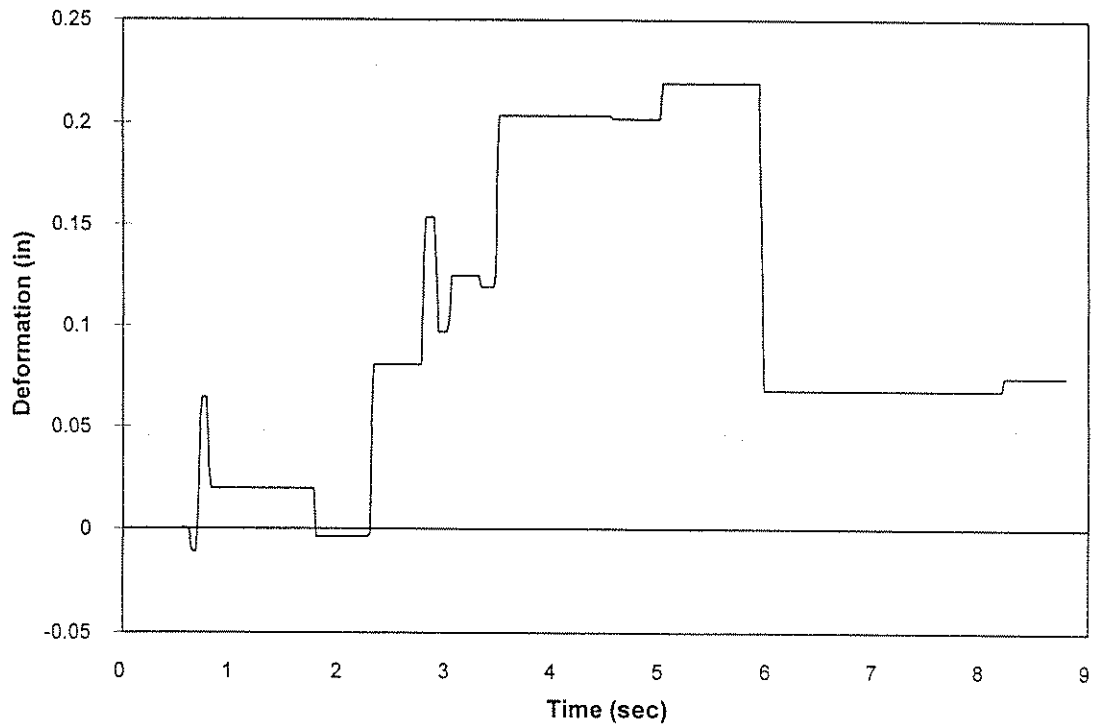


Figure 4-49 -Nonlinear Deformation History of the Middle Hinge Shear Bolts in the Long. Dir. (3/4" TBG and 1" SG)

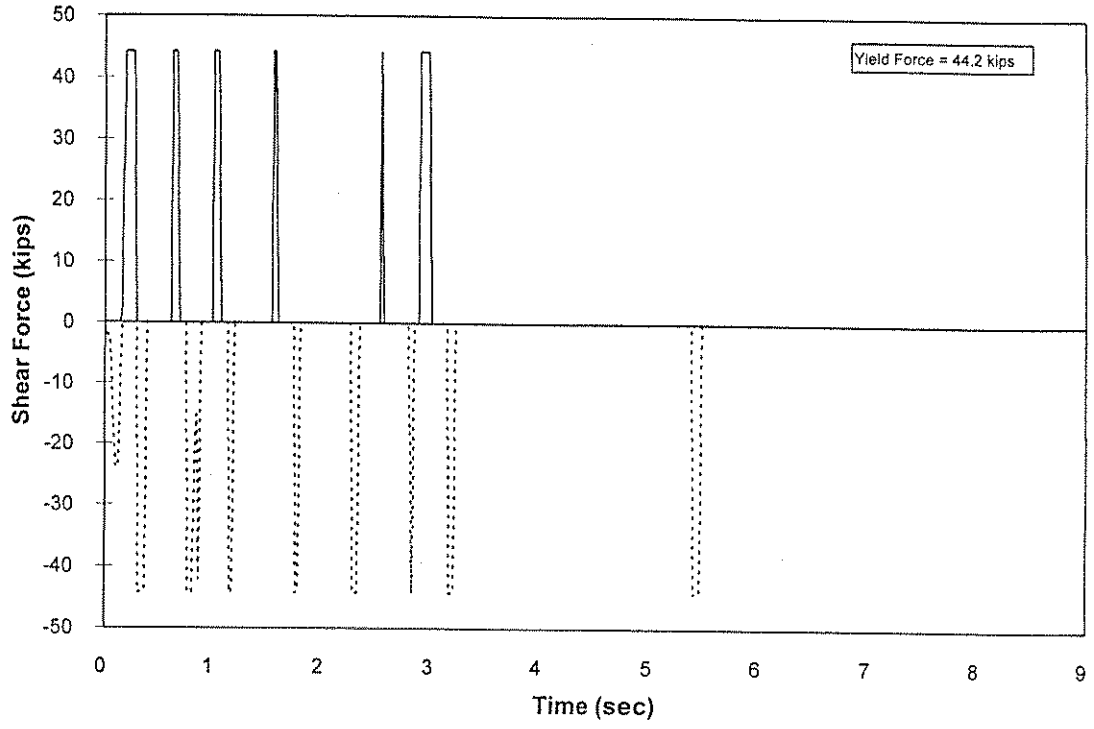


Figure 4-50 -Shear Force History of the Middle Hinge Shear Bolts in the Trans. Dir. (3/4" TBG and 1" SG)

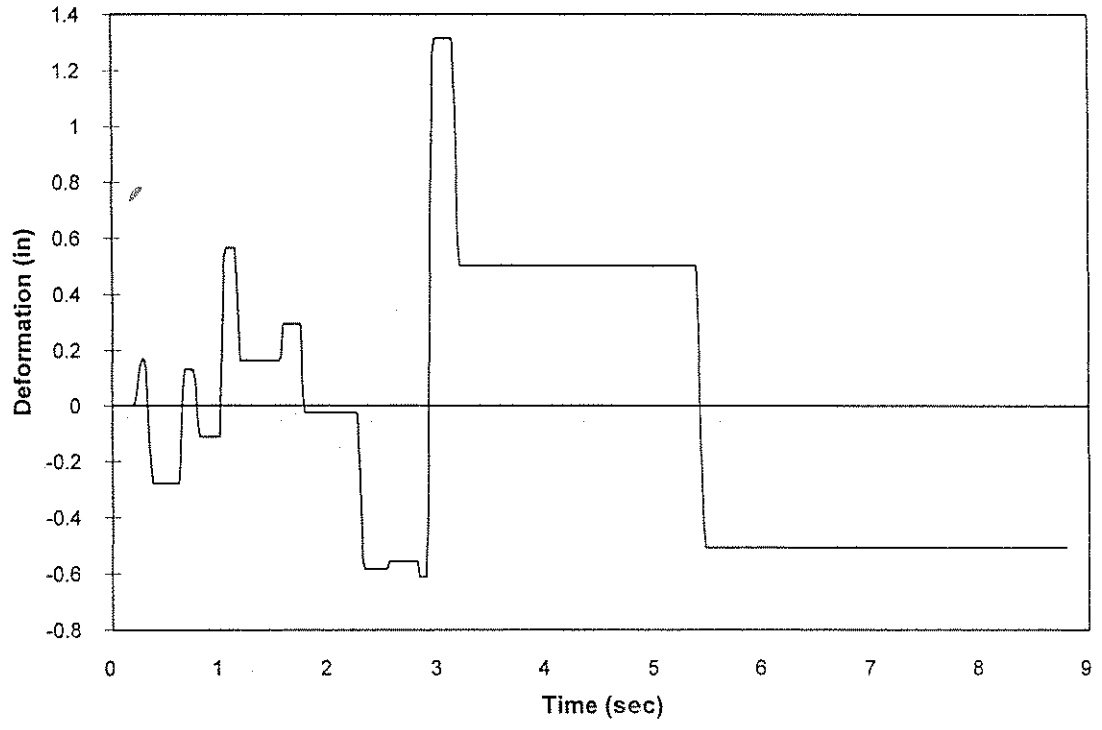


Figure 4-51 -Nonlinear Deformation History of the Middle Hinge Shear Bolts in the Trans. Dir. (3/4" TBG and 1" SG)

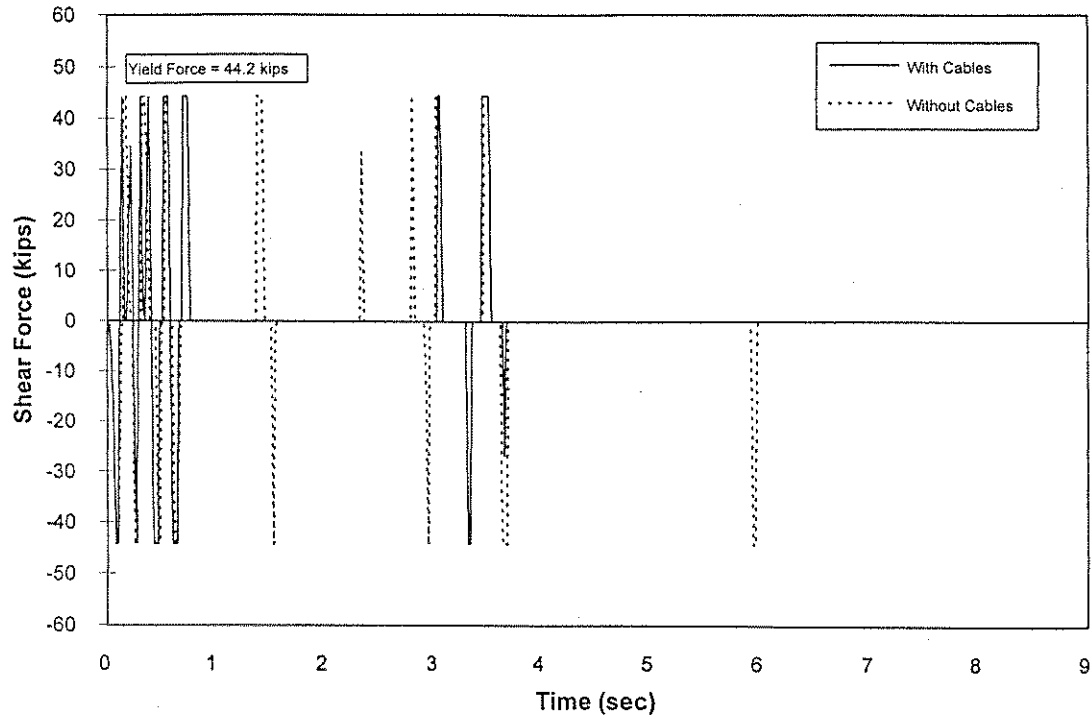


Figure 4-52 -Shear Force History of the Middle Hinge Shear Bolts in the Long. Dir. (Motion Normalized to 0.7g)

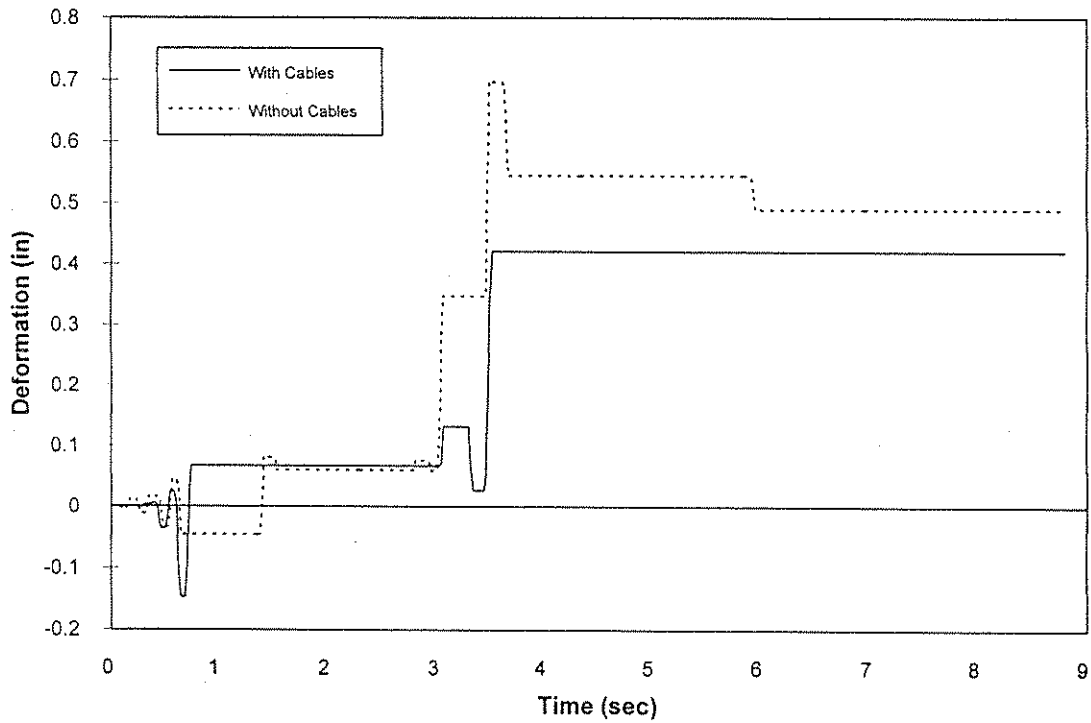


Figure 4-53 -Nonlinear Deformation History of the Middle Hinge Shear Bolts in the Long. Dir. (Motion Normalized to 0.7g)

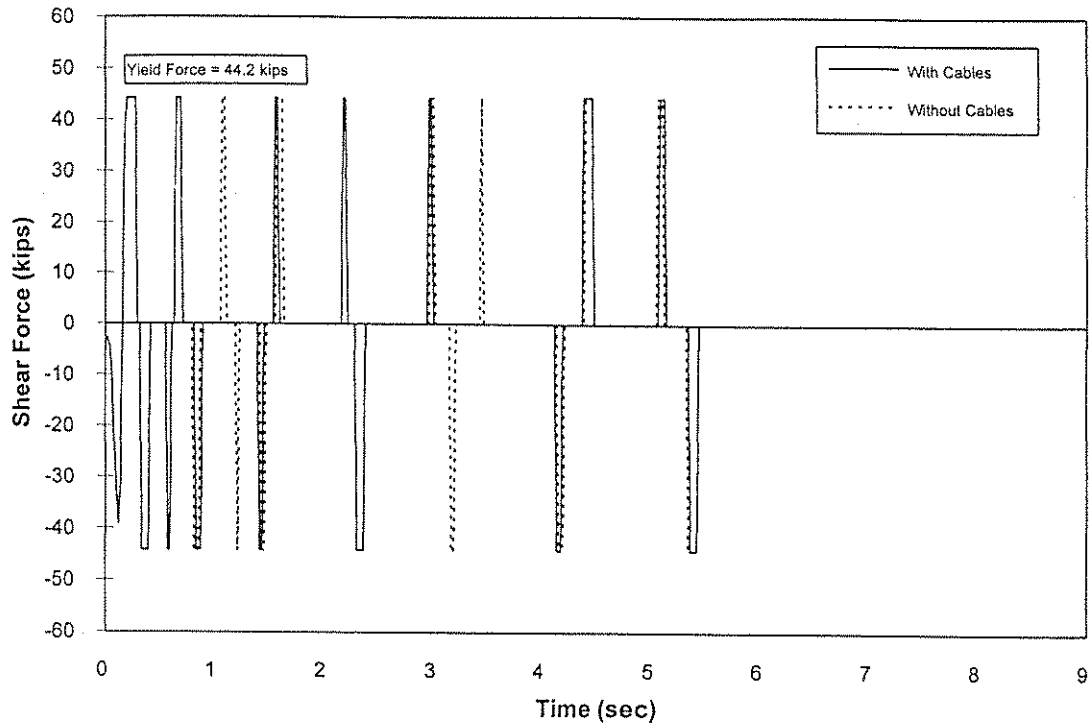


Figure 4-54 -Shear Force History of the Middle Hinge Shear Bolts in the Trans. Dir. (Motion Normalized to 0.7g)

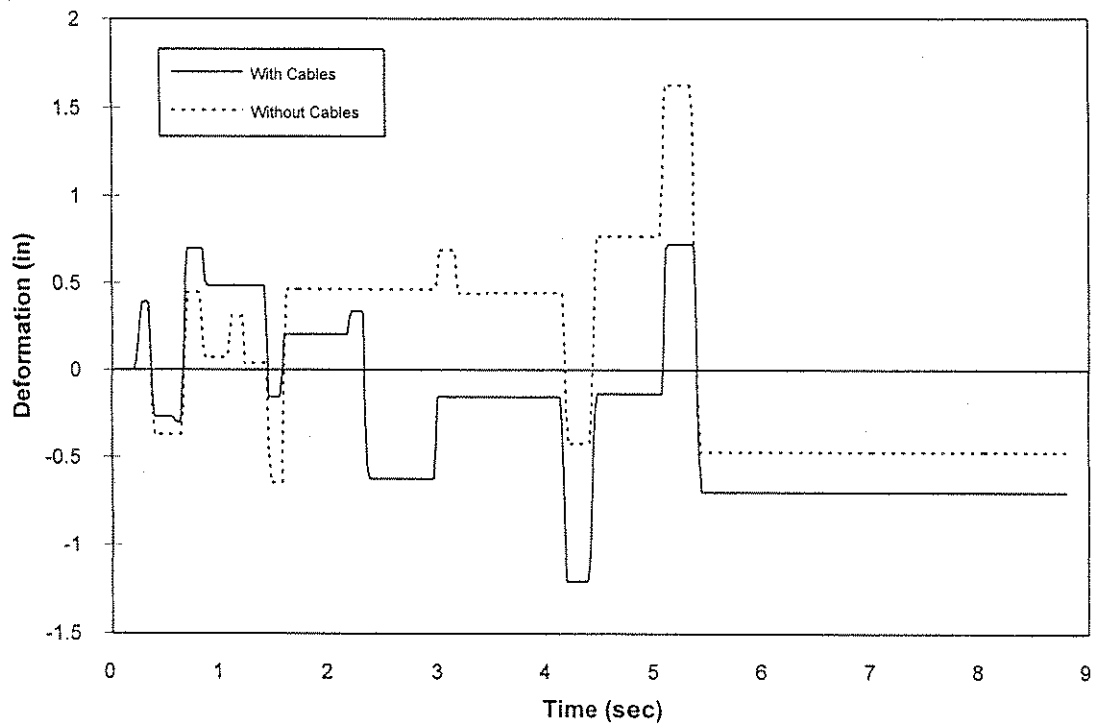


Figure 4-55 -Nonlinear Deformation History of the Middle Hinge Shear Bolts in the Trans. Dir. (Motion Normalized to 0.7g)

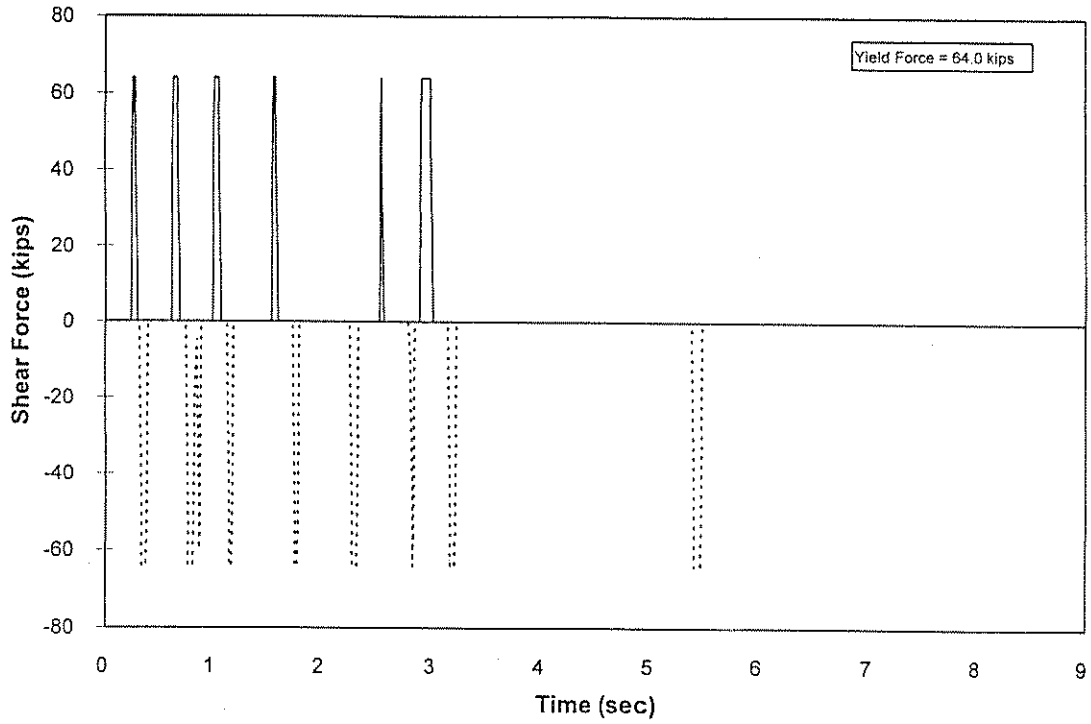


Figure 4-56 -Shear Force History of the Middle Hinge Shear Pipes in the Trans. Dir. (3/4" TBG and 1" SG)

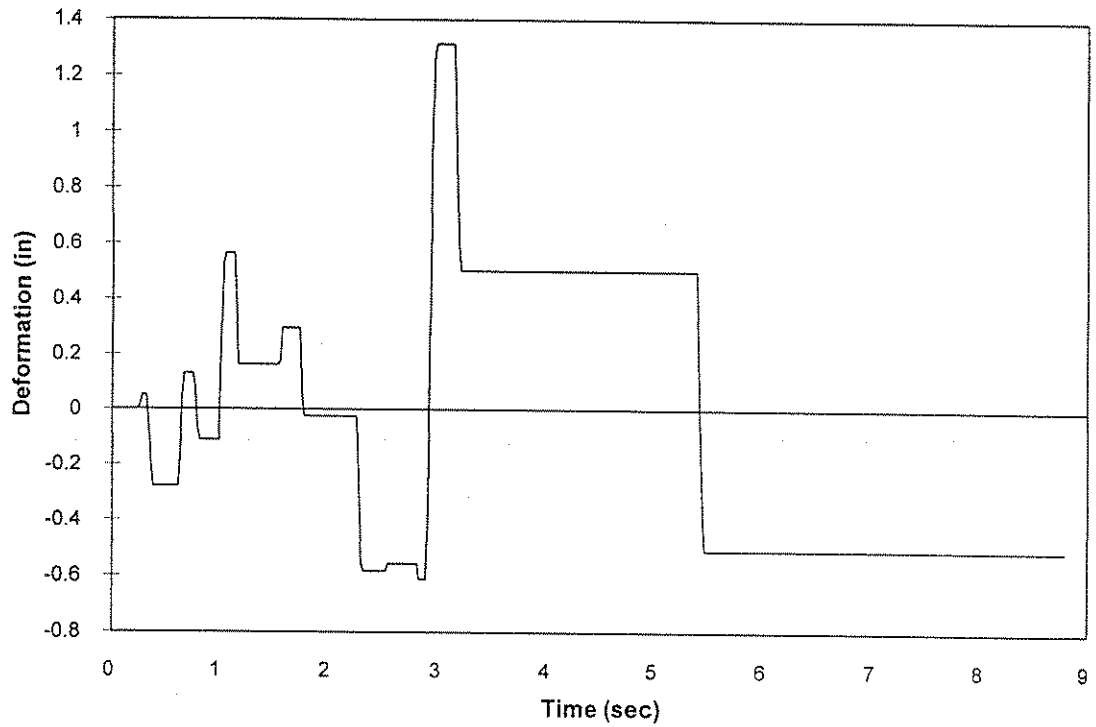


Figure 4-57 -Nonlinear Deformation History of the Middle Hinge Shear Pipes in the Trans. Dir. (3/4" TBG and 1" SG)

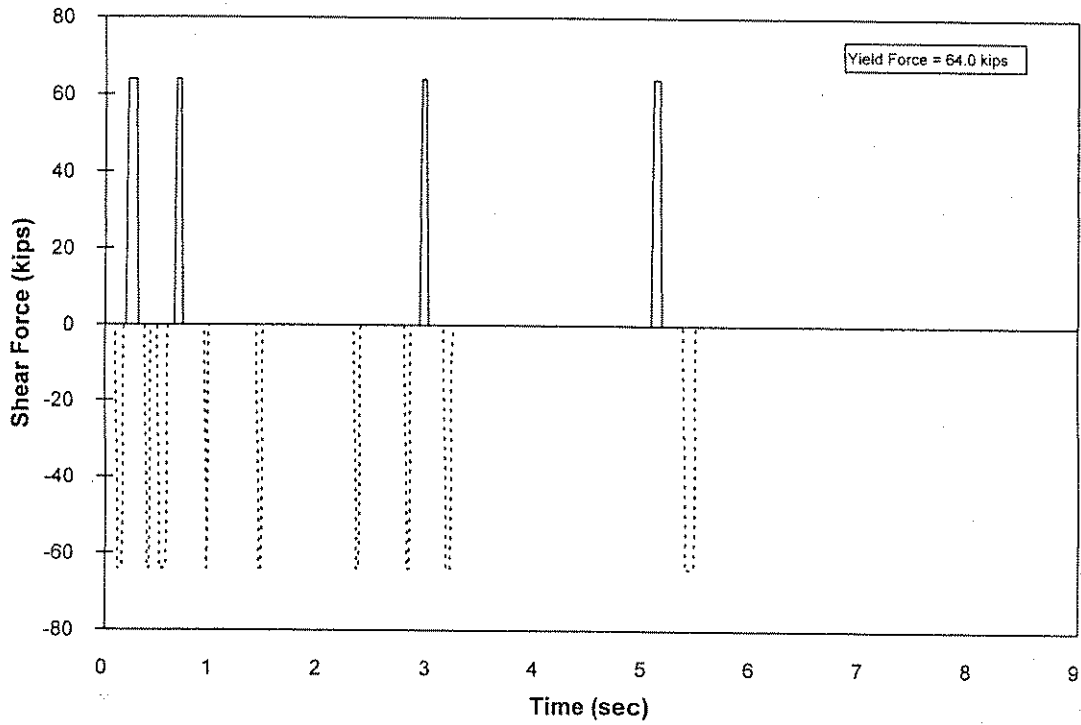


Figure 4-58 -Shear Force History of the Middle Hinge Shear Pipes in the Trans. Dir. (0" TBG, 1" SG, and W/O Shear Bolts)

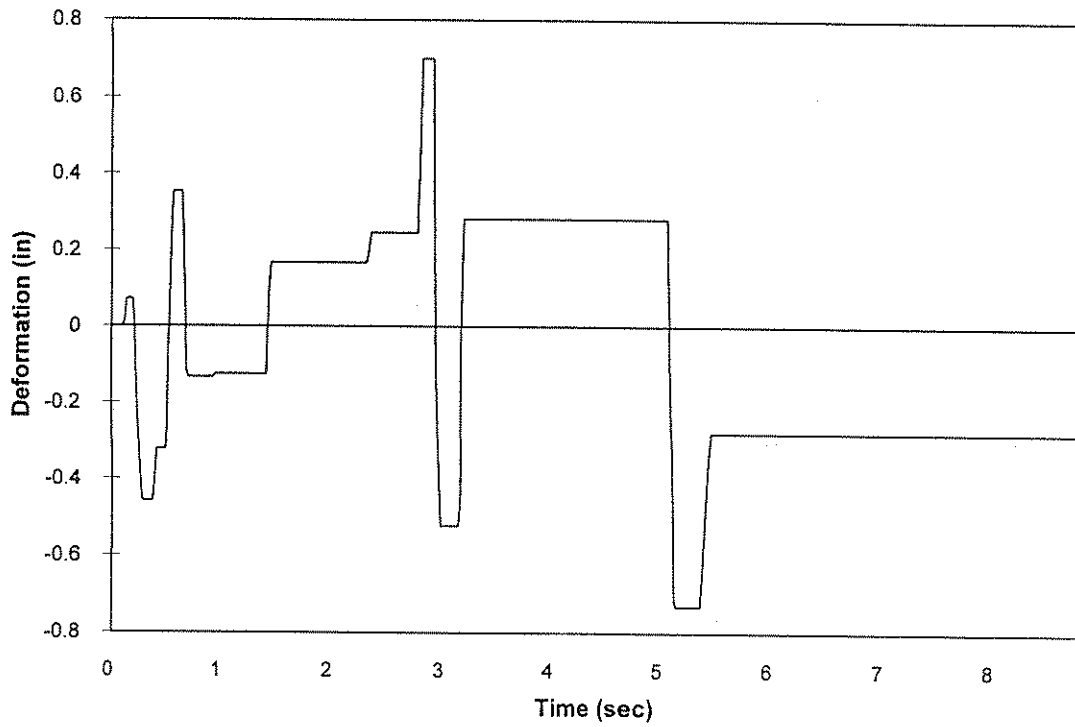


Figure 4-59 -Nonlinear Deformation History of the Middle Hinge Shear Pipes in the Trans. Dir. (0" TBG, 1" SG, and W/O Shear Bolts)

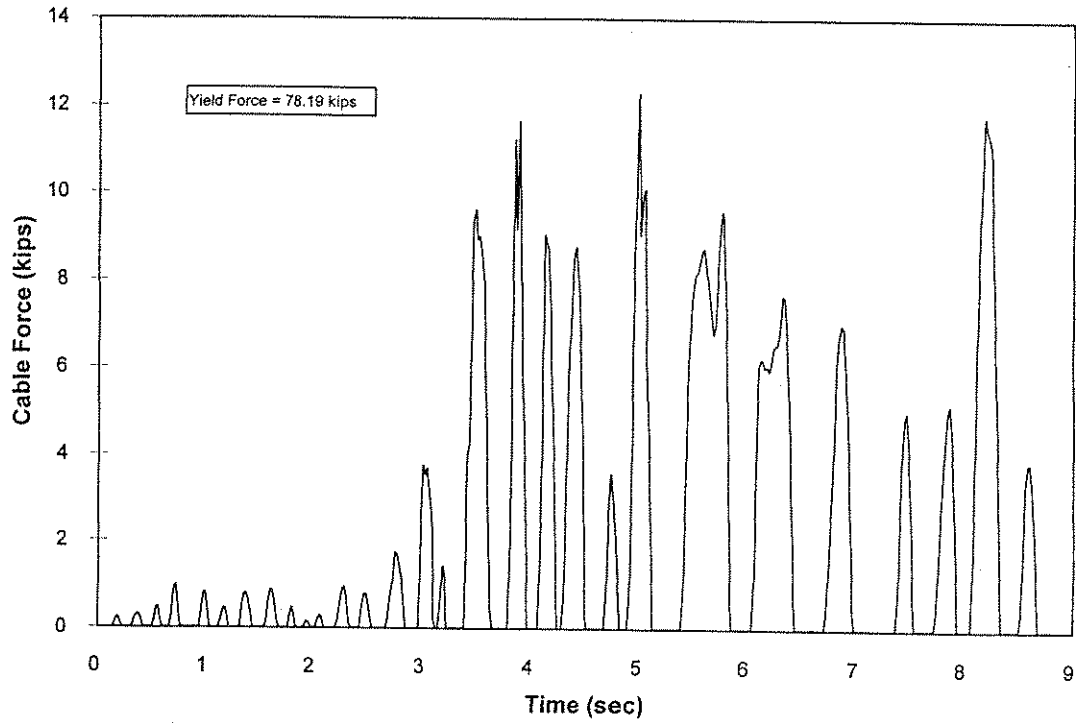


Figure 4-60 Tie Bar Force History of Abutment 1 Restrainers (0" TBG and 1" SG)

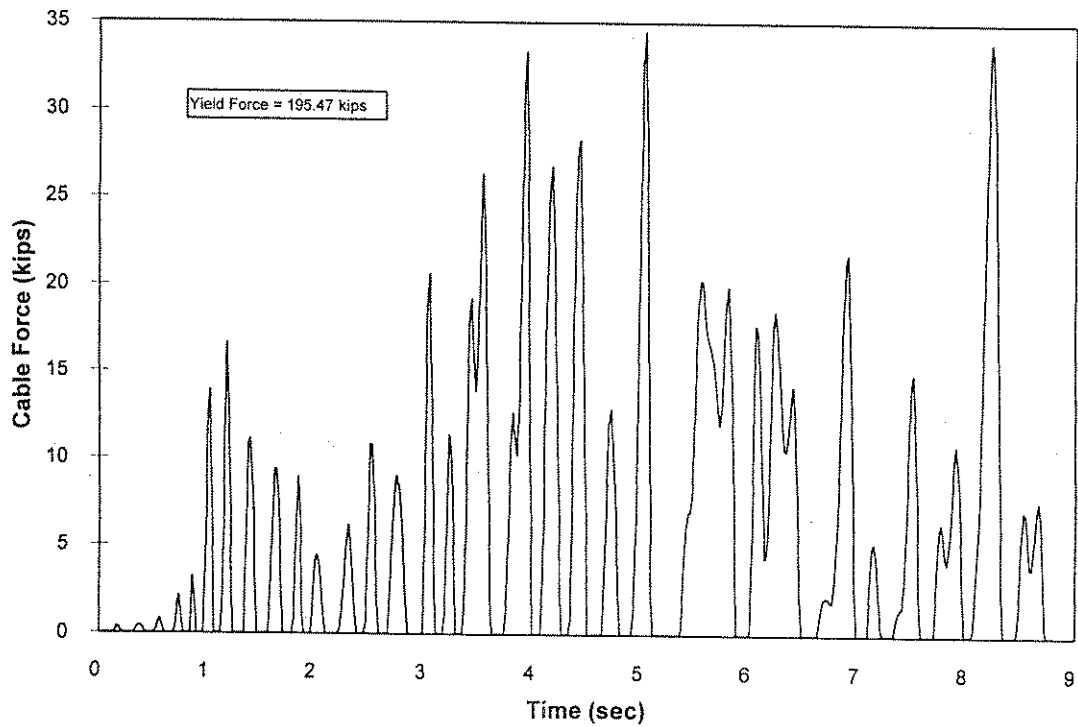


Figure 4-61 -Tie Bar Force History of the Middle Hinge Restrainers (0" TBG and 1" SG)

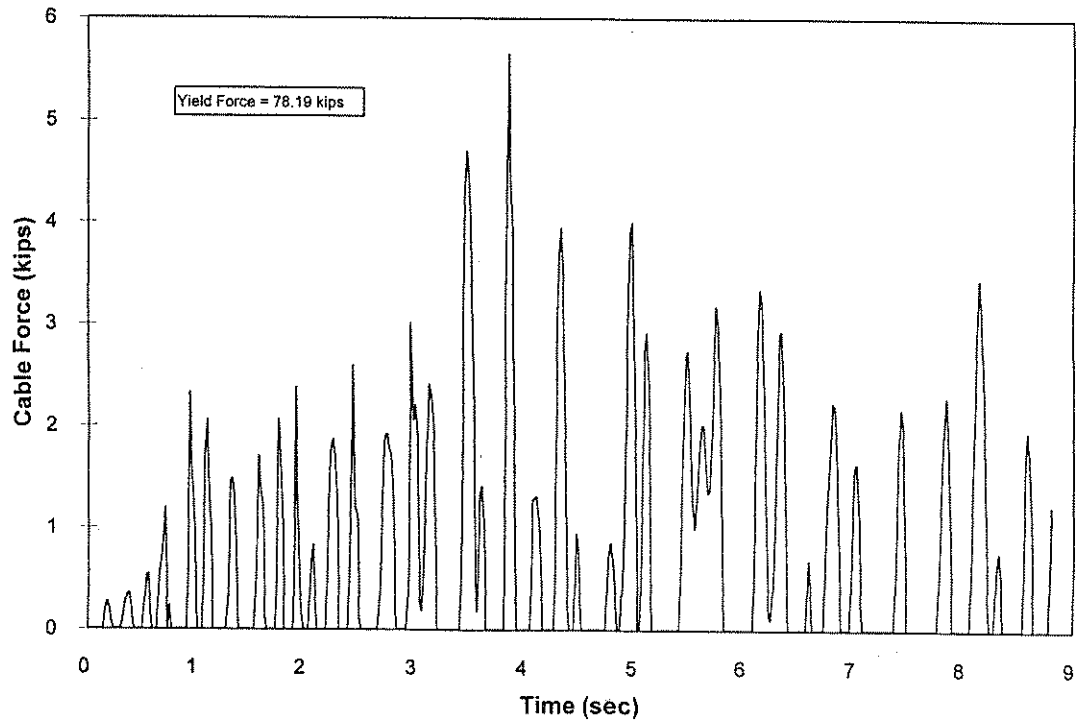


Figure 4-62 -Tie Bar Force History of Abutment 6 Restrainers (0" TBG and 1" SG)

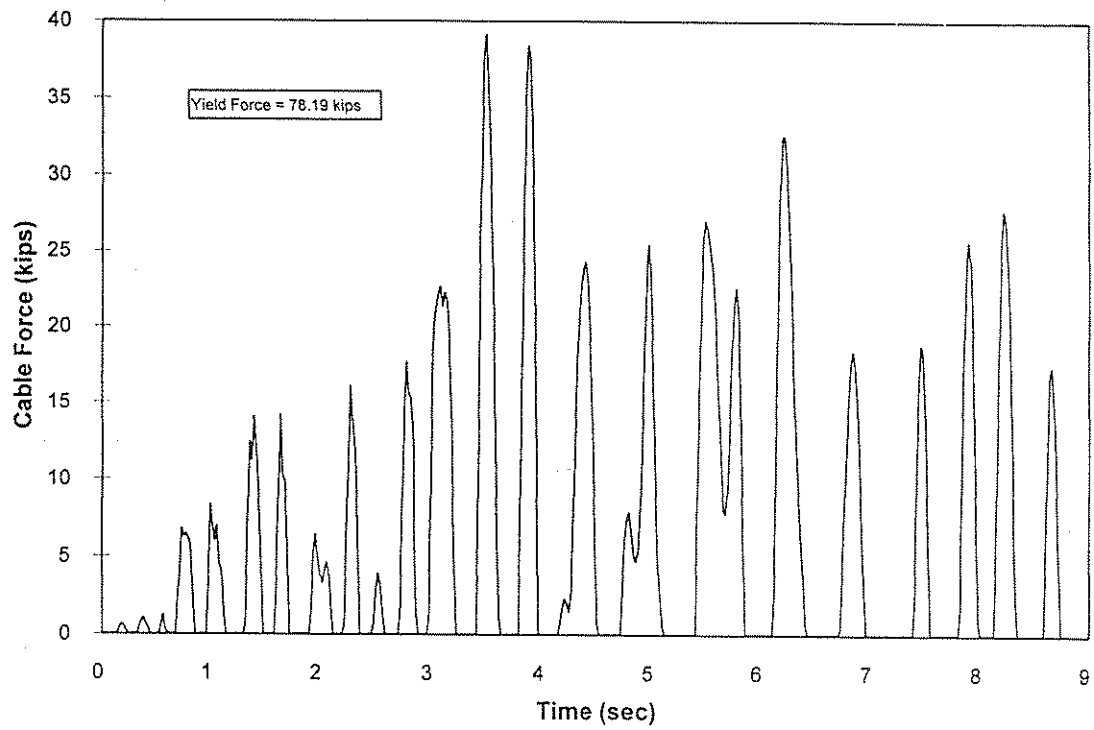


Figure 4-63 -Tie Bar Force History of Abutment 1 Restrainers (Motion Normalized to 1.0 g)

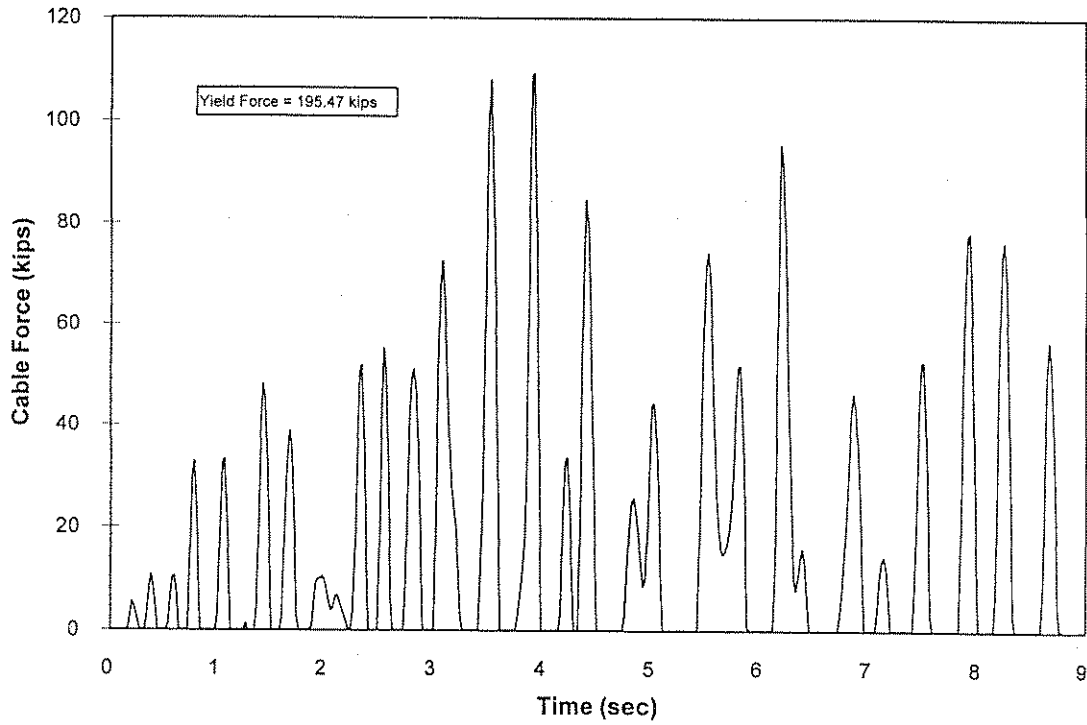


Figure 4-64 -Tie Bar Force History of the Middle Hinge Restrainers (Motion Normalized to 1.0 g)

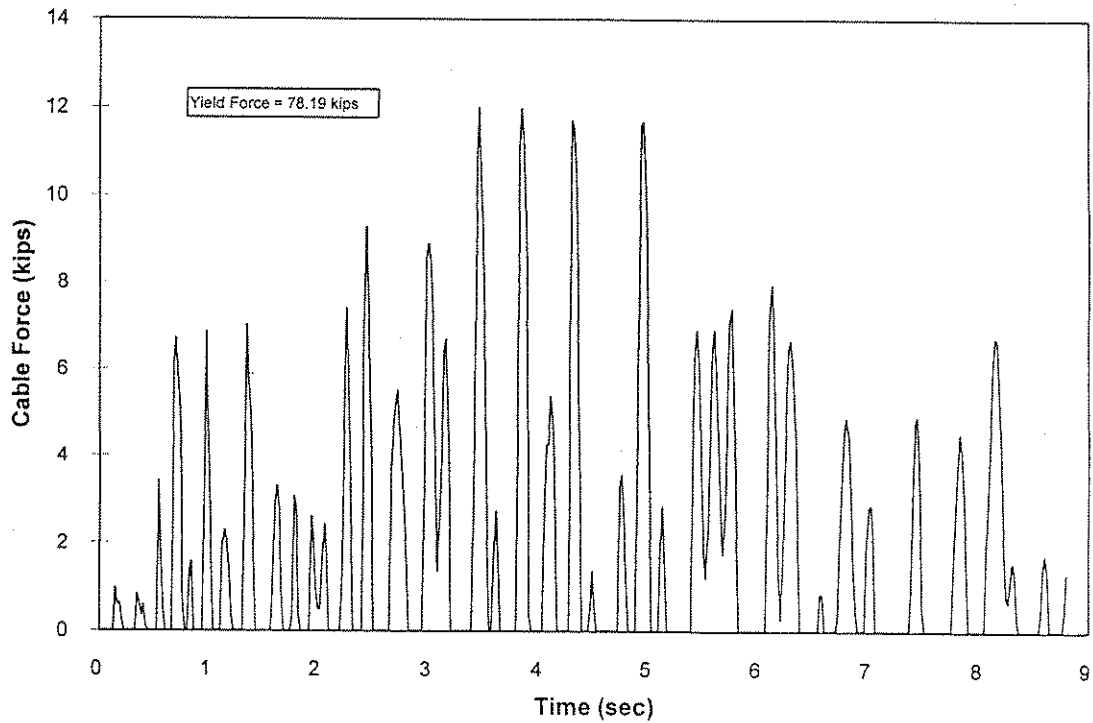


Figure 4-65 -Tie Bar Force History of Abutment 6 Restrainers (Motion Normalized to 1.0 g)

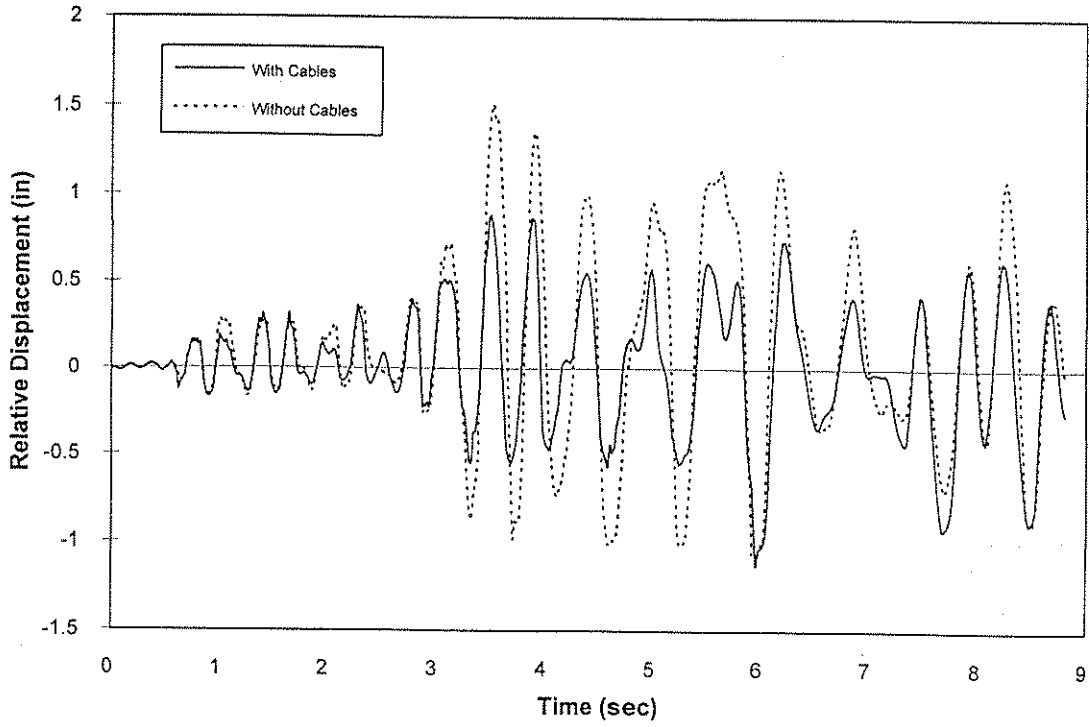


Figure 4-66 -Longitudinal Relative Displacement History at Abutment 1  
(Motion Normalized to 1.0 g)

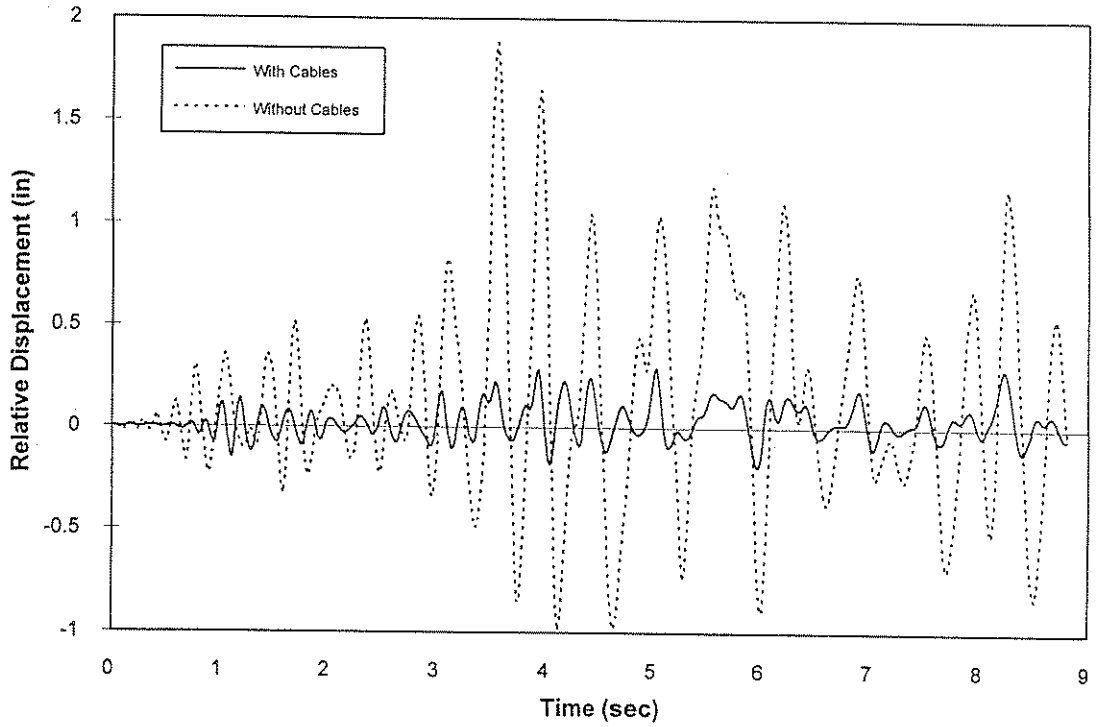


Figure 4-67 -Longitudinal Relative Displacement History at the Middle Hinge  
(Motion Normalized to 1.0 g)

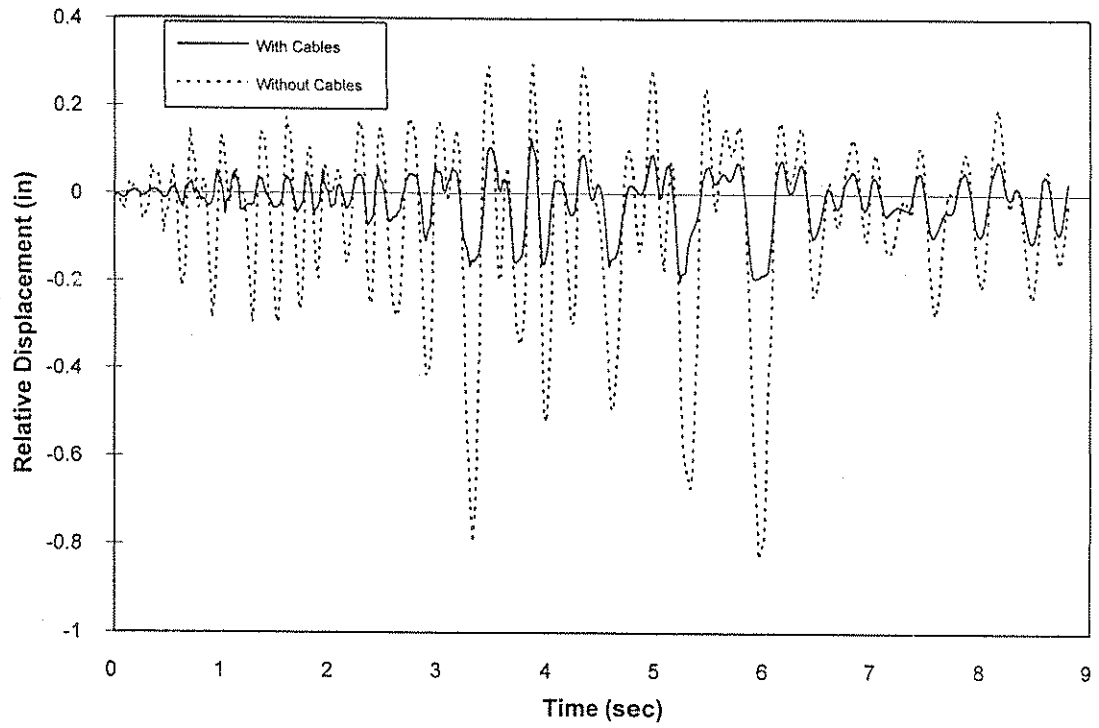


Figure 4-68 -Longitudinal Relative Displacement History at Abutment 6 (Motion Normalized to 1.0 g)

## List of CCEER Publications

<u>Report No.</u>	<u>Publication</u>
CCEER-84-1	Saiidi, M., and R. A. Lawver. "User's manual for LZAK-C64, a computer program to implement the Q-model on Commodore 64." <i>Report number CCEER-84-1</i> . Reno: University of Nevada, Department of Civil Engineering. January 1984.
CCEER-84-2	Douglas, B. M., and T. Iwasaki. "Proceedings of the first USA-Japan bridge engineering workshop," held at the Public Works Research Institute, Tsukuba, Japan. <i>Report number CCEER-84-2</i> . Reno: University of Nevada, Department of Civil Engineering. April 1984.
CCEER-84-3	Saiidi, M., J. D. Hart, and B. M. Douglas. "Inelastic static and dynamic analysis of short R/C bridges subjected to lateral loads." <i>Report number CCEER-84-3</i> . Reno: University of Nevada, Department of Civil Engineering. July 1984.
CCEER-84-4	Douglas, B. "A proposed plan for a national bridge engineering laboratory." <i>Report number CCEER-84-4</i> . Reno: University of Nevada, Department of Civil Engineering. December 1984.
CCEER-85-1	Norris, G. M., and P. Abdollaholiaee. "Laterally loaded pile response: Studies with the strain wedge model." <i>Report number CCEER-85-1</i> . Reno: University of Nevada, Department of Civil Engineering. April 1985.
CCEER-86-1	Ghusn, G. E., and M. Saiidi. "A simple hysteretic element for biaxial bending of R/C columns and implementation in NEABS-86." <i>Report number CCEER-86-1</i> . Reno: University of Nevada, Department of Civil Engineering. July 1986.
CCEER-86-2	Saiidi, M., R. A. Lawver, and J. D. Hart. "User's manual of ISADAB and SIBA, computer programs for nonlinear transverse analysis of highway bridges subjected to static and dynamic lateral loads." <i>Report number CCEER-86-2</i> . Reno: University of Nevada, Department of Civil Engineering. September 1986.
CCEER-87-1	Siddharthan, R. "Dynamic effective stress response of surface and embedded footings in sand." <i>Report number CCEER-87-1</i> . Reno: University of Nevada, Department of Civil Engineering. June 1987.
CCEER-87-2	Norris, G., and R. Sack. "Lateral and rotational stiffness of pile groups for seismic analysis of highway bridges." <i>Report number CCEER-87-2</i> . Reno: University of Nevada, Department of Civil Engineering. June 1987.
CCEER-88-1	Orie, J., and M. Saiidi. "A preliminary study of one-way reinforced concrete pier hinges subjected to shear and flexure." <i>Report number CCEER-88-1</i> . Reno: University of Nevada, Department of Civil Engineering. January 1988.

- CCEER-88-2      Orie, D., M. Saiidi, and B. Douglas. "A micro-CAD system for seismic design of regular highway bridges." *Report number CCEER-88-2*. Reno: University of Nevada, Department of Civil Engineering. June 1988.
- CCEER-88-3      Orie, D., and M. Saiidi. "User's manual for Micro-SARB, a microcomputer program for seismic analysis of regular highway bridges." *Report number CCEER-88-3*. Reno: University of Nevada, Department of Civil Engineering. October 1988.
- CCEER-89-1      Douglas, B., M. Saiidi, R. Hayes, and G. Holcomb. "A comprehensive study of the loads and pressures exerted on wall forms by the placement of concrete." *Report number CCEER-89-1*. Reno: University of Nevada, Department of Civil Engineering. February 1989.
- CCEER-89-2a      Richardson, J., and B. Douglas. "Dynamic response analysis of the Dominion Road Bridge test data." *Report number CCEER-89-2*. Reno: University of Nevada, Department of Civil Engineering. March 1989.
- CCEER-89-2b      Vrontinos, S., M. Saiidi, and B. Douglas. "A simple model to predict the ultimate response of R/C beams with concrete overlays." *Report number CCEER-89-2*. Reno: University of Nevada, Department of Civil Engineering. June 1989.
- CCEER-89-3      Ebrahimpour, A., and P. Jagadish. "Statistical modeling of bridge traffic loads: A case study." *Report number CCEER-89-3*. Reno: University of Nevada, Department of Civil Engineering. December 1989.
- CCEER-89-4      Shields, J., and M. Saiidi. "Direct field measurement of prestress losses in box girder bridges." *Report number CCEER-89-4*. Reno: University of Nevada, Department of Civil Engineering. December 1989.
- CCEER-90-1      Saiidi, M., E. Maragakis, G. Ghosn, Jr., Y. Jiang, and D. Schwartz. "Survey and evaluation of Nevada's transportation infrastructure, task 7.2—highway bridges, final report." *Report number CCEER-90-1*. Reno: University of Nevada, Department of Civil Engineering. October 1990.
- CCEER-90-2      Abdel-Ghaffar, S., E. Maragakis, and M. Saiidi. "Analysis of the response of reinforced concrete structures during the Whittier earthquake of 1987." *Report number CCEER-90-2*. Reno: University of Nevada, Department of Civil Engineering. October 1990.
- CCEER-91-1      Saiidi, M., E. Hwang, E. Maragakis, and B. Douglas. "Dynamic testing and analysis of the Flamingo Road Interchange." *Report number CCEER-91-1*. Reno: University of Nevada, Department of Civil Engineering. February 1991.
- CCEER-91-2      Norris, G., R. Siddharthan, Z. Zafir, S. Abdel-Ghaffar, and P. Gowda. "Soil-foundation-structure behavior at the Oakland Outer Harbor Wharf." *Report number CCEER-91-2*. Reno: University of Nevada, Department of Civil Engineering. July 1991.

- CCEER-91-3 Norris, G. M. "Seismic lateral and rotational pile foundation stiffness at Cypress." *Report number CCEER-91-3*. Reno: University of Nevada, Department of Civil Engineering. August 1991.
- CCEER-91-4 O'Connor, D. N., and M. Saiidi. "A study of protective overlays for highway bridge decks in Nevada, with emphasis on polyester-styrene polymer concrete." *Report number CCEER-91-4*. Reno: University of Nevada, Department of Civil Engineering. October 1991.
- CCEER-91-5 O'Connor, D. N., and M. Saiidi. "Laboratory studies of polyester-styrene polymer concrete engineering properties." *Report number CCEER-91-5*. Reno: University of Nevada, Department of Civil Engineering. November 1991.
- CCEER-92-1 Straw, D. L., and M. "Saiid" Saiidi. "Scale model testing of one-way reinforced concrete pier hinges subjected to combined axial force, shear and flexure." *Report number CCEER-92-1*, ed. by D. N. O'Connor. Reno: University of Nevada, Department of Civil Engineering. March 1992.
- CCEER-92-2 Wehbe, N., M. Saiidi, and F. Gordaninejad. "Basic behavior of composite sections made of concrete slabs and graphite epoxy beams." *Report number CCEER-92-2*. Reno: University of Nevada, Department of Civil Engineering. August 1992.
- CCEER-92-3 Saiidi, M., and E. Hutchens. "A study of prestress changes in a post-tensioned bridge during the first 30 months." *Report number CCEER-92-3*. Reno: University of Nevada, Department of Civil Engineering. April 1992.
- CCEER-92-4 Saiidi, M., B. Douglas, S. Feng, E. Hwang, and E. Maragakis. "Effects of axial force on frequency of prestressed concrete bridges." *Report number CCEER-92-4*. Reno: University of Nevada, Department of Civil Engineering. August 1992.
- CCEER-92-5 Siddharthan, R., and Zafir, Z. "Response of layered deposits to traveling surface pressure waves." *Report number CCEER-92-5*. Reno: University of Nevada, Department of Civil Engineering. September 1992.
- CCEER-92-6 Norris, G., and Zafir, Z. "Liquefaction and residual strength of loose sands from drained triaxial tests." *Report number CCEER-92-6*. Reno: University of Nevada, Department of Civil Engineering. September 1992.
- CCEER-92-7 Douglas, B. "Some thoughts regarding the improvement of the University of Nevada, Reno's national academic standing." *Report number CCEER-92-7*. Reno: University of Nevada, Department of Civil Engineering. September 1992.
- CCEER-92-8 Saiidi, M., E. Maragakis, and S. Feng. "An evaluation of the current Caltrans seismic restrainer design method." *Report number CCEER-92-8*. Reno: University of Nevada, Department of Civil Engineering. October 1992.

- CCEER-92-9 O'Connor, D. N., M. Saiidi, and E. A. Maragakis. "Effect of hinge restrainers on the response of the Madrone Drive Undercrossing during the Loma Prieta earthquake." *Report number CCEER-92-9*. Reno: University of Nevada, Department of Civil Engineering. December 1992.
- CCEER-92-10 O'Connor, D. N., and M. Saiidi. "Laboratory studies of polyester concrete: Compressive strength at elevated temperatures and following temperature cycling, bond strength to portland cement concrete, and modulus of elasticity." *Report number CCEER-92-10*. Reno: University of Nevada, Department of Civil Engineering. December 1992.